Chance Constrained Optimization of Process Systems under Uncertainty

vorgelegt von
Diplom-Ingenieur
Harvey Arellano-Garcia
aus Piura-Perú

von der Fakultät III- Prozesswissenschaften
der Technischen Universität Berlin
zur Erlangung des akademischen Grades

Doktor der Ingenieurwissenschaften
- Dr.-Ing. -

genehmigte Dissertation

Promotionsausschuss:

Vorsitzender: Prof. Dr.-Ing. F. Ziegler
Gutachter: Prof. Dr.-Ing. G. Wozny
Gutachter: Prof. Dr.-Ing. G. Tsatsaronis

Tag der wissenschaftlichen Aussprache: 20. Oktober 2006

Berlin 2006

D83

Persönliches Vorwort

Die vorliegende Arbeit entstand während meiner Tätigkeit als wissenschaftlicher Mitarbeiter am Fachgebiet Dynamik und Betrieb technischer Anlagen in der Fakultät Prozesswissenschaften der Technischen Universität Berlin. Sie wurde von der Deutschen Forschungsgemeinschaft (DFG) finanziell gefördert.

Meinem Doktorvater, Herrn Prof. Dr.-Ing. Günter Wozny, danke ich sehr herzlich für die kontinuierliche Unterstützung während der Anfertigung dieser Arbeit sowie die persönlichen Impulse.

Herrn Prof. Dr.-Ing. George Tsatsaronis danke ich für die Übernahme des Mitberichts, Herrn Prof. Dr.-Ing. Felix Ziegler für die Übernahme des Vorsitzes der Prüfungskommission. Weiterhin bedanke ich mich bei Prof. Ignacio Grossmann von der Carnegie Mellon University, USA, für die externe Begutachtung sowie das stets gezeigte Interesse an meiner Arbeit.

Für die große Diskussions- und Hilfsbereitschaft danke ich speziell Dr.-Ing. Moritz Wendt. Dank auch an Herrn Prof. Dr.-Ing. Pu Li für die freundliche Begleitung meines Werdegangs am Fachgebiet. Weiterhin haben Dipl.-Ing. Walter Martini und Dipl.-Ing. Tilman Barz zum Erfolg dieser Arbeit beigetragen. Die Arbeit in dieser Gruppe hat wirklich Spaß gemacht. Zu erwähnen sind auch die zahlreichen Studien-, Diplomarbeiter sowie Austauschstudenten, die mit Ihrem Engagement zum Erfolg weiterer wissenschaftlicher Nebentätigkeiten beigesteuert haben.

Den Kolleginnen und Kollegen am Fachgebiet danke ich für das gute Arbeitsklima. Besonders hohen Anteil daran hatten Dipl.-Ing. Irisay Carmona, Dipl.-Ing. Richard Faber, Dipl.-Ing. Olivier Villain, Dipl.-Ing. Robin Thiele und Dipl.-Ing. Diethmar Richter. Die fachgebietsübergreifende Kooperation mit Frau Dr.-Ing. Anja Drews hat die Endphase dieser Arbeit angenehm gestaltet.

Schließlich bedanke ich mich bei meinen Eltern. Diese Arbeit ist meiner Frau Carolina und den Kindern gewidmet.

Berlin, im Oktober 2006 Harvey Arellano-Garcia

Contents

Notations

Acronyms

LP	Linear Programming
NLP	Nonlinear Programming
MI	Mixed-Integer
MINLP	Mixed-Integer Nonlinear Programming
SQP	Sequential Quadratic Programming
MIMO	Multiple-Input Multiple-Output
NMPC	Nonlinear Model Predictive Control
EKF	Extended Kalman-Filter

List of Symbols

Symbols in Optimization Problems

a, b, c, d, e	Vectors of known parameters
$\mathbf{A}, \mathbf{B}, \mathbf{C}, \mathbf{E}$	Parameter matrices
A, B, C	Price factors
C, c	Cost factor
$\mathcal{C}$	Cost objective function
ψ	Deterministic performance criterion
$\mathbf{d}$	Array of design variables
f	Function
$\mathfrak{F}, f$	Objective function, performance metric
$\mathbf{g}, \mathfrak{g}$	Array of equality constraints
$\mathbf{h}, \mathfrak{h}, \mathbf{k}$	Array of inequality constraints
$\mathbf{i}$	Array of initial conditions
$\mathcal{J}$	Objective function
n_k	Number of scenarios
NK	Number of collocation points
t	Time
t_f	Total batch time, end time-point
t_C	Predefined time-point
$\mathcal{R}$	Feasible region
$\mathbf{p}$	Array of uncertain parameters (deterministic type)
$\mathbf{u}$	Array of control (independent) variables
$\mathbf{v}$	Array time-invariant optimization variables
UT	Utility costs
x	Continuous variable

$\mathbf{x}$	Array of dependent output variables
$\mathfrak{X}$	Feasibility index
$\mathbf{y}$	Array of dependent constrained output variables
$\mathbf{y}^{C}$	Non-measured output variables
y	Discrete variable
ω	Weighting factor
ν	Supplier amount fraction
λ, β	Ratios

Symbols in Probability and Stochastic

A_i	Events
α	Probability level
ξ	Uncertain variable
$\boldsymbol{\xi}$	Vector of uncertain variables
$\boldsymbol{\Xi}$	Uncertain domain or space
E	Expected value of a function
Φ	Probability distribution function
σ	Standard deviation
R_y	Covariance of the output variables
$\mathbf{R}$	Covariance matrix of the output variables
φ	Standard density function
$\hat{\varphi}$	Standard normal density function
ρ	Probability distribution function
$\mathcal{P}$	Probabilistic functional of the objective function
$\mathcal{P}_i$	Probabilistic functional of the constraints
$\mathcal{P}r$, Pr	Probability
r_{ij}	Correlation coefficients
S_i	Combination of probabilities
γ_k	Scenario probability
μ	Mean value
$\Sigma, \hat{\Sigma}$	Covariance matrix
θ	Parameter to describe correlation
$\boldsymbol{\theta}$	Inflow random vector
z	Upper bound of an uncertain variable

Symbols used in Examples

Latin letters

a	Heat capacity parameters
a	Catalyst activity A-B
A	Heat exchange surface
A_e	Tray area
A_f	Free area of a tray, m^2

a, b, c	Model parameters
A, B, C	Antoine constants
A, B, C	Components of a multi-component system
D, X, Y	Components of a multi-component system
C_{i0}	Molar concentration
c_p	Heat capacity
C_W	Weir constant
d	Reactor diameter
D	Distillate flow rate
D	Total amount of product alcohol
E	Energy consumption, MJ
E, E_A	Activation energy
F_e	Inlet flow rate
$F, feed$	Feed flow rate
F_R	Recycle feed flow
g	Acceleration due to gravity
h	Enthalpy of a component
h_{0i}	Specific standard enthalpies
h^{ω}	Clear liquid height
$h^{0\omega}$	Froth height
H	Enthalpy of a mixture
HU	Holdup
K	Phase equilibrium constant
k	Reaction rate constant
k_0	Frequency factor
k_{HT}	Heat transfer coefficient
K_{decay}	Catalyst decay rate
L	Liquid flow rate
L	Reflux flow rate
l_W	Weir length
$M, \tilde{M}$	Molecular weight, g/mol
M	Total feed amount
N	Number of intervals
n_A, n_B, n_C	Component mol fraction
$\dot{n}_i$	Molar flow
N_U	Number of controls
N_1, N_2	Past and future time intervals
NK	Number of collocation points
NK	Number of components
NST	Number of trays
p	Pressure, bar
P	System pressure
PB	Amount of product
p^0	Component partial pressure

Q	Reboiler duty
R	Gas constant
R_V	Reflux ratio
r	Reaction rate
t	Time
t_u	Switching time-point between the fractions
T	Temperature, K
T	Reactor temperature
T_F	Feed temperature
ΔT_{ad}	Adiabatic temperature rise
T_{ad}	Adiabatic end temperature
T_c	Control horizon
T_P	Prediction horizon
V	Vapor flow rate
V , V_R	Reactor volume
w	Gas velocity
x	Liquid composition

Greek letters

ς_W	Fraction factor for calculating dry pressure drop
η	Tray efficiency
γ	Activity coefficient
ρ	Density of a component
ε	Volumetric vapor fraction
λ	Manipulated variable variation weighting factor
δ	Offset weighting factor

List of Sub/Superscripts and Operations

Subscripts:

0	Start
a, b	Interval bounds
A, B, C, D	Component
X, Y, R	Component
B	Bottom
cool	Cooling medium
D	Distillate
f	End
in	Inlet
i	Index of components or collocation points
j	Index of trays or collocation points
l	Index of time intervals
k	Period or scenario
min	Lower bound
max	Upper bound

out	Outlet
reac	Reaction
s	Number of uncertain variables

Superscripts:

~	Corrected bounds within the moving horizon
HT	Heat transfer
k	Index of iteration
L	Liquid
L, LB	Lower bound
min	Lower bound
max	Upper bound
V	Vapor
SP	Set-point
U, UB	Upper bound
u	Input variables
y	Output variables
–	Average

List of Abbreviations

$\mathcal{SFI}$	Stochastic flexibility index
PDF	Probability Density Function
MCS	Monte Carlo Sampling
LHS	Latin Hyper-Cube Sampling
HSS	Hammersley Sequence Sampling
EM	Empty state
LA	Liquid Accumulation
VLE	Vapor-Liquid Equilibrium
LII	Linear Inverse Interpolation
BM	Bisectional Method
D-RTO	Dynamic Real-Time Optimization

With regards to the definition of chance-constrained optimization problems in Figure 4.3:

L	Linear process
S	Steady state process
N	Nonlinear process
D	Dynamic process
C	Time-invariant uncertainty
T	Time-dependent uncertainty
S	Single chance constraint
J	Joint chance constraint

Chapter 1

Introduction

Robust decision making under uncertainty is deemed to be a crucial factor in many discipline and application areas. The competitive nature of the market environment imposes reliability requirements in meeting product demands and quality standards. The chemical industry is, therefore, required to make design and operating decisions which satisfy several conflicting goals in an optimal and safe manner. However, uncertainty and variability are inherent characteristics of any process system. They arise due to the unpredictable and instantaneous variability of different process conditions, such as temperature and pressure of coupled operating units, market conditions, (recycle) flow rates and/or compositions or other model parameters such as kinetic constants or equilibrium parameters. These uncertainties or disturbances are often multivariate and form correlated stochastic sequences which have a chain-effect on each unit operation of a production line.

In industrial practice, uncertainties are usually compensated for by using conservative measures such as over-design of process equipment and then retrofits to overcome operability bottlenecks, or overestimation of operational parameters caused by worst case assumptions of the uncertain parameters, which leads to a significant deterioration of the objective function in an optimization problem. In other deterministic approaches, the expected values are used, which most likely leads to violations of the constraints when the decision variables are implemented on site. Moreover, using feedback control to compensate the uncertainty effects can not ensure adherence to the constraints on the open-loop variables. In several cases, particular variables describing product properties like composition, viscosity, density, and etc. can not be measured online. These variables are open-loop under the uncertainties, but they are supposed to be confined to a specific region corresponding to the product specifications. It should be noted that even measurable disturbance variables are also stochastic variables, because they may have been measured to the present time point, but their future values are unknown. However, in conventional design methods for feedback control systems the description of disturbances is not rigorous. Step change and white noise are the two types of disturbances typically considered thus far. Consequently, the consideration of uncertainties/disturbances and their stochastic properties in optimization approaches are necessary for robust process design, operation, and control.

In this thesis, the main focus is related to the application to transient processes. The optimization of such inherent dynamic processes is usually performed using model-based optimization techniques. In most previous studies, a nominal model is considered, with which the outcomes of a deterministic optimization allow neither variation nor uncertainty on operating conditions or model parameters. Moreover, it is not possible to generate highly accurate phenomenological models for most chemical processes because of the imprecise values of their physical parameters, and the lack of complete understanding of the underlying physical phenomena. The usually limited quality and quantity of input-output data used to fit the model implies that the model will not be an exact representation of the real process. Thus, the practical implementation of model-based techniques often leads to a significant discrepancy between reality and simulation. Therefore, the existence of these uncertainties has a detrimental impact on the optimized process and raises questions like: what would be the probability of complying with the constraints in accordance with the optimized operating policy? Handling uncertainty, which becomes important especially in the presence of constraints on quality and safety, has not been adequately addressed so far and constitutes a significant bottleneck in applying optimization techniques to real processes. Therefore, accounting for the uncertainties involved in an optimization problem formulation, any improvement obtained regarding a specified economic objective function may occasionally become irrelevant, i.e. safety, reliability, and operability are often decisive, and more crucial than an economic objective (Grossmann and Morari (1984)). However, these issues are more complex and there is no obvious approach to suitably assess them (Figure 1.1). Thus, in most cases, conservative decisions based on heuristics or empirical rules are made which might lead to a substantial profit decrease. Accordingly, it demands systematic methods to evaluate the trade-off between profitability and reliability of a planned operation.

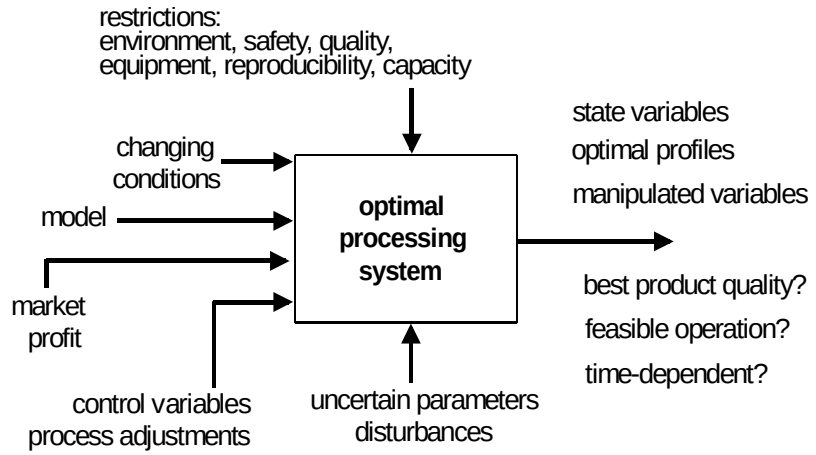

Figure 1.1: General operational objective targets.

During the past decades several approaches have been suggested to address these problems in a systematic manner. These techniques mostly differ in how uncertainty is handled as well as in the objectives that may include process flexibility, profitability, and/or robustness. In general, the direct solution can be problematic due to the difficulty in both evaluating the integral over the uncertain parameter space and ensuring feasibility of the inequalities for all parameter values instances (Samsatli et al., 1998). Overview of developments in the area of process design and operations under uncertainty are given in comprehensive reviews of Grossmann et al. (1983), Kall and Wallace (1994), Pistikopoulos (1995b), Wets (1996), Diwekar (2003), Sahinidis (2004). The emphasis of these studies, particularly in chemical engineering, has been mainly on process design problems. While most of the researchers were concerned about independent uncertain variables, Rooney and Biegler (1999, 2001) studied

the effect of correlated uncertain variables on plant design. Two approaches have been used to represent uncertain variables: discrete and continuous distribution. In the former, the bounded uncertain variables are discretized into multiple intervals such that each individual interval represents a scenario with an approximated discrete distribution (Halemane and Grossmann, 1993; Subrahmanyam et al., 1994; Pistikopoulos and Ierapetritou, 1995a; Rooney and Biegler, 1999). Thus, so-called multiperiod optimization problems are formulated. The second approach considers the continuous stochastic distribution of the uncertain variables, in which a multivariate numerical integration method will be chosen. This leads to a stochastic programming problem. An approximated integration through a sampling scheme (Diwekar and Kalagnannam, 1997) and a direct numerical integration (Bernado et al., 1999) have been used. Alternatively to sampled optimization algorithms, the stochastic problem can be relaxed to an equivalent NLP problem and then solved by using standard techniques. Thus, the optimization problem needs to be reformulated. If the uncertain variables have an impact on the objective function, it is usually formulated as the expected value of the objective function (Torvi and Herzberg, 1997; Acevedo and Pistikopoulos, 1998). Practically most of the previous cited works employed the two-stage programming method with the recourse formulation to deal with inequality constraints. In this approach the first-stage decision variables are predetermined before the realization of the uncertain variables, while the second-stage variables are decided after their realization. Moreover, in the recourse formulation, violation of the constraints is allowed, but penalized through penalty terms in the objective function. This leads to additional costs regarding the second-stage decisions. This approach is suitable when the objective function and constraint violations can be described by the same measurement, for example process planning problems under demand uncertainties (Clay and Grossmann, 1997; Gupta and Maranas, 2000). This compensation, however, requires a common measurement to describe the objective function and the constraint violations.

Decision making, however, inherently involves however consideration of uncertain outcomes. Thus, one is confronted with decisions a priori for the future operation. The decision though should be made before the occurrence of the random inputs. These uncertain variables can be constant or time-dependent in the future horizon. The stochastic distribution of the uncertain variables may have different forms. The mean and variance values can be determined based on historical data analysis. However, while computational advances in mathematical programming tools have aided decision making in many areas, their greatest impact may lie in enhancing decision making under uncertainty through stochastic programming. One method of stochastic programming is the probabilistic or chance-constrained approach which focuses on the reliability of the system, i.e., the system's ability to meet feasibility in an uncertain environment. This reliability is expressed as a minimum requirement on the probability of satisfying constraints. Thus, the objective function is expressed in terms of expected value, while the constraints are expressed in terms of fractiles. In fact, stochastic optimization even with an approximated distribution is more reliable than a deterministic optimization. For the numerical optimization under probabilistic constraints, some methods have been developed and applied to several disciplines like finance and management (Prekopa, 1995; Uryasev, 2000). In chemical process operations a few applications are known to date (Arellano-Garcia et al., 1998, 2003a). It has been used by, for instance, Maranas (1997) for molecular design and Petkov and Maranas (1997) for planning und scheduling of multiproduct batch plants. Additionally, several studies on model predictive control using probabilistic programming have been carried out for linear processes (Schwarm and Nikolaou, 1999; Wendt, 2005). In the case of a linear relation between the uncertain input and the output constraints, an efficient approach is presented by Prekopa (1995) for stochastic variables with correlated multivariate normal distribution, where numerical integration and sampling methods are combined. For the nonlinear case, sampling techniques can generally be employed. As an alternative to efficient

sampling techniques (Diwekar and Kalagnanam, 1997), Wendt et al., 2002 proposed in a previous work a computational method for nonlinear chance programming which is suitable, though, for steady state processes with only one single probabilistic constraint.

1.1 Scope

Deterministic optimization approaches have been well developed and widely used in the process industry to accomplish off-line and on-line process optimization. The challenge in this thesis is to address large-scale, complex optimization problems under various uncertainties. To deal with the unknown operating reality a priori, optimization under both parameter uncertainty and disturbance uncertainty has to be considered. Unlike the worst case analysis, for the presented approaches the stochastic characteristics (mean, covariance, correlation) of the uncertain variables will be involved in the optimization problem. While most parameter uncertainties are usually steady-state in nature, disturbance uncertainties are dynamic and will be described as stochastic processes. Uncertainties can be generally divided into external uncertainties like feed rate and/or its composition, recycle flows, temperature and pressure of the coupled operating units, supply of raw material and utilities, customer demand, prices, market conditions and internal uncertainties representing the unavailability of process knowledge such as model parameters. Model parameters are often regressed from a limited number of experimental data. While internal uncertainties have been well studied, external uncertainties have not been much emphasized. However, these uncertain variables will propagate through the process to the output variables and the outputs will also be uncertain, i.e., for a nonlinear process it is very difficult to analytically describe the distribution of the outputs. To overcome this problem, chance constrained programming is proposed in this thesis to deal basically with inequality constraints, which are based on the process requirements or limitations. This implies new approaches to high-order nonlinear integration of the joint probability density function.

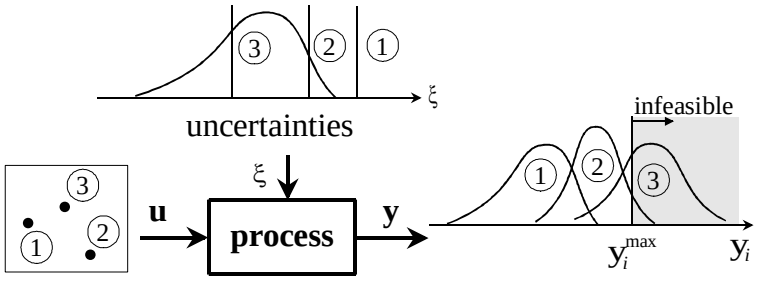

Figure 1.2: Strategies based on different uncertainty estimations.

Thus, the main propose is to make robust decisions accounting for uncertainties and unknown unexpected disturbances a priori. The main problem is illustrated in Figure 1.2. Whenever uncertainties are overestimated, the controls **u** will infer a conservative output distribution with regard to the constrained output and thus will lead to greater operational costs than actually needed (point 1 in Fig. 1.2). Unlike this, if the uncertainties are underestimated, the resulting strategy will be too aggressive which inevitably results in a high probability of constraint violation (point 3). Moreover, in practice, the presence of nonlinear (possibly time-varying) unmodelled dynamics and non-stationary noise or disturbances complicates the situation. How does one determine an optimal decision in such a complex setting? What is proposed in this thesis is a quantitative analysis of the probability of violating constraints by following a determined optimal strategy (point 2) based on the explicit integration of the available stochastic information of the uncertain variables. This requires a prior knowledge

about the probability distribution of the output variables. Generation of this information represents one of the main contributions of this thesis.

In summary, a novel analysis and optimization framework is proposed for optimization problems under uncertainty. Based on the method of chance constrained programming, efficient solution approaches are developed to different process systems engineering problems in order to make optimal decisions by taking both performance (through the objective function) and reliability into account. The essential challenge in solving such problems lies in the computation of the probabilities of holding the constraints as well as their gradients. Due to the fact that a desired compromise between optimality and the reliability of complying with the constraints can be induced, as a result, the derived strategy is thereby neither conservative nor aggressive.

1.2 Objectives

In this thesis, new approaches for chance constrained programming of large-scale nonlinear dynamic systems under time-dependent uncertainty are introduced. The stochastic nature of the uncertainties is explicitly considered in the problem formulation in which some input and state constraints are to be complied with predefined probability levels. The developed methods consider a nonlinear relation between the uncertain input and the constrained variables. Efficient algorithms are applied to compute the probabilities and, simultaneously, the gradients through integration by collocation in finite elements. The formulation of single or joint probability limits incorporates the consideration of feasibility and that of the trade-off between robustness and profitability regarding the objective function values. The new approaches are relevant to all cases when uncertainty can be described by any kind of joint correlated multivariate distribution function. The potential and the efficiency of the presented systematic methodology are illustrated with application to different processes under uncertainty, in particular, transient processes. Moreover, the functionality and efficiency of the developed chance constrained framework are demonstrated throughout on examples of design, operation and control problems. Furthermore, two model-based approaches are developed to provide a close integration of dynamic real-time optimization and control and to cope with uncertainty.

1.3 Overview

This thesis is devoted to the development of suitable algorithms and numerical techniques for the efficient solution of process engineering problems involving uncertainties. The proposed chance-constrained optimization framework forms the basis for addressing design, operation and control problems under uncertainty. The rest of the thesis is structured in seven additional Chapters. The problem formulation in **Chapter 2** reveals the necessity to explicitly incorporate the uncertainties into the optimization problems and underlines the importance of the chance constrained framework developed in this thesis. Moreover, the sources and characteristics of uncertainty and their analysis are highlighted. **Chapter 3** reviews the main approaches which have been proposed for optimization under uncertainty. **Chapter 4** describes the main principles and properties of chance constrained programming problems focusing on linear and steady-state processes. In **Chapter 5**, the new framework for chance-constrained programming of large-scale nonlinear dynamic systems under time-dependent uncertainty is introduced. The stochastic nature of the uncertainties is explicitly included in the optimization problem formulation. The method is based on the analysis of the relationship between the output constraints and the uncertain variables. The new approach involves

efficient algorithms for an indirect computation of the output probability distribution so that the probabilities and their gradients can be obtained by numerical integration of the probability density function of the multivariate uncertain variables by collocation in finite elements. Furthermore, depending on the process characteristics (linear, nonlinear, steady state, dynamic), the uncertainty type (constant, time-dependent) and the form of the chance constraints (single, joint), there are 16 different possible formulations of chance-constrained problems, as illustrated in Figure 4.3, which can in principle be solved using the proposed framework in this thesis.

In order to demonstrate the efficiency of the developed approaches, in **Chapter 6** the chance-constrained optimization framework is applied to an industrial scale process, namely a reactive semi-batch distillation process. The comparison of the stochastic results with the deterministic results is presented to indicate the robustness of the stochastic optimization. These achievements are an important step towards the implementation of robust optimal operating policies on real uncertain processes.

In **Chapter 7** two methods based on a Nonlinear Model Predictive Control (NMPC) scheme are introduced to solve close-loop dynamic optimization problems within an online framework. The key idea lies in the consideration of unknown and unexpected disturbances in advance i.e. anticipating, in particular, violation of output hard-constraints. Here, the solution of the posed novel chance-constrained NMPC problem has the features of prediction, robustness and being closed-loop. Based on the moving horizon strategy, the developed control strategy is extended to on-line optimization under uncertainty. In addition, towards an integration of dynamic real-time optimization and control of transient processes, a two-level strategy is considered.

Additionally, in all chance-constrained optimization problems under uncertainty treated in this thesis, the formulation of individual pre-defined probability limits of complying with the restrictions incorporates the issue of feasibility and the evaluation of trade-off between profitability and reliability.

Finally, a summary of the most important conclusions and key contributions are presented in **Chapter 8**. Furthermore, some suggestions and an outlook of potentially interesting future developments are presented.

Chapter 2

Problem Formulation

In chemical industry, decisions are often made based on limited knowledge about the processes and the corresponding underlying phenomena. This may result in poor process performance. Moreover, in industrial practice, there is a requirement for simultaneous process development, scale up and chemical production and for testing with incomplete process knowledge. In addition, it is required to accomplish as much process validation as possible in the pilot plants rather then in the real plant or production environment. On the other hand, there is a high reliance on experimentation and empiricism in obtaining process feasibility regions with little time devoted to process model development. Even in some processes most of the knowledge is empirical or with little understanding of the underlying mechanisms and it is rarely compatible with models derived from first principles. Thus, models used may be unreliable and the results inaccurate due to a number of non measurable external influences and limitations of models used for scale-up. As a consequence, the significance of a model-based approach in supporting and influencing practical decisions is limited by the low reliability of the results obtained. However, based on the agreement that process modeling can considerably benefit the process development and since the models represent the existing process knowledge in mathematical form, it becomes obvious that evaluation of the uncertainty effects in the process knowledge should not be ignored.

In order to improve the decision-making process, model-based deterministic optimization techniques have been successfully applied to a large number of engineering problems. However, it is widely recognized that in any engineering system there are always uncertainties due to variations in design conditions, loading and material properties, physical dimensions, and operating conditions. Deterministic approaches do not consider the impact of such variations, and as a result, the solution may be very sensitive to these variations. Moreover, deterministic optimization lacks the ability to achieve specified levels of constraint satisfaction especially for reliability and safety requirements. Therefore, the nominal deterministic model-based solution may be infeasible or over-conservative. On the other hand,

it is obvious that compared with the feasible region for deterministic optimization, the size of the feasible region will be reduced after considering robustness requirements. This raises the questions:

- *How to describe feasibility under the effect of uncertainty and variability to maintain robustness*?

- *What kind of constraint model should be adopted to ensure the accuracy in evaluating levels of constraint satisfaction*?

The design and simulation of chemical processes requires knowledge of thermodynamic properties, rate constants, transport coefficients, etc. However, exact values for many of these parameters are often not available, and this uncertainty must nevertheless be taken into account. For instance, an important factor in risk analysis and performance studies is the uncertainty associated with thermodynamic models. It exposes the importance of this topic for decision making in process safety and economic profitability analysis. Recent studies confirm the importance of this problem by analyzing the effect of thermodynamic data on estimated process performance (Vasquez and Whiting, 2000, Xin and Whiting, 2000). Generally, thermodynamic models are greatly affected by property inaccuracies because most of the parameters in the models are obtained via nonlinear regression procedures using experimental data (Fig. 2.1). Moreover, the measurements may be imprecise and even a small change in composition may be quite significant and thus any error of this magnitude can not be tolerated.

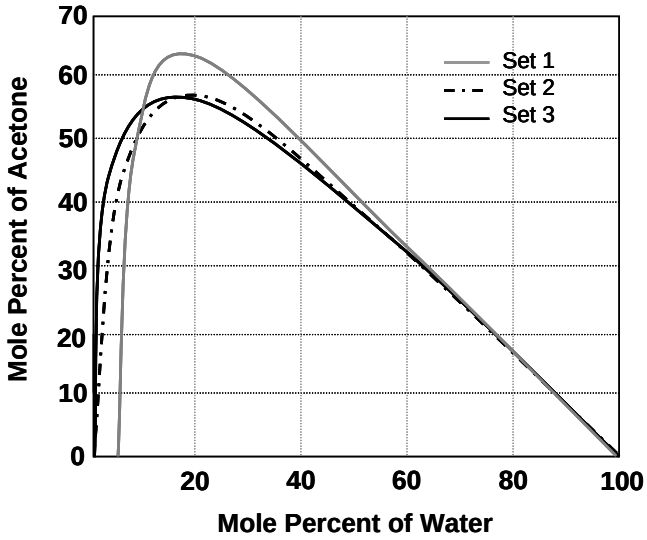

Figure 2.1: Predicted binodal curves for the liquid-liquid equilibrium of the ternary system chloroform-acetone-water 25°C using the NRTL model. NRTL parameters are regressed from different experimental data sources as indicated (Vasquez, V. R., W. B. Whiting, 2000).

In industrial practice, uncertainty is usually compensated for by means of overdesign. The design of even a simple piece of equipment often involves considering several uncertain parameters whose effects may be in opposition. Let us consider as a case study the design of a vacuum distillation column separating a temperature sensitive mixture. Uncertainty in tray efficiency leads to overdesign through the use of more than the optimum number of trays computed assuming complete knowledge. These trays are added to avoid penalties associated

with using reflux ratios higher than the optimum. However, in the separation of temperature sensitive mixtures the temperature in the reboiler is often limiting. The uncertainty in the temperature at which decomposition occurs often suggests using a temperature lower than the maximum allowed. The temperature in the reboiler of vacuum distillation columns is fixed through the phase rule by the pressure in the reboiler. In this context, higher pressure translates to higher temperature. The pressure in the reboiler depends on the number of trays in the column. The more trays there are, the higher the pressure in the reboiler. Hence, for this situation, uncertainty in tray efficiency indicates that more trays should be used while uncertainty in the decomposition temperature requires fewer trays.

In the daily production of chemical industry many plants are operated accounting for product requirements. Following the optimal operation planning, predefined steady-state operating points for continuous processes, e.g. a distillation column, are assigned to a process control system. The objective of the feedback control system is then to reject known or unknown disturbances so that the a priori set-points can be maintained. For several processes, however, the optimal productivity is close to the inherent limitations, product constraints or equipment capacity limits. Moreover, these restrictions may in fact vary while the process is running (horizontal and vertical lines in Fig. 2.2). In the neighborhood of such inherent limitations the process dynamics often exhibit highly nonlinear behavior. Thus, conservative operating points are usually chosen. However, controllers do not work perfectly, i.e. the controlled variables oscillate around their set-points (point A and B in Fig. 2.2.). Furthermore, depending on the control quality the fluctuations may be large or small. This is graphically represented as circles around the actual set-points (Fig. 2.2 – 2.4), where the bottom product x_B and the distillate product x_D are considered as constrained output.

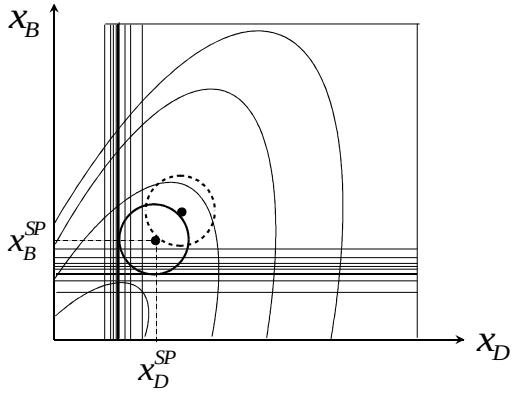

Figure 2.2: Constraints variations during process operation.

Also, the constrained variables are often monitored for safety considerations but not close-loop controlled. The disturbances behave randomly and even measured disturbances are stochastic variables since their values can not be precisely predicted for a future time point. Thus, it may be necessary to back off from the nominal optimal value of the constraints (point A in Fig. 2.3 *left*) which are difficult to measure or to control due to the poor dynamics. Since multivariate disturbances often exist in a large plant, it is difficult to decide a proper value. However, the back-off values are usually overestimated and thus leading to a conservative operation. For instance, it is well known that compositions are often not measurable online. Instead, temperatures are selected as reference variables for composition control. However, the specified points for temperature control do not necessarily guarantee the product purity specifications (e.g. if the pressure of the plant swings). Consequently, because of the conservative decisions concerning the temperature set-points (point B in Figure 2.3 *left*), a

much purer product than specified will be achieved which causes much higher operating costs than actually needed.

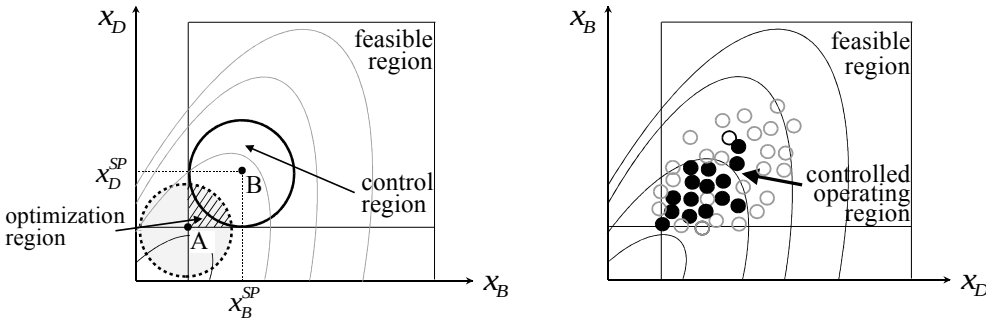

Figure 2.3: Steady state operating set-points by feedback control.

To overcome the outlined problems, taking into account the influence of uncertainty on the optimization problems for different purposes is proposed in this work. Thus, for instance, considering the operating point of a distillation column system defined by the distillate and bottom product specifications (Fig. 2.2 and 2.3), the values of the setpoints and controls can be adjusted so that the target area in Figure 2.3 *right* will be tailored according to the changing disturbances. Thus, in comparison to the conventional feedback control shown in Figure 2.3 *left*, the operating points can be moved closer to the nominal point A which leads to a higher profit.

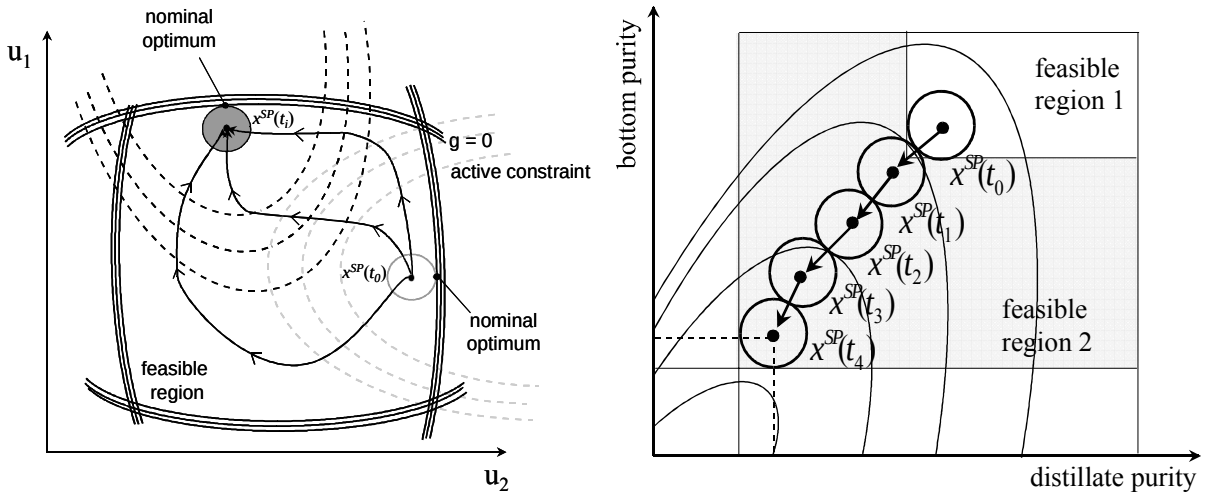

Figure 2.4: Dynamic operating set-points trajectories.

Another important aspect of process operation is that most chemical processes exhibit nonlinear and time-dependent behavior and large numbers of variables. Thus, it is very difficult to find optimal solutions a priori or even feasible solutions only by using heuristic rules. Therefore, systematic methods incorporating uncertainty information are neccesary. In Figure 2.4, the dynamic operating set-point trajectories for a time-varying process with changing (active) constraints (Fig. 2.4 *left*) and a stationary process with set-point modifications (Fig. 2.4 *right*) are illustrated to explain this issue. The size of the dynamic operating region around the optimum is affected by fast disturbances. Moreover, the true process optimum lies on the boundary of the feasible region defined by the active constraints (g=0). Due to the uncertainty in the parameters and the measurement errors, the process optimum and the set-point trajectory would be infeasible. Therefore, the optimal policy (set-

point profiles) needs to be adapted based on the current state, the disturbances and the available model parameters. To track the optimal set-points for transient processes, adaptive control strategies are required due to the changing dynamics of the operating process. By this means, robust approaches are required to relocate the region of the set-point trajectory within the feasible region of the process in order to guarantee, on the one hand, feasible operation, and to operate the process, on the other hand, still as closely to the true optimum as possible.

2.1 Sources and characteristics of uncertainty

When operating in a changing and uncertain environment, it is essential for market success to design processing systems capable of acceptably satisfying multiple conflicting goals (e.g. changeovers in customer demands, product specification, feed stocks and environmental regulations) in an optimal and safe manner. In industrial practice, uncertainties are compensated for by using conservative decisions like over-design of process equipment or overestimation of operational parameters based on worst case assumptions of the uncertain parameters, which leads to significant deterioration of the objective function in an optimization problem. Traditionally design and control are treated in a sequential way. Moreover, design stage calculations are conventionally performed under deterministic optimization paradigms: an economic objective function is optimized and leads to single-point solutions in the decision space, without taking into consideration different sorts of uncertainty.

However, almost all systems encountered in the process industries have uncertainty associated with them. From the viewpoint of process operation, the source of uncertainty may be either internal such as inaccurate model parameters and/or external such as unknown future feedstock. These disturbances are often multivariate and correlated stochastic sequences which have a chain-effect on each unit operation of a production line. In order to incorporate these uncertainties, two approaches: *deterministic* and *stochastic*, can generally be distinguished. In the former case, parametric uncertainties are described through lower and upper bounds or via a finite number of fixed parameter values (periods, scenarios). However, since a number of parameters are frequently estimated at the same time from a single set of experimental data, simple lower and upper bounds may not capture the actual uncertainty. Previous results have shown that failure to account for correlation amount the uncertain parameters can also lead to conservative estimates of the influence of uncertainty, infeasible operation, or both. Moreover, additional complications arise in process systems engineering problems because of highly nonlinear systems. Modeling the parametric uncertainty in these instances may require a more detailed statistical analysis. Therefore, the *stochastic* method takes a more general approach describing the uncertainties description by probability distribution functions.

2.1.1 Uncertainty classification

In the context of chemical engineering process systems, Ierapetritou et al. (1996a) proposed the following classification of the uncertainty types involved in process models:

(I) *Model-inherent uncertainty*: includes kinetic constants, physical properties and transfer coefficients. Information is usually obtained from experimental and pilot-plant data and the uncertainty is described via either a range of possible realizations or some approximation of a probability distribution function.

(II) *Process-inherent uncertainty*: it comprises flowrate/temperature variations, stream quality fluctuations and so on. This uncertainty type is usually described by

probability distributions obtained from (on-line) measurements. Here, any desired range of uncertain parameter realizations could theoretically be achieved through the implementation of a suitable control scheme.

(III) *External uncertainty*: it includes uncertainty in feed stream availability, product demands, prices and environmental conditions. Forecasting techniques based on historical data, customers´ orders and market indicators are typically used to obtain approximate ranges of uncertainty levels or the corresponding probability distributions.

(IV) *Discrete uncertainty*: this type is used to describe equipment availability and other random discrete events. A (discrete) probability distribution function can commonly be obtained from available data and manufactures´ specifications.

A further classification can be made in relation to the uncertain time dependence in the future horizon. The representation of uncertainty is an important modeling question. The potential effect of variability on process decisions regarding process design and operations constitutes another challenging problem. Moreover, the uncertain variables may be correlated or uncorrelated. However, they are undetermined before their realization. It means that either the measurable uncertain variables have been measured or the uncertain parameters newly estimated. In this thesis, the developed approaches are mainly concerned with uncertainties associated with the first three types (I-III) enumerated above.

2.1.2 Quantification of Uncertainty

Currently, process simulation models and other tools allow engineers to design, simulate, and to optimize chemical processes. However, there is a large need to incorporate uncertainties as a key issue to study the effect of variability on decisions related to process performance and quality. The quantification of uncertainty in stochastic process systems requires the quantification and characterization of the uncertain input. These are modeled by considering them as random variables. The assumed distributions for model parameter uncertainties depend on the obtainable information and the parameters nature. On the other hand, diverse probability distributions are possible for the different random inputs which are obtained based on measurements. Furthermore, a risk associated with a processing sequence is represented via particulars measures in the distributed output performance criteria predicted by the stochastic system. The general function for a stochastic output criterion measure involves the evaluation of the expected value E of the performance metric f, for a deterministic output performance criterion Ψ. This can be expressed analytically by the probability integral given in Equation 2.1.

$$E\left\{f\left(\Psi\left(\xi\right)\right)\right\} = \int_{-\infty}^{+\infty} f\left(\Psi\left(\xi\right)\right)\rho\left(\Psi\right)\, d\Psi \tag{2.1}$$

Accounting for the fact that the precise forms of the output and the probability density function $\rho(\Psi)$ are both unknown, it is more appropriate to express the expected value E as a multi-dimensional integral over the joint probability distribution function of the stochastic inputs $\rho(\xi)$,

$$E\left\{f\left(\Psi\left(\xi\right)\right)\right\} = \int_{\xi\in\Xi} f\left(\Psi\left(\xi\right)\right)\rho\left(\xi\right)\, d\xi \tag{2.2}$$

In equation (2.2) the whole uncertain space is denoted by Ξ. The probability distribution function can be either estimated from experimental data or assumed using regular distributions. The expected value is given as

$$E\{\Psi(\xi)\} = \int_{\xi \in \Xi} \Psi(\xi)\rho(\xi)\, d\xi \tag{2.3}$$

The variance of a random variable (or equivalently, of a probability distribution) is a measure of its statistical dispersion, indicating how its possible values are spread around the mean (Eq. 2.4). The variance Var is given as follows:

$$Var\{\Psi(\xi)\} = \int_{\xi \in \Xi} \left(\Psi(\xi) - E\{\Psi(\xi)\}\right)^2 \rho(\xi) d\xi \tag{2.4}$$

The presence of outliners can drastically influence the variance. In case the outliners are considered not as important as the width of the desired confidence interval or that between lower and upper fractiles, the variance can be employed as a measure to determine the uncertainty in the distribution bulk merely. The square root of the variance is the standard deviation. This is another measure of variability.

The uncertainty space, from which the system output response results, is formed by characterizing of the stochastic inputs to the system. This mostly affects the probability distribution functions contained in the joint confidence regions or confidence intervals. Nevertheless, it assumes a priori data availability in order to estimate the description of a particular parameter or set of parameters. In the absence of sufficient data, evaluation of realistic estimates of the parameter limits and the importance of the distributions analytical form are recommended. Under the assumption that parameters are independent of each other, the joint sampling space may be described as a hyper-rectangle where each dimension represents one uncertain input bounded by its respective upper and lower confidence limits. When no data is available, confidence limits around the assumed nominal values are defined as some percentage of the nominal values. In a multi-parameter model where the parameters are estimated simultaneously, a joint confidence region (e.g. normally distributed) provides a more appropriate measure of the uncertainty space in comparison to a hyper-rectangle comprising the individual confidence intervals. Rooney and Biegler (1999) demonstrate the importance of including parameter correlations in design problems by using elliptical joint confidence regions to describe the correlation among the uncertain model parameters.

Once the uncertain input space is defined in terms of its limits and distribution form, the next step is to quantitatively describe the related system outputs with regard to the performance criteria. Because of the use of highly nonlinear input probability distributions and complex (deterministic) model equations, as well as nonlinear constraints, it is very difficult or impossible to determine the system output probability distribution function or to derive nonlinear probability integral measures analytically (Fig. 2.5). Thus, approximation approaches are applied which usually situate observations within the input uncertainty distribution space at which the actual deterministic model is solved. They are generally classified into *sampling techniques* and *numerical integration* approximation formulas.

In sampling-based techniques, the performance response is estimated over the entire space of the uncertainties. However, the choice of successive inputs to obtain the information on the

stochastic output is very important when it is necessary to keep the number of observations small for computational efficiency reasons. Independently of the sampling technique, the deterministic model is simulated using the observed values of the stochastic inputs found with the help of the sampling strategy. This is based on the distribution characteristics of the input uncertainties. Here, general statistical metrics can be applied to quantify various aspects of the generated sample output distribution, such as the sample expected value and variance. An important advantage of the sampling techniques based on pseudo-random number sequences is that they do not always require more sample observations as the problem dimension (number of uncertainties) increases (Diwekar, 2003).

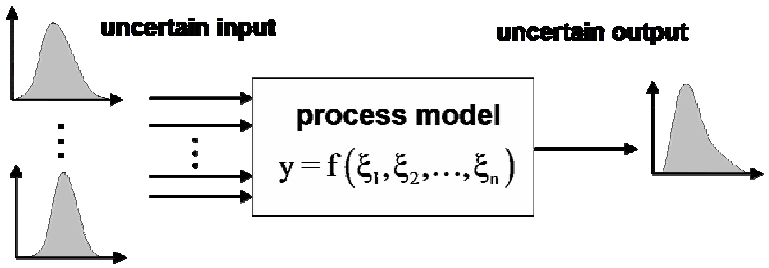

Figure 2.5: Uncertainty propagation.

In cases where the distribution function is known or approximated, numerical integration methods are generally applied. Here the different scenarios are weighted pursuant to the extent of fulfillment of some condition (Fig. 2.5). Approaches like Gaussian quadrature and cubature methods are presented in (Bernardo et al., 1999). Gaussian quadrature is a common numerical approximation approach for multi-dimensional integrals. It has used in optimal chemical process design under uncertainty approaches by Straub and Grossmann (1993), Pistikopoulos and Ierapetritou (1995a), and Terwiesch et al. (1998). In order to calculate Gauss product and cubature, enhanced integration formulas were proposed by Bernardo et al. (1999). They can be employed in order to improve the accurateness of the numerical integration over the multidimensional probability distribution.

2.2 Uncertainty analysis and sampling

To evaluate uncertainty, sensitivity analysis through a series of multiple runs can be performed. However, usually only one or two parameters at a time are varied in a simulation framework, where the underlying model may contain a large number of independent variables. Consequently, important interactions and scenarios may not be evaluated. Although a larger number of cases may be run as part of a sensitivity study, the volume of the output generated makes the results cumbersome or difficult to interpret. Even where many cases are analyzed, sensitivity analysis still provides no information as to the likelihood of different outcomes (Diwekar et al., 1991a).

Uncertainty analyses basically comprise the proliferation of uncertainty in model parameters and model structure to attain confidences statements for the estimate of risk and identify model components of critical importance. This is required especially when there is no *a priori* knowledge about the system uncertainty. Uncertainty analysis aims to provide a quantification of the uncertainty associated with a stochastic system in terms of the output performance distribution to the distributions of the (stochastic) inputs. The analysis of uncertainties is even more important when the technical or economical variables of the process are not determined

or the system design is incomplete. At the simulation stage, the computation results of the thermodynamic equations can be different due to the process states or the available parameter ranges. Thus, both earlier stochastic analysis capability and model accuracy are necessary in order to treat uncertainties efficiently. A well-established method for estimating model uncertainties is through model validation. But, it is often restricted because of the lack of data, limited experimental opportunities, and insufficient financial resources. However, characterizations of uncertainty sources enhance the value of model predictions by allowing for quantification of their precision, thus increasing the confidence one can have in them. Uncertainty is introduced into a simulation model in several ways, and its propagation is manifested as uncertainty or variability in the model output (Fig. 2.5). Thus, uncertainty analysis requires stochastic modeling environments.

Approaches involving uncertainty and sensitivity methods have predominantly paid attention to the simulation assessment of continuous processes, in particular, those unit operations which employ thermodynamic models and chemical reaction kinetic models subject to physical property and kinetic parameter uncertainties. In the past, several articles have investigated uncertainties in rigorous physical properties in chemical engineering applications (Maranas, 1997; Tørvi and Hetzberg, 1998; Terwiesch et al., 1998; Whiting et al., 1999; Vasquez and Whiting, 1999 and 2000; Tayal and Diwekar, 2001; Ulas and Diwekar, 2004). Approaches examining the dynamic propagation of uncertainty (Phenix et al., 1997) and others approximating the evolution of probability distribution functions in uncertain dynamic systems (Tørvi and Hetzberg, 1998) have been proposed. Due to the use of the quadrature for the integration under the multivariate distribution function, the latter method is limited to small numbers of uncertain factors.

2.2.1 General approach to uncertainty analysis and stochastic simulation

Systems process modeling can significantly benefit the process development. The created mathematical models represent the process knowledge. Consequently, the assessment of the uncertainty effects should not be overlooked. Computational and time resources may impose limits on the accuracy which can be obtained from uncertainty und sensitivity analysis. The stochastic simulation constitutes a general approach to perform parameter uncertainty analysis. For the purpose of simulation, uncertainty in process model systems is now explicitly considered using sampling techniques based on pseudo-random number sequences. The latter exhibits a number of desirable advantages for uncertainty and sensitivity analysis. They are not only conceptually simple but also flexible to in accomodating various situations such as the estimation of different statistical measures which include not only the mean and variance but also one-sided deviation functions. They also exploit the full range of the input uncertainties and the output performance distributions can be estimated without the use of intermediate models. The major disadvantage of these techniques is the large number of samples required to obtain good accuracy and the lack of uniformity, which may be apparent in the sample. To execute a quantitative uncertainty analysis, probability distributions must be allocated to each of the uncertain parameters. The distribution may result directly from data obtained from an appropriate experimental design, but usually expert judgment must be used to estimate the probability for the unknown value of a parameter to lie within a specified range. One common method for probabilistic or stochastic simulation follows an iterative procedure which can be generally formulated as follows:

a) Perform an inventory of all uncertain key input parameters
b) Define the maximum range of the appropriate unknown parameter values
c) Designate a probability distribution within this range

d) Establish and validate correlations amongst parameters
e) Sampling the distribution of the specified parameter
f) Derive quantitative assessment of the uncertainty e.g. in terms of confidence intervals for the unknown value
g) Perform sensitivity analysis to rank the key parameters involvement
h) Spread the effect of uncertainty through the model and estimate the probability distribution of the model predictions
i) Acquire supplementary data for the significant model parameters and reiterate steps b) to h)
j) Apply statistical techniques to evaluate the outcomes

2.2.1.1 Specifying probability distributions for uncertain model parameters

In engineering models uncertainty or variability can be expressed in terms of probabilistic distributions. The type of distribution chosen for an uncertain variable reflects the amount of available information. Experimental and plant data may contain systematic errors, erroneous data and outliners. In this thesis, systematic errors are not specifically considered. However, the chosen probability distributions show the range of values which the variable could assume and the probability of occurrence of each value within the range. In this way, the distributions give a description of the probability measures associated with the values of a random *uncertain* variable. Probability distributions may be viewed as cumulative distribution functions, or by selected parameters, such as fractiles and moments (e.g. mean and variance). A detailed review of these methods can be found in Diwekar and Rubin (1991a, 1994).

In order to better capture the diverse nature of uncertainty, different distributions can be employed for an uncertain variable. For instance, the uniform and log-uniform distributions represent an equal likelihood of a value to lie anywhere within a specified range, on either a linear or logarithmic scale, respectively. Uniform distribution is used when information is poor and only the limiting values are known. As it has no central tendency, uncertainties result in a broad value distribution of the output variables. In contrast, a normal distribution reveals a symmetric but varying probability of a parameter value being above or below the mean value. On the other hand, some distributions such as a lognormal distribution are distorted such that there is a high probability of values lying on one side of median than the other. Different distributions may be apparent for other stochastic input properties which are directly based on physical measurements. Besides, user-specified distributions can be used to represent any arbitrary characterization of uncertainty; including probabilistic constraints i.e. fixed probabilities. However, once probability distributions are assigned to the uncertain parameters, the next step is to perform a sampling operation from the multivariable uncertain parameter domain.

2.2.1.2 Sampling

To obtain representative values from the parameter space frequently, the sampling approach is used. This is the case, for instance, when performing uncertainty analysis of regression models. The primary purpose is to acquire reliable results for the output distributions of the variable analyzed. However, common sampling techniques e.g. Monte Carlo, though easy to employ, require numerous model evaluations for accurate results. Furthermore, techniques like Perturbation Methods and Stochastic Finite Elements though efficient, need access to model equations, i.e. a “black box” approach is not possible. In past chemical engineering applications sampling techniques, in particular Monte Carlo and Latin Hyper-Cube LHS strategies have been used. The Monte Carlo sampling technique (MCS) is one of the most widely used techniques for sampling from a probability distribution. This sampling approach

is based on a pseudorandom generator used to approximate a uniform distribution. The specific values for each input variable are selected by inverse transformation over the cumulative probability distribution. The computational effort required to achieve sufficient accuracy depends directly on the number of deterministic model simulations. Thus, an efficient sampling method for a large number of input uncertainty factors is necessary. In comparison to the MCS and LHS, the Hammersley Sequence Sampling HSS (Diwekar and Kalagnaman, 1997) appears to be the most efficient. The authors provide evidence that the convergence rate of samples propagated through diverse functions are claimed to be between 3 and 100 times faster for HSS than the MCS, LHS and median LHS techniques, over the range of linear and non-linear functions and correlation structures, they considered. The HSS method uses a quasi-random number generator based on the Hammersley points to uniformly sample a unit hypercube, and inverts these points over the multivariate probability distribution to provide a sample set for the variables of interest. Due to the distribution uniformity of the Hammersley points in the hypercube, the HSS sampling method exhibits a high efficiency. A disadvantage is that it imposes a correlation structure on the sample, which appears to change the uniformity properties of the low discrepancy design. Another disadvantage is that as a sampling based approach, a large sample number may still be required to achieve a reasonable accuracy. The sampled results of two variables with correlated normal distribution are shown in Figure 2.6. The difference between Monte-Carlo and Hammersley can easily be observed.

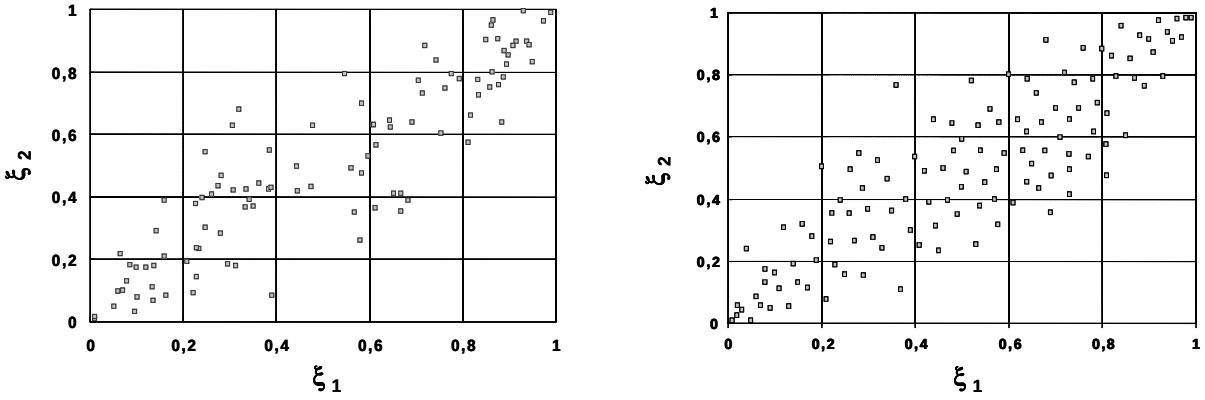

Figure 2.6: Two random variables with correlated normal distribution after sampling with MCS (left) and HSS (right).

After propagating the effects of uncertainties through the corresponding model, the next step is to analyze the results by application of statistical techniques. Here, the main task is the importance ranking of the uncertain parameters and their potential contribution to the total risk. Finally, uncertainty analyses are effective when they are conducted in an iterative manner providing a major tool for decision making. Additional reading on this issue can be obtained from a number of authors (Diwekar, 2003).

2.2.2 Advantages of an uncertainty and sensitivity analysis

In process simulation probability is generally applied to describe uncertainty. Provided that statistical methods are employed with no process knowledge, the physical implications of the outcomes can not be explicated. The analysis results give an idea about the tendency of the modification in the process variables uncertainties, in the relevance of the variables, and in the relation between them. For this purpose, the deterministic models can be emloyed in any usual simulator without adaptations. After that, a sensitivity analysis can be used in order to understand the system behavior by making out the main contributions of the considered

random outputs. In connection with the contributions of the uncertain inputs to the stochastic system, this analysis also offers quantitative measures of the strength of certain relationships between uncertain parameters to the predicted output variables. These measures are primarily sub-classes of the variance-based methods (Saltelli et al., 2000). Furthermore, given that discrete events are also handled by process simulations e.g. start-up, shut down, batch processes, for these discrete events the concepts of event und state can be used. While an event takes place at a time point, the system state is changed to a different one by an event. However, for an implicit event the time of occurrence is not known. On the contrary, for an explicit event it is known. Thus, either a point action is taken once at the moment when the event occurs or a continuous action is taken for the time period while a precondition is fulfilled. Uncertainties changes can be conveyed as variations of the distribution parameters.

The stochastic simulation is a helpful tool to validate a process model and to anticipate the unsteady state behavior of a process under diverse uncertainties. Overall, this generalized stochastic modeling capability can be practical for performance analysis, economic analysis, determination of over-design factor, error and sensitivity analysis, feasibility studies, risk analysis, identification of process R&D priorities and planning.

2.3 Illustrative example

In this section, the optimization of a batch distillation process is used as an example. The objective of the case study is to evaluate the influence of uncertainties on the process performance. Batch distillation processes are time-varying and this ever changing process also provides flexibility in operating and configuring the column in various ways. A distinctive feature of batch distillation is that it produces not only the desired products but also off-cuts. Conventionally, off-cuts are recycled to the reboiler of the column for the next batch. In this case study, an alternative operation mode for batch distillation is proposed, namely, the off-cuts will be recycled in form of a continuous feed flow into the column (Arellano-Garcia et al., 2002). The separation effect is promoted in this way and thus economical benefits can be achieved. Here, simulation and deterministic optimization based on a rigorous model are carried out to show the properties and feasibility of this operation mode and develop optimal operating policies.

In the proposed recycle strategy, the time of adding adds one further degree of operational freedom. The second principle of thermodynamics provides again useful indications. Since mixing is accompanied by irreversibility, the addition of an off-cut to the reboiler should be done when the two compositions are as close as possible. Since the composition of the off-cuts lies between the initial composition in the reboiler and that of the distillate, feeding the off-cuts to a certain stage of the column shortens the way of separation. The main problem is to decide when and how much recycle can be profitable.

The process considered is a batch distillation with a packed column for separating a 4-component mixture with A, B, C, D representing from the lightest to the heaviest component (Fig. 2.8). Furthermore, three main cuts (fractions A and C from the top of the column as well as one fraction D from the reboiler) will be obtained during the batch. An off-cut mainly containing B will be also received from the distillate. The heaviest component D has no vapor phase and remains in the reboiler during the batch. Moreover, in this system there is an azeotropic point. The VLE relationships of the other three components (A, B, C), which are distillated through the top of the column during the batch, show an abnormal behavior, especially those involving the least volatile component C. By “normal” and “abnormal” are

meant the x-y diagrams of a binary system given in Figure 2.7a and b, respectively. The relationship between component B and C in the mixture has the form of (b) in Fig. 2.7, from which one can imagine how drastically the state will change, when component C appears and goes up through the batch column.

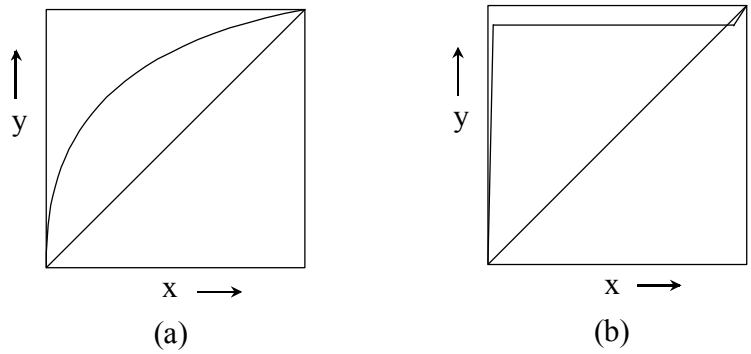

Figure 2.7: x-y diagram of a binary system: (a) normal and (b) abnormal.

In addition, because component C is much heavier than A and B, the column pressure has to be decreased during the period of distilling of fraction C. This means that besides the reflux ratio, the policy of the column pressure should be considered as a decision variable for the optimization. Until now, column pressure has been considered as a fixed parameter in previous studies on optimization of batch distillation. As we know, the variation of column pressure leads to a strong nonlinearity of the entire process and thus causes more severe convergence problems in the simulation. The optimization of column pressure is of interest, because an increase of the column pressure allows an increase of the total mass flow of vapor stream at the same vapor load term (*F-factor*). On the other hand, an increase in the column pressure also causes a decrease of the relative volatility that necessitates a higher reflux ratio to fulfill the purity constraints of the distillate products. To describe the packed column we use a detailed dynamic tray-by-tray model (Wendt et al., 2000). The number of the theoretical trays is calculated corresponding to the height of the packing. The holdup of each theoretical tray is computed with the correlation model proposed by by Engel et al. (1997). The vapor load from the reboiler to the column is restricted by the F-factor of the column as well as the heating capacity of the plant.

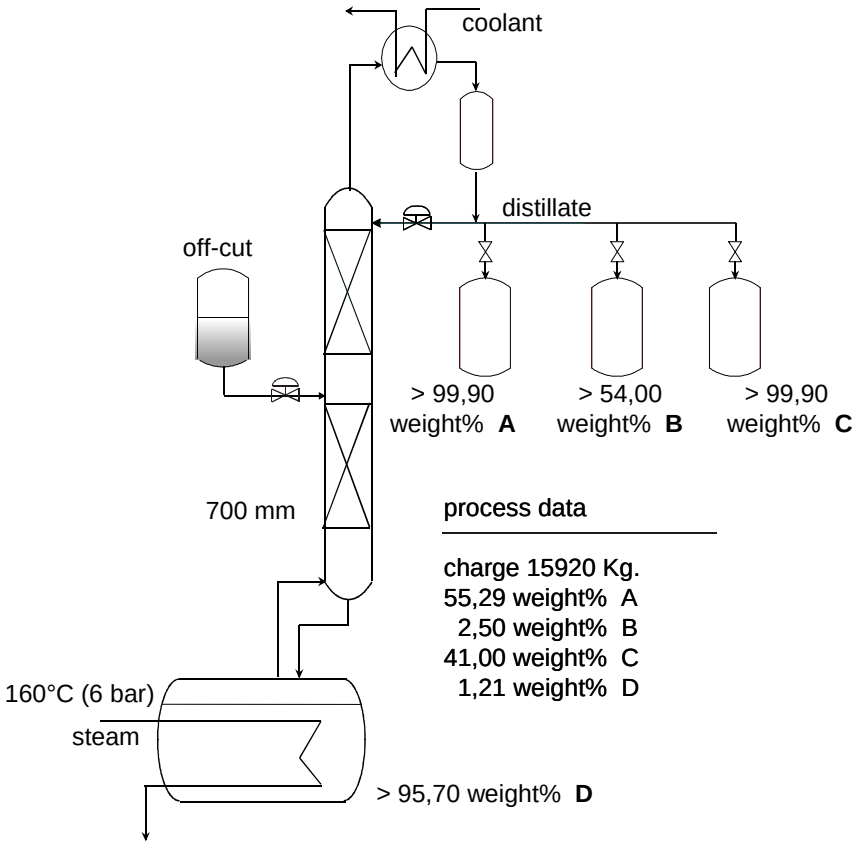

Figure 2.8: Batch distillation system with the proposed operation mode and their specifications.

2.3.1 Deterministic optimization

In industrial practice, it is often desired to minimize the duration of the batch processing. Thus we consider the time-optimal problem to find optimal policies for the proposed operation mode, which can be described as follows:

$$
\begin{aligned}
&\min\ t_f\ \left(F_R(t),\ P(t),\ R_V(t),\ t_{u1}, t_{u2},\ t_f\right)\\
&\text{s.t. the model equation system and}\\
&x_A(t_{u1}) \geq x_A^{SP}\\
&x_B(t_{u2}) \geq x_B^{SP}\\
&x_C(t_f) \geq x_C^{SP}\\
&x_D(t_f) \geq x_D^{SP}\\
&\int_{t_0}^{t_f} F_R(t)dt \leq M_1\\
&F_R^L \leq F_R(t) \leq F_R^U\\
&P^L \leq P(t) \leq P^U\\
&R_V^L \leq R_V(t) \leq R_V^U
\end{aligned}
\qquad (2.5)
$$

The decision variables are the reflux ratio R_V, the feed flow rate of the recycled off-cut F_R and the system pressure P. The different time intervals are also regarded as decision variables in order to properly identify the switching time-points between the different fractions as well as the total batch time. The output constraints are the specifications of the average composition in the three cuts and the final composition in the reboiler. The considered process features a strong nonlinear behavior and the model leads to a large-scale DAE system. To efficiently simulate and optimize the processes, collocation on finite elements is used to discretize the dynamic model equations. Through this discretization the dynamic optimization problem is transformed into a nonlinear programming (NLP) problem. It should however be noted that the choice of the feed tray for the recycle stream can also be optimized. To prevent the problem from becoming too complicated, simulations have been carried out to decide the feed tray.

Due to the amount of component A in the off-cut to be fed, its whole content should be pumped into the column by the end of the first main cut period. Thus, only in this period, the differences between the conventional and the new operation mode can be seen. Figure 2.9 *left* shows the optimal trajectories of the reflux in this period for both the conventional and the new operation mode.

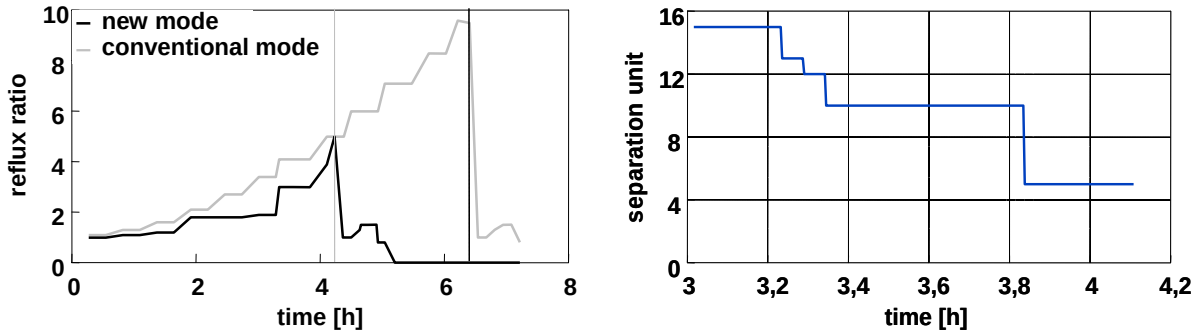

Figure 2.9: Optimal reflux ratio for the conventional and the new operation mode (left) and the optimal feed position of the recycle stream (right).

In Figure 2.9 *right* the optimal feed position of the recycle stream corresponding to the theoretical tray number is illustrated. This is approximately corresponding to the position in the column where the composition is equal to the feed composition. Figure 2.10 *left* shows the optimal recycle flow rate during the first period. It has to be noted that the difference concerning the optimal policies of the column pressure are only marginal, since a higher pressure is favorable in case of a constant F-Factor during the first main cut period. But the pressure is restricted by an upper bound due to the temperature of the reboiler heating steam.

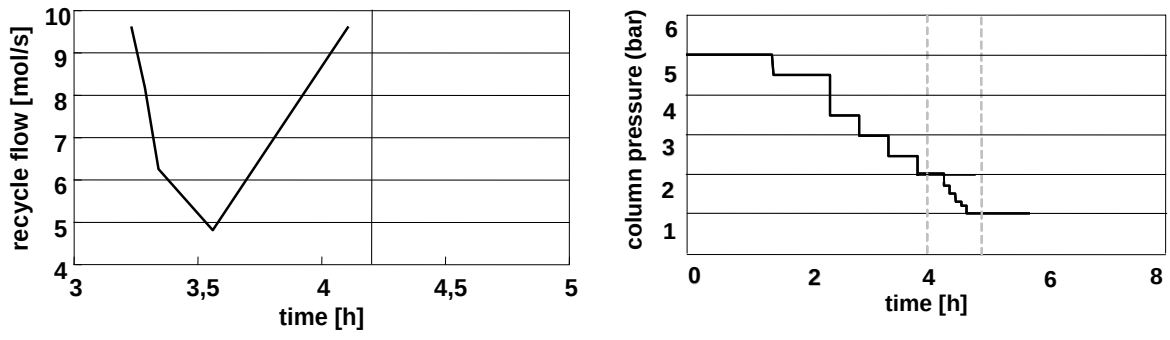

Figure 2.10: Optimal recycle flow rate and pressure policy.

The column pressure, as shown in Figure 2.10, should be high during the first fraction so that the column will have a large vapor load, because there is a large amount of component A in the reboiler at the beginning of the batch. After that the pressure should be decreased, since the effect of separation is more and more important as the mixture in the reboiler becomes heavier. This result illustrates the compensation between the amount and purity of the distillate by regulating the column pressure. The total batch time resulted from the optimized policy is about 6 hours, which is only 40% of the batch time needed for the conventional operation.

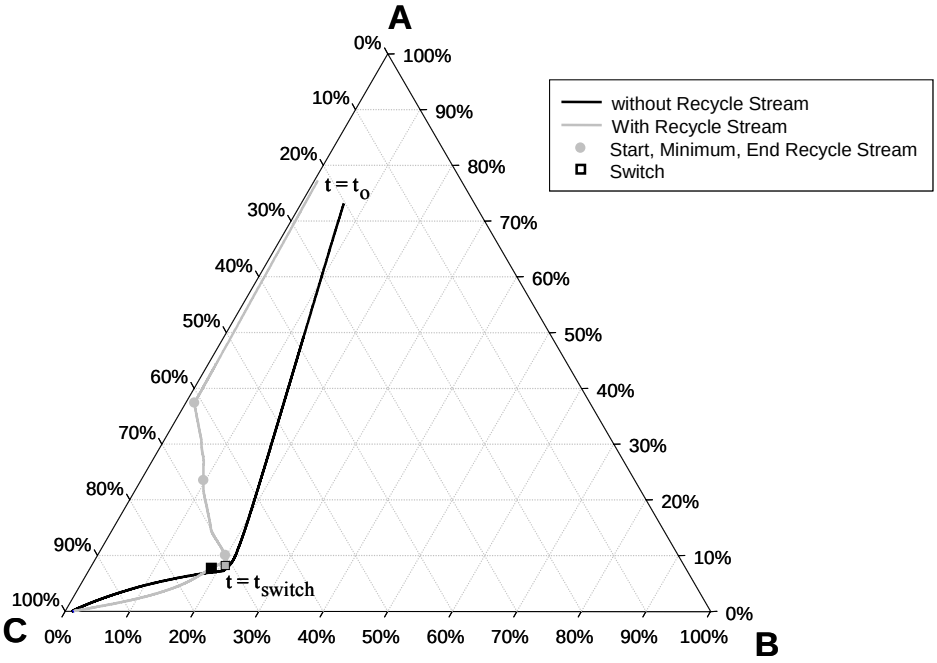

Figure 2.11: Optimal time-dependent reboiler compositions of A, B and C.

Due to the fact that in the new operation mode the off-cut of the previous batch is kept separated from the liquid mixture in the reboiler from the beginning (Fig. 2.11), it has only a little amount of component B compared to the composition in the conventional operation mode (Fig. 2.11). This leads to the fact that at the beginning the VLE interaction between component A and C is more dominating, which causes an increasing volatility and thus a much lower reflux rate is required for fulfilling the purity constraint of the first fraction. However, due to the decreasing amount of component A in the column during the batch, the supply of the recycle flow has to begin at a certain time as a compensation of this decrease. On the other hand, the content of the feed tank has to be depleted early enough before the first switch to the next fraction, in order to provide sufficient time for separating the remaining amount of component A, which originally comes from the recycle flow.

The computed trajectory of the recycle flow indicates two physical phenomena. With the proceeding time, by means of a decreasing amount of component A, a stronger compensation and thus a larger feed flow rate is desired. On the other hand, large liquid flows in later time intervals also cause a longer period until the first switch to the next fraction can be done due to the higher amount of liquid in the column, which needs to be distilled. Thus, the optimized curve indicates a trade-off between those two contradictory requirements. However, it should be noted that the shape of the curve does not have a strong impact on the targets of this optimization problem.

2.3.2 Uncertainty consideration

In the previous section, a deterministic optimization approach has been applied using a model with constant parameters. However, since the operation policy developed is highly sensitive towards variations in model parameters and boundary conditions, the product specifications may be violated when implementing it in the real plant. Furthermore, the amount and composition of the initial charge are also uncertain, since they are mostly product outputs of the previous batch. Therefore, simulation studies have been exemplarily carried out in order to determine the influence of uncertainty consideration on the distillate composition of the lightest product A which is constrained to 99 weight percent during the first main-cut period. For the purpose of this analysis, the values of the concentration of the heaviest component D in the reboiler, the initial charge, the concentration of component B in the recycle feed amount as well as the recycle feed amount, all of them at the beginning of the batch run, were varied around their expected values (from the deterministic optimization) (Fig. 2.12a).

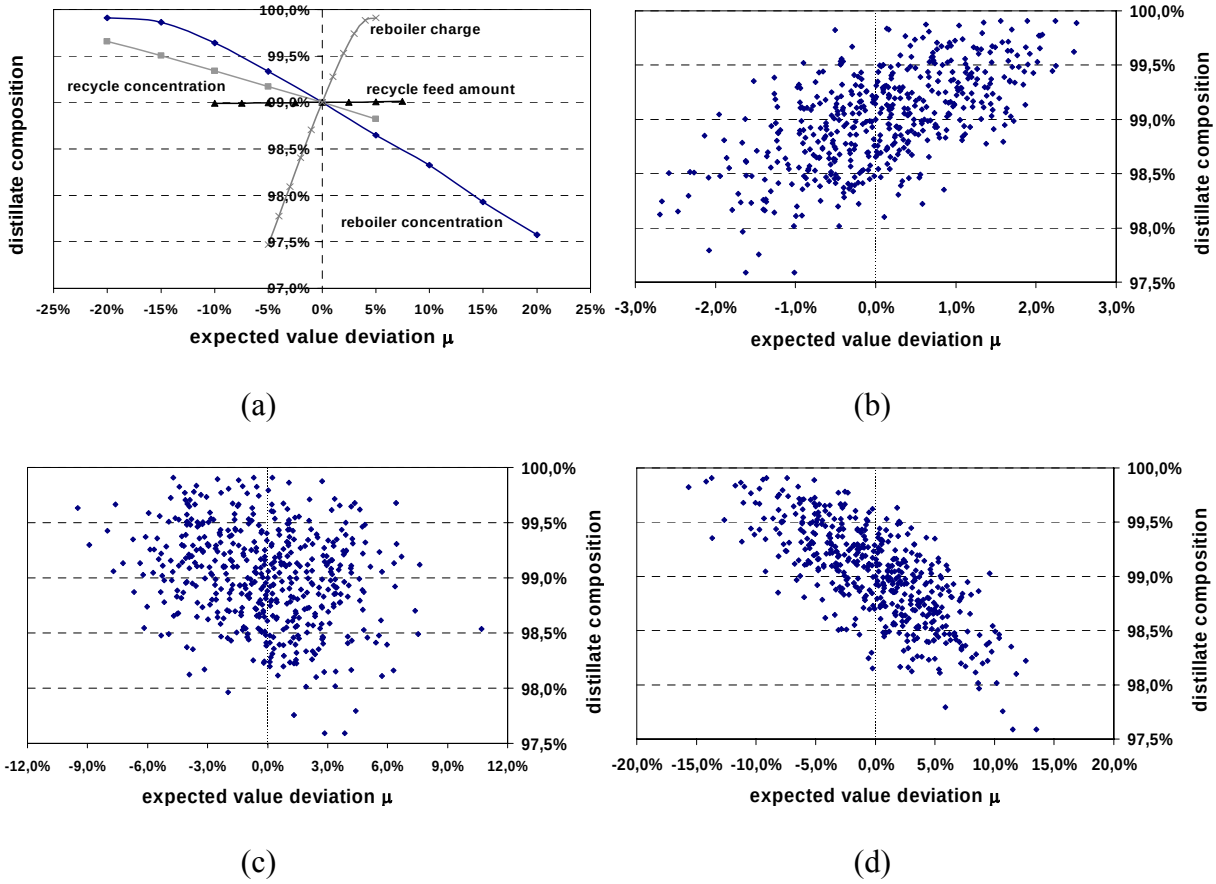

Figure 2.12: Changes of the distillate composition with regard to component A based on (a) simulation studies and stochastic simulations with a standard deviation of (b) initial charge 1%; (c) component B in the recycled off-cut 3%; (d) component D in the reboiler 5%.

Moreover, in order to analyze the reliability of the developed operation policies, stochastic simulations have been performed. For this purpose, the Monte Carlo sampling approach using the nominal operating policies was used to obtain representative values from the uncertain space. Thus, the uncertain inputs such as amount and composition of both the initial charge and the recycled off-cut are considered in this case study (Fig. 2.12a-d).

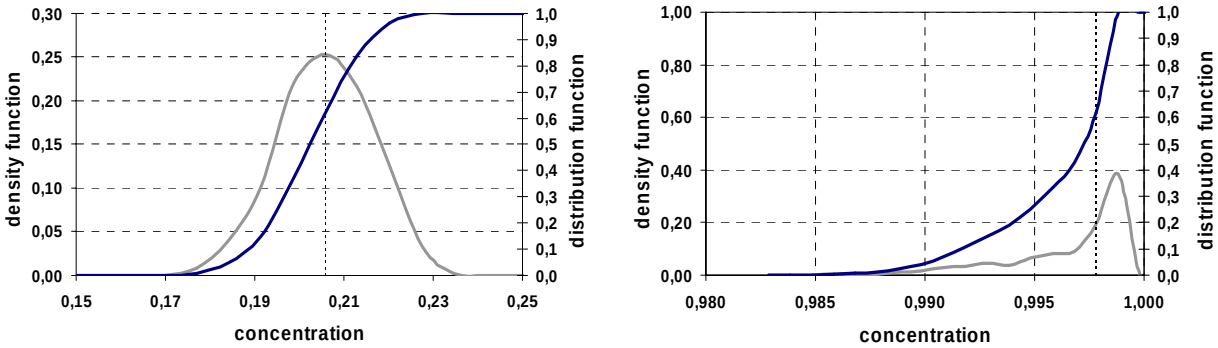

Figure 2.13: Stochastic distribution of the product concentration A (*right*) in the first main-cut with uncertain initial concentration of D in the reboiler (*left*).

The uncertainties are assumed to be normally distributed. From the results with 500 sample points it can be seen that the risk of violating the purity restriction in the first main-cut is 47,4%. The presented results show that although the expected values of the product concentrations and objective are satisfactory, there is a significant variability resulting in a high probability that the product quality constraint will be violated. Thus, the optimal policies from the deterministic optimization can not be reliable. From Figure 2.13, it can clearly be recognized that although the uncertain input is assumed to be normally distributed the output distribution is not. This effect is due to the nonlinear propagation of the random input.

2.4 Summary

In any decision-making process where the data or information upon which decisions are based, may be uncertain and where the entailing strategy involves a significant risk, quantitative risk and uncertainty evaluation studies provide an important aid. As shown in this chapter, for a quantitative understanding and control of e.g. time varying phenomena in process systems, it is essential to relate the observed dynamic behavior to mathematical models. These models usually depend on a number of parameters whose values are unknown or with insufficient accuracy. Furthermore, often only a part of the system's dynamics can be measured. Therefore, a plant model unavoidably involves uncertainties. In this context, a further challenging problem constitutes the potential effect of variability on process decisions which is an inherent property of the system and cannot usually be reduced but compensated.

Accounting for this problem, characterizations of uncertainty sources enhance the value of model predictions by allowing for quantification of their precision, thus increasing the confidence one can have in them. However, the available data quality and quantity in order to build process models has a large impact on the uncertainty connected with their parameters. Experimental data may enclose outliners, systematic errors and erroneous data. An illustrative example on a batch distillation column has demonstrated that an optimal operation based on nominal parameters values can result in poor overall performance when evaluated accounting for typical uncertainty levels. The underlying model parameter uncertainty has a detrimental impact on the process performance. More significantly, the probability of the constraint being violated in this case is almost 50%. In order to reduce this risk and increase the robustness of the operating policies, a quantitative measure of the trade-off between compliance with the constraints and the objective function is required. Thus, in this thesis, new approaches to robust optimization are introduced in order to improve the objective function performance while keeping the probability of a constraint violation within defined bounds.

Chapter 3

Optimization under Uncertainty

Studies on dynamic optimization have recently been performed to aid in optimal design and operation of increasingly intensified processes. Most of these studies make use of deterministic nonlinear optimization methods which have been developed to solve large-scale NLP problems (Gill et al., 1997; Leineweber et al., 1997). They can be classified into simultaneous and sequential approaches. The former includes all discretized variables usually resulting in extremely large NLP problems (Steinbach, 1995; Cervantes and Biegler, 1998, Biegler et al., 2002). The latter approach uses a simulation step to compute the dependent variables. Therefore, only the independent variables are explicitly varied by NLP (Logsdon and Biegler, 1992; Vassiliadis et al., 1994a,b; Li et al., 1998; Feehery and Barton, 1998). These approaches have been successfully applied to a number of primarily continuous chemical processes e.g. reactive, azeotropic distillation or batch distillation (Logsdon and Biegler, 1989; Li et al., 1998; Wendt et al., 2000). However, the optimization results are only applicable when the real operating conditions are precisely reflected in the optimization.

It is well-known that chemical processes are subject to large uncertainties. In industrial practice, they are usually compensated for by using conservative decisions like over-design of process equipment or overestimation of operational parameters based on worst case assumptions about the uncertain parameter values, which leads to significant deterioration of the economic performance (objective function) in an optimization problem. Moreover, uncertainties may have detrimental effects on equipment decisions, plant operability, and economical analysis. Thus, systematic methods are required for integrating the available stochastic information about the uncertain parameters into the process operation decisions. These uncertainties or disturbances are often multivariate and correlated stochastic sequences which have an influence like a chain-effect to each unit operation of the production line. In order to reduce it to a negligible level, a complex modeling effort is required. In the last

decades, aiming to determining the optimal operational policies, many deterministic model-based approaches have been developed. Depending on the objectives, decision variables, and constraints, in the literature the deterministic optimization problems are formally classified as Linear Programming (LP), Non-Linear Programming (NLP), Integer Programming (IP), Mixed Integer LP (MILP), and Mixed Integer NLP (MINLP). However, due to the high modeling complexity, model-based approaches are often impossible to implent in industrial processes. Furthermore, uncertainty compensation without considering its properties has several drawbacks. Optimization under uncertainty tackles these problems. It is a kind of optimization where the stochastic properties of the uncertainties in the data and the model are taken into account and is popularly known as Stochastic Programming or stochastic optimization problems. "*Stochastic Programming handles mathematical programming problems where some of the parameters are random variables...*" (Prekopa, 1995) is one of the simpler definitions given for Stochastic Programming. In this terminology, stochastic refers to the randomness, and programming refers to the mathematical programming techniques like LP, NLP, IP, MILP, and MINLP. There are probabilistic techniques like Simulated Annealing and Genetic Algorithms; these techniques are occasionally referred to as the stochastic optimization techniques because of the probabilistic nature of the search algorithms. In general, however, Stochastic Programming and stochastic optimization imply optimal decision making under uncertainties (Diwekar, 2003).

In the literature, several methods have been proposed to systematically solve optimization problems which are subject to uncertainties. The techniques introduced differ in the way of handling the sources of uncertainty or solving resulting problems. Rather than giving an exhaustive literature review, the reader is recommended to read the comprehensive reviews of Grossmann et al. (1983), Pistikopoulos (1995), Wets (1996), Diwekar (Review), Sahinidis (2004). In this chapter an overview of the approaches applied to this problem, in particular, some of the more recent articles in this area are highlighted.

The first works which considered stochastic uncertainties aimed at formalizing the calculation of safety factors commonly used to over-design the processes. Several works appeared in the 1970s including the ones by Takamatsu et al. (1973) and Damert et al., 1977, in which the distinction between design and control variables for continuous plants was proposed for the first time. This distinction becomes important with the assumption that the control variables can be adjusted for any possible realizations of the uncertainty. However, a large amount of the process system engineering literature refers to optimization under uncertainty concerning the simultaneous equipment design and control variable optimization. Nevertheless, the emphasis of previous studies has been mainly on process design problems. Parameter design methods were used to obtain robust design in the sense of reducing the source of variations.

Generally, the literature on optimization under uncertainty very often divides the problems into categories such as "*wait and see*", and "*here and now*". The former implies the assumption of perfect control adjustment and its validity extent relies on both the ability to detect feedback information from on-line process measurements, and the quality of the available information for close-loop control adjustment of certain process variables. For the latter when design and control variables are considered equivalent only a single operating policy is obtained in a conservative "here and now" strategy. Thus, the relative influence of different parameter values and disturbances on the optimization problem must be defined.

3.1 "Wait and See" Approach

The approach in which the expected values of the uncertainties are used in the problem formulation is the so-called "*wait-and-see"* approach. In such cases when additional measurement information on the uncertainties becomes available, the operational strategy can be adapted. But, since the complete future trajectory will rarely be known, this approach is not suitable for handling time-varying disturbances. Thus, provided that the main uncertainties are associated with time-invariant parameters e.g. raw materials, measurements of the parameter values following this approach may provide the required variable values. However, the wait and see strategy is, in fact, compensation without considering the uncertainty properties and has several drawbacks. First of all, the actions taken are always a *posteriori*. Second, a feedback control can not ensure constraints on open-loop variables. Moreover, these input uncertainties will propagate through the process to the output variables e.g. composition, temperature. In particular, for *nonlinear* processes the analytical description of the output distribution is challenging. In this case the term *nonlinear* describes the relationship between the uncertain and the constrained variables. As described in Chapter 2, a scheme of simulation with sampling can address this issue. In "wait and see" one waits until an observation is made on the random elements, and then solves the deterministic problem. This strategy requires the solution of several deterministic optimization problems in order to find the deterministic optimal decision at each scenario or random sample. The problem can be formulated in the following general form:

$$\begin{aligned} \max_{\mathbf{u}} \quad & \mathcal{F} = f(\mathbf{u}, \boldsymbol{\xi}) \\ s.t \quad & g_i(\mathbf{u}, \boldsymbol{\xi}) = 0 \\ & h_i(\mathbf{u}, \boldsymbol{\xi}) \geq 0 \end{aligned} \tag{2.1}$$

Since the optimization procedure is repeated for each uncertain variable sample, as shown in Figure 2.1, $\boldsymbol{\xi}$ corresponds to the vector of uncertain variable values associated with each scenario or sample. Thus, a probabilistic representation of the uncertain output can be obtained. The shortcoming of this strategy is that it can not guarantee satisfaction of inequality constraints.

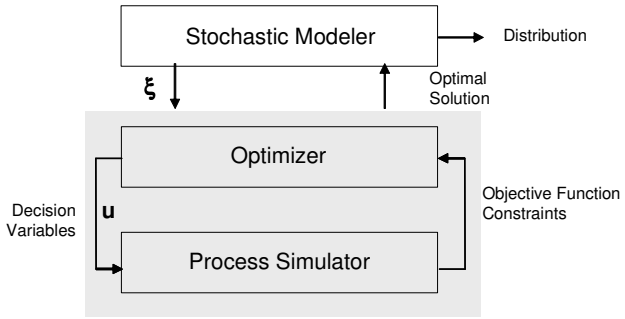

Figure 2.1: "Wait and See" Approach.

3.2 "Here and Now" Approach

While in the "*wait-and-see"* approach the expected values of the uncertainties are used in the problem formulation, the "*here-and-now"* problems involve the definition of both the objective function and constraints in terms of some probabilistic representation (e.g. expected

value, variance, fractiles). Furthermore, the decision variables are detached from the uncertain parameters (see Figure 2.2). A "*here-and-now"* problem can be formulated as follows:

$$\begin{aligned} \max_{\mathbf{u}} \quad & \mathfrak{P} = \mathcal{P}_1\left(\mathfrak{g}_1\left(\mathbf{u}, \boldsymbol{\xi}\right)\right) \\ s.t \quad & \mathcal{P}_1\left(\mathfrak{g}_1\left(\mathbf{u}, \boldsymbol{\xi}\right)\right) = 0 \\ & \mathcal{P}_2\left(\mathfrak{h}_1\left(\mathbf{u}, \boldsymbol{\xi}\right) \geq 0\right) \geq \alpha \end{aligned} \tag{2.2}$$

As can be seen in (2.2), in contrast to the deterministic optimization problem, the stochastic optimization considers the probabilistic functionals of the objective function and the constraints. Thus, $\mathcal{P}$ represents a cumulative distribution functional e.g. expected value, variance, or fractiles. To solve such problems the use of stochastic modeling is required. Accordingly, an iterative probabilistic model representing the discretized uncertainty space is embedded in the simulation stage as a part of the optimization loop in Figure 2.2.

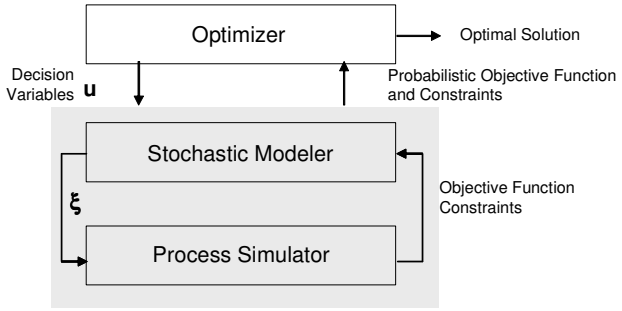

Figure 2.2: "*Here and Now"* Approach.

As described above, both "*here and now"* and "*wait and see"* problems require representation of uncertainties in the probabilistic space and then propagate these uncertainties through the model to obtain the probabilistic representation of the output. This is the main dissimilarity between stochastic and deterministic optimization problems. In process system engineering there are many problems which incorporates both "*here and now"*, and "*wait and see"* problems. After separating the decisions into these two categories, a coupled approach can be employed to deal with such problems. However, stochastic or deterministic uncertainty models are only approximations of the true model-plant mismatch, the potential variability and disturbances of the true process. The selection of a realistic type and extent of uncertainty representations require a careful judgment in order to properly balance robustness and conservativeness regarding the extent of probable variations. A general optimization or control problem under uncertainty can be formulated mathematically as:

$$\min_{\mathbf{u}(t,\xi),\, \mathbf{v}(\xi),\, t_C} \mathrm{E}_{\xi}\left\{ f\left(\dot{\mathbf{x}}, \mathbf{x}, \mathbf{y}, \mathbf{u}, \mathbf{v}, t_C; \xi\right)\right\} = \min_{\mathbf{u}(t,\xi),\, \mathbf{v}(\xi),\, t_C} \int_{\xi \in \Xi} \rho(\xi)\, f\left(\dot{\mathbf{x}}, \mathbf{x}, \mathbf{y}, \mathbf{u}, \mathbf{v}, t_C; \xi\right) d\xi$$

subject to

$$\begin{aligned} & \mathbf{g}\left(\dot{\mathbf{x}}, \mathbf{x}, \mathbf{y}, \mathbf{u}, \mathbf{v}, t; \xi\right) = 0, \\ & \mathbf{h}\left(\dot{\mathbf{x}}, \mathbf{x}, \mathbf{y}, \mathbf{u}, \mathbf{v}, t; \xi\right) \geq 0, \\ & \mathbf{i}_0\left(\dot{\mathbf{x}}(0), \mathbf{x}(0), \mathbf{y}, \mathbf{u}(0), \mathbf{v}, t_C; \xi\right) = 0, \\ & \mathbf{u}_{\min} \leq \mathbf{u} \leq \mathbf{u}_{\max}\,,\; t_0 \leq t_C \leq t_f \end{aligned} \tag{2.3}$$

where $E_\xi\{f\}$ is the expected value of f, $\rho(\xi)$ the joint probability density function, f the performance metric to be optimized, $\mathbf{x}$ the differential state variables, $\dot{\mathbf{x}}$ their derivatives with respect to the time, $\mathbf{y}$ are the algebraic state variables, $\mathbf{u}$ the time-dependent optimization variables, $\mathbf{v}$ the time-invariant optimization variables, t the time, t_C certain time points, t_f the final time, ξ the uncertain model parameters over the domain Ξ. The equality constraints $\mathbf{g}$ generally represent the process model equations but also could similarly include constraints on the process or performance requirements. The inequality constraints $\mathbf{h}$ are usually related to equipment limitations, safety regulations, environmental and/or performance restrictions (e.g. product purity specifications). The initial conditions of the system are represented by $\mathbf{i_0}$.

The explicit uncertainty consideration adds information to the optimization model (2.3) and allows for more robustness. However, a stochastic optimization problem has to be solved whose complexity may exceed the complexity of the corresponding deterministic problem by several orders of magnitude. The uncertainty nature, which includes time dependency or its significance in the objective and the constraints, leads to different classes of stochastic optimization formulations. Several approaches have been suggested to formulate and solve this problem (2.3), differing in how uncertainty is handled in the constraints as well as in the objectives that may include process flexibility, profitability, and/or robustness. In general, the direct solution can be problematic due to the difficulty in both evaluating the integral over the uncertain parameter space and ensuring feasibility of the inequalities for all parameter realizations.

Concerning the way uncertainty is handled, the choice of uncertainty characterization is the key assumption which strongly influences the way in which several methods have been developed. Most of the methods proposed to solve optimization problems under uncertainty, especially those relating to design, are associated with the verification of the limits of the feasible region. Other methods allow some infeasibility during the optimization procedure without explicit definition of the feasible region. Generally speaking, three different approaches can be distinguished:

1) ***Scenario-based optimization approach***, where the uncertainty is described by a set of scenarios (periods) using either discrete probability distributions or the discretization of continuous probability functions, and the expectation of a certain performance criterion, resulting in a multi-period optimization problem.

In scenario-based optimization, the bounded uncertain parameters are discretized into multiple intervals such that each individual interval represents a scenario associated with an approximated discrete distribution. Each instance is called a *scenario* and represents a certain event or history of events. The scenarios may be determined *explicitly* if the most important combinations of parameter values and the associated probabilities are known a priori. Otherwise, they may be generated *implicitly* by assuming probability density functions for the parameters. Generally, this leads to a multi-period optimization problem that provides the solution which is feasible only for the selected points. Thus, the feasibility problem must be then tested over the entire range of parameters. In precise probabilistic terms this corresponds to a discrete distribution given by a finite probability. Scenario-based approaches provide a simple way to incorporate uncertainty. But, they inevitably expand the size of the problem significantly as the number of scenarios augments exponentially with the number of uncertain parameters. This main drawback prevents the application of these approaches to solve practical problems with large numbers of uncertain parameters. The problems following the scenario-based approach can be formulated as follows:

$$\min_{\mathbf{u}(t,\xi),\,\mathbf{v}(\xi),\,t_C} E_\xi\left\{f\left(\dot{\mathbf{x}},\mathbf{x},\mathbf{y},\mathbf{u},\mathbf{v},t_C;\xi\right)\right\} = \min_{\mathbf{u}(t,\xi),\,\mathbf{v}(\xi),\,t_C} \sum_{k=1}^{n_k} \gamma_k f_k\left(\dot{\mathbf{x}}_k,\mathbf{x}_k,\mathbf{y}_k,\mathbf{u},\mathbf{v},t_C;\xi_k\right)$$

subject to

$$\begin{aligned} &\mathbf{g}_k\left(\dot{\mathbf{x}},\mathbf{x},\mathbf{y},\mathbf{u},\mathbf{v},t;\xi\right)=0, && \forall k=1..n_k \\ &\mathbf{h}_k\left(\dot{\mathbf{x}},\mathbf{x},\mathbf{y},\mathbf{u},\mathbf{v},t;\xi\right)\geq 0, && \forall k=1..n_k \\ &\mathbf{i}_{0k}\left(\dot{\mathbf{x}}(0),\mathbf{x}(0),\mathbf{y},\mathbf{u}(0),\mathbf{v},t_C;\xi\right)=0, && \forall k=1..n_k \end{aligned} \tag{2.4}$$

Where n_k is the number of scenarios and γ_k is the associated probability of occurrence of scenario k. It should be noted that in (2.4), **u** is independent of the scenarios (here and now) but that dependence on the scenarios could be included to represent "wait and see" case where controls are optimally adjusted for the values of the uncertain parameters realized in the scenario (Samsatli et al., 1998). Abel and Marquardt, (2000) integrated time varying uncertainties into the robust optimization of operating policies for dynamic hybrid (discrete continuous) systems. Optimization approaches are formulated considering uncertainty not only in model parameters but also in the process model structure resulting either in a single-level or bi-level scenario integrated optimization problems. These provide solutions comprising different control policies for the various switching times, at which the model structure and uncertainty may change.

2) ***Stochastic approach***, where the uncertainty parameters are described through a joint probability density function (PDF) resulting in a stochastic optimization problem.

3) ***Parametric approach***, where the problem is solved parametrically in the space of the uncertain parameters.

More recently, parametric programming ideas have been developed for design and control under uncertainty (Acevedo and Pistikopoulos, 1998; Vassiliadis and Pistikopoulos, 1998; Bansal et al. 2000, 2002). The advantage of such a technique is that it is based on building a complete map of the model validity for different regions of uncertainty. This can then be used to generate all optimal solutions as the operating conditions change as a function of the parameter uncertainty. For nonlinear models including integer variables, the parameter programming solution approaches have been limited to either only a single model uncertain parameter or several uncertain parameters varying in a single direction. Dua and Pistikopuolos, (2002) proposed algorithms for the solution of multiparametric mixed-integer nonlinear optimization (mp-MINLP) problems where uncertainty is described by a set of parameters constrained by lower and upper bounds. However, the computational complexity of these approaches is expected to increase significantly with the problem dimensionality. Thus, the implementation as well as the application of such algorithms to large-scale processes, and their extension for the case of non-convex models is still a challenge to be tackled.

To summarize, the first two approaches are based on the characterization of the uncertain parameter space by considering either discrete scenarios or stochastic distributions, assuming that some information regarding the uncertainty is provided either in the form of the expected nominal point or specific range of values or in the form of a probability distribution function. In the parametric framework, no assumptions are made about the uncertainty model and the objective function is obtained as a function of the uncertain parameters over the demand space.

The direct solution of (2.3) is challenging due to the difficulty in both evaluating the integral over the uncertain parameter space and guaranteeing feasibility of the inequalities for all parameter realizations. In process systems engineering, the previous studies on decision making under uncertainty have been concerned mainly with process design problems. One of the most widely used techniques is two-stage programming (Liu and Sahinidis 1998, Petkov and Maranas 1998, Dantzig, 1955, Pistikopoulos, 1995b). In this method, the decision variables of the problem are divided into two sets. The *first-stage* variables (design variables) are to be predetermined before the actual realization of the uncertain parameters ("*here-and-now"* decisions). Therefore, when the random events occur, further design or operational policy improvements can be made by opting for, at a certain cost, the values of the *second-stage*, or *recourse*, variables ("*wait-and-see"* decisions). Conventionally, the second-stage variables are understood as corrective measures or recourse against any infeasibility arising due to a particular realization of uncertainty. However, the second-stage problem may also be an operational-level decision problem following a first-stage strategy and the uncertainty realization. Due to uncertainty, the second-stage cost is a random variable. The idea is to select the first-stage variables so that the sum of the first-stage costs and the expected value of the random second-stage recourse costs are minimized. The concept of recourse has been applied to linear, integer, and nonlinear programming (Sahinidis, 2004).

The application of these different approaches to solving design optimization problems under uncertainty has extensively been studied in chemical engineering in the past. Grossmann et al. (1983) discussed two types of generic problems: *i) design for a fixed degree of flexibility*, where the plant is designed for optimal economics while maintaining operational feasibility over a pre-specified range of parameter uncertainties and *ii) design for an optimal degree of flexibility*, where a design is optimized for both economics and flexibility, and the degree of flexibility is quantified using a flexibility index. Usually, the problem of parameter uncertainty is then reduced to the general form of a multi-period problem. The discretization of the parameter uncertainty space generates a set of scenarios for which the control variables can be modified separately. The assumption is that during operation there is enough information about the uncertain parameters to optimally adjust the control variables. For a cost objective function $\mathcal{C}$, the two-stage problem can be defined as follows:

$$
\begin{aligned}
&\text{Design stage:}\\
&\min_{\mathbf{d}} \mathrm{E}_{\mathbf{p}\in\mathcal{R}}\left\{\mathcal{C}(\mathbf{d},\mathbf{p})\right\}\\
&\text{Operation stage:}\\
&\mathcal{C}(\mathbf{d},\mathbf{p}) = \min_{\mathbf{u}} \mathcal{C}(\mathbf{d},\mathbf{u},\mathbf{p})\\
&\text{s.t} \quad \mathfrak{g}(\mathbf{u},\mathbf{p}) = 0\\
&\qquad \mathfrak{h}(\mathbf{u},\mathbf{p}) \geq 0
\end{aligned}
\tag{2.5}
$$

The feasible region $\mathcal{R}$ associated with the design is given by,

$$\mathcal{R}(\mathbf{d}) = \left\{\mathrm{p} \middle| \forall \mathrm{p} \in \mathcal{R}\, \exists \mathbf{u} : \mathfrak{f}(\mathbf{d},\mathbf{u},\mathbf{p}) \leq 0\right\}$$

The original equalities and inequalities are reformulated into a new vector, $\mathfrak{f}$, which expresses the implicit elimination of the state variables from the problem. Two-stage design and operation approaches have extensively been investigated for the case of *deterministic* parameter uncertainties characterized by bounded ranges. Thus, a variety of technique have

been proposed to solve (2.5). However, the uncertain parameters are discretized into a number of values from their overall uncertainty description. These discretized points are often set to lower and upper bounds based on their confidence intervals. In other works, the discretized points are selected from elliptical joint confidence regions or the confidence region is derived from a likelihood ratio test (Seber and Wild, 1989; Gallant, 1987; Rooney and Biegler, 2001). This leads to a multi-period (or multi-stage) optimization problem which is solved in the design stage,

$$\begin{aligned} &\min_{\mathbf{d},\mathbf{u}_k} \left\{ f_0(d) + \sum_{k=1}^{\mathcal{K}} \omega_k f_k(\mathbf{d},\mathbf{u}_k,\mathbf{p}_k) \right\} \\ &\text{s.t.} \quad \mathfrak{f}(\mathbf{d},\mathbf{u}_k,\mathbf{p}_k) \le 0 \\ &\qquad \mathbf{p} \in P = \left\{ \mathbf{p} \middle| \mathbf{p}^{LB} \le \mathbf{p} \le \mathbf{p}^{UB} \right\} \\ &\qquad \forall k = 1,\cdots,\mathcal{K} \end{aligned} \tag{2.6}$$

where f_0 represents a function for the fixed costs, the index k is an index for the periods (scenarios), and ω_k stands for weight factors related to the discrete probability of each period. The vector of uncertain parameters **p** is characterized by bounded values, in a region P, which contains all possible parameter values. Based on this formulation, several methods with application to distillation sequence synthesis, design feasibility under uncertainty, multi-period multi-product batch plants, and scheduling under uncertainty have been developed to solve multi-period design optimization problems (Grossmann and Sargent, 1978, Varvarezos et al., 1992, Subrahmanyan et al., 1994). Its solution results in designs which are optimal only for the discretized values of the parameters, but not necessarily feasible for the entire region of uncertainty. Thereby a feasibility problem is solved to verify if the design variables operate over the entire uncertain region,

$$\mathfrak{X}\left(\mathbf{d}^*\right) = \max_{\mathbf{p}\in P} \min_{\mathbf{u}} \max \mathfrak{h}\left(\mathbf{d}^*,\mathbf{u},\mathbf{p}\right). \tag{2.7}$$

where the equality constraints, $\mathfrak{g}$, have been implicitly incorporated into the inequality constraints, $\mathfrak{h}$. If $\mathfrak{X}(\mathbf{d}^*) \le 0$ for all $\mathbf{p} \in P$, the current design d^* is feasible. If $\mathfrak{X}(\mathbf{d}^*) \ge 0$ for any $\mathbf{p} \in P$, then the current design is not feasible. The solution of (2.7) results in critical values of the parameters where the greatest constraint violation arises because there is a part of P where the feasible region is an empty space. The discretization can then be updated with the critical point, and another multiperiod design problem is solved. Numerous methods have been proposed to solve (2.7) comprising vertex search methods where the critical points are located at vertices of the hyper-rectangle (Halemane and Grossmann, 1983; Swaney and Grossmann, 1985a,b; Ostrovsky et al., 1994) and the active-set approach with mixed-integer strategies suggested by Grossman and Floudas (1987) based on the a priori identification of potential active constraints which limit flexibility. Ostrovsky et al. 1998, 2000 proposed different bounding methods for the flexibility analysis with which a global solution can be found based upon global search using interval analysis. However, a steady-state point of view renders an unrealistic control schema and thus a dynamic analysis is required. Dimitriadis and Pistikopoulos (1995) formulate the dynamic feasibility problem and define a dynamic flexibility index which represents the largest scaled deviation of the uncertain parameter profile that the design can tolerate while remaining feasible within the time horizon considered. The main drawbacks are the high dimension of the optimization even for small problems, and the assumption that the direction in the parameter space for the critical point

locations is either known or is at one of the vertices in the dynamic hyper-rectangle. This concept was then extended to stochastic flexibility for linear dynamic systems (Adjiman et al., 1998, Floudas et al., 2001).

3.3 Probabilistic feasible region approaches

In order to determine the feasible region more accurately than the hyper-rectangle characterization, different methods using probabilistic definitions of uncertainty have been proposed to incorporate a superior information level in comparison to bounded range deterministic uncertainty approaches. Thus, stochastic flexibility analysis procedures were defined which are concerned with the probability of feasible operation for linear systems, subject to combined discrete and continuous uncertainties, described by probability distributions, but for which perfect control is assumed. Straub and Grossmann (1993) presented an approach to assess the stochastic flexibility of a nonlinear convex feasible region under perfect control. For a total of P uncertain parameter dimensions the stochastic flexibility index $\mathcal{SFI}$ is defined as,

$$\mathcal{SFI} = \int_{p_1^{LB}}^{p_1^{UB}} \int_{p_2^{LB}(p_1)}^{p_2^{UB}(p_1)} \cdots \int_{p_P^{LB}(p_1,p_2,\ldots,p_{P-1})}^{p_P^{UB}(p_1,p_2,\ldots,p_{P-1})} \rho(\mathbf{p})\, dp_P \cdots dp_2\, dp_1 \,. \tag{2.8}$$

Where p^{UB} and p^{LB} are the upper and lower bounds of each dimension in the feasible region using Gaussian quadrature in order to approximate the multidimensional integral and $\rho(\mathbf{p})$ represents the truncated correlated joint distribution function. The application of this approach to design optimization involves again iteration between a design *master problem* and an operating stage *sub-problem* (2.6) applying Benders decomposition. (Birge and Louveaux, 1997, Dantzing and Wolfe, 1960, Benders, 1962). For continuous probability distributions, this challenge has been primarily tackled through the explicit/implicit discretization of the probability space for approximating the multivariate probability integrals. The key advantage of these methods lies in the fact that they are largely insensitive to the type of probability distribution. However, this suffers from the disadvantage that there is an exponential increase in the number of optimization sub-problems that must be solved as the numbers of uncertain parameters and quadrature points increase. Further, $\mathcal{SFI}$ produces feasible designs, but they may show larger quadratic loss. More efficient integration techniques than Gaussian quadrature have also been proposed in the context of stochastic design optimization, such as specialised quadratures and cubatures for normally distributed parameters (Bernardo et al., 1999) and efficient sampling techniques (Diwekar and Kalagnanam, 1997; Acevedo and Pistikopoulos, 1998). However, the difficulty in applying these methods to stochastic flexibility evaluation is that each of the generated integration points has to be tested to verify if it lies within the feasible region of uncertain parameters. Balasubramanian and Grossmann (2003) proposed a multiperiod MILP model for scheduling multistage flowshop plants with uncertain processing times. They developed a special branch and bound algorithm with an aggregated probability model. The scenario-based approaches provide a straightforward way to implicitly incorporate uncertainty. However, they inevitably enlarge the size of the problem significantly as the number of scenarios increases exponentially with the number of uncertain parameters.

3.4 Limited feasibility approaches

Guaranteeing feasibility in a specified region is a significant issue in the conceptual problems described above. However, it is also relevant to examine the effect that regions of non-feasibility may have on the process. Therefore, an approach which provides optimal decisions under the complete uncertainty range while capturing the dynamic/continuous and non-linear effects modelled in the system of integrated processes is required. Thus, in other approaches the solutions do not assure feasibility over a specified feasible region but rather allow partial feasibility by evaluating the entire uncertainty space. For this purpose, a stochastic constraint is defined as a constraint on a stochastic variable. This constraint may be considered as either *hard* or *soft*, for which some violations are accepted at the expense of a finite penalty (Saltelli et al., 2000). Such approaches are different from flexibility analyses which deal with all constraints as hard and attempt to ensure feasibility within the uncertainty space presupposing perfect control when reacting to uncertainties.

To consider the uncertainties, the optimization problem needs to be reformulated. Thus, some special manipulations of the objective function and the equality and inequality constraints have to be performed in order to relax the stochastic problem to an equivalent NLP problem so that it can be solved by the existing optimization routines. If the uncertain variables have an impact on the objective function, it is usually re-formulated as the expected value of the objective function. To handle the inequality constraints under uncertainty during the time horizon, two main types of formulation have been used: the **recourse formulation** and the formulation of **chance constraints**. In the recourse formulation, violation of the constraints is allowed, but penalized through a penalty term in the objective function. This approach is recommendable when the objective function and constraint violations can be described by the same measurement, for example process planning problems under demand uncertainties (Subrahmanyam et al., 1994; Liu and Sahinidis, 1996; Ahmed and Sahinidis, 1998; Gupta and Maranas, 2000). In many situations, however, a model of such costs is not easily available or even nonsense, particularly, when the constraints are related to safety requirements (Kall and Wallace, 1994). In such situations, it is preferable not to compensate for violations by additional costs, but rather to maintain a high level of reliability which implies that the constraints have to be satisfied at least with a probability exceeding some pre-selected value.

Several methods following this strategy have been developed. An efficient approach for linear systems was proposed with stochastic variables with correlated multivariate normal distribution, where numerical integration and sampling methods are combined (Prékopa, A., 1995). Chance constraints can indeed be computed by sampling techniques. The disadvantage of sampling approaches is that some effort might be wasted on optimizing when approximation is not accurate (Birge and Louveaux, 1997). In nearly all stochastic optimization problems, the major bottleneck is the computational time spent for generating and evaluating probabilistic functions of the objective function and constraints. The accuracy of the estimates for the actual mean and the actual standard deviation is particularly important so as to obtain realistic estimates of any performance or economic parameter. However, this accuracy is dependent on the number of samples and the number of uncertain parameters. The number of samples required for a given accuracy in a stochastic optimization problem depends upon several factors, such as the type of uncertainty, and the point values of the decision variables (Painton and Diwekar, 1995). Especially for optimization problems, the number of samples required also depends on the location of the trial point solution in the optimization space. Therefore, the selection of the number of samples for the stochastic optimization procedure is a crucial and challenging problem. A combinatorial optimization

algorithm that automatically selects the number of samples and provides a trade-off between accuracy and efficiency is presented in Ki-Joo Kim and Diwekar (2002).

3.5 Summary

The outcomes of a deterministic optimization allow neither variation nor uncertainty on operating conditions or model parameters. However, the existence of these uncertainties raises questions like: *what will be the corresponding probability of complying with the constraints in accordance with the optimized operating policy?* Handling uncertainty, which becomes important especially in the presence of constraints on quality and safety, has not been adequately addressed and constitutes the main bottleneck in applying optimization techniques to real processes. Therefore, in relation to the uncertainties involved in an optimization problem formulation, the comparative improvement obtained due to a specified economic objective function may occasionally become irrelevant, i.e. safety, reliability, and operability are often decisive, and more crucial than an economic objective (Grossmann and Morari (1984)). However, these issues are more complex and there is no established approach to assess them appropriately. Thus, in most cases, conservative decisions based on heuristics or empirical rules have to be made which might lead to a substantial profit decrease. Therefore, systematic methods to evaluate the relationship between profitability and reliability of a planned operation are required.

Chapter 4

Chance-Constrained Optimization under Uncertainty

Decision making inherently involves consideration of uncertain outcomes. While computational advances in mathematical programming tools have aided decision making in many areas, their greatest impact may lie in enhancing decision making under uncertainty through stochastic programming. During the past decades several approaches have been suggested to address these problems in a systematic manner. One method of stochastic programming is the probabilistic or chance-constrained approach which focuses on the reliability of the system, i.e., the system's ability to remain feasible in an uncertain environment. The reliability is expressed as a minimum requirement on the probability of satisfying the system constraints. Specifically in complex dynamic systems there are parameters which are usually uncertain, but may have a large impact on the objective function and the constrained outputs. Thus, the challenge is to make decisions *a priori* for the future operation. However, the decision is needed to be made before the realization of the uncertain inputs. Consequently, under the consideration of uncertainties, the following questions should be answered: 1) how to achieve an economically optimal operation? 2) How to ensure that the constraints of the output variables are satisfied? 3) How to prevent the propagation of the uncertainties to downstream processes? And 4) how to design a proper feedback control system? A stochastic programming problem has to be defined and solved to answer these questions.

Most current approaches to process operations are based either on heuristic rules or on deterministic optimization, where uncertainties of several parameters are not taken into consideration. Furthermore, in many practical applications, only some uncertain outputs involved and critical for quality control are available for online measurement. For instance, pressure, and temperature in non-isothermal reactors are usually available online while the values of product and reactant concentrations are often available only via off-line analysis. Alternatives such as state observers are commonly developed using a perfect knowledge of the system parameters. Especially concerning process kinetics, it is difficult to define error bounds and there is often a large uncertainty on these parameters. However, uncertainty in the model parameters can result in a possibly large bias in the estimation of the unmeasured states. The limiting factors are, among others, the insufficient knowledge about the key parameters, which are often estimated with poor initial guesses; the large variations of the operating conditions, in particular, in batch processes; the inaccuracy of the initial estimates of the state variables; the imprecise measurement of the feed amount and its composition. To deal with the unknown operating reality a priori, two general methods are known in the chemical industry: the worst-case and the base-case analysis have commonly been used

(Fig.4.1). The latter uses the nominal (mean) values of the uncertain variables. However, the realized values will deviate from the nominal values and hence the constraints will almost certainly be violated by the implementation of the developed strategies for the base-case analysis. The former is a simplistic approach to the evaluation of feasibility and robustness. It is usually applied to problems in which the distributions of random variables are not given. The worst case analysis assumes that all fluctuations may occur simultaneously in the worst possible combinations. The worst case analysis is conservative since it is unlikely that the worst cases of variable or parameter deviations will simultaneously occur. However, in spite of the low achievable profit, worst case analysis is used widely in many areas of optimization applications due to its simplification and reliability in ensuring the constraints. It should be pointed out that operability and reliability become increasingly important issues in operations planning. In this thesis, a systematic approach is formulated which is capable of evaluating the balance between the reliability and the profitability of future operations.

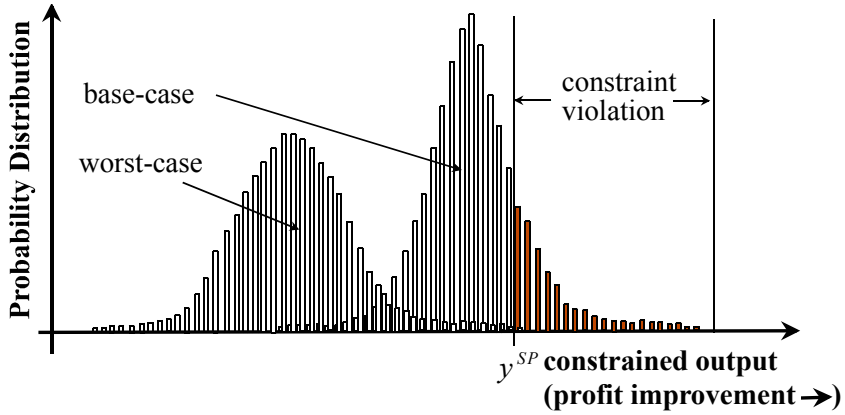

Figure 4.1: Trade-off between reliability and profitability

A general optimization or control problem under uncertainty can be formulated as:

$$\min f\left(\mathbf{x}, \mathbf{y}, \mathbf{u}, t_C; \boldsymbol{\xi}\right)$$

subject to

$$\begin{aligned} &\mathbf{g}\left(\dot{\mathbf{x}}, \mathbf{x}, \mathbf{y}, \mathbf{u}, t; \boldsymbol{\xi}\right) = 0, \\ &\mathbf{h}\left(\dot{\mathbf{x}}, \mathbf{x}, \mathbf{y}, \mathbf{u}, t; \boldsymbol{\xi}\right) \geq 0, \\ &\mathbf{i}_0\left(\dot{\mathbf{x}}(0), \mathbf{x}(0), \mathbf{y}, \mathbf{u}(0), t_C; \boldsymbol{\xi}\right) = 0, \\ &\mathbf{u}_{\min} \leq \mathbf{u} \leq \mathbf{u}_{\max}, \; t_0 \leq t_C \leq t_f \end{aligned} \tag{4.1}$$

where f is a time-variant performance criterion to be optimized, $\mathbf{x} \subseteq \Re^n$ are the differential state variables, $\dot{\mathbf{x}}$ their derivatives with respect to the time, $\mathbf{y} \subseteq \Re^L$ the constrained output variables, $\mathbf{u} \subseteq \Re^M$ the optimization variables, t time, t_C certain time points, t_f the final time, and $\boldsymbol{\xi} \subseteq \Re^S$ the uncertain parameters over the domain Ξ. The equality constraints $\mathbf{g} \subseteq \Re^{n+L}$ generally represent the process model equations but could also include constraints on the process or performance requirements. The inequality constraints $\mathbf{h} \subseteq \Re^L$ are usually related to equipment limitations, safety, and/or performance restrictions. The known initial conditions of the system are represented by $\mathbf{i_0}$. Since the model involves uncertainty, process output predictions are also uncertain. This uncertainty in process output predictions may result in

adverse violation of the constraints on the outputs. Thus, incorporation of uncertainty into the output constraints is necessary and needs to be included in the problem formulation. As stated in chapter 2, a process may have internal uncertainties such as inaccurate model parameters or structures and external uncertainties such as unknown future feedstock or atmospheric temperature. While internal uncertainties have been well studied in the framework of robust control in the past (Morari and Zafiriou, 1989, Calafiore and Dabbene, 2000), external uncertainties have not been much emphasized.

The characteristics of these uncertainties or stochastic disturbances, such as mean, covariance or probability distribution, may be known from statistical analysis of historical data (Bates, 1988). In chemical process industry, there has been an explosive growth of computer-based process monitoring systems in the last two decades, which makes it relatively easy to acquire process data to be utilized for distribution analysis (Jobson, 1991, Pearson, 2001). The probability distribution of different variables may have different forms. Normal distribution is frequently regarded as an appropriate assumption for some uncertain variables in the engineering practice. This statement is based on the central limit theorem (Loeve, 1963; Maybeck 1995). Accordingly, if a random variable is generated as the sum of effects of different independent random parameters, the variable distribution is close to a normal distribution regardless of the distribution of each individual parameter. However, stochastic optimization with even an approximated distribution is more reliable than a deterministic optimization. In most of the examples in this thesis, uncertainties are assumed to have a correlated multivariate normal distribution, but the developed approach does not depend on the particular distribution form.

In problem (4.1) the major difficulty is due to the optimal decisions that have to be made prior to the observation of random parameters. Thus, it is complicated to find any decision which would definitely exclude later constraint violations caused by unexpected random effects. As explained in chapter 3, in several cases such constraint violation can be balanced afterwards by some compensating decisions made in the second stage. In many applications, however, compensations simply do not exist (e.g. safety restrictions) or can not be modeled in any reasonable way. In such circumstances, a chanced-constrained approach can be used in which a user-defined probability level of holding the constraints (reliability of being feasible) will be ensured. A generic way to express such probabilistic or chance constraint as an inequality is

$$\mathcal{P}r\left(\mathfrak{h}\left(\mathbf{u},\boldsymbol{\xi}\right)\geq 0\right)\geq \alpha \tag{4.2}$$

Here, $\mathbf{u}$ and $\boldsymbol{\xi}$ are decision and random vectors, respectively. The value $\alpha \in [0, 1]$ represents the probability level. Since α can be defined by the user, it is possible to select different levels and make a compromise between the objective function value and the risk of constraint violation. In engineering practice, inequality constraints are commonly used to specify or restrict some of the output variables:

$$y_i^{min} \leq y_i\left(\mathbf{u},\boldsymbol{\xi}\right) \leq y_i^{max} \qquad i=1,\ldots,L \tag{4.3}$$

where y_i^{min} and y_i^{max} are the output lower and upper bounds, respectively. In continuous operation they may be constant, while in batch processes they are often time dependent. Holding these constraints is usually critical to ensure safe production. The proposed approach in this thesis relies on formulating output constraints of the form (4.3) as chance constraints as follows:

$$\Pr\left\{ y_i^{min} \le y_i(\mathbf{u},\boldsymbol{\xi}) \le y_i^{max} \right\} \ge \alpha_i, \qquad i = 1,\ldots,L \tag{4.4}$$

With this representation single probabilities of ensuring each inequality for $t \in [t_0, t_f]$ will be calculated. In this form, different confidence levels can be assigned to different outputs based on their requirements. Another form is the joint chance constraint, where all inequalities are included in the probability computation and they must be satisfied simultaneously with the one given confidence (probability) level

$$\Pr\left\{ y_i^{min} \le y_i(\mathbf{u},\boldsymbol{\xi}) \le y_i^{max}, \quad i = 1,\ldots,L \right\} \ge \alpha \tag{4.5}$$

The values of α or α_i are not given by explicit formulae, but are rather defined as probabilities of some implicitly defined regions in the space of the random parameter ξ in such a way that the feasible region will shrink if the confidence level is increased, which will imply a more conservative decision. Increasing the confidence levels brings, however, the advantage of keeping a more stable operation, but it may reduce the system flexibility with respect to the variations required. Moreover, as shown in Figure 4.2, the feasibility in (4.5) includes the one in (4.4), but the reverse is not true.

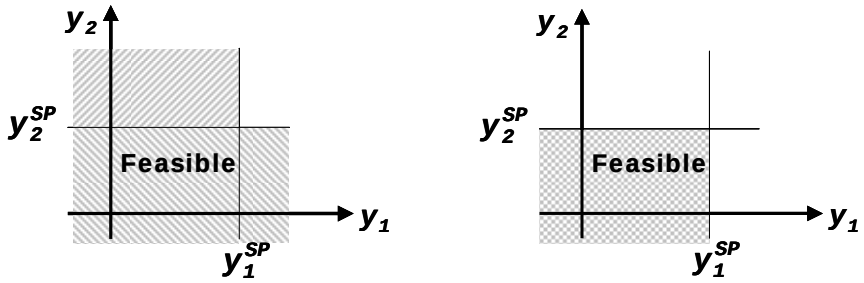

$\Pr_i\left\{ y_i(\mathbf{u},\boldsymbol{\xi}) \le y_i^{SP} \right\} \quad i = 1,2$ $\qquad$ $\Pr\left\{ y_i(\mathbf{u},\boldsymbol{\xi}) \le y_i^{SP}, i = 1,2 \right\}$

Figure 4.2: Reliability in single and joint constraints

The main challenge in chance-constrained programming lies in calculating values, gradients and possibly Hessians of these functions. However, the main difference between (4.4) and (4.5) lies in their reliability. While a joint chance constraint demands for reliability in the output feasible region as a whole, single chance constraints call for reliability in the individual output feasible region. Thus, single chance constraints may be used when some output constraints y_i^{SP} are more critical than the others. On the other hand, if the constraints are related to safety considerations in process operation, a joint constraint may be more convenient. With regard to the equalities in problem (4.1) which are the process model equations, they have to be satisfied with any realization of the uncertain variables. Moreover, the effect of the model equations is a projection of the space of the random variables $\boldsymbol{\xi}$ as inputs to a space of state variables **x** and **y**, with given controls **u**. Consequently, the equalities can be eliminated through an integration of the equations in the space of the uncertain variables. This means that the sequential approach may be suitable for solving such problems.

To treat the objective function in problem (4.1), minimizing the expected value and the variance of the objective function has usually been adopted (Darlington et al., 1999):

$$\min E\left[f(\mathbf{x},\mathbf{u},\boldsymbol{\xi}) \right] + \omega D\left[f(\mathbf{x},\mathbf{u},\boldsymbol{\xi}) \right] \tag{4.6}$$

E and *D* are the operators of expectation and variation, respectively, ω is a weighting factor between the two terms. By these means, the objective function in (4.1) is now relaxed to a deterministic function through these two operators. Accordingly, a general chance constrained problem can be formulated starting from (4.1) by using the objective function from (4.6) and (4.4) as the single constraints

$$
\begin{aligned}
&\min \mathrm{E}\left[\mathrm{f}\left(\mathbf{x}, \mathbf{y}, \mathbf{u}, \mathrm{t_C}; \boldsymbol{\xi}\right)\right] + \omega \mathrm{D}\left[\mathrm{f}\left(\mathbf{x}, \mathbf{y}, \mathbf{u}, \mathrm{t_C}; \boldsymbol{\xi}\right)\right] \\
&\text{s.t.} \quad \mathbf{g}(\dot{\mathbf{x}}, \mathbf{x}, \mathbf{y}, \mathbf{u}, \mathrm{t}, \boldsymbol{\xi}) = 0, \\
&\qquad \Pr_{\mathrm{i}}\left\{\ \mathbf{h}\left(\dot{\mathbf{x}}, \mathbf{x}, \mathbf{y}, \mathbf{u}, \mathrm{t}; \boldsymbol{\xi}\right) \geq 0\right\} \geq \alpha_{\mathrm{i}} \quad \mathrm{i} = 1, \cdots, \mathrm{L} \\
&\qquad \mathbf{i}_0\left(\dot{\mathbf{x}}(0), \mathbf{x}(0), \mathbf{y}, \mathbf{u}(0), \mathrm{t_C}; \boldsymbol{\xi}\right) = 0, \qquad , \\
&\qquad \mathbf{y}_{\min} \leq \mathbf{y} \leq \mathbf{y}_{\max}, \\
&\qquad \mathbf{u}_{\min} \leq \mathbf{u} \leq \mathbf{u}_{\max}, \\
&\qquad \mathrm{t_0} \leq \mathrm{t_C} \leq \mathrm{t_f}
\end{aligned}
\tag{4.7}
$$

or (4.5) as the joint constraint.

$$
\begin{aligned}
&\min \mathrm{E}\left[\mathrm{f}\left(\mathbf{x}, \mathbf{y}, \mathbf{u}, \mathrm{t_C}; \boldsymbol{\xi}\right)\right] + \omega \mathrm{D}\left[\mathrm{f}\left(\mathbf{x}, \mathbf{y}, \mathbf{u}, \mathrm{t_C}; \boldsymbol{\xi}\right)\right] \\
&\text{s.t.} \quad \mathbf{g}(\dot{\mathbf{x}}, \mathbf{x}, \mathbf{y}, \mathbf{u}, \mathrm{t}, \boldsymbol{\xi}) = 0, \\
&\qquad \Pr\left\{\ \mathbf{h}_{\mathrm{i}}\left(\dot{\mathbf{x}}, \mathbf{x}, \mathbf{y}, \mathbf{u}, \mathrm{t}; \boldsymbol{\xi}\right) \geq 0, \quad \mathrm{i} = 1, \cdots, \mathrm{L}\right\} \geq \alpha \\
&\qquad \mathbf{i}_0\left(\dot{\mathbf{x}}(0), \mathbf{x}(0), \mathbf{y}, \mathbf{u}(0), \mathrm{t_C}; \boldsymbol{\xi}\right) = 0, \\
&\qquad \mathbf{y}_{\min} \leq \mathbf{y} \leq \mathbf{y}_{\max}, \\
&\qquad \mathbf{u}_{\min} \leq \mathbf{u} \leq \mathbf{u}_{\max}, \\
&\qquad \mathrm{t_0} \leq \mathrm{t_C} \leq \mathrm{t_f}
\end{aligned}
\tag{4.8}
$$

Therefore, as shown in Figure 4.3, such problems can be classified based on process properties, uncertainties and constraint forms. According to the Figure 4.3, there are total 16 different possible formulations.

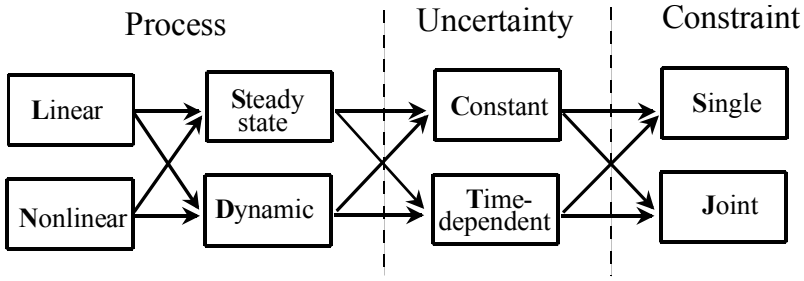

Fig. 4.3: Classification of chance constrained problems

The solution of such problems will lead to an expected optimal value of the objective function by searching for the decision in a feasible region defined with a given confidence level to be held. The initial letters are used to denote the different chance constrained problems. For example, a linear steady state process with constant uncertainties under single chance constraint is called an LSCS problem. It is interesting to note that LSTS and NSTS can be solved separately for each interval, while for LSTJ and NSTJ (a quasi-dynamic problem) the whole time horizon should be considered. To solve such problems with an existing

optimization routine, the probability of holding the constraints has to be computed. Moreover, the gradients of the probability function with respect to the controls are also required. Since α can be defined by the user, it is possible to select different levels and make a compromise between the objective function value and risk of constraint violation. Different problems have different degrees of complexity for computing these values, which will be discussed in the following sections.

For numerical optimization under probabilistic constraints, some methods have been developed and applied to several disciplines like finance and management (Prekopa, 1995; Uryasev, 2000). In chemical process operations few applications have been made (Arellano-Garcia et al., (1998, 2003b), Henrion et al., 2001). It has been used by, for instance, Maranas (1997) for molecular design and Petkov and Maranas (1997) for planning und scheduling of multiproduct batch plants. Additionally, several studies on model predictive control using probabilistic programming have been carried out for linear processes (Schwarm and Nikolaou, 1999; Wendt, 2005).

4.1 Linear Chance-Constrained Optimization

Due to the fact that the uncertain input variables propagate through the process to the output variables, the outputs are also uncertain. However, chance constrained linear problems can be relatively easily treated and have some affable properties. In systems where the relation between uncertain input and constrained variables is linear, the type of the multivariate probability distribution function of the constrained output is the same as the one of the uncertain input. Thus, in this thesis, *linear* systems are referred to those systems where a linear relation between the uncertain variables and the constrained variables exists. Optimization of linear steady state systems (LSCS and LSCJ) under constant uncertain variables has been well studied (see Kall and Wallace, 1994). Especially in production planning, linear input-output relations for process modeling are commonly used. In the framework of a *linear* system, the solution of a problem with *single* chance constraints can be derived simply by a coordinate transformation. For the cost minimization, a generic chance constrained linear optimization problem under single probabilistic constraints can be formulated as follows:

$$
\begin{aligned}
\min \quad & \mathrm{Cost} = \sum_{j=1}^{m} c_j^u u_j - \sum_{i=1}^{n} c_i^y y_i \\
\text{s.t.} \quad & \Pr\left\{ u_r^\theta = \sum_{i=1}^{n} a_{r,i} y_i + \sum_{j=1}^{m} b_{r,j} u_j \le \theta_r \right\} \ge \alpha_r \quad r = 1,\ldots,R \\
& \Pr\left\{ y_s^\xi = \sum_{i=1}^{n} d_{s,i} y_i + \sum_{j=1}^{m} e_{s,j} u_j \ge \xi_s \right\} \ge \alpha_s \quad s = 1,\ldots,S \\
& y_{min} \le y \le y_{max}, \\
& u_{min} \le u \le u_{max}
\end{aligned}
\tag{4.9}
$$

The formulation under one joint probabilistic constraint is,

$$\begin{aligned}
&\min \ \text{Cost}=\sum_{j=1}^{m} c_j^u u_j - \sum_{i=1}^{n} c_i^y y_i \\
&\text{s.t.} \quad \Pr\left\{\begin{array}{ll} u_r^\theta = \sum_{i=1}^{n} a_{r,i} y_i + \sum_{j=1}^{m} b_{r,j} u_j \le \theta_r, & r=1,\ldots,R \\ y_s^\xi = \sum_{i=1}^{n} d_{s,i} y_i + \sum_{j=1}^{m} e_{s,j} u_j \ge \xi_s, & s=1,\ldots,S \end{array}\right\} \ge \alpha \\
&\qquad y_{\min} \le y \le y_{\max}, \\
&\qquad u_{\min} \le u \le u_{\max}
\end{aligned} \tag{4.10}$$

Where $\mathbf{c}^u, \mathbf{c}^y$ represent the price vectors of the input and output variables, and {**a**, **b**, **d**, **e**} are vectors with known parameters. The inflow and outflow random vectors are $\boldsymbol{\theta} \subseteq \Re^R$ and $\boldsymbol{\xi} \subseteq \Re^S$, respectively. Additionally $\mathbf{u} \subseteq \Re^m$ and $\mathbf{y} \subseteq \Re^n$ are vectors of the input and output decision variables. It should be noted that the uncertain variables have no impact on the objective function and the feasible region of problem (4.10) is a subset of that of problem (4.9). In order to characterize the uncertain variables, it will be assumed that the probability density function of θ and ξ are identified as $\rho_r(\theta_r)$ and $\rho_s(\xi_s)$. According to this, the probability distribution functions are then expressed as,

$$\begin{aligned}
\Phi_r(u_r^\theta) &= \Pr\left\{\theta_r \le u_r^\theta\right\} = \int_{u_r^\theta}^{\infty} \rho_r(\theta_r)\, d\theta_r \quad r=1,\ldots,R \\
\Phi_s(z_s^\xi) &= \Pr\left\{\xi_s \le y_s^\xi\right\} = \int_{-\infty}^{y_s^\xi} \rho_s(\xi_s)\, d\xi_s \quad s=1,\ldots,S
\end{aligned} \tag{4.11}$$

Where Φ is the probability distribution function with $\Phi(\infty)=1$. The form of probability distribution of different variables can vary. In some cases the uncertain variables may be uncorrelated; however, they usually have correlations. Therefore, this leads to the formulation of a unified density function for the correlated variables,

$$\begin{aligned}
\Phi_r(u_r^\theta) &= \int_{-\infty}^{\infty} d\theta_1 \cdots \int_{-\infty}^{u_r^\theta} d\theta_r \cdots \int_{-\infty}^{\infty} \rho(\theta_1,\cdots,\theta_R)\, d\theta_R \quad r=1,\cdots,R \\
\Phi_s(z_s^\xi) &= \int_{-\infty}^{\infty} d\xi_1 \cdots \int_{z_1^\xi}^{\infty} d\xi_s \cdots \int_{-\infty}^{\infty} \rho(\xi_1,\cdots,\xi_S)\, d\xi_S \quad s=1,\cdots,S
\end{aligned} \tag{4.12}$$

4.1.1 Relaxation of the probabilistic constraints

The solution strategy to probabilistic programming problems defined in (4.9) and (4.10) is to relax them into equivalent deterministic problems, so that they can be solved by available commercial optimization tools. Based on (4.11) and (4.12), problem (4.9) can be converted into the following equivalent deterministic problem

$$
\begin{aligned}
\min \quad & \text{Cost} = \sum_{j=1}^{m} c_j^u u_j - \sum_{i=1}^{n} c_i^y y_i \\
\text{s.t.} \quad & \sum_{i=1}^{n} a_{r,i} z_i + \sum_{j=1}^{m} b_{r,j} u_j \le \Phi_r^{-1}(1-\alpha_r) \quad r = 1,\cdots,R \\
& \sum_{i=1}^{n} d_{s,i} y_i + \sum_{j=1}^{m} e_{s,j} u_j \ge \Phi_s^{-1}(\alpha_s) \quad s = 1,\cdots,S \\
& y_{min} \le y \le y_{max}, \\
& u_{min} \le u \le u_{max}
\end{aligned}
\tag{4.13}
$$

The operator Φ^{-1} represents the inverse function of (4.11) and (4.12). Its value is only dependent on the specified confidence levels. However, this is a linear programming (LP) problem that can be solved with any LP solver such as the simplex method. Unfortunately, the relaxation of problems under a joint probabilistic constraint (4.10) leads to a NLP problem. If the uncertain variables are uncorrelated, the joint probability is merely the multiplication of the single probabilities. Thus, problem (4.10) can be reformulated as

$$
\begin{aligned}
\min \quad & \text{Cost} = \sum_{j=1}^{m} c_j^u u_j - \sum_{i=1}^{n} c_i^y y_i \\
\text{s.t.} \quad & \prod_{r=1}^{R} \left[1 - \Phi_r \left(\sum_{i=1}^{n} a_{r,i} y_i + \sum_{j=1}^{m} b_{r,j} u_j \right) \right] \prod_{s=1}^{S} \Phi_s \left(\sum_{i=1}^{n} d_{s,i} y_i + \sum_{j=1}^{m} e_{s,j} u_j \right) \ge \alpha \\
& y_{min} \le y \le y_{max}, \\
& u_{min} \le u \le u_{max}
\end{aligned}
\tag{4.14}
$$

In order to solve problem (4.14), a NLP solver such as SQP is required. Furthermore, it should be noted that the gradient of a probability function is the value of the density function. In the case of correlated uncertain variables, as denoted in (4.12), the joint probability results in an integration form, and thus problem (4.10) is then,

$$
\begin{aligned}
\min \quad & \text{Cost} = \sum_{j=1}^{m} c_j^u u_j - \sum_{i=1}^{n} c_i^y y_i \\
\text{s.t.} \quad & \left[\int_{u_1^\theta}^{\infty} d\theta_1 \cdots \int_{u_R^\theta}^{\infty} \rho(\theta_1,\cdots,\theta_R) d\theta_R \right] \left[\int_{-\infty}^{z_1^\xi} d\xi_1 \cdots \int_{-\infty}^{z_S^\xi} \rho(\xi_1,\cdots,\xi_S) d\xi_S \right] \ge \alpha \\
& y_{min} \le y \le y_{max}, \\
& u_{min} \le u \le u_{max}
\end{aligned}
\tag{4.15}
$$

To compute the constraint values in (4.15) a multivariate integration is necessary, which is generally complicated. However, in order to avoid the multivariate integration, marginal distributions can be used in (4.13) and (4.14) to cope with correlated uncertain variables. But, such formulation does not appropriately reproduce the real problem and thus may lead to an incorrect solution.

4.1.2 Linear steady state problem - an illustrative example

In this section a *linear* system is considered where the whole process is steady state including constant random variables, a LSCS problem. In this example, a blending problem is considered with specified outflow and uncertain inflow. Generally, given a characterization of variability in the properties comprising a blend, one may ask the following questions: how the blend quality should be expressed in terms of constraints and the probability of exceeding those constraints due to the variability in the properties? Given an explicit probabilistic description of acceptable blend quality, how can the blend be optimized to minimize the cost? What is the trade-off between different objectives for blending (e.g., minimizing expected cost, or variance? Answers to these questions can be given taking into account the probabilistic nature of the properties and the effects of changes in properties on plant performance, and cost.

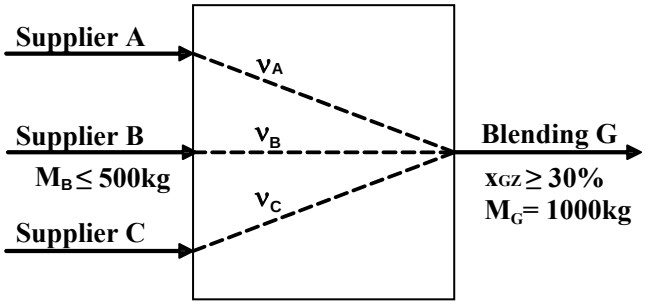

Figure 4.4: Process representation for the blending problem

Here a simplified blending problem is introduced as an illustrative example. The amounts recived from the respective suppliers to form the total blending outflow are given by ν_i. The aim of the optimization is the cost minimization of the blending process shown in Figure 4.4. The process will produce a blend product (output) by using three different suppliers A, B, C (inputs). These inputs consist of raw material as feedstock (see Table 4.1). Altogether 1000kg of mixture G, which consists of the components y and z, are to be produced at minimal costs. The content of z in the outflow should be greater than 30 percent. Furthermore, the delivery amount of the supplier B is restricted to an upper bound of 500 Kg. Its supply may have a degree of uncertainty. The suppliers A and C can provide much larger amounts as requested. On the outlet side, the blend composition can be treated as a decision variable, if it can be sold out on the market, and, thus, its amount may depend on random demands of customers. Due to changing market conditions these demands are uncertain in the planned future time horizon, but their stochastic distributions may be known or at least a range of values they may assume. For such production problems, linear input-output relations for process modeling are typically used. The parameters in these relations are supposed to be available. Hence, it is possible to represent the uncertain variables with the decision variables.

	Supplier A	Supplier B	Supplier C
Composition x_y (kg/kg)	50%	80%	90%
Composition x_z (kg/kg)	50%	20%	10%
Cost c (€/kg)	4,00	1,00	2,00

Table 4.1: The composition and the costs for the different supply quantities

The deterministic optimization problem can be defined as follows:

$$\begin{aligned} \min \text{Cost} &= f\left(v_A, v_B, v_C\right) \\ &= M_G \sum_i v_i c_i \\ \text{s.t.} \quad & \sum_i v_i = 1 \\ & \sum_i v_i x_{iz} \geq 30\% \\ & v_B M_G \leq 500\,\text{Kg} \\ & v_A, v_B, v_C \geq 0,0\% \end{aligned} \tag{4.16}$$

In Figure 4.5 the feasible region in terms of the amounts "*v*" from suppliers A and B is represented (see left Fig. 4.5), which is limited through the sum relation of v_i, the restrictions of the delivery amount of B and the blending composition x_{GZ}. Also, the objective function invariant lines are shown on the right in Fig. 4.5.

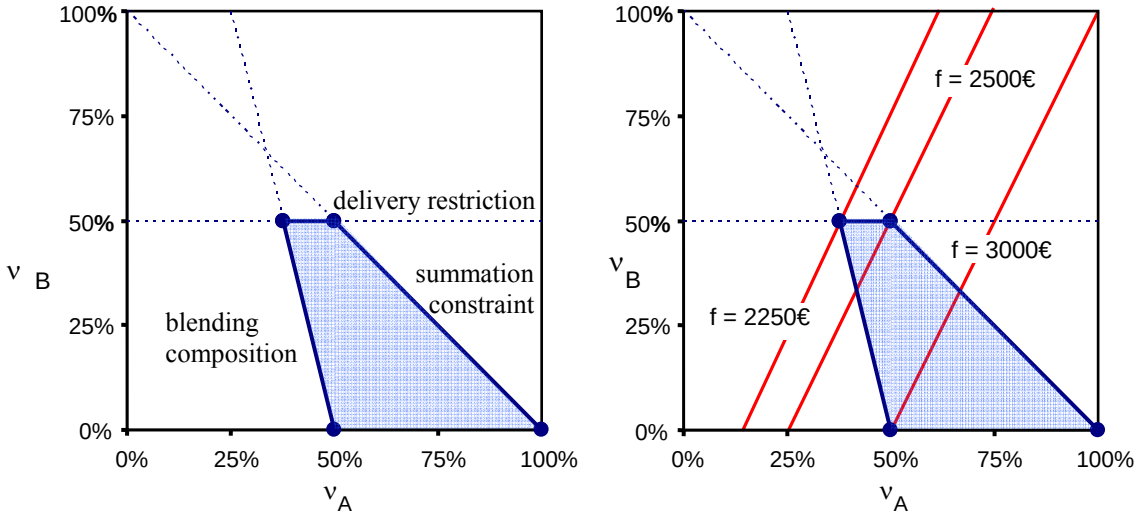

Figure 4.5: Feasible region and the objective function values

The linear deterministic optimization problem can be solved with the Simplex-Method. The solution is $v_A^* = 37,5\%$, $v_B^* = 50,0\%$, $v_C^* = 12,5\%$, $f^* = 2250\,€$. For the case of single chance constraints the original problem (4.16) can be reformulated into the following equivalent chance constrained linear problem.

$$\begin{aligned} &\min \; f(\mathbf{x}) = \mathbf{c}^T \mathbf{x} \\ &\text{s.t.} \; \Pr\left\{\mathbf{a}_i^T \mathbf{x} + b_i \geq \xi_i\right\} \geq \alpha_i \quad i = 1, \cdots, L \end{aligned} \tag{4.17}$$

where $\mathbf{x}$ is the vector of the decision variables. $\mathbf{c}, \mathbf{a}_i$ are vectors with known parameters and b_i, α_i are scalars. Defining $z_i = \mathbf{a}_i^T \mathbf{x} + b_i \geq \xi_i$ Equation (4.17) can be transformed into

$$\Pr\left\{\xi_i \leq z_i\right\} \geq \alpha_i \quad i = 1, \cdots, L \tag{4.18}$$

For the normal distribution $\xi_i \sim N(\mu_i, \sigma_i^2)$, the following expression can be derived

$$\Phi(z_i) = \Pr\left(\frac{\xi_i - \mu_i}{\sigma_i} \le \frac{z_i - \mu_i}{\sigma_i}\right) \ge \alpha_i \tag{4.19}$$

where Φ is the probability function of the standard normal distribution. From the monotonic nature of the probability function, it follows from (4.19) for each single chance constraint that:

$$z_i - \mu_i - \sigma_i \Phi^{-1}(\alpha_i) \ge 0 \tag{4.20}$$

Equation (4.20) represents a deterministic linear inequality. Thus, the optimization problem in (4.17) has been converted to a deterministic linear programming problem. In the case of an upper bound on an uncertain variable, the chance constraint is formulated as

$$\Pr\left\{z_i = a_i^T x + b_i \le \xi_i\right\} \ge \alpha_i \quad i = 1, \cdots, L \tag{4.21}$$

and thus,

$$\Pr\{\xi_i \le z_i\} = 1 - \Pr\{\xi_i \ge z_i\} \tag{4.22}$$

from which the following expression can be obtained

$$z_i - \mu_i + \sigma_i \Phi^{-1}(\alpha_i) \le 0 \tag{4.23}$$

Therefore, the stochastic optimization problem can be transformed into a deterministic LP problem at any rate. First, the problem described in equation (4.24) is solved for three different example cases,

$$\begin{aligned} \min \text{Cost} &= f(v_A, v_B, v_C) \\ &= M_G \sum_i v_i c_i \\ \text{s.t.} \quad & \sum_i v_i = 1 \\ & \sum_i v_i x_{iz} \ge \xi_1 \\ & v_B M_G \le \xi_2 \\ & v_A, v_B, v_C \ge 0,0\% \end{aligned} \tag{4.24}$$

a) $\xi_1 = 25,0\%$, $\xi_2 = 600$, $v_A^* = 22,5\%$, $v_B^* = 60,0\%$, $v_C^* = 17,5\%$, $f^* = 1850\,€$

b) $\xi_1 = 30,0\%$, $\xi_2 = 500$, $v_A^* = 37,5\%$, $v_B^* = 50,0\%$, $v_C^* = 12,5\%$, $f^* = 2250\,€$

c) $\xi_1 = 35,0\%$, $\xi_2 = 400$, $v_A^* = 52,5\%$, $v_B^* = 40,0\%$, $v_C^* = 7,5\%$, $f^* = 2650\,€$

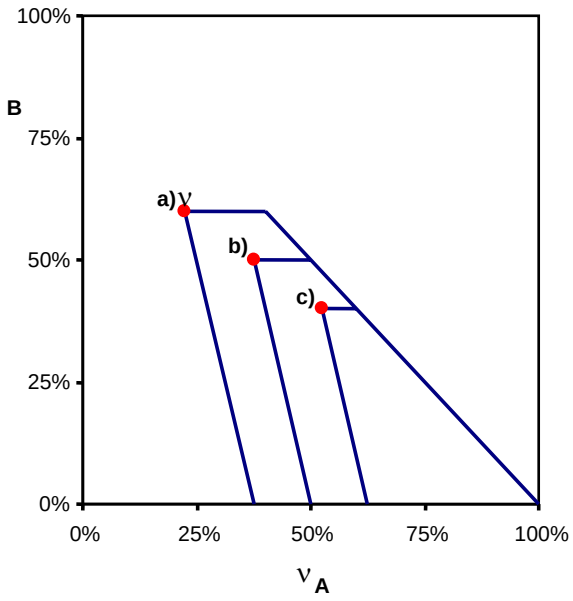

Figure 4.6: Alteration of the feasible region boundaries.

The diagram in Figure 4.6 shows the changes to the feasible region boundaries due to the different uncertainties. Thus, since the actual realization of these values can not be predicted, uncertainties are described with their probability distributions. Consequently, it will be assumed that the random variables are normally distributed, namely $\xi_1 \sim N(30\% , 5\%^2)$, $\xi_2 \sim N(500 , 150^2)$. As a result, a single chance-constrained optimization problem based on equations (4.16) and (4.20) is formulated as follows,

$$\begin{aligned} &\min \text{Cost} = M_G \sum_i v_i c_i \\ &\text{s.t.} \quad \sum_i v_i = 1 \\ &\quad \Pr\left\{\sum_i v_i x_{iz} \geq \xi_1\right\} \geq 90\% \\ &\quad \Pr\left\{v_B M_G \leq \xi_2\right\} \geq 90\% \\ &\quad v_A, v_B, v_C \geq 0,0\% \end{aligned} \quad \Rightarrow \quad \begin{aligned} &\min \text{Cost} = M_G \sum_i v_i c_i \\ &\text{s.t.} \quad \sum_i v_i = 1 \\ &\quad \sum_i v_i x_{iz} \geq 30 - 5\Phi^{-1}(0.9) \\ &\quad v_B M_G \leq 500 - 150\Phi^{-1}(0.9) \\ &\quad v_A, v_B, v_C \geq 0,0\% \end{aligned} \qquad (4.25)$$

The optimization problem formulated in equation (4.25) is again a LP problem, and its solution is $v_A^* = 58,3\%$, $v_B^* = 30,8\%$, $v_C^* = 10,9\%$, $f^* = 2858,74\,€$. It should be noted that in comparison to the deterministic solution, the total cost increases. This is obviously the price for the reliability increase.

The following diagram in Figure 4.7 shows different assumed types of probability distribution regarding the uncertain input.

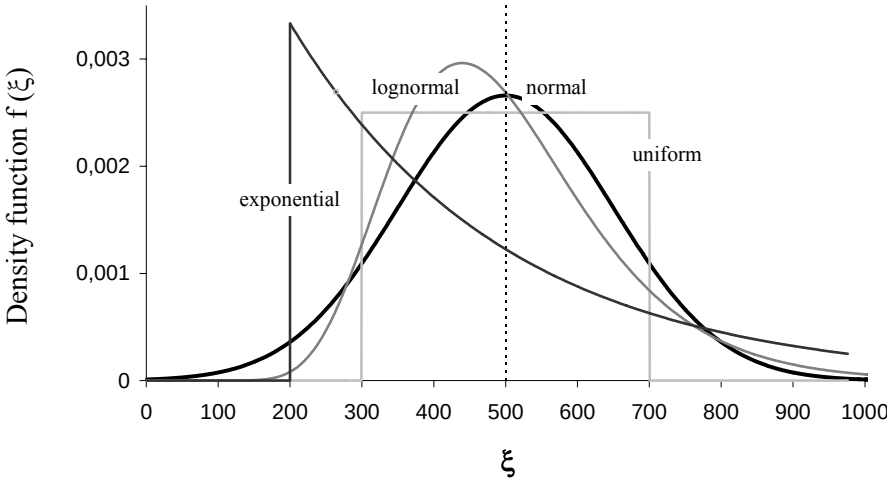

Figure 4.7: Probability densities of a continuous random variable: delivery amount of B.

Figure 4.8 shows distinct operating regions of the problem where various confidence levels are assigned to the restriction concerning the delivery amount of B. Thus, the sensitivity of the total cost to the reliability of the uncertain inflow can be analyzed considering different probability density functions. The solution provides a relationship between the objective function and the risk of constraint violation. If a higher probability level is chosen, the strategy derived will be more reliable, but the total cost will considerably increase. Consequently, a suitable confidence level should be specified with which an appropriate trade-off between objective function and reliability can be established.

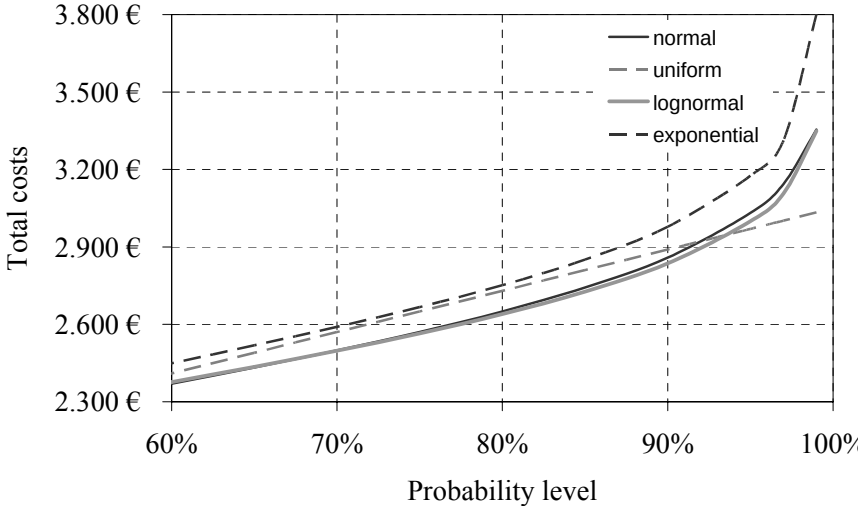

Figure 4.8: Total cost vs. probability level

The presented approach to stochastic programming under chance constraints can easily be extended to those problems (e.g. planning problems) which also include integer decision variables. These discontinuous variables can represent the case where plants in a production line will be out of operation due to, for instance, market conditions. The superstructure of a plant operation as described in Li et al., (2003) is illustrated in Figure 4.9. By means of linear mass and energy balances of the plants as well as of the process, a large-scale dynamic MILP problem under single chance constraints can be formulated. Based on the stochastic distribution of the uncertain variables, the problem is then relaxed to an equivalent

deterministic mixed-integer-linear-programming (MILP) problem. A further detailed description of the transformation can be found in Arellano-Garcia et al., 1998. Thus, the model presented above can be transferred to the following MILP problem,

$$\begin{aligned} &\min \ \mathbf{c}^T\mathbf{x} + \mathbf{d}^T\mathbf{y} \\ &\text{s.t.} \ \ \mathbf{A}\mathbf{x} + \mathbf{B}\mathbf{y} \geq \mathbf{b} \\ &\qquad \mathbf{x} \geq 0, \ \ \mathbf{y} \in \{0,1\} \end{aligned} \tag{4.26}$$

where **x** and **y** are continuous and integer decision variables, respectively. The integer variables stand for discrete decisions such as operation status of equipment, as well as capacity and design logic.. The vectors c, b, d, and the matrices A, B are known constants. The problem in (4.26) can then be solved with a standard MILP solver.

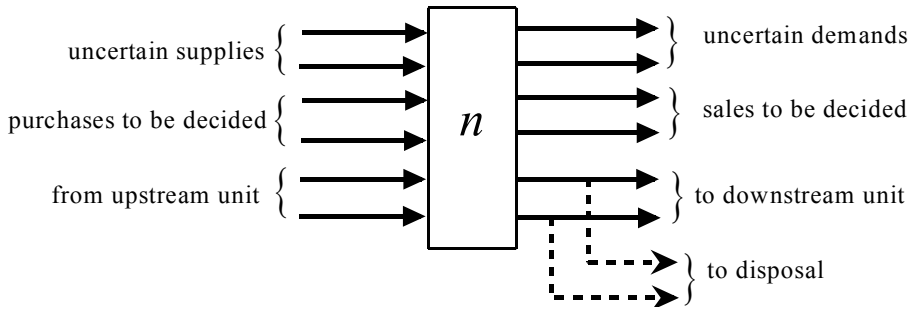

Figure 4.9: Superstructure of a plant (n=1,…,N) (Li et al., 2003).

The relaxation and solution of chance constrained optimization problems for *linear* systems under single constraints, as shown before, is not problematic. However, the introduction of joint chance constraints implies the focus on the success of operation as a whole, i.e. all the constraints must be satisfied simultaneously for the specified confidence level. Furthermore, the relaxation of the optimization problem under joint probabilistic constraints leads to a NLP problem. Similarly to equation (4.17) the problem with a joint constraint can be formulated as,

$$\begin{aligned} &\min \ \ f(\mathbf{x}) = \mathbf{c}^T\mathbf{x} \\ &\text{s.t.} \ \ \Pr\left\{\mathbf{a}_i^T\mathbf{x} + b_i \geq \xi_i, \quad i = 1,\cdots,L\right\} \geq \alpha \end{aligned} \tag{4.27}$$

The uncertain variables in the inequality constraint can be converted through standardization

$$z_i = \frac{\mathbf{a}_i^T + b_i - \mu_i}{\sigma_i} \geq \frac{\xi_i - \mu_i}{\sigma_i} = \xi_{s,i}, \quad i = 1,\ldots,L \tag{4.28}$$

Thus the chance constraint in Equation (4.27) corresponds to

$$\Phi\left(z_1,\ldots,z_L\right) = \Pr\left\{\xi_{s,i} \leq z_i, \quad i = 1,\ldots,L\right\} \geq \alpha \tag{4.29}$$

Using (4.29), it can be seen that the correlation effect between the uncertain variables can now be taken into account. The main challenge lies in the computation of the probability and their gradients. For the illustrative example in section 4.1.2, the problem with a joint constraint is formulated as:

$$\begin{aligned} &\min \text{Cost} = \mathrm{M_G} \sum_{\mathrm{i}} v_{\mathrm{i}} \mathrm{c_i} \\ &\text{s.t.} \quad \sum_{\mathrm{i}} v_{\mathrm{i}} = 1 \\ &\qquad \Pr\left\{ \begin{matrix} \sum_{\mathrm{i}} v_{\mathrm{i}} \mathrm{x_{iz}} \geq \xi_1 \\ v_{\mathrm{B}} \mathrm{M_G} \leq \xi_2 \end{matrix} \right\} \geq 90\% \\ &\qquad v_{\mathrm{A}}, v_{\mathrm{B}}, v_{\mathrm{C}} \geq 0,0\% \end{aligned} \tag{4.30}$$

Following the standardization in (4.28), the joint probability with two inequality constraints or "*events*" in (4.30) can be defined as:

$$\Phi\left(\mathrm{z}_1 \leq \xi_{\mathrm{s},1}, \mathrm{z}_2 \leq \xi_{\mathrm{s},2}\right) = \int_{\infty}^{\mathrm{z}_1} \int_{\infty}^{\mathrm{z}_2} \rho\left(\xi_{\mathrm{s},1}, \xi_{\mathrm{s},2}\right) \mathrm{d}\xi_{\mathrm{s},1}\, \mathrm{d}\xi_{\mathrm{s},2} \tag{4.31}$$

$$= \frac{1}{2\pi\sigma_1\sigma_2\sqrt{(1-\mathrm{r}_{12}^2)}} \int_{-\infty}^{\mathrm{z}_1} \int_{-\infty}^{\mathrm{z}_2} \exp\left[-\frac{1}{2(1-\mathrm{r}_{12}^2)} \left(\frac{(\xi_1-\mu_1)^2}{\sigma_1^2} - 2\mathrm{r}_{12} \frac{(\xi_1-\mu_1)(\xi_2-\mu_2)}{\sigma_1\sigma_2} + \frac{(\xi_2-\mu_2)^2}{\sigma_2^2} \right) \right] \mathrm{d}\xi_1 \mathrm{d}\xi_2$$

The resulting probability can then be computed through numerical integration. Thus, for the bivariate standard normal distribution in (4.31) the next equation can be used

$$\frac{\partial \Phi\left(\mathrm{z}_1, \mathrm{z}_2\right)}{\partial \mathrm{z}_1} = \Phi\left(\frac{\mathrm{z}_2 - \mathrm{r}_{12}\mathrm{z}_1}{\sqrt{1-\mathrm{r}_{12}^2}} \right) \rho\left(\mathrm{z}_1\right) \tag{4.32}$$

The joint probability gradients are computed through evaluation of the probability function Φ and the density function ρ of each uncertain variable. Consequently, the gradient with respect to the decision variables **x** in (4.27) is computed by

$$\frac{\partial \Pr}{\partial \mathrm{x_i}} = \frac{\partial \Phi\left(\mathrm{z}_1, \mathrm{z}_2\right)}{\partial \mathrm{z}_1} \frac{\partial \mathrm{z}_1}{\partial \mathrm{x_i}} + \frac{\partial \Phi\left(\mathrm{z}_1, \mathrm{z}_2\right)}{\partial \mathrm{z}_2} \frac{\partial \mathrm{z}_2}{\partial \mathrm{x_i}} \tag{4.33}$$

Based on the mathematical derivation above, the formulated optimization problem in (4.27) can then be solved with a NLP solver. Following (4.14), if the uncertain variables are uncorrelated (r_{12}=0), the computation will be simplified to,

$$\begin{aligned} \mathrm{F}(\mathrm{z}_1, \mathrm{z}_2) &= \frac{1}{\sqrt{2\pi}\sigma_1} \int_{-\infty}^{\mathrm{z}_1} \exp\left[-\frac{1}{2} \frac{(\xi_1-\mu_1)^2}{\sigma_1^2} \right] \mathrm{d}\xi_1 \frac{1}{\sqrt{2\pi}\sigma_2} \int_{-\infty}^{\mathrm{z}_2} \exp\left[-\frac{1}{2} \frac{(\xi_2-\mu_2)^2}{\sigma_2^2} \right] \mathrm{d}\xi_2 \\ &= \Phi\left(\frac{\mathrm{z}_1 - \mu_1}{\sigma_1} \right) \Phi\left(\frac{\mathrm{z}_2 - \mu_2}{\sigma_2} \right) \end{aligned} \tag{4.34}$$

Figure 4.10 shows the probability distributions of the strongly correlated bivariaten standard-normal distributed variables. The influence of the correlation can easily be observed. The stronger the correlation is, the larger is the common feasible area of the two events (deterministic constraints). For the extreme case $r_{12} \to 1$, the optimal solution will approach closely the one of the case with single chance constraints.

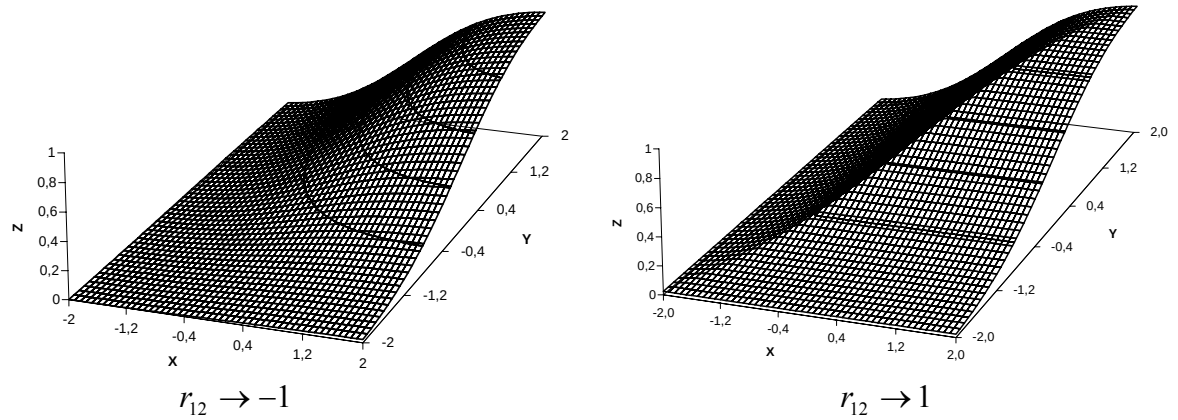

Figure 4.10: PDF of correlated bivariate standard normal distributed variables.

4.1.3 Probability computation for multivariate systems

In cases of problems with *joint* chance constraints, an explicit solution cannot be obtained, since the calculation of a joint probability of multivariate uncertain variables is needed. Unfortunately, it is not trivial to compute these probability values even numerically, when the dimension is larger than 3. A simulation scheme proposed by Szántai (1988) to estimate multivariate integrals seems to be very efficient. A detailed description of this method can be found in Prékopa (1995). The idea is to relax the stochastic problem to a deterministic nonlinear programming problem. For a linear problem with a joint chance constraint, the relaxed problem is convex (Kall and Wallace, 1994). Theoretically, it is possible to perform the joint probability computation of linear systems through numerical multivariate integration of Equation (4.27). However, with increasing the value of L, the computation time increases exponentially. For this reason, several sampling techniques have been developed. In most of the previous studies, Monte-Carlo method has been used (Fishman, 1999). Recently, efficient sampling methods have been developed such as the Hammersley sequence sampling (HSS) proposed by Diwekar and Kalagnanam (1997), which has an increase of efficiency up to 3 to 100 times in comparison to the Monte-Carlo method. Furthermore, it is also possible to combine numerical integration techniques with efficient sampling methods. An integration method based on the simulation scheme of Szántai (1988) and Prékopa (1995), where the probabilities and gradients of the constraints composed of stochastic variables with multivariate normal distribution can efficiently be computed, was implemented for correlated variables with normal distributions (Arellano-Garcia et al., 1998).

The idea is based on evaluating the joint probability of N events $A_1, A_2, \ldots, A_N$ (i.e., $A_i : \xi \le z_i,\ i = 1, \ldots, N$) through application of the following:

$$\Pr(A) = P(A_1 \cap A_2 \cap \ldots \cap A_N) = 1 - \Pr(\bar{A}_1 \cup \bar{A}_2 \cup \ldots \cup \bar{A}_N) \tag{4.35}$$

where $\bar{A}_1, \bar{A}_2, \ldots, \bar{A}_N$ are the complement i.e. violation of the events. According to the *inclusion-exclusion* principle: the number of elements in a finite set that have at least one out of N properties is equal to the number of elements having exactly one of the properties (corresponding to S_1), less the number having exactly two properties (S_2), plus the number having exactly three properties (S_3), and so on, up to the number having all N (S_N). (See Figure 4.11).

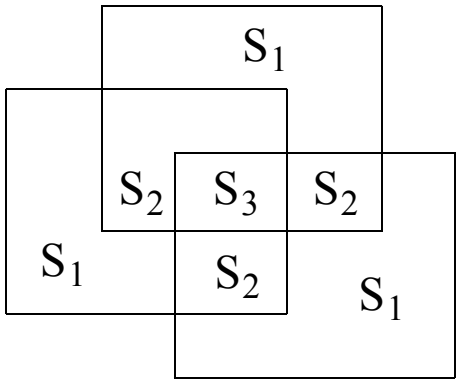

Figure 4.11: Illustration of the inclusion-exclusion principle.

Thus, the inclusion-exclusion formulas is defined as

$$\Pr(A) = 1 - \bar{S}_1 + \bar{S}_2 - \bar{S}_3 + \cdots + (-1)^N \bar{S}_N \tag{4.36}$$

$$\bar{S}_k = \sum_{i \le i_1 < \cdots < i_k \le N} \Pr(\bar{A}_{i_1} \cap \cdots \cap \bar{A}_{i_k}) \tag{4.37}$$

where $\bar{S}_1$ and $\bar{S}_2$ are the combinations of the probabilities of violating the constraints for single and bivariate normal events which can be computed exactly for the given normal distribution function by means of series expansions (Prékopa, 1995). However, for $\bar{S}_k$ with $k \ge 3$, the computation will be very difficult. Therefore, the fundamental idea of the simulation method is based on the computation of the probability of the combinations of the single and the bivariate events ($\bar{S}_1$ and $\bar{S}_2$) accurately and to approximate the rest of the inclusion-exclusion formula (4.36) through sampling from the given multivariate normal distribution. Accordingly, let N_T be the length of the sample set, corresponding to each sample s, the number of violations k_S of the events can be observed. Then the following expression represents an estimate of $\bar{S}_k$:

$$\bar{S}_k \approx \frac{1}{N_T} \sum_{S=1}^{N_T} \binom{k_S}{k} \tag{4.38}$$

Consequently, three estimates for $\Pr(A)$ can be obtained:

$$\hat{\Pr}_0 = \nu_0, \ \hat{\Pr}_1 = 1 - \bar{S}_1 + \nu_1, \ \hat{\Pr}_2 = 1 - \bar{S}_1 + \bar{S}_2 + \nu_2 \tag{4.39}$$

where

$$\nu_0 = \frac{1}{N_T}\sum_{S=1}^{N_T} k_S$$

$$\nu_1 = \frac{1}{N_T}\sum_{S=1}^{N_T} \max(k_S - 1,\ 0) \tag{4.40}$$

$$\nu_2 = \frac{-1}{N_T}\sum_{S=1}^{N_T} k'_S \quad \text{and} \quad k'_S = \begin{cases} \binom{k_S - 1}{2} & \text{if } k_S \geq 2 \\ 0 & \text{if } k_S < 2 \end{cases}$$

Subsequently, an optimal weighted sum of the three estimates will represent the approximation of $\Pr(A)$,

$$\hat{\Pr} = \omega_0\hat{\Pr}_0 + \omega_1\hat{\Pr}_1 + \omega_2\hat{\Pr}_2 \tag{4.41}$$

with $\omega_0 + \omega_1 + \omega_2 = 1$, where $\omega_0, \omega_1, \omega_2$ are chosen so that the variance of $\hat{\Pr}$ is minimized. Let **C** be the covariance matrix of the three estimates. **C** can also be calculated through sampling. Then the variance of $\hat{\Pr}$ is $\boldsymbol{\omega}^T C\boldsymbol{\omega}$, where $\boldsymbol{\omega} = (\omega_0, \omega_1, \omega_2)^T$ can be obtained by solving the following problem:

$$\begin{aligned} &\min\ \boldsymbol{\omega}^T\mathbf{C}\boldsymbol{\omega} \\ &\text{s.t. } \omega_0 + \omega_1 + \omega_2 = 1 \\ &\omega_0, \omega_1, \omega_2 \geq 0 \end{aligned} \tag{4.42}$$

To compute the probability function gradients of the joint normal distribution, N probability distribution function values have to be computed, each of which is a value of a (N-1)-dimensional normal probability distribution function (Prékopa, 1995). However, the computation may be too large. To overcome this problem, Wendt (2005) proposed a reduced gradient approach where the gradients of $\overline{S}_1$ and $\overline{S}_2$ are accurately computed, while the gradients of the remaining terms of the inclusion-exclusion formula are approximated by sampling. For this purpose, a small perturbation is given on each sample so as to observe the increment of the number of violations. In this way, the probability and their gradients can be computed simultaneously (Li et al., 2002).

4.1.4 Feasibility Analysis

An important aspect in formulating and solving probabilistic programming problems is the feasibility analysis. In Equation (4.13) the feasible region is formed by cutting-planes, whereas the feasible regions in (4.14) or (4.15) are constructed by a curvature. However, the feasible definition area region of the problem is dependent on the user-predefined probability level α. Thus, tuning the value of α is an issue of the relation between feasibility and profitability. Obviously, a high confidence level of compliance with the constraints is in principle preferred. But, the solution of a chance-constrained problem is only able to arrive at a maximum value α^{max} which is dependent on the properties of the uncertain inputs and the restriction of the controls and outputs. If a greater value is chosen, the solver (e.g. SQP) will not find a solution to the problem. In previous studies, Prekopa (1995) suggested a probability maximization step to obtain the maximum probability value α^{max}. For linear systems, Li, Wendt, Arellano-Garcia, Wozny (2002) propose an easy-to-use method to compute the

maximum feasible confidence level. The basic idea is to map the stochastic inputs to the outputs and analyze the output properties. In the following section is shown that the joint probability has the maximum value if the mean values of the outputs are in the middle of the restricted region [y^{min}, y^{max}]. Thus, α^{max} can be obtained by a simulation run.

4.1.4.1 One-step horizon

Consider the following general linear system

$$y(i+1) = ay(i) + bu(i) + c\xi(i) \tag{4.43}$$

where a, b and c are known model parameters, y and u are the input and output variables, correspondingly. The sampling time instant is indicated by i, ξ are the non-zero mean correlated stochastic disturbance variables described by the probability density function of a multivariate normal distribution

$$\varphi_N(\xi) = \frac{1}{|\Sigma|^{1/2}(2\pi)^{N/2}} \; e^{-\frac{1}{2}(\xi-\boldsymbol{\mu})^T \Sigma^{-1}(\xi-\boldsymbol{\mu})} \tag{4.44}$$

where $\boldsymbol{\mu}$ is a mean value vector in $\mathbb{R}^N$ and Σ is a non-degenerate symmetrical positive definite covariance $N \times N$ matrix. They can be represented as follows:

$$\boldsymbol{\mu} = \begin{bmatrix} \mu_1 \\ \mu_2 \\ \cdots \\ \mu_N \end{bmatrix} \qquad \boldsymbol{\Sigma} = \begin{bmatrix} \sigma_1^2 & \sigma_1\sigma_2 r_{12} & \cdots & \sigma_1\sigma_N r_{1N} \\ \sigma_1\sigma_2 r_{12} & \sigma_2^2 & \cdots & \sigma_2\sigma_N r_{2N} \\ \cdots & \cdots & \cdots & \cdots \\ \sigma_1\sigma_N r_{1N} & \sigma_2\sigma_N r_{2N} & \cdots & \sigma_N^2 \end{bmatrix} \tag{4.45}$$

where σ_i is the standard deviation of each individual stochastic variable, and $r_{ij} \in [-1,1]$ are the correlation coefficients between ξ_i and ξ_j. It should be stressed that a strong correlation between the uncertain variables often exists, in particular, for time-varying stochastic processes. A positive correlation ($r_{ij} > 0$) means that if a variable is larger (smaller) than the mean value in a time interval, then the variable is likely to be larger (smaller) than the mean value in the next time interval too. The opposite is true if the sign of the correlation coefficient is negative. However, the presence of a correlation will lead to larger output deviations from the expected values and, thus, generates a higher probability of violating the output constraints. The inequality constraint for one future point can reduced to

$$\Pr\{y_{min} \le y(1) \le y_{max}\} \ge \alpha \tag{4.46}$$

From (4.43) the mean and the standard deviation of $y(1)$ can be derived

$$\mu_{y(1)} = ay(0) + bu(0) + c\mu_1 \tag{4.47}$$

$$\sigma_{y(1)} = |c| \;\; \sigma_1 \tag{4.48}$$

Furthermore, the input value may change the mean value of the future output but has no effect on its variance. In the context of *linear systems*, for a normally distributed disturbance the output of the system is also normally distributed. The chance constraint (4.46) is then equivalent to

$$\Phi_1\left(\frac{y_{max}-\mu_{y(1)}}{\sigma_{y(1)}}\right)-\Phi_1\left(\frac{y_{min}-\mu_{y(1)}}{\sigma_{y(1)}}\right)\geq\alpha \tag{4.49}$$

where Φ_1 is the one-dimensional (1-D) standard normal probability distribution function. The interactions of the parameters in (4.49) are represented in Fig. 4.12. For the range of output variances resulting from (4.48), the probability will assume different values. This issue is shown in Fig. 4.12 for $\sigma'_y < \sigma''_y < \sigma'''_y$. With the output standard deviation σ'_y, we have the option to reallocate $\mu_{y(1)}$ with $u(0)$ due to the large possible feasible region. In case of σ''_y there will be no choice, i. e. $u(0)$ must have such value that $\mu_{y(1)}$ is located in the central point of $[y_{min}, y_{max}]$. Thus, the feasible region is diminished to one point. For a value of $\sigma_{y(1)}$ greater than σ''_y, such as σ'''_y, no feasible solution can be found for the problem. Therefore, providing an unconstrained input, σ_1 determines the feasibility of the system. Consequently, in order to guarantee a feasible problem solution, the following formulation based on (4.49) should be used

$$\sigma_1 \leq \frac{y_{max}-y_{min}}{2\ |c|\ \Phi_1^{-1}\left(\frac{\alpha+1}{2}\right)} \tag{4.50}$$

where Φ_1^{-1} denotes the inverse function of Φ_1. Hence, it can be concluded that an infeasible problem can be relaxed by decreasing the probability level α or by expanding the specified output region $[y_{min}, y_{max}]$.

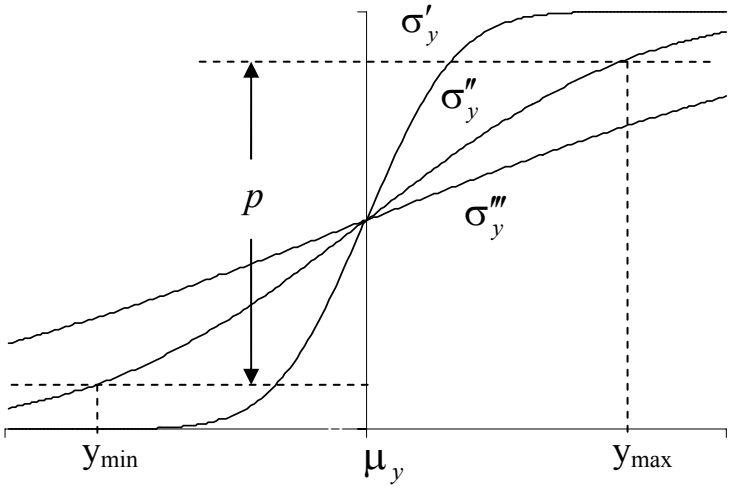

Figure 4.12: Probability profiles w. r. t the output.

4.1.4.2 N-step horizon

For a horizon with *N* predictive points, from (4.43) the output on each time point can be described as

$$y(i) = a^i y(0) + b\sum_{l=1}^{i} a^{l-1} u(i-l) + c\sum_{l=1}^{i} a^{l-1}\xi(i-l) \qquad i = 1,\cdots,N \tag{4.51}$$

The mean of the output is then from (4.45):

$$\mu_{y(i)} = a^i y(0) + b\sum_{l=1}^{i} a^{l-1} u(i-l) + c\sum_{l=1}^{i} a^{l-1}\mu_{i-l+1} \tag{4.52}$$

The covariance of the output between point i and j ($j \geq i,\ i = 1,\cdots,N$) can be calculated by

$$\begin{aligned} R_y(i,j) &= E\left\{\left[\, y(i) - \mu_{y(i)} \,\right]\ \left[\, y(j) - \mu_{y(j)} \,\right]\right\} \\ &= c^2 E\left\{\left[\sum_{l=1}^{i} a^{l-1}[\xi(i-l) - \mu_{i-l+1}]\right]\ \left[\sum_{m=1}^{j} a^{m-1}[\xi(j-m) - \mu_{j-m+1}]\right]\right\} \\ &= c^2 \sum_{l=1}^{i}\sum_{m=1}^{j} a^{i+j-l-m}\sigma_l\sigma_m r_{l,m} \end{aligned} \tag{4.53}$$

which will contribute to the correlation of these two points. The variance of the output at point i is in that case:

$$\sigma_{y(i)}^2 = R_y(i,i) = c^2 \sum_{l=1}^{i}\sum_{m=1}^{i} a^{2i-l-m}\sigma_l\sigma_m r_{l,m} \tag{4.54}$$

which is part of the covariance (4.53). However, it is again evident from 4.52 and 4.54 that the input can only affect the means of the outputs which horizontally shift the individual probability profile (Fig. 4.12). From (4.53) and (4.54), on the other hand, the output covariance and variance are determined by the covariance of the disturbance at different time points as well as by the model parameters (a, c). Furthermore, the shape of the probability curve will be influenced by the covariance. Thus, in connection with a problem with N predictive points, the feasibility relies on the output covariance matrix provided that the input is unconstrained or the allowable input region is sufficiently large. Moreover, due to the high order exponential terms, both mean and covariance of the outputs are highly sensitive to the values of the model parameter a.

Single chance constraints

Since the output of a linear system disturbed by a normally distributed sequence is also normally distributed, in case of single chance constraints, Equation (4.49) can be applied to the inequality constraint of each individual output point. This means

$$\Phi_1\left(\frac{y_{max} - \mu_{y(i)}}{\sigma_{y(i)}}\right) - \Phi_1\left(\frac{y_{min} - \mu_{y(i)}}{\sigma_{y(i)}}\right) \geq \alpha \qquad i = 1,\cdots,N \tag{4.55}$$

where $\mu_{y(i)}, \sigma_{y(i)}$ are computed from (4.52) and (4.54), respectively. Manipulating u(i) such that $\mu_{y(i)}$ is in the middle of $[y_{\min}, y_{\max}]$, the possible maximum value of the individual probability will be

$$\alpha^{\max}(\mathrm{i}) = 2\Phi_1\left(\frac{\mathrm{y_{max}} - \mathrm{y_{min}}}{2\sigma_{\mathrm{y(i)}}}\right) - 1 \qquad \mathrm{i} = 1, \cdots, \mathrm{N} \tag{4.56}$$

By means of comparison between $\alpha^{\max}(\mathrm{i})$ and α, one can then identify whether the problem is feasible or not. The required input values u(i) corresponding to this achievable probability can be calculated through (4.52).

Joint chance constraint

In case of a joint chance constraint with N output points it is not possible to obtain an explicit probability representation similar to (4.55) and (4.56). Large absolute values of the elements in the output covariance matrix may cause an infeasible problem. Thus, from (4.53) and (4.54) the following relationships between the output covariance of a point and that of the point before can be derived,

$$\mathrm{R_y(i, i+1)} = \mathrm{c^2}(\mathrm{a}\sigma^2_{\mathrm{y(i)}} + \sum_{\mathrm{l=1}}^{\mathrm{i}} \mathrm{a^{i-l}}\sigma_{\mathrm{l}}\sigma_{\mathrm{i+1}}\mathrm{r_{l,i+1}}) \tag{4.57}$$

$$\sigma^2_{\mathrm{y(i+1)}} = \mathrm{c^2}(\mathrm{a^2}\sigma^2_{\mathrm{y(i)}} + \sum_{\mathrm{l=1}}^{\mathrm{i+1}} \mathrm{a^{i+1-l}}\ \ \sigma_{\mathrm{l}}\sigma_{\mathrm{i+1}}\mathrm{r_{l,i+1}} + \sum_{\mathrm{m=1}}^{\mathrm{i}} \mathrm{a^{i+1-m}}\sigma_{\mathrm{m}}\sigma_{\mathrm{i+1}}\mathrm{r_{i+1,m}}) \tag{4.58}$$

Based on these equations, the change of the output covariance (variance) values from one time point to the next can be followed. Moreover, in addition to the variance of the disturbance at each individual point, the correlation between the points of the stochastic sequence effectively increases the variance of the next output. For small element values in the output covariance matrix, it is preferred to have small correlation coefficients $r_{i,j}$ in the disturbance covariance matrix. For instance, for the model parameters, it can be concluded from (4.57) and (4.58) that $|c| < 1$ and $|a| < 1$ is favorable for the feasibility of the system. An additional factor which has an influence on the value of the covariance (variance) is the horizon length. For example, if $\mathrm{a} = 1,\ \sigma_{\mathrm{i}} = \sigma,\ \mathrm{r_{i,j}} = 0,\quad (\mathrm{i} \neq \mathrm{j},\ \mathrm{i, j} = 1, \cdots, \mathrm{N})$, the output variance at point N will be

$$\sigma^2_{\mathrm{y(N)}} = \mathrm{c^2}\sigma^2\mathrm{N} \tag{4.59}$$

In comparison to (4.51), the output variance at point N is N-times greater than the value at the first point. In this case, however, a larger N will most likely lead to an infeasible problem. Furthermore, there is no explicit function to calculate the joint multivariate probability. The maximum achievable probability value can be computed, however (see Appendix A1). It can be proven that the joint probability reaches its maximum value whenever the mean values of the output vector are in the middle of $[\mathrm{y_{min}},\ \mathrm{y_{max}}]$ for $\mathrm{i} = 1, \cdots, \mathrm{N}$, i.e.,

$$\mu_{\mathrm{y(i)}} = \frac{\mathrm{y_{min}} + \mathrm{y_{max}}}{2} \qquad \mathrm{i} = 1, \cdots, \mathrm{N} \tag{4.60}$$

After substituting $\mu_{y(i)}$ in (4.52) with $\mu_{y(i)}$ from (4.60), the resulting input vector can be calculated by:

$$u(i-1)=\frac{1}{b}\mu_{y(i)}-\frac{a^{i}}{b}y(0)-\frac{c}{b}\sum_{l=1}^{i}a^{l-1}\mu_{i-l+1}-\sum_{l=2}^{i}a^{l-1}u(i-l) \qquad i=1,\cdots,N \tag{4.61}$$

Based on this control vector, the maximum achievable joint probability can be computed through one simulation run by the method described above. However, it should be remarked that with an increase of the standard deviation value of the disturbance variables, the largest obtainable probability will decrease. Furthermore, a strong correlation between the variables leads more likely to constraint violations.

4.1.5 Linear dynamic problems

As demonstrated in the previous section, the solution of a problem within the framework of a *linear* system with single chance constraints can basically be derived by a coordinate transformation. In cases of linear problems with a *joint* chance constraint, the relaxed problem is a convex NLP provided that the probability distribution function of the uncertain variables is quasi-concave. Thus, it can be solved with an NLP solver. The probabilities and gradients of the constraints, composed of stochastic variables with multivariate normal distribution, can be computed using an efficient simulation approach. The approaches have been applied to linear predictive control problems (Schwarm and Nikolaou, 1999, Li et al., 2000b, Wendt, 2005). However, optimization of linear steady state systems (LSCS and LSCJ) under constant uncertain variables has been well studied (Kall and Wallace, 1994). It can be applied in process design and planning under uncertainty.

In this section, *linear dynamic* systems with *time dependent* uncertain inputs are considered (LDTS and LDTJ). Consequently, the outputs in the future horizon depend on the current state, the future and past controls as well as uncertain inputs. The uncertain inputs can include both uncertain parameters and disturbances. The controls in the horizon will be decided to optimize some objective function and ensure the chance constraints for the outputs. However, for the computational treatment of linear dynamic processes, the time dependence of all variables has to be taken into account. Furthermore, for the mathematical and numerical treatment it is also important to differentiate whether there is a time dependence of the uncertain variables or not as well. In the case of no time dependency (*steady* random variables), the probability computation follows the same pattern as described in the previous section, since the dynamics of the process has only an impact on the deterministic variables.

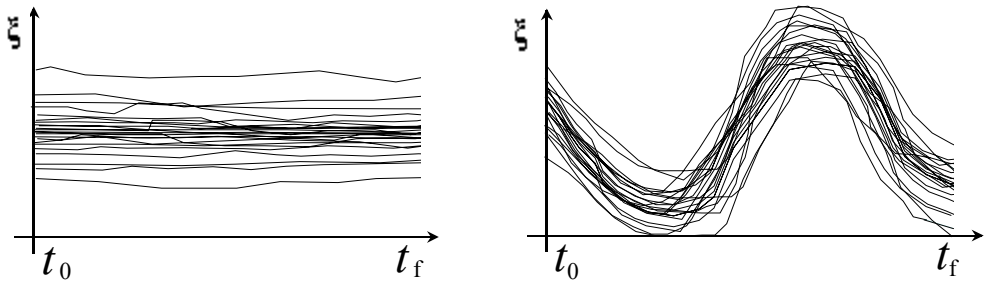

Figure 4.13: Static and dynamic uncertain variables.

Dynamic random variables have either to be discretized into a finite number of time intervals or described by a finite number of other auxiliary uncertain variables so as to approximate a linear relation between a certain number of uncertain inputs and constrained outputs. Noteworthy examples, where a stochastic optimization problem of *linear* systems with dynamic random variables is relevant, are predictive control problems which include chance constraints in its mathematical formulation (Schwarm and Nikolaou, 1999, Li et al., 2000b).

$$
\begin{aligned}
\min \ & \sum_{i=1}^{N} \left[\mathbf{u}(i) - \mathbf{u}(i-1) \right]^2 \\
\text{s.t.} \ & \mathbf{x}(i+1) = \mathbf{A}\mathbf{x}(i) + \mathbf{B}\mathbf{u}(i) + \mathbf{C}\boldsymbol{\xi}(i) \\
& \mathbf{y}(i) = \mathbf{E}\mathbf{x}(i) \\
& \Pr\left\{ \mathbf{y}(i) \le \mathbf{y}^{SP}(i), \quad i = 1, \cdots, N \right\} \ge \alpha \\
& \mathbf{u}_{min} \le \mathbf{u}(i) \le \mathbf{u}_{max} \\
& \mathbf{x}(t_0) = \mathbf{x}_0
\end{aligned}
\tag{4.62}
$$

In these works, the model uncertainty is described as the uncertainty of the step-response coefficients. Thus, in order to predict future outputs both model and disturbance uncertainties are considered to have multivariate normal distributions. Moreover, strong correlations are taken into account to properly estimate the real system. Based on the moving horizon strategy, each output within the horizon is to be restricted between specific upper and lower bounds with a corresponding probability level. Since the outputs are restricted by these chance (probabilistic) constraints, the objective function of the predictive control problem basically comprises the input moves which are to be minimized within the horizon. Furthermore, when considering a multi-input/multi-output (MIMO) linear system, the outputs in the future horizon are functions of the current state, the future and past controls and of the uncertain disturbances. Thus, the control policy will be computed by solving the optimization problem on the basis of the initial state, the model uncertainties and also the uncertain disturbances in the new horizon. This leads, however, to an optimization problem under joint chance constraints. So for instance, assuming that each of the model and disturbance uncertainties is a sequence (over N time intervals) of stochastic variables with multivariate normal distribution, the joint probability in (4.62) can be formulated as follows:

$$
\Pr\left\{ \begin{array}{c}
y_{1,min}(k+1) \le y_1(k+1) \le y_{1,max}(k+1) \\
y_{1,min}(k+2) \le y_1(k+2) \le y_{1,max}(k+2) \\
\cdots \quad \cdots \quad \cdots \\
y_{1,min}(k+N) \le y_1(k+N) \le y_{1,max}(k+N)
\end{array} \right\} \ge \alpha_1
\tag{4.63}
$$

Immediately after the first control is applied in response to the disturbance, the new state at the next time point t+1 is available. Then, the computation proceeds to the next horizon. In addition, since there may be varying uncertain properties at each horizon move, the uncertainty characteristics such as mean, variance and correlation play a decisive role in the optimal control advance. However, with the joint probability the problem becomes an NLP problem. Unfortunately, it is not possible to easily compute those probability values even numerically, if the dimension is larger than 3. In Chapter 7, the performance of the predictive controller with its extension to a robust NMPC under chance constraints is explained in detail.

4.2 Nonlinear Chance-Constrained Optimization

In systems where the relationship between uncertain and constrained variables is *nonlinear*, the type of the probability distribution function of the uncertain input is not the same as the one of the constrained output. Unlike linear systems, a multivariate normal distribution of the uncertain input never causes a multivariate normal distribution of the output. Furthermore, due to the nonlinear propagation, it is difficult to obtain the stochastic distribution of output variables. Thus, nonlinear chance constrained programming remained as an unresolved problem. The output probability distribution function is often not even known exactly and has to be estimated from historical data (Johnston and Kramer, 1998). Moreover, even a given multivariate distribution (such as multivariate normal) can not be calculated exactly in general but has to be approximated by simulations or bounding arguments. However, a linear relationship can rarely be found in process system engineering. On the other hand, the relation is nonlinear, but, it shows very often a *monotonic* relationship between uncertain input and constrained output.

4.2.1 Monotonic relationship between uncertain input and output

In order to introduce the concept of *monotony* with reference to the relationship between a constrained uncertain output and a random input, in this section, a very simple derivation is carried out for a random variable function. So for instance, if $\xi \in \Xi$ is a random variable, any other variable $y \in \mathbf{Y}$ defined as function of ξ will also be a random variable. In such case, $\rho_{\Xi}(\xi)$ and $F_{\Xi}(\xi)$ denote the probability density and distribution functions of ξ, respectively. The main difficulty is to find the density function $\rho_{\mathbf{Y}}(y)$ and the distribution function $F_{\mathbf{Y}}(y)$ of the random output variable y. Assuming the following functional relation,

$$\mathbf{Y}=\gamma(\Xi) \tag{4.64}$$

The distribution function of **Y** is then the probability of realizing **Y** less than or equal to y, by definition. Furthermore, it results that,

$$F_{\mathbf{Y}}(y) = \Pr(\mathbf{Y} \le y) = \Pr(\gamma \le y) = \int_{\gamma(\xi)\le y} \rho_{\Xi}(\xi)\, d\xi \tag{4.65}$$

whereas the integration is to be carried out over all values of ξ for which $\gamma(\xi)\le y$. The probability density function of **Y** is defined as,

$$\rho_{\mathbf{Y}}(y) = \frac{\partial}{\partial y}\left[F_{\mathbf{Y}}(y)\right] \tag{4.66}$$

The relationships formulated in (4.65) and (4.66) are general and can be applied to any function $\gamma(\xi)$. If $\gamma(\xi)$ is a monotonically increasing or decreasing function, as diagramed in Fig. 4.14, the integration bounds can be set up without any difficulty.

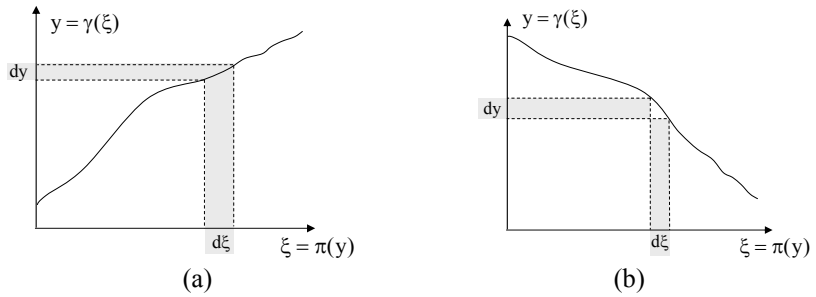

Figure 4.14: Monotonic relations: (a) monotonic increasing; (b) monotonic decreasing.

In this case, the inverse relation of (4.64) can be stated as

$$\xi = \gamma^{-1}(y) = \pi(y) \tag{4.67}$$

From (4.67), it can be seen that ξ is a single valued function of y. Based on (4.67), it follows that:

$$d\xi = \left|\frac{d\pi}{dy}\right| dy = \left|\pi'(y)\right| dy \tag{4.68}$$

where the absolute value is introduced to deal with both the increasing and the decreasing type of functions. From (4.65) and (4.68) results then:

$$F_Y(y) = \int_{-\infty}^{y} \rho_\Xi\left[\pi(y)\right]\left|\pi'(y)\right| dY \tag{4.69}$$

Furthermore, the differentiation of $F_Y(y)$ provides,

$$\rho_Y(y) = \rho_\Xi\left[\pi(y)\right]\left|\pi'(y)\right| \tag{4.70}$$

However, if a process system is modeled by the functional relationship from (4.64) and if the relation between uncertain input and uncertain output is *nonlinear*, the generation of the inverse relation (4.67) or reverse projection is not a trivial task. Particularly, when a correlated multivariate distribution function is considered, the correlation between the variables leads to a rather complicated integration due to the overlap of the uncertain variables´ spaces.

4.2.2 Solution strategy

The basic idea of chance-constrained optimization is to integrate explicitly the available stochastic information. The essential challenge here lies in the computation of the probabilities of complying with the constraints, and their gradients. Following the idea of monotony described in 4.2.1, Wendt et al. (2002) propose a probability computation method for steady state problems under only one single chance constraint.

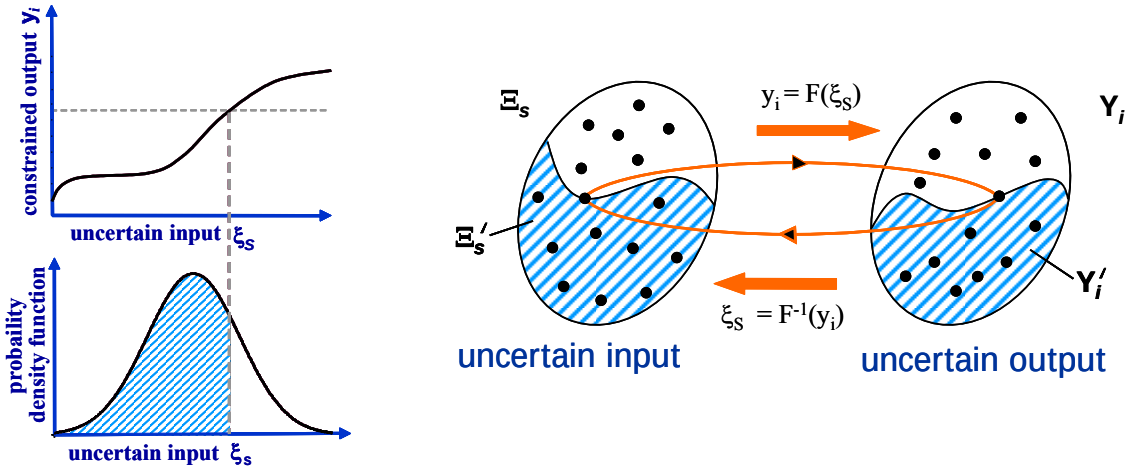

Figure 4.15: Mapping between an uncertain input variable and an output variable.

By means of the monotony of the output variables with respect to one of the uncertain variables, the output feasible region is mapped back to a region of the uncertain input variables. Thus, the probability of holding the output constraints can be achieved by integration of the probability density function of the multivariate uncertain variables (Fig. 4.15). The main idea relies upon the case of a *monotonic* relationship between a constrained output variable $y_i \in Y_i$ and at least one of the uncertain input variables $\xi_s \in \Xi_s$ where Ξ_s is a subspace of Ξ. This study can be performed easily by analyzing the operation of the process considered via simulation. As shown on the right in Fig. 4.15, the confined feasible region is considered that will formed by the nonlinear projection of the uncertain input region for some given controls **u** (hatched area in the uncertain output). Thus, the points in Fig. 4.15 represent some realizations of the variables based on their distribution functions. That means a point in Ξ_s leads to a point in Y_i through the projection $y_i = F(\xi_s)$. Consequently, a point $y_i \in Y_i$ can simply lead to one value of ξ_s through the reverse projection $\xi_s = F^{-1}(y_i)$. Hence, the boundary of the constrained value y^{SP} in the output region corresponds to a limiting value ξ_s^L for ξ_s in the input region. In Fig. 4.15 the entire output region is represented by Y_i, while the hatched sub-area Y_i' includes only those values of y_i which do not exceed the constrained bound y^{SP} so that the constraint

$$\Pr\left\{ y_i \le y_i^{SP} \right\} \ge \alpha \tag{4.71}$$

is satisfied. The hatched sub-area Ξ_s' displays the uncertain input region with the bound ξ_s^L which corresponds to the output constraint y^{SP}. Thus, one can come to the conclusion that if the positive monotony $y_i \uparrow \Rightarrow \xi_i \uparrow$ exists then the chance constraint in (4.71) can be formulated as

$$\Pr\left\{ \xi_s \le \xi_s^L \right\} \ge \alpha \tag{4.72}$$

On the other hand, if a negative monotony $y_i \uparrow \Rightarrow \xi_i \downarrow$ is in force then the representation

$$\Pr\left\{ \xi_s \geq \xi_s^L \right\} \geq \alpha \tag{4.73}$$

is equivalent to (4.71). Generally, in the case of a negative monotony, an upper bound of the constrained output corresponds to a lower bound of the random input variable and vice versa. In contrast, in case of a positive monotonic relation there is no change between upper and lower bound. It should be noted that all uncertain variables which have an impact on y_i are taken into account when computing $\Pr\left\{ y_i \leq y_i^{SP} \right\}$. In addition, the values of the decision variables **u** also have an impact on the projected region. Thus, the bound ξ_s^L will change based on the realization of the individual uncertain variables ($\xi_1, \cdots \xi_{s-1}$) and the value of **u** as follows

$$\xi_s^L = F^{-1}\left(\xi_1, \cdots, \xi_{s-1}, y_i^{SP}, \mathbf{u}\right) \tag{4.74}$$

The limiting value ξ_s^L is computed by solving the model equations with given decision variables and the boundary value y^{SP}. This implies that the probability of complying with the output constraint can be transformed to a multivariate integration in the corresponding limited region of the uncertain inputs

$$\begin{aligned} \Pr\left\{ y \leq y^{SP} \right\} &= \Pr\left\{ \xi_s \leq \xi_s^L, \xi_k \subseteq \Re^s, s \neq k \right\} \\ &= \int_{-\infty}^{\infty} \cdots \int_{-\infty}^{\xi_s^L} \cdots \int_{-\infty}^{\infty} \rho\left(\xi_1, \cdots, \xi_{s-1}, \xi_s\right) d\xi_k \cdots d\xi_s \cdots d\xi_1 \end{aligned} \tag{4.75}$$

where $\rho(\xi)$ is the joined distribution function of ξ. The right-hand side of (4.75) represents a multivariate integration over the region of Ξ excluding the section beyond the confining value ξ_s^L. Consequently, the probability of the constrained output is attained by computing the value of the probability density function of the random inputs. In principle, this solution approach can be used to solve problems under uncertainties with any kind of joint correlated multivariate distribution function, provided that the density function is available or it can be approximated.

4.2.2.1 Mapping approach- elementary illustration

To illustrate the mapping approach (Fig. 4.15), the following problem with a joint normal distribution of two uncertain variables is considered. The information which defines the stochastic properties of the uncertain input is given in Table 4.2.

Random input	expected value	standard deviation	correlation matrix
ξ_1	4.0	0.5	$\begin{bmatrix} 1.0 & -0.6 \\ -0.6 & 1.0 \end{bmatrix}$
ξ_2	4.0	0.7	

Table 4.2: Stochastic properties of the uncertain inputs

Here, the nonlinear relation between the constrained output, y, and the random inputs ξ_1 and ξ_2 is specified by:

$$y = (2\xi_1 - 8)^3 - \xi_2 + 6.2 \tag{4.76}$$

and the probability of complying with the constraint $\Pr\{y \le 2.5\}$ needs to be calculated. A monotonic relationship between y and ξ_2 is assumed. Through reverse projection (mapping) of the constrained output to the region of the random input, the bound of the uncertain input region is obtained

$$\xi_2^L = (2\xi_1 - 8)^3 + 3.7 \tag{4.77}$$

This represents the integration bound which is required for the computation of the output constraint probability:

$$\Pr\{y \le 2.5\} = \int_{-\infty}^{\infty} \int_{-\infty}^{(2\xi_1-8)^3+3.7} \varphi_2(\xi_1, \xi_2)\, d\xi_2\, d\xi_1 \tag{4.78}$$
$$\Pr\{y \le 2.5\} = 71.44\%$$

where φ_2 denotes the density function of the bivariate normal distribution. Figure 4.16 illustrates the reliability of the results, and the mapping concerning the compliance of the bound through variation of the uncertain variables obtained by Monte Carlo simulations (1000 samples).

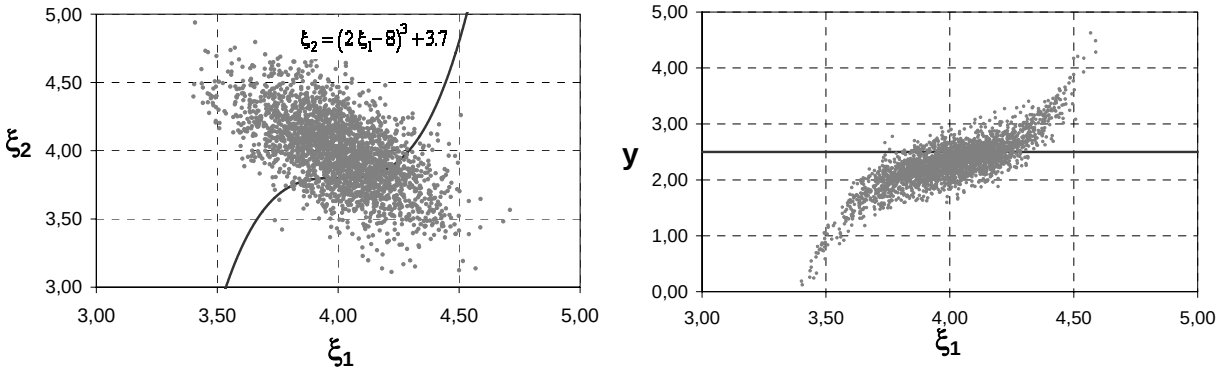

Figure 4.16: Mapping of the constrained output to the uncertain input region.

In spite of the difficulty in describing the output distribution due to the *nonlinearity*, the probability of holding the output constraint can be calculated. About 71% of the points in Fig. 4.16 are below the bounds. Figure 4.17 shows the resulting integration limit over the uncertain variables.

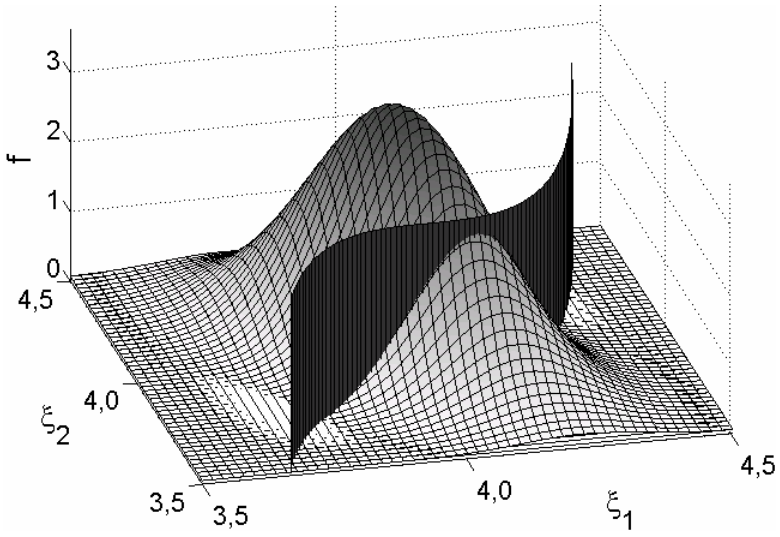

Figure 4.17: Density function and the integration limit (black solid area) over the uncertain input.

4.2.2.2 Computation of the probability gradients

The solution strategy is basically to relax the nonlinear chance-constrained programming problem in order to transform it to a deterministic NLP problem. Thus, the computational strategy is a sequential NLP as illustrated in Fig. 4.18. Here the input boundary ξ_s^L is computed by the Newton-Raphson method for more complex models based on the output value of y^{SP}. Since this boundary depends on the realization of the uncertain variables (ξ_1 ,...,ξ_{s-1}) according to Equation (4.74), it has to be computed on each collocation point of these variables. In this way, the equality constraints (model equations) are eliminated by expressing the state variables in terms of decision and uncertain variables. Furthermore, to link the chance-constrained approach to a NLP framework, the gradients of the output constraint probabilities with regard to the decision variables **u** need to be computed. From (4.74) and (4.75) the decision variables, **u,** have an impact on the value of the probability through the integration bound of the corresponding region of the random inputs. Thus, the gradients can be computed as follows

$$\frac{\partial \Pr\left\{ y_i \le y_i^{SP} \right\}}{\partial u} = \int_{-\infty}^{\infty} \cdots \int_{-\infty}^{\infty} \rho\left(\xi_1, \cdots, \xi_{s-1}, \xi_s^L\right) \frac{\partial \xi_s^L}{\partial u} d\xi_1 \cdots d\xi_k \tag{4.79}$$

where $\frac{\partial \xi_s^L}{\partial u}$ represents the gradient vector. It should be noted that for the gradient computation the number of integrals will be reduced by one integral in comparison to (4.75). The right-hand side of (4.79) can simultaneously be computed to (4.75) by numerical integration in the input region.

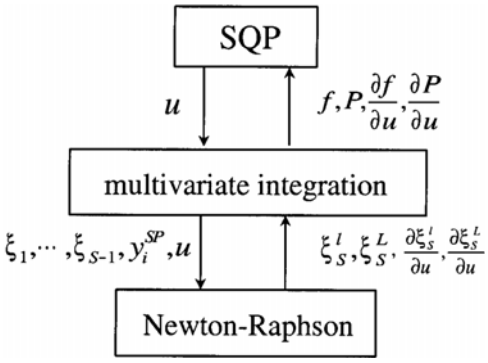

Figure 4.18: Computational strategy for solving steady-state problems with one single chance constraint

As mentioned earlier, collocation in finite elements is used to discretize the bounded region of the uncertain inputs. We refer here to the appendix A2 for supplementary details concerning the orthogonal collocation approach. It should be noted, however, that for normal distributions the boundaries of the infinite integrals in (4.75) are chosen as [-3σ, 3σ]. In the next section, a nested computational scheme for performing the multivariate integration is presented based on the fact that the S-dimensional integration can be computed by an S-1 dimensional integration (Wendt 2005).

4.2.3 Numerical approach to multivariate integration

In this section, the numerical approach to the multivariate integration used in this thesis is presented. It is derived from the orthogonal collocation on finite elements. The random inputs are supposed to be an *S*-dimensional joint normal distribution with the probability density function

$$\varphi_S(\xi) = \frac{1}{|\Sigma|^{1/2}(2\pi)^{S/2}} e^{-\frac{1}{2}(\xi-\mu)^T \Sigma^{-1}(\xi-\mu)} \tag{4.80}$$

where μ and Σ are known expected values and the covariance matrix of the stochastic variables, respectively. They have the following form:

$$\mu = \begin{bmatrix} \mu_1 \\ \mu_2 \\ \cdots \\ \mu_S \end{bmatrix} \quad \Sigma = \begin{bmatrix} \sigma_1^2 & \sigma_1\sigma_2 r_{12} & \cdots & \sigma_1\sigma_S r_{1S} \\ \sigma_1\sigma_2 r_{12} & \sigma_2^2 & \cdots & \sigma_2\sigma_S r_{2S} \\ \cdots & \cdots & \cdots & \cdots \\ \sigma_1\sigma_S r_{1S} & \sigma_2\sigma_S r_{2S} & \cdots & \sigma_S^2 \end{bmatrix} \tag{4.81}$$

The standard deviation of each individual random variable is represented by σ_i, and $r_{i,j} \in (-1, 1)$ is the correlation coefficients between ξ_i and ξ_j $(i, j = 1, \cdots, S)$. However, by definition, the probability of the random inputs in a certain region can be obtained starting from the standard probability distribution function Φ_S,

$$\Phi_S(z_1^{(1)}, \cdots, z_S^{(1)}, \hat{\Sigma}^{(1)}) = \int_{-\infty}^{z_1^{(1)}} \cdots \int_{-\infty}^{z_S^{(1)}} \hat{\varphi}_S(\hat{\xi}_1, \cdots, \hat{\xi}_S) d\hat{\xi}_1 \cdots d\hat{\xi}_S \tag{4.82}$$

where $\hat{\varphi}_S$ is the standard density function and z the integration limits. $\hat{\xi}$ and $\hat{\Sigma}$ refer to the linear transformation of ξ and the covariance matrix, respectively. Both constitute the standard normal distribution with zero mean. $\hat{\Sigma}$ denotes the correlation matrix which features unit diagonal elements. Further, Equation (4.82) can be rewritten as

$$\Phi_S(z_1^{(1)},\cdots,z_S^{(1)},\hat{\Sigma}^{(1)}) = \int_{-\infty}^{z_1^{(1)}} \Phi_{S-1}(z_2^{(2)},\cdots,z_S^{(2)},\hat{\Sigma}^{(2)})\hat{\varphi}_1(\hat{\xi}_1^{(1)})d\hat{\xi}_1^{(1)} \tag{4.83}$$

where Φ_{S-1} stands for the S-1-dimensional standard probability distribution function while $\hat{\varphi}_1$ is the standard normal density function of a single random variable (Prekopa, 1995). A general characterization of (4.83) can be formulated as follows,

$$\Phi_{S-j}(z_1^{(j+1)},\cdots,z_S^{(j+1)},\hat{\Sigma}^{(j+1)}) = \int_{-\infty}^{z_{j+1}^{(j+1)}} \Phi_{S-j-1}(z_{j+2}^{(j+2)},\cdots,z_S^{(j+2)},\hat{\Sigma}^{(j+2)})\hat{\varphi}_1(\hat{\xi}_{j+1}^{(j+1)})d\hat{\xi}_{j+1}^{(j+1)} \tag{4.84}$$

and

$$z_k^{(j+1)} = \frac{z_k^{(j)} - r_{k,j}^{(j)}\hat{\xi}_j^{(j)}}{\sqrt{1-r_{k,j}^{(j)^2}}}, \quad j=1,\cdots,S-1; \quad k=j+1,\cdots,S \tag{4.85}$$

$\hat{\Sigma}^{(j)}$ is the $(S-j+1)\times(S-j+1)$ correlation matrix with the elements

$$r_{k,i}^{(j+1)} = \frac{r_{k,i}^{(j)} - r_{k,j}^{(j)} r_{i,j}^{(j)}}{\sqrt{1-r_{k,j}^{(j)^2}}\sqrt{1-r_{i,j}^{(j)^2}}}, \qquad k,i=j+1,\cdots,S \tag{4.86}$$

Repeating this procedure for $S-2$ transformation steps from (4.83, 4.85, and 4.86) the following 2-dimensional integration is obtained

$$\Phi_2(z_{S-1}^{(S-1)},z_S^{(S-1)},\hat{\Sigma}^{(S-1)}) = \int_{-\infty}^{z_{S-1}^{(S-1)}} \Phi_1\left[z_S^{(S)}\right]\hat{\varphi}_1\left(\hat{\xi}_{S-1}^{(S-1)}\right)d\hat{\xi}_{S-1}^{(S-1)} \tag{4.87}$$

where Φ_1 is the standard probability function of a normally distributed variable. Since an analytic solution of (4.87) is not available, numerical integration is required. For this purpose, collocation on finite elements, which has been regarded as an efficient method (Finlayson, 1989), is used. In the collocation framework, the integration interval $(-\infty, z_{S-1}^{(S-1)}]$ is discretized into subintervals. In this thesis, for the standard normal distribution, the domain $[-3, z_{S-1}^{(S-1)}]$ is used for most of the examples presented. However depending on the optimization problem there may also exist lower bounds. Based on the equations (4.80)-(4.87), a nested computational approach has been developed. Derived from the collocation method, the values of Φ_2 on the collocation points of the random variable are calculated. These values will then be employed to compute the values of Φ_3 and the procedure will proceed upwards until the values of Φ_S are finally computed.

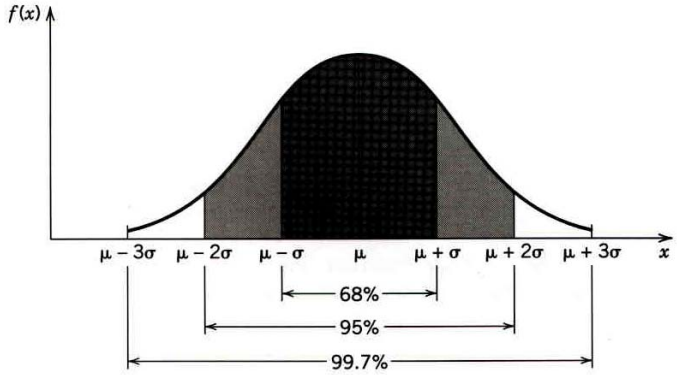

Figure 4.19: Probabilities associated with the normal distribution.

The selection of the number of intervals and the number of collocation points defines a trade-off between accuracy and computational time. A large number of intervals and collocation points will result in high accuracy, but the computation time will considerably increase. Simulation results have demonstrated that four intervals with 3-point-collocation or two intervals with 5-point-collocation can reach a probability error of less than 1%. Table 4.3 shows the results corresponding to the normal distribution.

number of collocation points	number of intervals	total number of points	error
3	4	12	0.5%
5	2	10	0.1%
5	1	5	1%

Table 4.3: Integration of the standard normal distribution with orthogonal collocation

To implement the numerical approach, it is necessary to determine the standardized value $z_S^{(1)}$ for each integration step. The corresponding real value $\xi_S^{true} = \xi_S^L$ is then calculated from (4.74) based on the model equations so that:

$$z_S^{(1)} = \frac{\xi_S^{true} - \mu_S}{\sigma_S} \tag{4.88}$$

Besides, the real values of the other remaining uncertain variables $\xi_k^{true} = \xi_k$ (with k=1,..,S-1) are also required for the computation of $\xi_S^{true} = \xi_S^L$ in every integration step. This results from (4.85), being the starting point the collocation points NK which are distributed on the corresponding integral for each uncertain variable and, thus, they are set as fixed values $\hat{\xi}_{j,w}^{(j)}$ with $j = 1,...,S-1$ and $w = 1,...,NK$. The relationship (4.85), based on which the transformation of the integration limits is described, can also be used for any other points within the integral such that

$$\hat{\xi}_k^{(j)} = \hat{\xi}_k^{(j+1)} \cdot \sqrt{1 - r_{k,j}^{(j)^2}} + r_{k,j}^{(j)} \cdot \hat{\xi}_j^{(j)}, \quad j = 1,\cdots,S-1; \quad k = j+1,\cdots,S-1 \tag{4.89}$$

Under the assumption of a normal distribution, the computation of the gradients (4.79) can be carried out similarly to the previously described procedure. However, from (4.74) and the fact

that merely the very last bound value of the integral in (4.82) are concerned with the decision variables u, the gradient vector can be computed from (4.83) as follows,

$$\frac{\partial \mathbf{\Phi}_S}{\partial \mathbf{u}} = \int_{-\infty}^{z_1} \frac{\partial \mathbf{\Phi}_{S-1}}{\partial \mathbf{u}} \hat{\varphi}_1(\hat{\xi}_1) d\hat{\xi}_1 \tag{4.90}$$

Furthermore, given that

$$\mathbf{\Phi}_{S-1}(z_1^{(2)}, \cdots, z_S^{(2)}, \hat{\Sigma}^{(2)}) = \int_{-\infty}^{z_2^{(2)}} \mathbf{\Phi}_{S-2}(z_3^{(3)}, \cdots, z_S^{(3)}, \hat{\Sigma}^{(3)}) \hat{\varphi}_1(\hat{\xi}_2^{(2)}) d\hat{\xi}_2^{(2)} \tag{4.91}$$

The following relation can be read

$$\frac{\partial \mathbf{\Phi}_{S-1}}{\partial \mathbf{u}} = \int_{-\infty}^{z_2^{(2)}} \frac{\partial \mathbf{\Phi}_{S-2}}{\partial \mathbf{u}} \hat{\varphi}_1(\hat{\xi}_2^{(2)}) d\hat{\xi}_2^{(2)} \tag{4.92}$$

If the procedure is carried forward for $S-2$ steps i.e. transformations, it results in

$$\frac{\partial \mathbf{\Phi}_2}{\partial \mathbf{u}} = \int_{-\infty}^{z_{S-1}^{(S-1)}} \frac{\partial \mathbf{\Phi}_1}{\partial \mathbf{u}} \hat{\varphi}_1\left(\hat{\xi}_{S-1}^{(S-1)}\right) d\hat{\xi}_{S-1}^{(S-1)} \tag{4.93}$$

along with

$$\frac{\partial \mathbf{\Phi}_1}{\partial \mathbf{u}} = \hat{\varphi}_1(z_S^{(S)}) \frac{\partial z_S^{(S)}}{\partial \mathbf{u}} \tag{4.94}$$

The gradient $\frac{\partial z_S^{(S)}}{\partial \mathbf{u}}$ can be obtained from $\frac{\partial \xi_S^L}{\partial \mathbf{u}}$ which refers to the real physical value. For this purpose, the same transformation chain from (4.88) and (4.89) is adopted. Consequently, for the computation of the gradients using multivariate integration, the same orthogonal collocation points can be used which are used for the probability computation. Thus, the gradients of the probability, from (4.94) back to (4.90), can be calculated simultaneously with the computation of $\mathbf{\Phi}_S$.

4.2.4 Illustrative example: design of a reactor-separator system

One important aspect in process design is to reduce the effect of the system uncertainties such as unpredictable variations in the values of plant parameters around their nominal values which are often encountered in operation of process plants. However, the design of chemical processes requires data, most of which are obtained from experiments or are estimated from correlations. This introduces into the design uncertainties with even unknown magnitudes. To reduce the probability of inadequate system performance, overdesign factors are applied to account for these uncertainties in the design parameters. Often, these safety factors are, however, based on experience or heuristics and are only partially related quantitatively to possible causes of system malfunctions.

The following example will demonstrate the efficiency of the approach presented until this point. Here, the design of a prototype chemical process shown in Fig. 4.20 and presented by Dittmar and Hartmann (1976), Grossmann and Sargent (1978), Ostrovsky et al. (2000), is investigated.

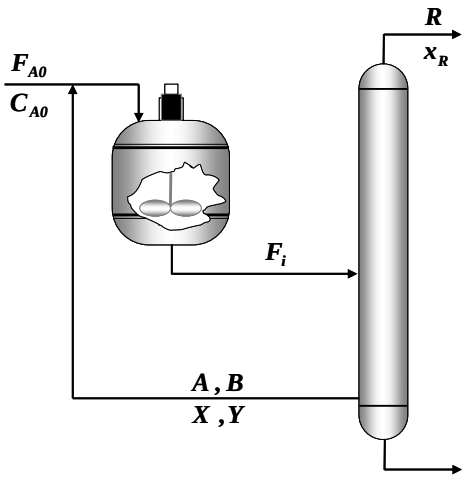

Figure 4.20: Reactor-separator system

The system consists of a continuous stirred tank reactor, in which Denbigh´s reaction takes place with first-order irreversible kinetics. The CSTR is connected in series with an ideal separator. The Denbigh kinetics are given as follows,

$$\begin{array}{ccccc} A & \xrightarrow{k_B} & B & \xrightarrow{k_R} & R \\ \downarrow{\scriptstyle k_X} & & \downarrow{\scriptstyle k_Y} & & \\ X & & Y & & \end{array} \tag{4.95}$$

The feed flow of raw material into the reactor comprises only component A in a molar concentration C_{A0}. The reaction product includes all components. From the separator overhead, a product stream containing the desired product R is drwan while the rest of the components are either recycled or sent downstream for further processing. Components A and B are recycled at the ratio of λ, and components X and Y at the ratio of β with reference to the amount of these components in the separator feed. The ratios of molar concentrations C_i of the components (i = A, B, R, X, Y) to C_{A0} are denoted with x_i, the molar flow rate of raw material with F_{A0}, and the molar flow rate of the reactor feed with F_i. However, the steady-state process operation, assuming isothermal conditions, constant density, and liquid-phase reaction are then described by the following set of nonlinear equations:

$$\begin{aligned}
&F_{A0} + \lambda F_i x_A - F_i x_A - V(k_B + k_X) C_{A0} x_A && = 0 \\
&\lambda F_i x_B - F_i x_B + V C_{A0} \{k_B x_A - (k_R + k_Y) k_B\} && = 0 \\
&\beta F_i x_X - F_i x_X + V C_{A0} k_X x_A && = 0 \\
&\beta F_i x_Y - F_i x_Y + V C_{A0} k_Y x_B && = 0 \\
&-F_i + V C_{A0} k_R x_B && = 0 \\
&x_A + x_B + x_R + x_X + x_Y - 1 && = 0
\end{aligned} \tag{4.96}$$

The required amount of R and the sum of the molar concentrations of the products X and Y are given:

$$\begin{aligned} F_i\, x_R &= q_1 \\ C_{A0}\left(x_X + x_Y\right) &= q_2 \end{aligned} \tag{4.97}$$

The nominal values and the data necessary for simulation and optimization are listed in Table 4.5. The aim of the design optimization is to minimize the total cost of the system which is defined by the equipment (reactor volume) and the recycle costs. C_1 and C_2 denote the respective prices.

$$\mathcal{J} = C_1 V + C_2 \left\{\lambda F_i \left(x_A + x_B\right) + \beta F_i \left(x_X + x_Y\right)\right\} \tag{4.98}$$

The deterministic optimization problem for the reactor-separator design is first solved using the nominal values of the model parameters. The optimization problem is defined by the objective function (4.98) and the constraints (4.96) and (4.97) while complying with a product concentration restriction of $x_R \geq 25\%$. The decision variables are the reactor volume V, and the factors λ and β.

Table 4.5: Data for the reactor-separator system

$F_{A0} = 100\,\text{mol/h}$	$C_{A0} = 0.1\,\text{mol/l}$	$k_X = 0.02\,\text{h}^{-1}$
$C_1 = 0.01\,\text{u€/l}$	$C_2 = 0.125\,\text{u€/(mol/h)}$	$k_Y = 0.01\,\text{h}^{-1}$
$q_1 = 70\,\text{mol/h}$	$q_2 = 0.005\,\text{mol/h}$	
$k_B = 0.4\,\text{h}^{-1}$	$k_R = 0.1\,\text{h}^{-1}$	

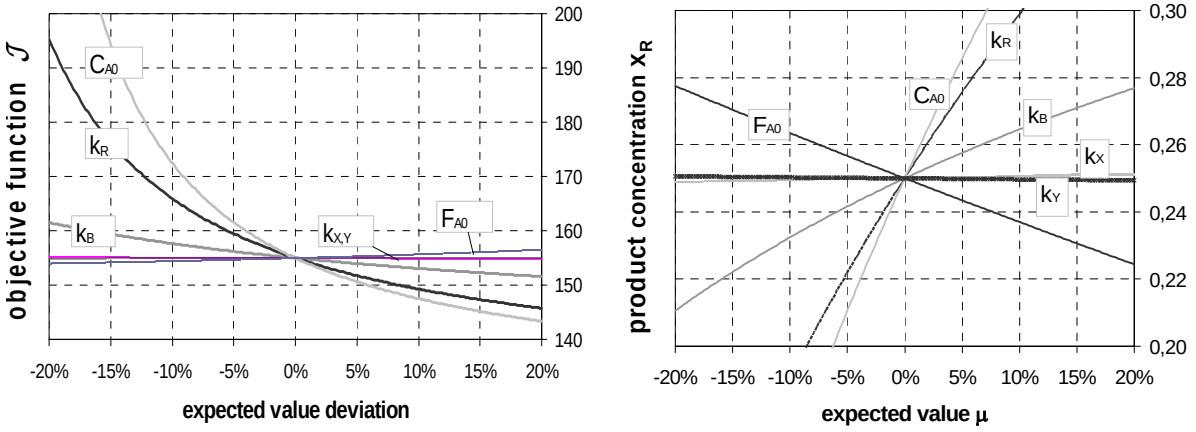

(a) (b)

Figure 4.21: Objective function and product concentration x_R in dependence on the expected value deviation of the model parameters.

In Fig. 4.21 the simulation studies based on the deterministic optimization results show the influence of the different reaction rates, the feed flowrate F_{A0} and its concentration C_{A0} on the objective function $\mathcal{J}$ and on the product concentration. For this purpose, the parameters were varied 20% around their expected values. From Figure (4.21b), the perturbation analysis on the deterministic outcomes demonstrates that the three most relevant parameters are the feed flowrate F_{A0}, and the reaction rates k_B, k_R. However, provided that C_{A0} is constant, these

parameters are assumed to be the only sources of uncertainty. They are assumed to be distributed normally with a standard deviation of 5% from the mean value. The resulting probability density and distribution functions are given in Figure 4.22.

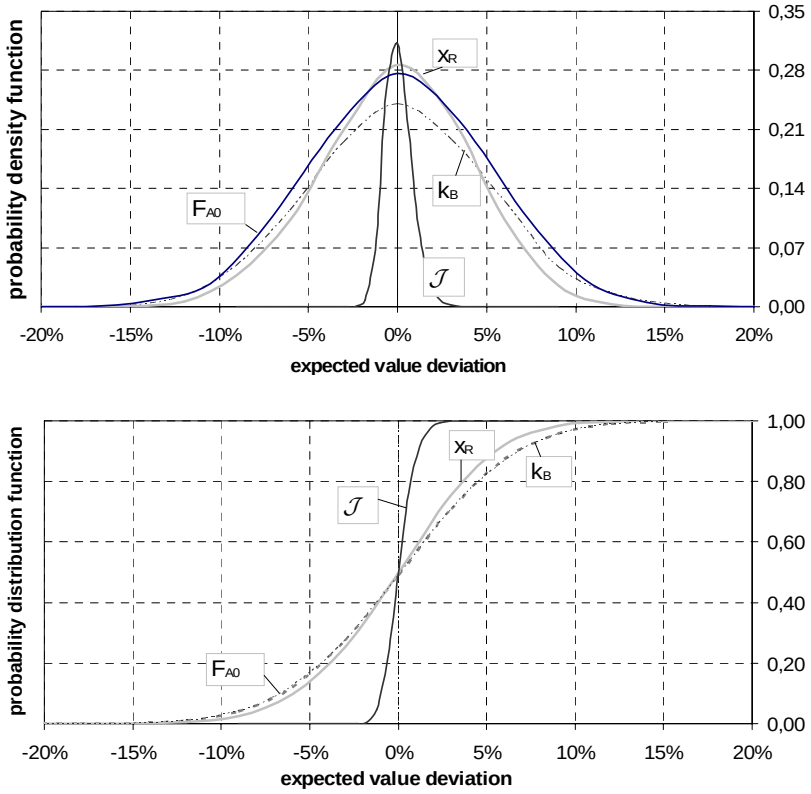

Figure 4.22: Probability density and distribution function

Monte Carlo simulations (5000 samples) have been performed to determine the effect of uncertainty on the deterministic optimization results. The results in Figure 4.23 show the high probability (~50%) for the product quality constraint violation. Therefore, for a robust design the explicit consideration of uncertainties within the optimization problem is needed.

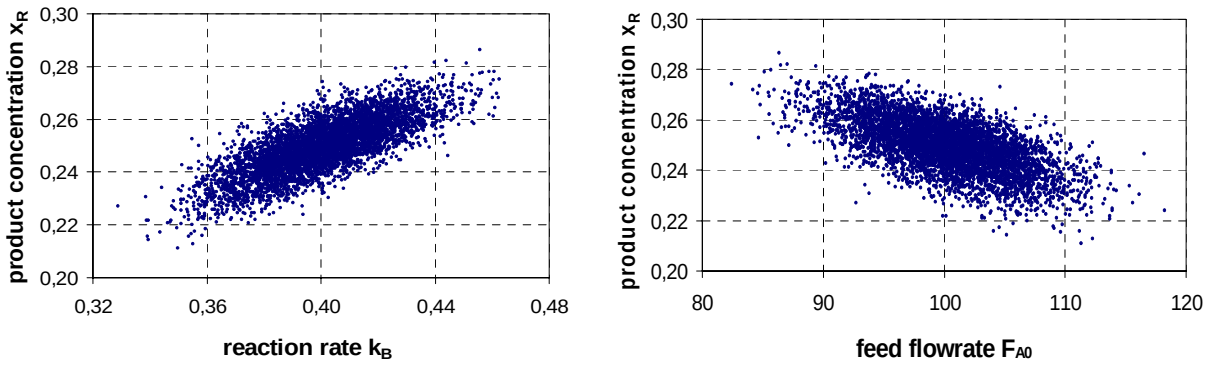

Figure 4.23: Performance of the deterministic optimization through Monte Carlo simulations.

In order to formulate the chance-constrained optimization problem, the uncertain parameters form the joint normal distribution. Here, the correlation matrix elements may result from parameter estimation. Derived from Figure (4.21b) and further simulation results, a strict monotonic relation between the constrained output (product quality) and the nominated

uncertain parameters can be determined. Since the monotony of at least one uncertain parameter is only required for the application of the *nonlinear* chance-constrained approach, the reaction rate k_B is selected as the random variable to compute the bound of the region of the uncertain variables. Thus, the chance-constrained optimization problem can be formulated as follows,

$$\begin{aligned} &\min \quad \mathcal{J} \\ &\text{s.t.} \quad \text{equality constraints (4.96) and (4.97)} \\ &\qquad \Pr(x_R \geq x_R^{SP}) \geq \alpha \\ &\qquad 0 \leq \lambda \leq 1 \\ &\qquad 0 \leq \beta \leq 1 \\ &\qquad 0 \leq x_A, x_B, x_R, x_X, x_Y \leq 1 \end{aligned} \tag{4.99}$$

The decision variables are the reactor volume, λ and β. Due to the dependence of the product concentration on the random variables, the fulfilment of the inequality constraint is described as a chance constraint. It can then be shown that a positive monotonic relation exists, namely $x_R \uparrow \Rightarrow k_B \uparrow$ and, thus, $P\{x_R \geq x_R^{SP}\}$ can be restated as $1 - P\{k_B \leq k_B^L\}$ compliant with (4.71) and (4.72). Besides, based on the realization of the other uncertain variables, the product quality restriction x_R^{SP}, as well as the value of the decision variables, the upper bound for the random variable k_B is then:

$$k_B^L = F^{-1}(F_{A0}, k_R, x_R^{SP}, V, \lambda, \beta) \tag{4.100}$$

Therefore, following (4.75) k_B^L can be used as the upper bound for the numerical integration,

$$\Pr\{x_R \geq x_R^{SP}\} = \int_{-\infty}^{\infty} \cdots \int_{-\infty}^{\infty} \int_{-\infty}^{k_B^L} \rho(F_{A0}, k_R, k_B) dk_B dk_R dF_{A0} \tag{4.101}$$

Based on the computational scheme described in section 4.2.3, the multivariate integration in (4.101) is computed with the three-point-collocation and an inaccuracy less than 10^{-6}. The outcomes of the robust design optimization under uncertainty are depicted in Figure 4.24. The robustness of the optimal design is thereby demonstrated by sampling the random parameters.

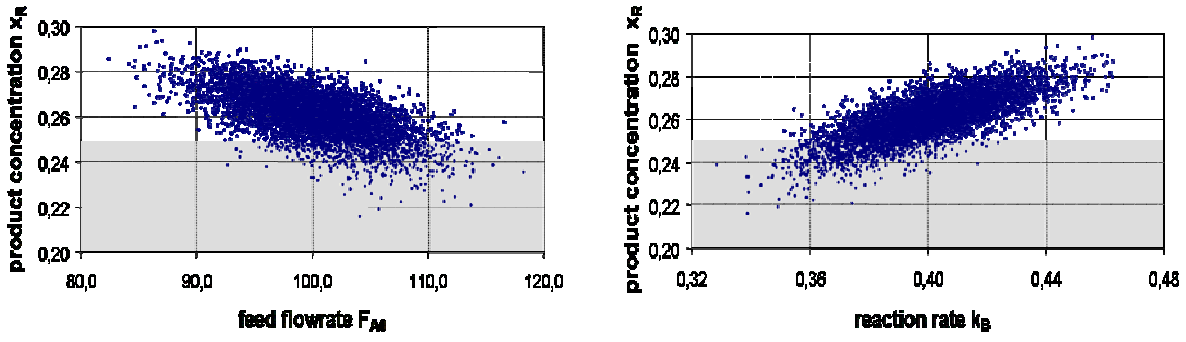

Figure 4.24: Scatter plots showing the impact of parameter uncertainties on the constrained output.

However, the Monte Carlo simulations (5000 samples) indicate that, as anticipated, a risk of constraint violation of 10% results from the stochastic optimization for $\alpha = 0.9$. Table 4.6 provides additional details from the results of the chance-constrained optimization in comparison with those of the deterministic optimization. Here, the deterministic case and three additional stochastic cases are listed with regard to different probability levels.

	$\mathcal{J}$	α	x_R^{SP}	V	λ	β
deterministic	154.2995	--	0.25	12759.927	0.919	0.275
Stochastic	160.5967	0.90	0.25	11957.747	0.943	0.448
	172.1216	0.93	0.25	11746.478	0.956	0.549
	184.9851	0.96	0.25	11260.653	0.963	0.613

Table 4.6: Deterministic and stochastic optimization results

The uncertainties are not only compensated for by variation of the reactor volume but also by further change of the decision variables λ and β. It can also be seen that the total cost increases if a higher probability level is required, i.e. the total cost resulting from the deterministic optimization is lower. But, implementations of decisions based on the deterministic results are not appropriate due to the high risk of constraint violation (see Fig. 4.23). One important effect observed is that the stochastic optimization results become increasingly sensitive to the specified probability level α as it approaches the maximum achievable probability of complying with the constraint. In Chapter 6, this issue is discussed in detail for a large-scale process system.

4.3 Summary

Under the framework of *linear* systems, which are defined through a linear relation between the uncertain input and the output constraints, efficient approaches are presented with stochastic variables with correlated multivariate normal distribution combining numerical integration and sampling methods. Thus, for instance, a continuous process with constant uncertain inputs leads to a *steady-state* problem, while a continuous process with time-dependent uncertain inputs represents a *dynamic* problem under uncertainty. However, in case of a *nonlinear* process it is very difficult to describe the distribution of the outputs analytically. In this case, sampling techniques can generally be employed. For this purpose, a scheme of *simulation* with sampling can address this problem. According to their distributions, random values are generated. After simulation runs with the sampled data, the probability distribution of the outputs can be obtained. Besides Monte-Carlo, some other efficient sampling strategies also have been proposed (Diwekar and Kalagnanam, 1997).

As an alternative to sampling techniques, a method for nonlinear chance-constrained programming has been introduced in this Chapter. The basic idea of the method is to map the output distribution onto that of the uncertain input variables. Since the uncertainty properties are taken into account, the solution of the problem is a decision *a priori*. A predefined probability to satisfy the constraints will be held under the uncertainty and thus the decision is robust. The solution provides a comprehensive relationship between the performance criteria and the probability level of satisfying the constraint (Section 4.2.4). For linear systems, an easy-to-use method is proposed to determine the maximum feasible confidence level by simulation.

However, the performance of the method is limited to the problem definition of steady state processes with just one single chance constraint. For other relevant processes, in particular, dynamic systems including operation and control tasks under uncertainty (e.g. time-dependent uncertainties), the approach needs to be extended including also those cases where the definition of multiple single probabilistic constraints is required. In this case, different confidence levels can be selected for different output constraints when some output constraints are more critical than the others. Furthermore, the extension of the approach to a joint chance-constrained problem is not a trivial task, but is necessary, if the constraints are related to e.g. safety considerations where reliability is required over the entire output feasible region. Moreover, as identified in section 4.1.4, an important open issue in solving chance-constrained programming problems is the feasibility analysis, which is still pending to be analyzed for nonlinear dynamic processes. Thus, development of more efficient methods to address high dimension problems, e.g. **N**onlinear **D**ynamic Systems under **T**ime-dependent Uncertainty and **J**oint constraints (NDTJ), represents a significant challenge. For this purpose, in the next Chapters, a new promising chance constrained optimization framework and its applications to process optimization and control under uncertainty is introduced and discussed to illustrate its efficiency and potential.

Chapter 5

A New Stochastic Optimization Framework for Nonlinear Dynamic Systems under Chance Constraints

In this Chapter, a new framework with different approaches for chance constrained programming of large-scale nonlinear *dynamic* systems under time-dependent and time-independent uncertainty is presented which focuses on the reliability of the system, i.e., the system's ability to meet feasibility in an uncertain environment. The stochastic property of the uncertainties is explicitly considered in the problem formulation in which some input and state constraints are to be complied with predefined probability levels. The method considers a *nonlinear* relation between the uncertain input and the constrained variables. Following the idea introduced in the previous Chapter, the concept is basically to map the output feasible region (distribution) back to a bounded region of the uncertain input variables; so that the probability of complying with the output constraints and their gradients can be achieved by numerical integration of the probability density function of the multivariate correlated uncertain variables by collocation in finite elements. By this means, the original idea is now applicable for dynamic optimization problems with larger scale. The framework involves new efficient algorithms for the required back-mapping as well as for the computation of single and joint probabilities and their gradients with an optimal number of collocation points. The formulation and tuning of predefined probability limits incorporate the issue of feasibility and the contemplation of trade-off between the objective function (profitability) and robustness. Thus, the results can be used to select optimal and robust operation policies. The approach is relevant to all cases when uncertainty can be described by any kind of joint correlated multivariate distribution functions.

In chemical process industry, transient process operations have significantly increased. Thus, from a practical viewpoint, the development of optimal policies and/or the design of a control system for optimal operation on time-varying trajectories pose a major challenge. However, approaches that consider the system capability to readily adjust in order to meet the requirements of changing conditions or to recover from process disturbances or dynamic plant behaviour are rather limited. In this Chapter, fundamental developments of a new chance-constrained optimization framework are described. To demonstrate its efficiency and potential, it is used to obtain among others strategies for operation planning as well as integrated process and control systems design, which are economically optimal and can cope

with model uncertainty and process disturbances. Based on a dynamic mathematical model describing the process, including path constraints, interior and end-point constraints such as product specifications and safety restrictions, and relations describing uncertain parameters and time-varying disturbances (probability distributions), the problem is posed as a stochastic nonlinear dynamic optimal formulation within a finite time horizon of interest.

5.1 Strict monotonic relationship between constrained output and uncertain input

The main significance of considering dynamic optimization problems under uncertainty is based on the fact that the solution of the chance-constrained problem has the feature of prediction and robustness. The predictive strategy is derived for a future time horizon where output constraints are to be complied with a certain probability level. This means, depending on the stochastic property of the uncertainties, the process operation will be planned so that large changes of the uncertain disturbances can optimally be compensated while complying with the output constraints and leading to a better performance of the objective function.

The key idea is to avoid direct computing the output probability distribution. Instead, an equivalent representation of the probability is derived by mapping the probabilistic constrained output region back to a bounded region of the uncertain inputs. Since dynamic systems with multiple time intervals are now considered, the reverse projection (mapping) of the output feasible region is not trivial. Furthermore, a more efficient *dynamic solver* is required in order to solve dynamic problems with time-dependent constraint variables and the uncertain parameters occurring throughout the entire operation time with different control parameters **u** in different time intervals.

The conceptual mathematical formulation is given by a set of differential and algebraic equations and inequalities of the following form:

$$
\begin{aligned}
&\min \mathrm{E}\left[\mathrm{f}\left(\mathbf{x}, \mathbf{y}, \mathbf{u}, \mathrm{t_C}; \boldsymbol{\xi}\right)\right] + \omega \mathrm{D}\left[\mathrm{f}\left(\mathbf{x}, \mathbf{y}, \mathbf{u}, \mathrm{t_C}; \boldsymbol{\xi}\right)\right] \\
&\text{s.t.} \quad \mathbf{g}(\dot{\mathbf{x}}, \mathbf{x}, \mathbf{y}, \mathbf{u}, \mathrm{t}, \boldsymbol{\xi}) = 0, \\
&\qquad \mathrm{Pr_i}\left\{\mathbf{h}\left(\dot{\mathbf{x}}, \mathbf{x}, \mathbf{y}, \mathbf{u}, \mathrm{t}; \boldsymbol{\xi}\right) \geq 0\right\} \geq \alpha_{\mathrm{i}} \quad \Rightarrow \quad \mathrm{Pr_i}\left\{\mathrm{y_i} \leq \mathrm{y_i^{SP}}\right\} \geq \alpha_{\mathrm{i}},\ \mathrm{i} = 1, \cdots, \mathrm{L} \quad \text{(single)} \quad \vee \\
&\qquad \mathrm{Pr}\left\{\mathbf{h}'\left(\dot{\mathbf{x}}, \mathbf{x}, \mathbf{y}, \mathbf{u}, \mathrm{t}; \boldsymbol{\xi}\right) \geq 0\right\} \geq \alpha \quad \Rightarrow \quad \mathrm{Pr}\left\{\mathrm{y_i} \leq \mathrm{y_i^{sp}},\ \mathrm{i} = 1, \cdots, \mathrm{M}\right\} \geq \alpha \quad \text{(joint)} \\
&\qquad \mathbf{k}\left(\mathbf{u}, \mathrm{t}\right) \geq 0 \qquad\qquad \mathbf{h}' \subseteq \Re^{\mathrm{M}};\quad \mathrm{M} \neq \mathrm{L} \qquad\qquad (5.1) \\
&\qquad \mathbf{i}_0\left(\dot{\mathbf{x}}(0), \mathbf{x}(0), \mathbf{y}, \mathbf{u}(0), \mathrm{t_C}; \boldsymbol{\xi}\right) = 0, \\
&\qquad \mathbf{y}_{\min} \leq \mathbf{y} \leq \mathbf{y}_{\max}, \\
&\qquad \mathbf{u}_{\min} \leq \mathbf{u} \leq \mathbf{u}_{\max}, \\
&\qquad \mathrm{t_0} \leq \mathrm{t_C} \leq \mathrm{t_f}
\end{aligned}
$$

Where:

$\mathrm{f} \subseteq \Re^{1}$	Time-dependent objective function
$\mathbf{g} \subseteq \Re^{\mathrm{n+L}}$	Dynamic model equations
$\mathbf{h} \subseteq \Re^{\mathrm{L}}$	Inequality constraints influenced by uncertain parameters
$\mathbf{k} \subseteq \Re^{\mathrm{H}}$	Inequality constraints independent of uncertain parameters

$\mathbf{x} \subseteq \Re^n$	Time-dependent unconstrained state (output) variables
$\mathbf{y} \subseteq \Re^L$	Time-dependent constrained state (output) variables
$\mathbf{u} \subseteq \Re^M$	Time-dependent decision variables
$\xi \subseteq \Re^S$	Uncertain variables
$\mathbf{y}^{SP} \subseteq \Re^L$	Output variables bounds

The equality constraints represent the process model equations but could also comprise constraints on the process or performance requirements. The inequality constraints are typically related to equipment limitations, safety regulations, environmental and/or product purity specifications, but some of them are not necessary dependent on the uncertain variables $\mathbf{k} \subseteq \Re^H$. They have to be satisfied throughout the period of operation or only imposed at specific times t_C. However, while inequality constraints regarding bounds on process inputs can be easily satisfied by the actual system, constraints on process outputs are more indefinable. Due to the uncertainty, process output predictions are then also uncertain leading to violation of constrained outputs. Thus, uncertainty incorporation into the output constraints is required and needs to be considered in the optimization problem formulation. The main challenge in chance constrained programming lies in calculating probability values, the gradients of the probability function to the controls and possibly Hessians. In case of dynamic systems, the problem has different degrees of complexity for computing these values, which will be discussed in the next sections.

5.1.1 Solution approach

In this section, a systematic methodology is presented which can be applied to large scale dynamic problems in a reasonable computation time. The method considers a nonlinear relation between the uncertain input and the constrained variables. The procedure of the dynamic solver implies two basic steps:

i) The reverse projection of the feasible region for solving dynamic problems
ii) The computation of the joint or multiple single probabilities and their sensitivities.

5.1.1.1 Reverse projection of the feasible region

The computation of the time-dependent uncertain variable boundaries through reverse projection according to

$$\xi_s^L = F^{-1}\left(\xi_1, \cdots, \xi_{s-1}, y_i^{SP}, t, \mathbf{u}\right), \tag{5.2}$$

is not trivial. Due to the model complexity, an explicit expression of (5.2) is usually not available. For steady-state problems a Newton-Raphson step has been found to be suitable (see section 4.2.2). However, in order to solve dynamic optimization problems under chance constraints, a more general and efficient approach is required. As a consequence of the model complexity, an additional iterative procedure is employed in order to calculate the limiting value ξ_s^L. Here, the desired value is approximated through multiple simulations embedded in the so-called *reverse projection approach* which is basically based on the bisectional method. Figure 5.1 shows a scheme of the restricted region by $[\xi_a, \xi_b]$ where the bound ξ_s^L according to the constrained output y^{SP} can be searched. This region corresponds to the integration area where the multivariate integration is also carried out. Firstly, the function values y_i of the

corresponding interval endpoints (ξ_a, ξ_b) are defined and verified to ensure that the reverse projection value is located inside of the interval (Fig. 5.1).

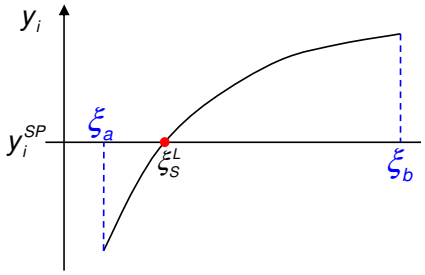

Figure 5.1: Search-space for the reverse projection

The reverse projection approach is a systematic, iterative method which is used to find a "root" $\xi_s^L\left(y_i^{SP}\right)$ of a monotonic continuous function (Fig. 5.2). The algorithm picks midpoints of ξ_S within the interval (ξ_a, ξ_b) and after computing their corresponding output value y_i, one of the interval endpoints is then changed depending on whether the y_i is greater or less than $y_i\left(\xi_a\right)$ or $y_i\left(\xi_b\right)$. Afterwards, half of the original interval is discarded and the midpoint is assigned to one of the endpoints. After a few iterations, the algorithm yields an approximation of the required bound value ξ_s^L, with a given specified tolerance. The only required inputs for the approach would be the tolerance, the endpoints of the original interval, the maximum number of iterations, and the function values from just one simulation run for each iteration step. By this means convergence can be guaranteed. Moreover, the success of the presented approach is based on the size of the original interval.

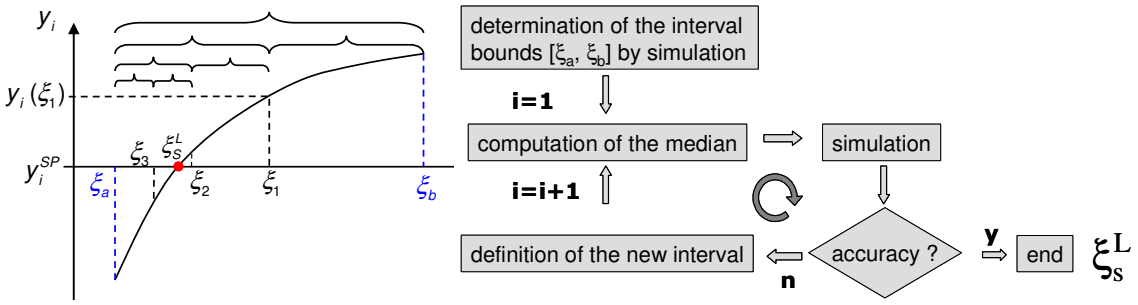

Figure 5.2: The reverse projection approach.

The approach converges linearly because the width of the bracketed range decreases by a factor of two after each iteration. However, it can be slightly improved by interpolating the successive approximated roots ξ_S between the function's values y_i at the interval endpoints. This modification leads to the method which is also known as linear inverse interpolation, the false-position method. It is similar to the method presented above, but instead of the midpoint we take a point defined by an intersection of the secant line joining the points $\left[\xi_a, y_i\left(\xi_a\right)\right]$ and $\left[\xi_b, y_i\left(\xi_b\right)\right]$ with the ξ_s-axis (Fig. 5.3).

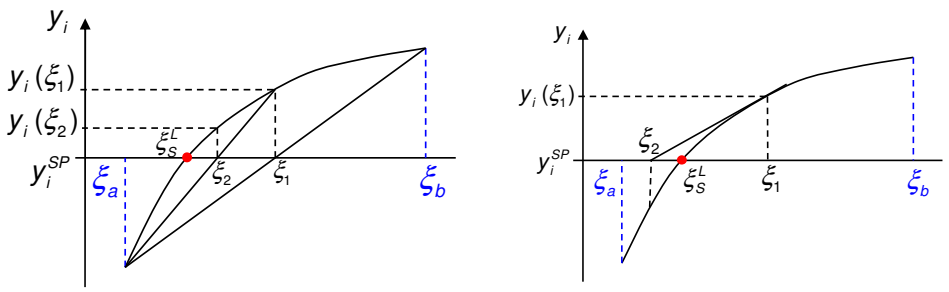

Figure 5.3: (a) Linear inversion interpolation (b) Newton Method

Both methods used in this work assume a monotonic continuous function. The linear inverse interpolation uses a pair of points, essentially to figure out the slope of the function, and hence where it will cross the axis. In contrast, Newton's method will linearize the unknown function, but its data is now all gathered at the latest point. The Newton's method is admittedly faster than the methods presented, but it unfortunately requires both the function and its derivative which makes the programming unnecessary complex apart from computing time. Furthermore, there is not always a guarantee for convergence.

5.1.1.2 Computing the gradients of the probability

The computation of the gradients of the output constraint probability gradients with respect to the decisions variables **u** is based on the formulation of the total differential of the model equations $\mathbf{g}\left(\mathbf{x},\mathbf{u},t,\xi_1,\cdots\xi_s^L\right)$,

$$d\mathbf{g}=\left[\frac{\partial \mathbf{g}}{\partial \mathbf{x}}\frac{\partial \mathbf{x}}{\partial \mathbf{u}}\right]d\mathbf{u}+\left[\frac{\partial \mathbf{g}}{\partial \xi_s^L}\frac{\partial \xi_s^L}{\partial \mathbf{u}}\right]d\mathbf{u}+\left[\frac{\partial \mathbf{g}}{\partial \mathbf{u}}\right]d\mathbf{u}=\mathbf{0}. \tag{5.3}$$

Firstly, according to the calculated boundary value ξ_s^L (Eq. 5.2), we define the following function $\mathfrak{F}$ corresponding to the feasible region

$$\begin{aligned}\Pr\left\{\ y\ \le y^{SP}\right\}&=\Pr\left\{\xi_s\le\xi_s^L,\xi_k\subseteq\Re^s,s\ne k\right\}\\&=\mathfrak{F}\left(\xi_s^L\right)=\int_{\Xi_s}\cdots\left[\int_{-\infty}^{\xi_s^L}\rho\left(\xi_1,\cdots,\xi_{s-1},\xi_s^L\right)d\xi_s\right]d\xi_1\cdots d\xi_k\end{aligned}. \tag{5.4}$$

The right-hand side of (5.4) represents the numerical integration in the bounded input region. Thus, the gradients computation can be formulated as follows

$$\frac{d\Pr}{d\mathbf{u}}=\frac{d\mathfrak{F}}{d\xi_s^L}\frac{\xi_s^L}{d\mathbf{u}}=\int_{\Xi_s}\cdots\left[\rho\left(\xi_1,\cdots,\xi_{s-1},\xi_s^L\right)\frac{d\xi_s}{d\mathbf{u}}\bigg|_{\xi_s^L}\right]d\xi_k\cdots d\xi_1, \tag{5.5}$$

whereas the values of $\left.\frac{d\xi_s}{d\mathbf{u}}\right|_{\xi_s^L}$ in (5.5) will be calculated in accordance with the model equations **g** through

$$\left[\frac{\partial \mathbf{g}}{\partial \mathbf{x}}\right] d\mathbf{x} + \left[\frac{\partial \mathbf{g}}{\partial \mathbf{u}}\right] d\mathbf{u} + \left[\frac{\partial \mathbf{g}}{\partial \xi_s^L}\right] d\xi_s^L = \mathbf{0} \quad , \tag{5.6}$$

which can be rewritten by the following way

$$\left[\frac{\partial \mathbf{g}}{\partial \mathbf{x}}\frac{\partial \mathbf{x}}{\partial \mathbf{u}}\right] d\mathbf{u} + \left[\frac{\partial \mathbf{g}}{\partial \xi_s^L}\frac{\partial \xi_s^L}{\partial \mathbf{u}}\right] d\mathbf{u} + \left[\frac{\partial \mathbf{g}}{\partial \mathbf{u}}\right] d\mathbf{u} = \mathbf{0}\,. \tag{5.7}$$

This leads to

$$\left[\frac{\partial \mathbf{g}}{\partial \mathbf{x}} \quad \frac{\partial \mathbf{g}}{\partial \xi_s^L}\right] \begin{bmatrix} \frac{\partial \mathbf{x}}{\partial \mathbf{u}} \\ \frac{\partial \xi_s^L}{\partial \mathbf{u}} \end{bmatrix} = -\left[\frac{\partial \mathbf{g}}{\partial \mathbf{u}}\right]. \tag{5.8}$$

To clarify the applicability of the presented solution strategy, let us consider a simple example for a dynamic process with the following attributes:

$y_1(t), y_2(t), y_3(t), y_4(t)$	4 time-dependent constrained state variables
$u_1(t), u_2(t), u_3(t)$	3 time-dependent control variables
$\xi_1, \xi_2 \left(\xi_1 \in \Xi_1, \xi_2 \in \Xi_2\right)$	2 static uncertain variables

With the initial state: $y_1(0), y_2(0), y_3(0), y_4(0)$, a process with one single output end-point chance constraint is contemplated, namely $y_1(t_f) \le y_1^{SP}$. The inequality output constraint is then formulated as a chance constraint of the form $P\{y_1 \le y_1^{SP}\}$ for $t \in [t_0, t_f]$. Based on the impacts of the uncertain parameters on the constrained output variable, a strict monotonic relation between ξ_1 and y_1 is assumed to be $\xi_1 \uparrow \Rightarrow y_1 \uparrow$ such that

$$P\{y_1 \le y_1^{SP}\} = P\{\xi_1 \le \xi_1^L, \xi_2 \in \Xi_2\}\,.$$

Using orthogonal collocation, the discretized nonlinear model equations in time interval j are represented as,

$$\begin{aligned}
g_1(y_1(j), y_2(j), y_3(j), y_4(j), u_1(j), u_2(j), u_3(j), \xi_1, \xi_2) &= 0 \\
g_2(y_1(j), y_2(j), y_3(j), y_4(j), u_1(j), u_2(j), u_3(j), \xi_1, \xi_2) &= 0 \\
g_3(y_1(j), y_2(j), y_3(j), y_4(j), u_1(j), u_2(j), u_3(j), \xi_1, \xi_2) &= 0 \\
g_4(y_1(j), y_2(j), y_3(j), y_4(j), u_1(j), u_2(j), u_3(j), \xi_1, \xi_2) &= 0
\end{aligned}.$$

If three time intervals with piecewise constant decision variables or controls **u** are considered, the upper bound of the integration is then expressed as a function of,

$$\xi_1^L(y_1(0), y_2(0), y_3(0), y_4(0), u_1(1), u_2(1), u_3(1), u_1(2), u_2(2), u_3(2), u_1(3), u_2(3), u_3(3), y_1^{SP}, \xi_2)$$

Analog to (5.5) the probability computation is then stated as follows,

$$\mathrm{P}\{\xi_1 \le \xi_1^{\mathrm{L}}, \xi_2 \in \Xi_2\} = \mathfrak{F}(\xi_1^{\mathrm{L}}) = \int_{\xi_2 \in \Xi_2} \left[\int_{-\infty}^{\xi_1^{\mathrm{L}}} \rho(\xi_1, \xi_2) \mathrm{d}\xi_1 \right] \mathrm{d}\xi_2$$

The gradient computation can be derived as

$$\frac{\mathrm{d}\,\mathrm{Pr}}{\mathrm{d}\mathbf{u}} = \frac{\mathrm{d}\mathfrak{F}}{\mathrm{d}\xi_1^{\mathrm{L}}} \frac{\mathrm{d}\xi_1^{\mathrm{L}}}{\mathrm{d}\mathbf{u}} = \int_{\xi_2 \in \Xi_2} \left[\rho(\xi_1^{\mathrm{L}}, \xi_2) \frac{\mathrm{d}\xi_1^{\mathrm{L}}}{\mathrm{d}\mathbf{u}} \right] \mathrm{d}\xi_2$$

with the unknown variables

$$\mathrm{y}_1(1), \mathrm{y}_2(1), \mathrm{y}_3(1), \mathrm{y}_4(1), \mathrm{y}_1(2), \mathrm{y}_2(2), \mathrm{y}_3(2), \mathrm{y}_4(2), \xi_1^{\mathrm{L}}, \mathrm{y}_2(3), \mathrm{y}_3(3), \mathrm{y}_4(3)$$

and given

$$\mathrm{u}_1(1), \mathrm{u}_2(1), \mathrm{u}_3(1), \mathrm{u}_1(2), \mathrm{u}_2(2), \mathrm{u}_3(2), \mathrm{u}_1(3), \mathrm{u}_2(3), \mathrm{u}_3(3), \xi_2,$$

the resulting equation system for 3 time intervals can be formulated as follows,

$$\begin{aligned}
\mathrm{g}_1(\mathrm{y}_1(1), \mathrm{y}_2(1), \mathrm{y}_3(1), \mathrm{y}_4(1), \mathrm{u}_1(1), \mathrm{u}_2(1), \mathrm{u}_3(1), \xi_1^{\mathrm{L}}, \xi_2) &= 0 \\
\mathrm{g}_2(\mathrm{y}_1(1), \mathrm{y}_2(1), \mathrm{y}_3(1), \mathrm{y}_4(1), \mathrm{u}_1(1), \mathrm{u}_2(1), \mathrm{u}_3(1), \xi_1^{\mathrm{L}}, \xi_2) &= 0 \\
\mathrm{g}_3(\mathrm{y}_1(1), \mathrm{y}_2(1), \mathrm{y}_3(1), \mathrm{y}_4(1), \mathrm{u}_1(1), \mathrm{u}_2(1), \mathrm{u}_3(1), \xi_1^{\mathrm{L}}, \xi_2) &= 0 \\
\mathrm{g}_4(\mathrm{y}_1(1), \mathrm{y}_2(1), \mathrm{y}_3(1), \mathrm{y}_4(1), \mathrm{u}_1(1), \mathrm{u}_2(1), \mathrm{u}_3(1), \xi_1^{\mathrm{L}}, \xi_2) &= 0
\end{aligned}$$

$$\begin{aligned}
\mathrm{g}_1(\mathrm{y}_1(2), \mathrm{y}_2(2), \mathrm{y}_3(2), \mathrm{y}_4(2), \mathrm{u}_1(2), \mathrm{u}_2(2), \mathrm{u}_3(2), \xi_1^{\mathrm{L}}, \xi_2) &= 0 \\
\mathrm{g}_2(\mathrm{y}_1(2), \mathrm{y}_2(2), \mathrm{y}_3(2), \mathrm{y}_4(2), \mathrm{u}_1(2), \mathrm{u}_2(2), \mathrm{u}_3(2), \xi_1^{\mathrm{L}}, \xi_2) &= 0 \\
\mathrm{g}_3(\mathrm{y}_1(2), \mathrm{y}_2(2), \mathrm{y}_3(2), \mathrm{y}_4(2), \mathrm{u}_1(2), \mathrm{u}_2(2), \mathrm{u}_3(2), \xi_1^{\mathrm{L}}, \xi_2) &= 0 \\
\mathrm{g}_4(\mathrm{y}_1(2), \mathrm{y}_2(2), \mathrm{y}_3(2), \mathrm{y}_4(2), \mathrm{u}_1(2), \mathrm{u}_2(2), \mathrm{u}_3(2), \xi_1^{\mathrm{L}}, \xi_2) &= 0
\end{aligned}$$

$$\begin{aligned}
\mathrm{g}_1(\mathrm{y}_1^{\mathrm{SP}}, \mathrm{y}_2(3), \mathrm{y}_3(3), \mathrm{y}_4(3), \mathrm{u}_1(3), \mathrm{u}_2(3), \mathrm{u}_3(3), \xi_1^{\mathrm{L}}, \xi_2) &= 0 \\
\mathrm{g}_2(\mathrm{y}_1^{\mathrm{SP}}, \mathrm{y}_2(3), \mathrm{y}_3(3), \mathrm{y}_4(3), \mathrm{u}_1(3), \mathrm{u}_2(3), \mathrm{u}_3(3), \xi_1^{\mathrm{L}}, \xi_2) &= 0 \\
\mathrm{g}_3(\mathrm{y}_1^{\mathrm{SP}}, \mathrm{y}_2(3), \mathrm{y}_3(3), \mathrm{y}_4(3), \mathrm{u}_1(3), \mathrm{u}_2(3), \mathrm{u}_3(3), \xi_1^{\mathrm{L}}, \xi_2) &= 0 \\
\mathrm{g}_4(\mathrm{y}_1^{\mathrm{SP}}, \mathrm{y}_2(3), \mathrm{y}_3(3), \mathrm{y}_4(3), \mathrm{u}_1(3), \mathrm{u}_2(3), \mathrm{u}_3(3), \xi_1^{\mathrm{L}}, \xi_2) &= 0
\end{aligned}$$

The equation system can generally be characterized by $\mathbf{g}(\mathbf{y}, \mathbf{u}, \xi_1^{\mathrm{L}}) = 0$ and its solution provides ξ_1^{L}. From (5.3) the total differential is,

$$\left[\frac{\partial \mathbf{g}}{\partial \mathbf{y}}\right] \mathrm{d}\mathbf{y} + \left[\frac{\partial \mathbf{g}}{\partial \mathbf{u}}\right] \mathrm{d}\mathbf{u} + \left[\frac{\partial \mathbf{g}}{\partial \xi_1^{\mathrm{L}}}\right] \mathrm{d}\xi_1^{\mathrm{L}} = \mathbf{0} \;\rightarrow\; \left[\frac{\partial \mathbf{g}}{\partial \mathbf{y}} \;\; \frac{\partial \mathbf{g}}{\partial \xi_1^{\mathrm{L}}}\right] \begin{bmatrix} \mathrm{d}\mathbf{y} \\ \mathrm{d}\xi_1^{\mathrm{L}} \end{bmatrix} = -\left[\frac{\partial \mathbf{g}}{\partial \mathbf{u}}\right] \mathrm{d}\mathbf{u}$$

This is a matrix vector system which can be written as follows

$$
\begin{bmatrix}
\frac{\partial g_{11}}{\partial y_{11}} & \cdots & \frac{\partial g_{11}}{\partial y_{41}} & 0 \cdots 0 & \frac{\partial g_{11}}{\partial \xi_1^L} \\
\vdots & \ddots & \vdots & \vdots \ddots \vdots & \vdots \\
\frac{\partial g_{41}}{\partial y_{11}} & \cdots & \frac{\partial g_{41}}{\partial y_{41}} & 0 \cdots 0 & \frac{\partial g_{41}}{\partial \xi_1^L} \\
\frac{\partial g_{12}}{\partial y_{11}} & \cdots & \frac{\partial g_{12}}{\partial y_{41}} & \frac{\partial g_{12}}{\partial y_{12}} \cdots \frac{\partial g_{12}}{\partial y_{42}} & \frac{\partial g_{12}}{\partial \xi_1^L} \\
\vdots & \ddots & \vdots & \vdots \ddots \vdots & \vdots \\
\frac{\partial g_{42}}{\partial y_{11}} & \cdots & \frac{\partial g_{42}}{\partial y_{41}} & \frac{\partial g_{42}}{\partial y_{12}} \cdots \frac{\partial g_{42}}{\partial y_{42}} & \frac{\partial g_{42}}{\partial \xi_1^L} \\
0 \cdots 0 & \frac{\partial g_{13}}{\partial y_{12}} & \cdots & \frac{\partial g_{13}}{\partial y_{42}} & \frac{\partial g_{13}}{\partial y_{13}} \cdots \frac{\partial g_{13}}{\partial \xi_1^L} \\
\vdots \ddots \vdots & \vdots & \ddots & \vdots & \vdots \\
0 \cdots 0 & \frac{\partial g_{43}}{\partial y_{12}} & \cdots & \frac{\partial g_{43}}{\partial y_{42}} & \frac{\partial g_{43}}{\partial y_{13}} \cdots \frac{\partial g_{43}}{\partial \xi_1^L}
\end{bmatrix}
\begin{bmatrix} dy_{11} \\ dy_{21} \\ dy_{31} \\ dy_{41} \\ dy_{12} \\ dy_{22} \\ dy_{32} \\ dy_{42} \\ dy_{13} \\ dy_{23} \\ dy_{33} \\ d\xi_1^L \end{bmatrix}
= -
\begin{bmatrix}
\frac{\partial g_{11}}{\partial u_{11}} & \cdots & \frac{\partial g_{11}}{\partial u_{31}} & 0 \cdots 0 & 0 \cdots 0 \\
\vdots & \ddots & \vdots & \vdots \ddots \vdots & \vdots \ddots \vdots \\
\frac{\partial g_{41}}{\partial u_{11}} & \cdots & \frac{\partial g_{41}}{\partial u_{31}} & 0 \cdots 0 & 0 \cdots 0 \\
0 \cdots 0 & \frac{\partial g_{12}}{\partial u_{11}} & \cdots & \frac{\partial g_{12}}{\partial u_{31}} & 0 \cdots 0 \\
\vdots \ddots \vdots & \vdots & \ddots & \vdots & \vdots \ddots \vdots \\
0 \cdots 0 & \frac{\partial g_{42}}{\partial u_{12}} & \cdots & \frac{\partial g_{42}}{\partial u_{32}} & 0 \cdots 0 \\
0 \cdots 0 & 0 \cdots 0 & & \frac{\partial g_{13}}{\partial u_{13}} & \cdots \frac{\partial g_{13}}{\partial u_{33}} \\
\vdots \ddots \vdots & \vdots \ddots \vdots & & \vdots & \ddots \vdots \\
0 \cdots 0 & 0 \cdots 0 & & \frac{\partial g_{43}}{\partial u_{13}} & \cdots \frac{\partial g_{43}}{\partial u_{33}}
\end{bmatrix}
\begin{bmatrix} du_{11} \\ du_{21} \\ du_{31} \\ du_{12} \\ du_{22} \\ du_{32} \\ du_{13} \\ du_{23} \\ du_{33} \end{bmatrix}
$$

Where the state variables are represented by, $y_{i,j}$, with i and j as variable and interval index, respectively. Furthermore, by means of Gauss elimination, the gradients can easily be computed. They correspond to the values of the last line of the eliminated matrix.

$$\frac{d\xi_1^L}{d\mathbf{u}} = \left[\frac{\partial \xi_1^L}{du_{11}}, \frac{\partial \xi_1^L}{du_{21}}, \ldots, \frac{\partial \xi_1^L}{du_{33}} \right]^T$$

Thus, we finally deal only with NLP problems (see Chapter 6). For the optimization itself, the sequential approach with a standard NLP solver is used. Consequently, the proposed approach employs a three-staged computation framework to decompose the problem (Fig. 5.4). The upper stage is a superior optimizer following the sequential strategy, where the optimization generates the values of the decision variables and supplies those to the lower stages i.e. simulation stage which also includes the multivariate integration where the probabilities and their gradients are finally calculated. These stages give the values of the objective function, the deterministic and probabilistic constraints, as well as the gradients back to the optimizer.

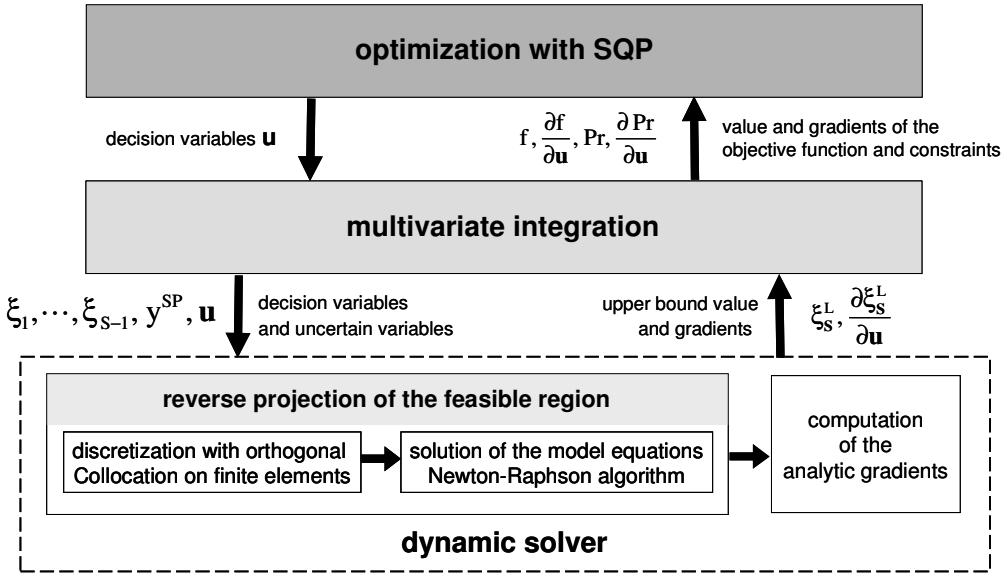

Figure 5.4: Chance-Constrained Optimization Framework

5.1.1.3 Convexity analysis

A critical issue in dealing with probabilistic constraints is the convexity analysis of the problem for nonlinear systems. An analytical result regarding this issue is given by Prekopa (1995). It states that if the constraints such as (5.4) form a convex set and if the density function is logarithmically concave, the corresponding problem is convex. Although distribution functions can never be concave or convex (they are bounded between zero and one), many of them turn out to be quasi-concave.

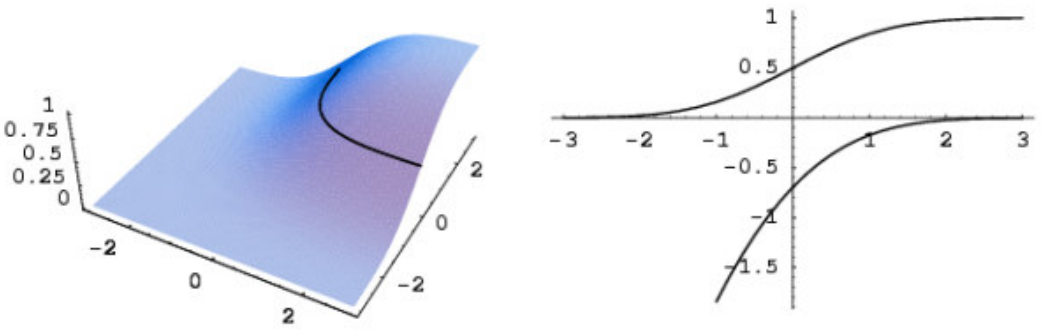

Figure 5.5: Bivariate normal distribution function (left) and standard normal distribution and its logarithm (right), Henrion et al., (1999a).

Figure 5.5 (left) shows the graph of the bivariate normal distribution function with independent components. It is neither concave nor convex, but all its upper level sets are convex. For algorithm purposes it is often desirable to know that the function defining an inequality constraint is not just quasi-concave but actually concave. However, most of the important multivariate distribution functions (multivariate normal, uniform distribution on convex compact sets, Dirichlet, Pareto, etc.) share the property of being log-concave. Figure 5.5 (right) shows the one dimensional normal distribution and its log (Henrion et al., 1999). The problem of normal distributions with correlated components is open. However, a complex system described with a rigorous model is frequently non-convex. Besides, the condition that the constrained output must be convex is difficult to be fulfilled. Thus, the solution with the gradient-based chance-constrained optimization normally provides a local optimum.

5.1.1.4 Illustrative example

Batch processes are inherently dynamic and, thus, the complete profiles of the degree of freedoms are required in order to define their optimal operating policies. The optimization of such processes is generally performed using model-based optimization techniques. In previous studies, deterministic optimization with a nominal model has normally been the common approach for batch distillation. Since uncertainties exist, the results obtained by deterministic approaches may however cause a high risk of constraints violations. To overcome these drawbacks, the developed approach is, at first, applied to the dynamic optimization of a simple batch distillation process (Fig 5.6) with a binary mixture and a single fraction (Arellano-Garcia et al., 2003b).

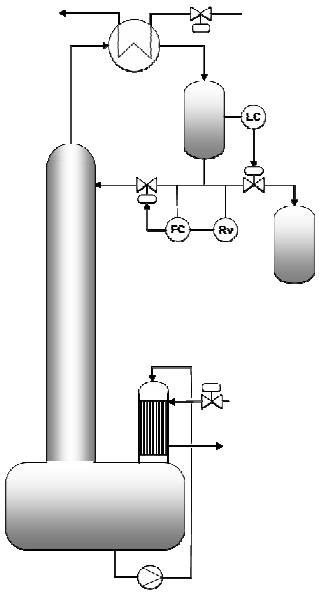

Impact of probability level on the reflux ratio

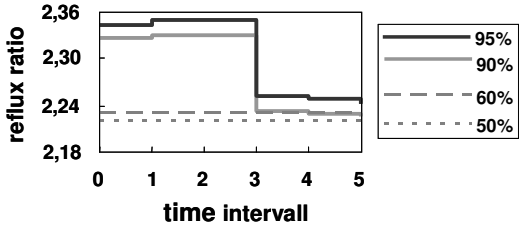

impact of probability level α on the objective

α	50%	60%	90%	95%
$\mathcal{PD}$	0.2294831	0.2290534	0.2274652	0.2267549

Figure 5.6: Simplified flowsheet of the batch distillation column (left); impact of the probability on the reflux ration and the objective function

The aim of the optimization is the maximization of the total amount of distillate product $\mathcal{PD}$ within a fixed time horizon t_f. The uncertain parameters are the initial feed composition and the tray efficiency as well. The product is restricted by a given purity specification of 0.99 mol/mol. Thus, in this example, the problem formulation includes a single chance constraint.

$$\Pr\left\{x_D(t_f) \geq 0{,}99\right\} \geq 0{,}96$$

The trajectory of the reflux ratio and the different lengths of the time intervals are the decision variables to be optimized. In Figure 5.6, the impact of the different probability levels is illustrated indicating the trade-off between the objective function and the robustness of the process. It can be noted that mainly in the beginning time intervals, the probability level has an impact on the optimal process operation policy. Thus, only these intervals are shown in Fig. 5.6. In Chapter 6, the application of the solution approach to a large-scale nonlinear dynamic system including multiple single and joint constraints will show its efficiency and potential.

5.1.2 Handling of single and joint constraints

The probability computation procedure from (5.4) can basically be augmented to multiple single chance constraints. This means, the probability computation for each constraint is formulated as follows

$$\begin{aligned}\Pr\left\{ y_i \leq y_i^{SP}\right\} &= \Pr\left\{\xi_s \leq \xi_s^L, \xi_k \subseteq \Re^s, s \neq k\right\} \\ &= \int_{-\infty}^{\infty} \cdots \int_{-\infty}^{\xi_s^L} \cdots \int_{-\infty}^{\infty} \rho\left(\xi_1, \cdots, \xi_{s-1}, \xi_s\right) d\xi_k \cdots d\xi_s \cdots d\xi_1 \qquad i = 1, \cdots, L\end{aligned} \tag{5.9}$$

It should be noted that distinct uncertain variables can be selected for different constraints. The extension of the approach to joint chance constrained problems is not a trivial task. Firstly, an uncertain variable ξ_S has to be found which is monotone to all constrained output variables i.e. to the joint probability. The choice of an appropriate uncertain variable is viable by carefully examining the relation between uncertain inputs and constrained outputs. This can be achieved by process simulation perturbing the uncertain variables or by analyzing the physical properties of the process. Then the uncertain variable has to be defined as an upper or lower bound according to the bounds of the constrained outputs and the characteristics of the monotony, respectively. In case there are several constrained outputs inducing several upper or lower bounds, then the lowest possible value of the upper bound and the highest possible value of the lower bound is chosen for the integration of ξ_S. Therefore, the joint probability with regard to the output constraints can be expressed as

$$\Pr\left\{ y_i \le y_i^{SP}, i = 1,\cdots,L \right\} = \Pr\left\{ \xi_s^{LB} \le \xi_s \le \xi_s^{UB} \right\} \tag{5.10}$$

where ξ_s^{LB} and ξ_s^{UB} are the upper and lower bound of the uncertain input region, correspondingly. This region is formed by the cutting planes mapped by $y_i(\mathbf{u},\boldsymbol{\xi}) \le y_i^{SP}, (i = 1,\ldots,L)$. In that case the joint probability (5.10) can be computed by

$$\Pr\left\{ y_i \le y_i^{SP}, i = 1,\cdots,L \right\} = \int_{-\infty}^{\infty} \cdots \int_{\xi_S^{LB}}^{\xi_S^{UB}} \cdots \int_{-\infty}^{\infty} \rho\left(\xi_1,\cdots,\xi_{s-1},\xi_s\right) d\xi_k \cdots d\xi_s \cdots d\xi_1. \tag{5.11}$$

It should be noted that if all constrained outputs have a positive monotonic relation to the uncertain input, there will be no lower bound, but the lowest possible value will become the upper bound (case 1). The different possible cases for joint constraints are listed below with regard to the integration bound value in case of a positive and/or negative monotonic relation. However, if all constrained outputs are affected by the same uncertain variables, the joint probability in (5.11) is applicable. For the sake of simplicity, the following assumptions are set:

Constrained outputs:	$y_1, y_2 \rightarrow y_i^{SP} \ge y_i$
Uncertain variable:	ξ
Monotonic functions:	$f_1, f_2 \rightarrow y_1 = f_1(\xi)$ and $y_2 = f_2(\xi)$

Case 1: positive monotonic i.e. $\frac{\partial f_1}{\partial \xi} > 0$ and $\frac{\partial f_2}{\partial \xi} > 0 \rightarrow \int_{-\infty}^{\xi^{UB}} \rho(\xi)\, d\xi = \Pr_j$

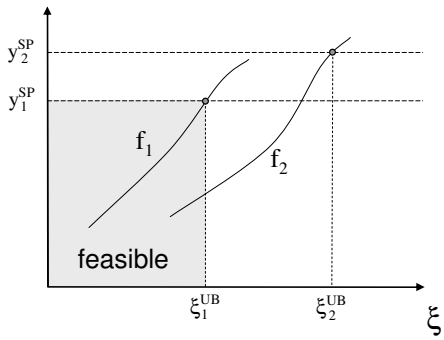

$$\xi^{UB} = \min\left\{\xi_1^{UB}, \xi_2^{UB}\right\} = \min\left\{f_1^{-1}\left(y_1^{SP}\right), f_2^{-1}\left(y_2^{SP}\right)\right\}$$

$$\xi_1^{UB} < \xi_2^{UB} \Rightarrow \Pr_j = \Pr_1$$

$$\Rightarrow \int_{-\infty}^{\xi_1^{UB}} \rho(\xi)\, d\xi = \Pr_1$$

Case 2: negative monotonic i.e. $\frac{\partial f_1}{\partial \xi} < 0$ and $\frac{\partial f_2}{\partial \xi} < 0 \rightarrow \int_{\xi^{LB}}^{\infty} \rho(\xi)\, d\xi = Pr_j = 1 - \int_{-\infty}^{\xi^{LB}} \rho(\xi)\, d\xi$

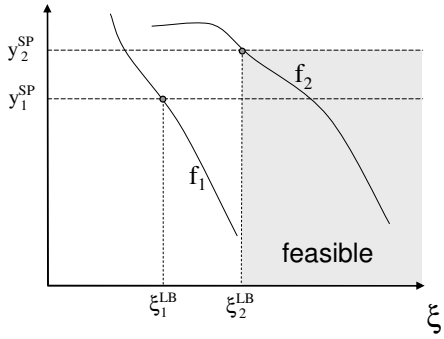

$$\xi^{LB} = \max\left\{\xi_1^{LB}, \xi_2^{LB}\right\}$$
$$= \max\left\{f_1^{-1}\left(y_1^{SP}\right), f_2^{-1}\left(y_2^{SP}\right)\right\}$$
$$\xi_2^{LB} > \xi_1^{LB} \Rightarrow Pr_j = Pr_2; \quad \Xi_2 \subseteq \Xi_1$$
$$\Rightarrow Pr_2 = 1 - \int_{-\infty}^{\xi_2^{LB}} \rho(\xi)\, d\xi$$

Case 3: if $\frac{\partial f_1}{\partial \xi} > 0$ and $\frac{\partial f_2}{\partial \xi} < 0 \rightarrow \int_{\xi^{LB}}^{\xi^{UB}} \rho(\xi)\, d\xi = Pr_j = \int_{-\infty}^{\xi^{UB}} \rho(\xi)\, d\xi - \int_{-\infty}^{\xi^{LB}} \rho(\xi)\, d\xi = Pr_1 - (1 - Pr_2)$

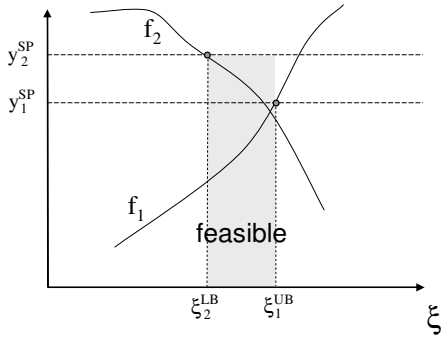

$$\xi_1^{UB} = f_1^{-1}\left(y_1^{SP}\right)$$
$$\xi_2^{LB} = f_2^{-1}\left(y_2^{SP}\right)$$
$$\text{If} \quad \xi_2^{LB} \geq \xi_1^{UB} \Rightarrow Pr_j = 0$$
$$\text{else} \quad Pr_j = Pr_1 - (1 - Pr_2) = Pr_1 + Pr_2 - 1$$

Case 4: $y_1 = f_1(\xi)$, $y_2 \neq f_2(\xi)$, $Pr_j = Pr_1 \cdot Pr_2$; $Pr_2 = \{0,1\}$

$$\Rightarrow Pr_j = \int^{f_1^{-1}(y_1^{SP})} \rho(\xi)\, d\xi \Leftrightarrow Pr_2 = 1$$

Furthermore, to link the chance-constrained approach to a NLP framework, the gradients of the output constraint probability in reference to the decisions variables **u** are required. From (5.2) and (5.11) the decision variables **u** have an impact on the value of the probability through the integration bound of the corresponding region of the random inputs. Thus, the gradients for multiple single constraints can be computed as follows

$$\frac{\partial \Pr\left\{ y_i \leq y_i^{SP} \right\}}{\partial u} = \int_{-\infty}^{\infty} \cdots \int_{-\infty}^{\infty} \rho\left(\xi_1, \cdots, \xi_{s-1}, \xi_s^L\right) \frac{\partial \xi_s^L}{\partial u} d\xi_1 \cdots d\xi_k \tag{5.12}$$

where $\frac{\partial \xi_s^L}{\partial u}$ represents the gradient vector. The right-hand side of Equation (5.12) can simultaneously be computed to (5.9) by numerical integration in the input region. For this purpose the optimal number of collocation points and intervals need to be determined in order to find a trade-off between computational time and accuracy. Table 4.3 shows the results corresponding to the normal distribution.

The gradients computation of a joint chance constraint (Eq. 5.11) can generally be described as follows,

$$\frac{\partial \Pr\left\{ y_i \le y_i^{SP}, i = 1,\cdots,n \right\}}{\partial u} = \\ = \int_{-\infty}^{\infty} \cdots \int_{-\infty}^{\infty} \left[\rho\left(\xi_1,\cdots,\xi_{s-1},\xi_s^{UB}\right) \frac{\partial \xi_S^{UB}}{\partial u} - \rho\left(\xi_1,\cdots,\xi_{s-1},\xi_s^{LB}\right) \frac{\partial \xi_S^{LB}}{\partial u} \right] d\xi_{S-1} \cdots d\xi_1 \tag{5.13}$$

where ξ_s^{LB} and ξ_s^{UB} are the upper and lower bound of the uncertain input region, respectively. These bound values are selected in a similar way to (5.10). However, following the idea of the solution method the stochastic problem is relaxed to a nonlinear programming problem, so that it can be solved with a standard NLP algorithm such as SQP (Figure 5.4).

In addition, there are, in fact, cases where different uncertain variables or subsets of the total number of uncertain variables have an influence on different constrained outputs. This is, for instance, the case of a stochastic dynamic optimization in which both the uncertain variables and the chance constraints have a selective point-in-time dependency $y(\mathbf{u},\xi,t_i) \le y_i^{SP}, i = 1,\ldots,m$. Then the joint probability has to be reformulated considering the upper and lower bounds of the different integrals

$$\Pr\left\{ \begin{array}{l} y_1^{min} \le y\left(\mathbf{u},\xi,t_1\right) \le y_1^{max} \\ y_2^{min} \le y\left(\mathbf{u},\xi,t_2\right) \le y_2^{max} \\ \cdots \\ y_m^{min} \le y\left(\mathbf{u},\xi,t_m\right) \le y_m^{max} \end{array} \right\} = \int_{\xi_1^{LB}}^{\xi_1^{UB}} \cdots \int_{\xi_{S-1}^{LB}}^{\xi_{S-1}^{UB}} \int_{\xi_S^{LB}}^{\xi_S^{UB}} \rho\left(\xi_1,\cdots,\xi_{S-1},\xi_S\right) d\xi_S \, d\xi_{S-1} \cdots d\xi_1 \tag{5.14}$$

The mathematical formulation of the process needs then to be discretized into time intervals such that the end of those intervals corresponds to the time points of the constrained outputs. Thus, the dynamic change of the random variable is discretized into a certain number of time intervals where it is assumed to be piecewise constant. Hence, when the whole time period of the process is divided into N time intervals, one dynamic random variable is converted into N random inputs $\xi(t_i) \le \xi_i$, with i=1,…,N. Consequently, each of those random inputs ξ_i corresponds to one partial integral in the multiple integral formulations on the right hand side of Equation (5.14). This means, the larger the number of those time intervals N, the higher the numerical expense for solving the multiple integral. Therefore, for discretization, a trade-off decision needs to be made between the real trajectory of $\xi(t)$ and the number of time intervals.

In general, for the numerical implementation, the most convenient way is when the time intervals of $\xi(t_i) \le \xi_i$, with i=1,…,N are exactly the same as those intervals between the time points where the specification bounds of the constrained outputs are defined, i.e. for N=m. Furthermore, since each integral in Equation (5.14) corresponds precisely to each time interval, the numerical treatment of the constrained output and the uncertain input can simultaneously be considered. Moreover, the existence of the required monotone relation guarantees that each specified bound of the constrained output, y_i^{min}, y_i^{max}, for a certain time point has exactly one corresponding bound of the uncertain input of the preceding time interval. This leads to the conclusion that in the multiple integral each partial integral has

upper and lower bounds ξ_i^{UB}, ξ_i^{LB} ; $i = 1,\ldots,S; \wedge S = N = m$, which are computed by the reverse function with the upper and lower bounds of the constrained variables y_i^{min}, y_i^{max} as the input. Thus, the mathematical formulation for the joint probabilistic constraint can be formulated by the multiple integral in Equation (5.14) with those bounds of the random inputs mentioned above. In order to numerically solve the multiple integral, a special characteristic of this problem has to be noted, namely, that each bound of the random input is influenced by all values of other random inputs and the control variables of all previous time intervals. This means, that for each integration step, the bounds of the random input will change and need to be recalculated by solving the reverse function with the corresponding constrained variable and new values of random inputs of the previous time intervals. A new approach to considering dynamic random variables in dynamic systems is introduced in section 5.3.

5.2 Non-monotonic relationship

In the previous section, a systematic approach to solving nonlinear chance constrained optimization problems, where the monotony of the constrained output to at least one uncertain input is utilized, so that the feasible region (output distribution) is mapped to a region of the uncertain variables. However, there are, in fact, some stochastic optimization problems where no monotone relation between constrained output and any uncertain input variable can be assured. By this means, when the required monotony can not be guaranteed, more than one uncertain input lead to the same unique uncertain output. For instance, such processes which imply complex reaction systems where the question of whether there is a monotony or not are strongly dependent on the policies of the decision variables.

To address this problem, a new efficient approach is proposed to chance constrained programming for nonlinear dynamic processes with no guarantee of a monotonic relation between constrained output and uncertain input.

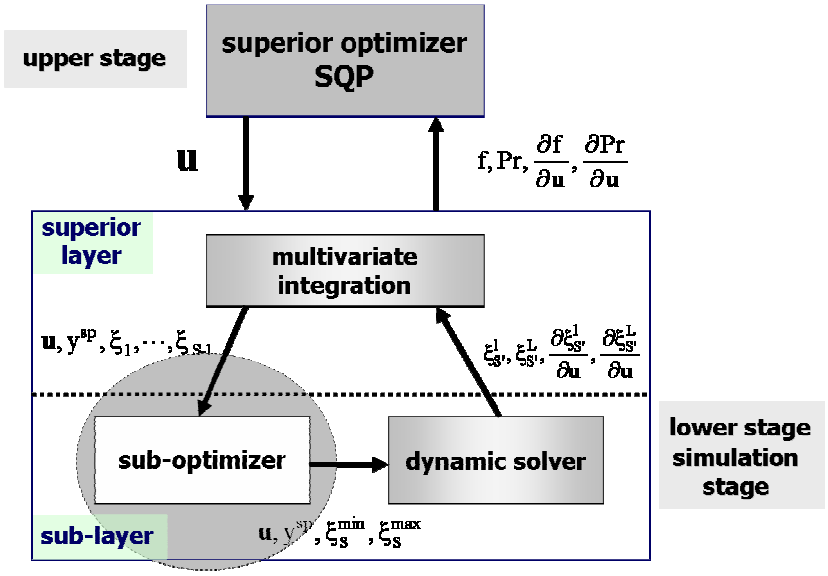

Figure 5.7: General Chance-Constrained Optimization Framework

5.2.1 Solution approach

The proposed approach uses a two-stage computation framework (Fig. 5.7). The upper stage is a superior optimizer following the sequential strategy. Inside the simulation layer there is a two-layer structure to compute the probabilistic constraints. One is the superior layer, where the probabilities and their gradients are finally calculated by multivariate integration. The main novelty is contained in the other, the sub-layer, and is the key to the computation of the chance constraints with non-monotonous relation. The main idea is that for the multivariate integration the bounds of the constrained output **y** and those for the selected uncertain variables $\boldsymbol{\xi}$ reflecting the feasible area concerning y are computed at temporarily given values of both the decision and the other uncertain variables. Thus, all local minima und maxima of the function reflecting y are first detected (Fig. 5.8). This computation of the required points of [min **y**($\boldsymbol{\xi}$)] and [max **y**($\boldsymbol{\xi}$)] can be achieved by an optimization step in the sub-layer (in case monotony exists, this optimization step can be neglected). With the help of those significant points, the entire space of $\boldsymbol{\xi}$ can be divided into monotonous sections in which the bounds of the subspaces of feasibility can be computed through a reverse projection by solving the model equations of this sub-layer in the following step.

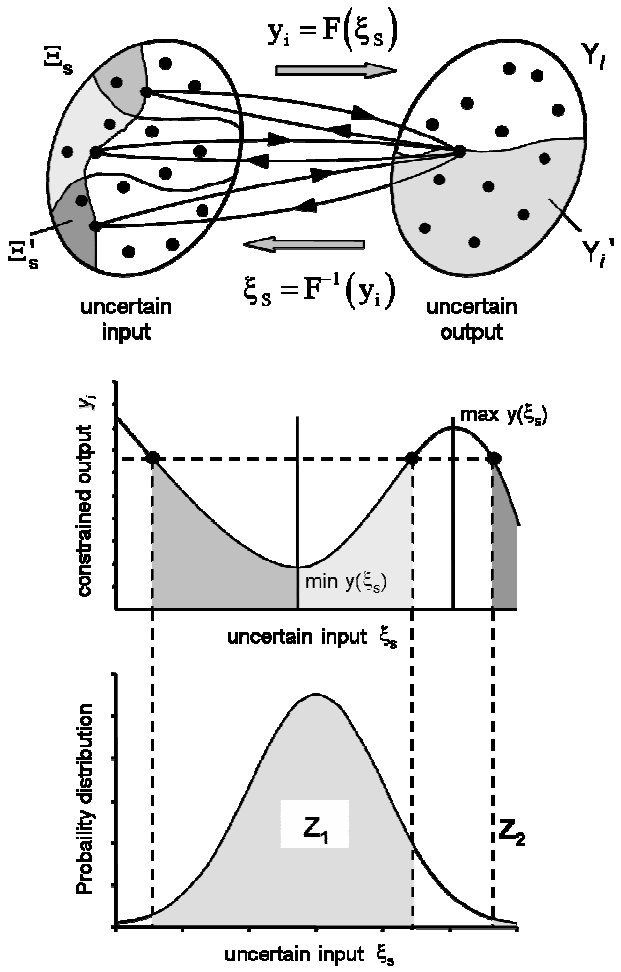

Figure 5.8: Mapping feasible regions and the non-monotonic sections

The bounds of feasibility are supplied to the superior multivariate integration layer, where the necessary probabilities Eqs. (5.15)-(5.16) and the gradients are computed by adding all those feasible fractions together (Fig. 5.8).

$$\Pr = \sum \Pr(z_i) \tag{5.15}$$

$$\Pr(z_i) = \int_{-\infty}^{\infty} \int_{-\infty}^{\infty} \cdots \int_{\xi_S^{\min,i}}^{\xi_S^{\max,i}} \rho\left(\xi_i; \mathbf{R}\right) d\xi_S \, d\xi_{S-1} \cdots d\xi_1 \tag{5.16}$$

5.2.1.1 Local *min* and *max* value of the constrained outputs

In the presence of multiple local optima, specific optimization methods have been developed for many classes of global optimization GO problems. Additionally, general techniques have been developed that appear to have applicability to a wide range of problems. However, considering also numerical efficiency issues, all rigorous GO approaches have an inherent computational demand which increases non-polynomially, as a function of problem-size, even in the simplest GO instances. Global convergence, however, needs to be guaranteed by the global scope algorithm component.

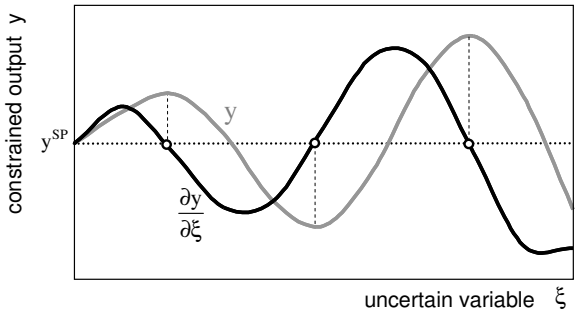

Figure 5.9: Identifying local extrema values.

Alternatively, to detect all local minima and maxima of the constrained output **y**, its gradients with respect to the uncertain variable $\boldsymbol{\xi}$ are calculated (Fig. 5.9). For this purpose, an ad hoc modification of the Mueller Method (Mueller, 1956) with different initial values is proposed. This computation leads to all values with zero gradient and therefore to the extreme values of the constrained outputs. These points represent the boundaries of the different monotone sections. The main challenge is again the mapping back or reverse projection.

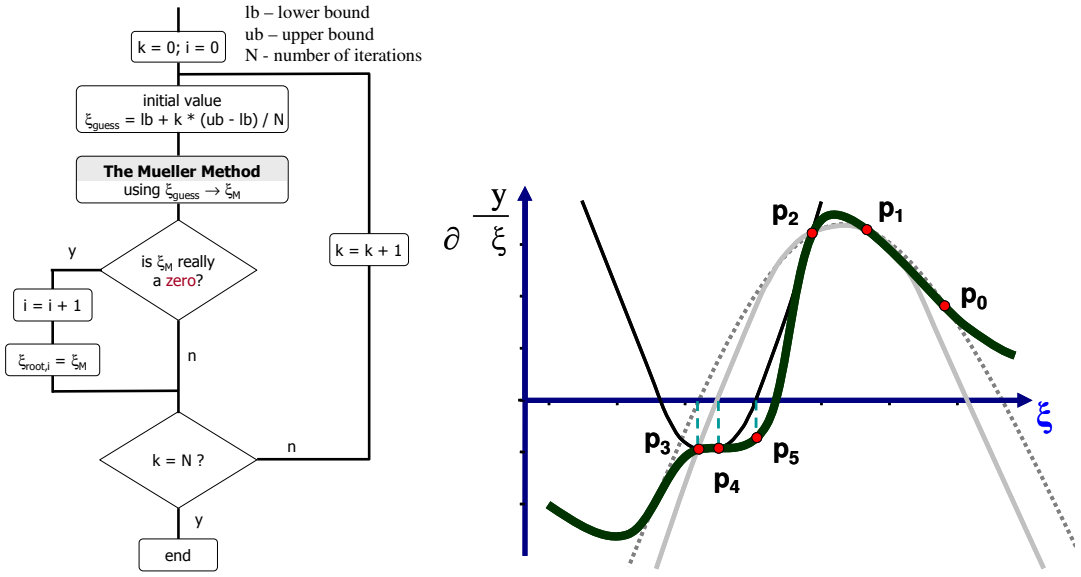

Figure 5.10: Root finding algorithm based on the Mueller method.

The Mueller method is a generalization of the secant method and assumes a function to be approximately quadratic in the region of interest. Each improvement is taken as the point where the approximating parabolic curve (defined by 3 points in each case) crosses the axis nearest to the last point. Since this method is intended to be used for polynomials, it can not be guaranteed that any initial values leads to a zero in our case. Therefore, the Mueller method is applied several times using different initial values between a lower and an upper bound for the uncertain variable. In order to ensure that no root is found twice with the algorithm described in Fig. 5.10, the function is divided by $(\xi-\xi_{0i})$. After having determined the boundaries of the monotone sections, the next step is to calculate the reverse projection of y^{SP} for each section.

5.2.1.2 Verification of the integration limits

In principle, six different cases can occur in such a monotone section (Fig. 5.11): either the constrained output increases with the uncertain variable ξ and crosses y^{SP} so that a reverse projection is possible (1) or stays above it (2) and (3). It can also decrease with the uncertain variable and cross the restriction, as seen in (4), or it stays completely below the constrained bound for the cases (5) and (6). In the cases (2), (3), (5), and (6), there is no change of the integration limits, whereas in the remaining cases a reverse projection of y^{SP} using the developed method in section 5.1.1 leads to a new integration limit. By repeating this procedure for every monotone section, all limits can be determined. They represent then the boundaries of the sections in which the constrained output y remains below its upper bound (Fig. 5.11) and can be used for calculating the probability by multivariate integration.

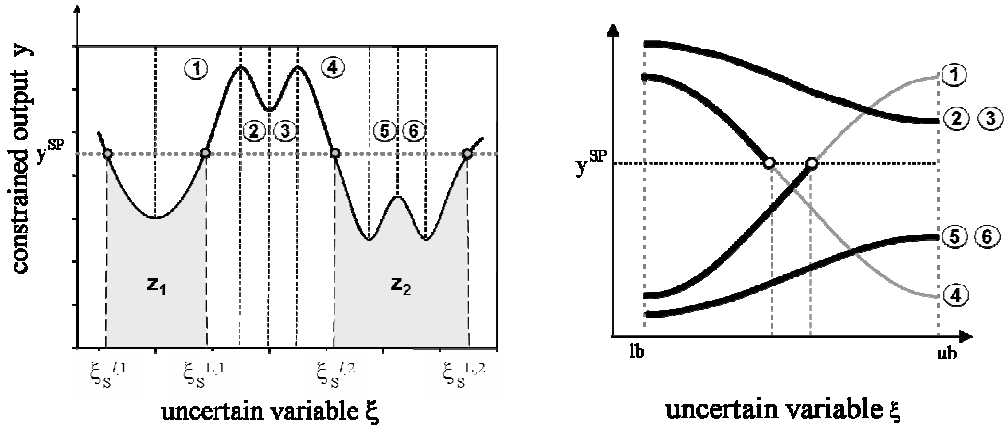

Figure 5.11: Integration limits of the non-monotonous function.

Arising changes of the integration limits are consistently verified for every monotone section. In case of variation, the reverse projection of y^{SP} leads to new integration limits, which are, then, employed to compute the probability by multivariate integration.

Similar to the elementary illustration in section 4.2.2.1, we consider the following problem with a joint normal distribution of two uncertain variables. The stochastic properties are given in Table 5.1.

Random input	expected value	standard deviation	correlation matrix
ξ_1	4.0	0.5	$\begin{bmatrix} 1.0 & -0.6 \\ -0.6 & 1.0 \end{bmatrix}$
ξ_2	4.0	0.7	

Table 5.1: Stochastic properties of the uncertain inputs.

The nonlinear relation between the constrained output, y, and the random inputs ξ_1 and ξ_2 is given by the function,

$$y = (2 \cdot \xi_1 - 7,6)^2 - 3 \cdot (\xi_2 - 4,2)^2 + 2,52 .$$

Here the probability of complying with the constraint Pr{y≤2,5} is to be computed. However, in this case, there is no monotonic relation between the constrained output and any of the uncertain inputs. The following figure illustrated this issue, where one of the uncertain inputs is kept at its expected value, respectively.

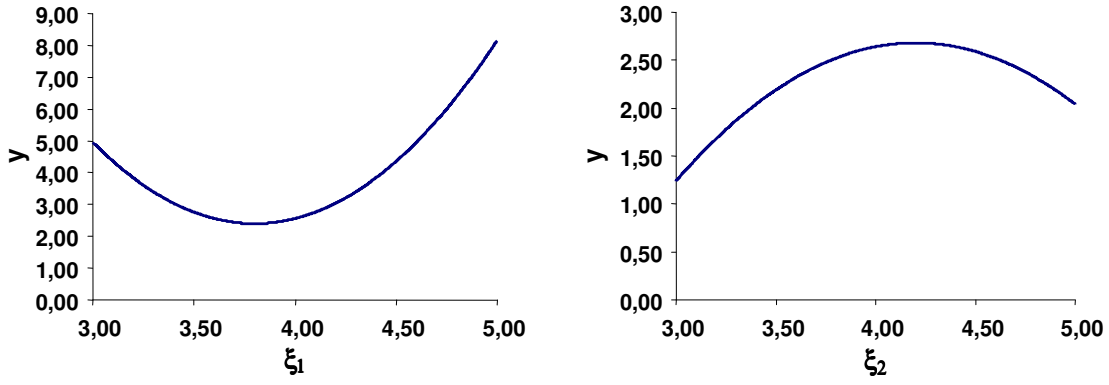

Figure 5.12: Non-monotonic relation between constrained output and uncertain input.

The integration limits for the probability computation are obtained through division of the function, y, into monotonous sections in which for each value of y again exactly one value of ξ_2 can be assigned. The required probability $\Pr\{y \le 2,5\} = 82,32\%$ arises then as a result of the integration over those monotonic sections and addition of the computed partial probabilities.

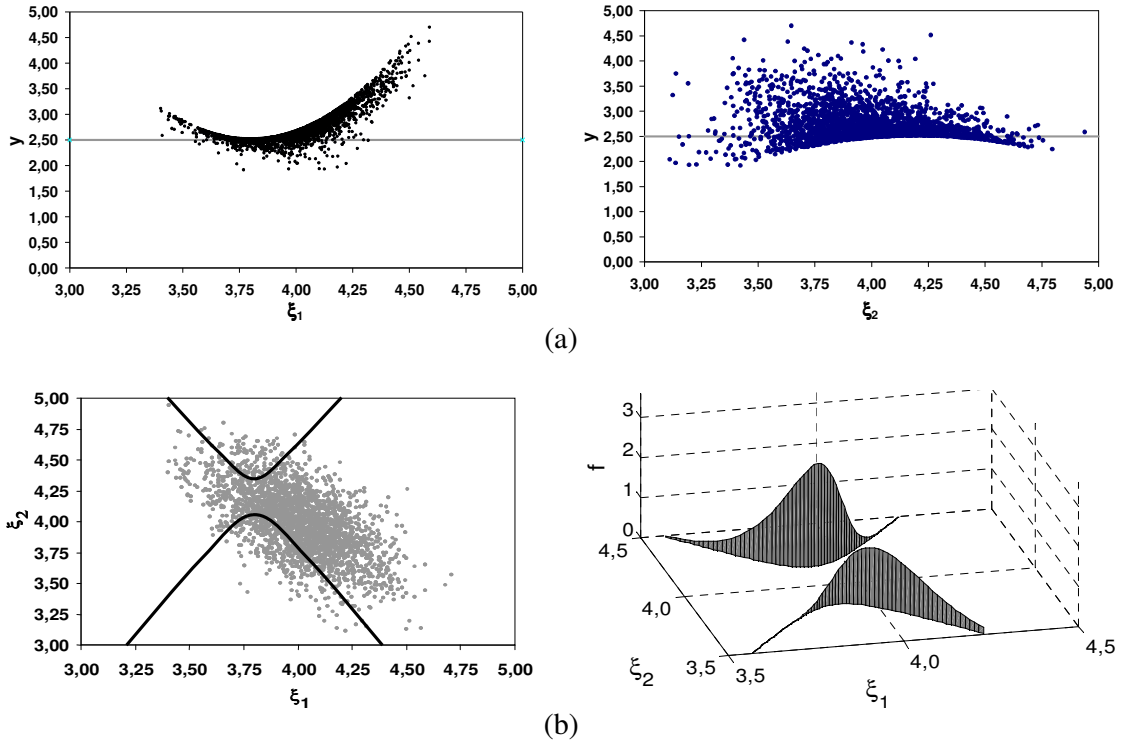

Figure 5.13: (a) Mapping of the uncertain input (b) integration limits over the uncertain variables.

The mapping of a joint normal distribution of the two uncertain variables (ξ_1 , ξ_2) is shown in Figure 5.13a. It also illustrated the reliability of the results, and the mapping concerning the compliance with the bound ($y \le 2,5$) through variation of the uncertain variables by Monte Carlo simulations (1000 samples). Moreover, in Figure 5.13b the resulting integration limits over the uncertain variables are illustrated.

5.2.2 Illustrative example: a dynamic reactor network system

The major challenge of design and operation lies in dealing with the conflicts between the objectives. Moreover, there are uncertainties that need to be taken into consideration in order to make the results more reliable for practical realization. In this example the introduced chance constrained optimization approach is used to address the problem of optimal process design under uncertainty, in which optimal operational considerations and robustness analysis are simultaneously considered. The formulation of individually pre-defined probability limits of complying with the restrictions incorporates the issue of feasibility and the contemplation of trade-off between profitability and reliability. As illustrated in Fig. 5.14, a two-stage reactor system is investigated as a practical example. The reactor network consists of two reactors connected in series, in which two main chain reactions take place. Component B (CB), as the intermediate product, is deemed to be the desired product. It is assumed that the

feed flow into the 1st reactor, F_0, is the product stream from an upstream plant, which is stored previously in a vessel as the middle buffer and can be supplied to the network with a controllable flow rate, but with a given composition and temperature. The corresponding model and additional data are summarized in Appendix A3.

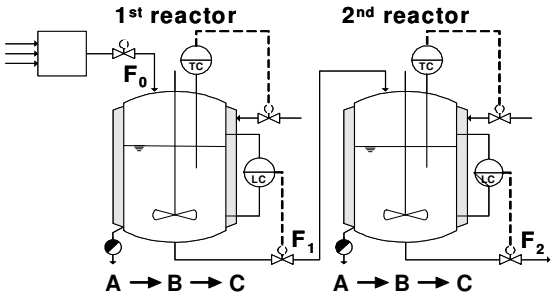

Figure 5.14: Reactor network flowsheet.

First of all, the potential for optimization needs to be investigated through preliminary simulation studies. The dynamic behavior of the process is computed through discretization by the collocation method on finite elements. The results of the simulation studies are illustrated in Figure 5.15, where the necessity for design and operational optimization is demonstrated.

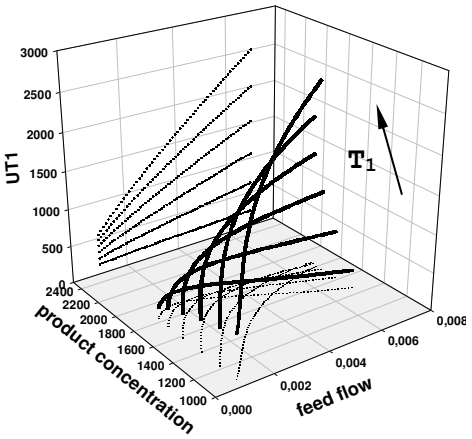

Figure 5.15: Optimization potential analysis.

As expected, the product concentration of component B depends on the reaction kinetics of both reactors, which actually depends on both the residence time and the temperature. Figure 5.15 is created for fixed volumes and thus F_0 can roughly be seen as a reciprocal measurement for the residence time. It can also be seen that an increasing temperature allows lower residence times for fulfilling the purity restriction concerning CB, which allows either higher feed flow rates, and thus higher product flow rates, or lower design costs related to the volumes. On the other hand, it induces higher utility costs (UT). With regard to the residence time, a decision is required between higher flow rates or smaller volumes. Those facts lead to the conclusion that, for cost minimization, overall trade-off decisions need to be made between the temperatures, the flow rates and the volumes. Due to the process dynamics a high degree of flexibility concerning the time-dependence of temperatures and flow rates will lead to better optimal results. In reality, however, the design optimization is often realized first, before optimal operation policies are computed based on the previously optimized design

parameters. The analysis of Figure 5.15 leads to the conclusion that better results are expected when design and dynamic operational optimization are both realized simultaneously in one optimization scheme.

Problem definition

The aim of the optimization is the minimization of total costs. Thus the objective function includes both the design which implies material costs of the reactor depending on the volumes (V_i) and operational costs (utilities UT_i) during the time period, minus a term indicating the total amount of the desired product (PB), which is assumed to be profitable. The objective function of the optimization problem can be written as follows with A, B and C as specific price factors:

$$\min f = \min \left(\sum_{i=1}^{2} A_i \cdot V_i^{2/3} - B \cdot PB + \sum_{i=1}^{2} C_i \cdot UT_i \right) \tag{5.17}$$

Additionally, there are lower bounds for the amount of the converted Product (PB) and upper bounds of utility supply for both reactors (UT_1 and UT_2) necessary to realize the desired trajectories of reactor temperatures in closed control loops. To achieve the optimization goal, the design parameters such as volumes (V_1 and V_2) of both reactors, as well as operational parameters such as flow rates and temperatures are used as free decision variables. The latter ones can be seen as time-dependent, which leads to greater improvement in the dynamic optimization problem.

It should be noted that utility costs are caused by both hot utility supply for sudden increase and cold utility supply for sudden decrease of reactor temperatures. Thus, the utility costs are proportional to the absolute value of the current temperature deviation. This may lead to complications concerning the gradient computation around the value of the current temperature, which could be critical for the implementation of NLP solvers such as SQP. To overcome this problem, the relation of the utility costs to the reactor temperature deviation is approximated by a self-formulated exponential function, which is smooth also around the point of the current temperature and thus easy to differentiate, and on the other hand close to the original curve (see Appendix A3).

In an attempt to make the optimization more robust and the results reliable, uncertainties of several parameters are taken into consideration. For this example the kinetic parameters and the reaction enthalpies are considered to be uncertain. However, since all constraints are affected by the uncertain parameters, they should be reformulated to chance constraints. The uncertain parameters also have an impact on the objective function. The usual way is to reformulate it to its expected value. However, for practical application, it is more convenient to assure a certain reliability of the realization of the calculated objective value. This can be achieved by minimizing an upper bound β and its compliance can be guaranteed with certain reliability by formulating an *additional* chance constraint. Thus, the entire dynamic stochastic optimization problem will be formulated as follows with α_i as the probability levels:

$$
\begin{aligned}
&\min \beta \\
&\text{s.t.} \quad \text{model equations} \\
&\Pr\{f \le \beta\} \ge \alpha_1 \\
&\Pr\{CB \ge CB^{SP}\} \ge \alpha_2 \\
&\Pr\left\{\left(PB - \int_0^{t_E} F_0\, CB_0 dt\right) \ge M_B^{SP}\right\} \ge \alpha_3 \\
&\Pr\{UT_1 \le UT_1^{SP}\} \ge \alpha_4 \\
&\Pr\{UT_2 \le UT_2^{SP}\} \ge \alpha_5 \\
&t_E \le t^{SP}
\end{aligned}
\tag{5.18}
$$

This formulation allows the user greater flexibility to control the reliability of certain bounds of the objective value. With this formulation, it is also possible to analyze the impact on the optimized value of β with a variation of the probability limit α_1. The created curve of β as a function of α_1 can be a base for trade-off decisions between the upper bound of costs and the reliability. For instance, the end of a section, where this curve is rather flat, could be an interesting point for the user, since a high increase of α_1 induces only a low increase of the cost limit.

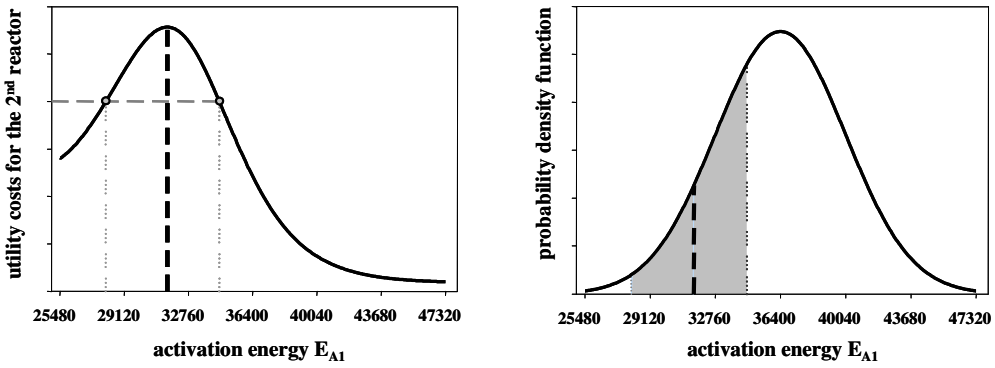

Figure 5.16: Non-monotony and pdf of the uncertain variable: activation energy E_{A1}.

Process analysis has resulted in the fact that the constrained utility costs are not monotone to any uncertain input for several sets of decision variables. For some cases even the other constrained variables such as the final product concentration and the conversion, are not monotone either. For the computation the activation energy has been selected as the uncertain input variable for the determination of the feasibility bounds, because of best convergence properties.

Figure 5.16 shows the upper bound of the utility costs for the second reactor against the uncertain activation energy at some given controls. It is an example of the non-monotonic relationship between constrained output and the uncertain input variable that can occur in the considered system. For a given bound of the utility costs two corresponding values for E_{A1} can be identified. These are then projected onto the probability density function and represent the bounds for the computation of the probability. Figure 5.17 shows the resulting optimal design and operation policies.

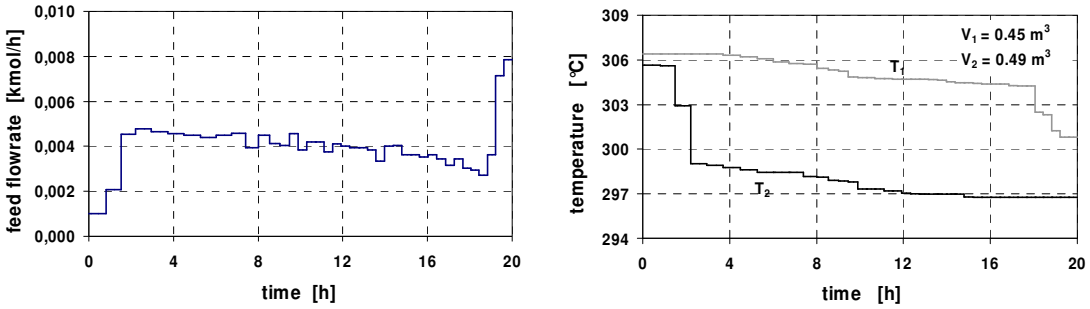

Figure 5.17: Optimal operation policies, feed flowrate (left) as well as reactor temperatures and optimal volumes (right).

Numerical results

Figures 5.18 illustrate the reliability of both the deterministic optimization results and the stochastic optimization results concerning the compliance of the upper bounds of the utility costs through variation of the uncertain parameters by Monte Carlo simulations. For the stochastic results only less than 5 % of the samples exceed the bounds of feasibility as claimed in the formulation of the chance constraints, while for the deterministic results the exceeding samples are close to 50%. Moreover, it is interesting to observe the difference concerning the distribution shapes of the utility costs in the second reactor caused by different values of the decision variables. This is due to the non-monotonous relation between the activation energy E_{A1} and that constrained output. While the simulation with deterministically optimized controls induces one minimum of the utility costs, the one with stochastically optimized controls induces at least two minima and one maximum. The fact that the shape of the curves and the number of peaks strongly depend on the values of the decision variables is illustrated in the two graphics at the bottom of the Figure 5.18 as the main reason why the development of this new approach has become necessary.

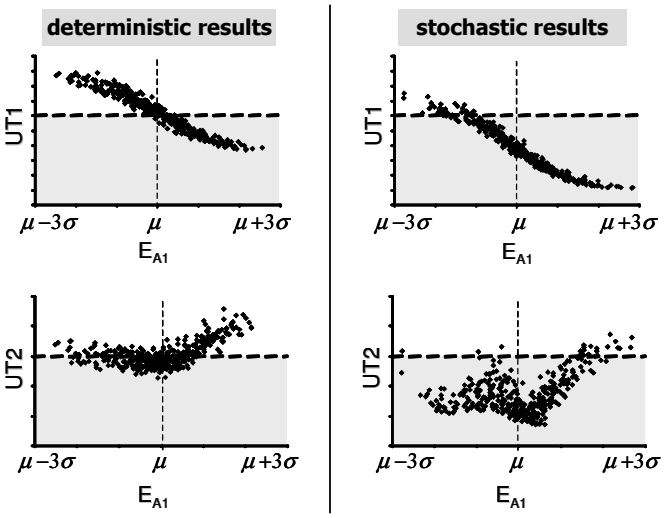

Figure 5.18: Optimization results

Due to the reformulation of the objective function, the computational results show that with the help of this new optimization framework a high degree of flexibility concerning trade-off decisions between the optimization target and the reliability is guaranteed. Moreover, the relationship between the probability levels and the corresponding values of the objective function can be used for a suitable trade-off decision between *profitability* and *robustness*. Tuning the value of α_i is also an issue of the relation between *feasibility* and profitability. The solution of a defined problem, however, is only able to arrive at a maximum value α^{max} which is dependent on the properties of the uncertain inputs and the restriction of the controls and outputs (Arellano-Garcia et al., 2004b).

Feasibility analysis

The knowledge of α^{max} is decisive; if a value greater than α^{max} is selected, the feasible region will be empty. For linear systems, an easy-to-use method has been introduced in the previous Chapter to compute the maximum feasible confidence level. Thus, α^{max} can be obtained by a simulation run. In this Chapter, a preceding probability maximization step is set up to find out the maximum probability value. For this purpose, in case of a joint constraint the original objective function is replaced with

$$\max \ \Pr\left\{ y_i^{min} \le y_i(\mathbf{u}, \xi) \le y_i^{max}, \quad i = 1, \ldots, L \right\}. \tag{5.19}$$

and then the optimization problem is solved. In case of single constraints the procedure is carried out iteratively for each chance constraint creating a multidimensional Pareto front.

5.3 Chance-constrained optimization under time-dependent uncertainty

Uncertainty and variability are inherent characteristics of any process system. Moreover, measurements often contain random errors that invalidate the process model used for optimization and control. This implies that neither the magnitude nor the sign of the error can be predicted with certainty. However, the uncertainties considered are continuous variables, not results of discrete events. This means that there is infinity of possible “discrete” values for

the events associated with continuous time-dependent variables. The only possible way these weaknesses can be characterized is by use of probability distributions. Besides, uncertain variables can be constant or time-dependent in the future horizon (Fig. 4.13). They are undetermined before their realization. Moreover, usually only a subset of variables can be measured. The unmeasured variables are though open loop but should be constrained under uncertain disturbances.

Therefore, in this section, the chance-constrained approach is extended to deal with time-dependent uncertainties. For this purpose, a dynamic process with NY time-dependent output state variables $\mathbf{y}(t)$, NU time-dependent control variables $\mathbf{u}(t)$, and NΦ time-dependent uncertain parameters $\boldsymbol{\xi}(t)$ is considered. The probability Pr of complying with a certain restriction which corresponds to the output state variable y^{SP} at every time point, t, during the process operation is to be calculated and formulated by the following expression:

$$\Pr\left\{ y\left(\mathbf{u}, t, \boldsymbol{\xi}\right) \le y^{SP}, \quad \forall t \in \left[t_0, t_f\right] \right\} \tag{5.20}$$

In order to transform the infinite number of time points to a finite number of representing values, the entire time horizon is divided into several short time intervals where both the control variables and the uncertain variables are piecewise constant. Due to the monotony between the restricted output y^{SP} and at least one uncertain parameter, the value of this uncertain parameter ξ^{SP}, which corresponds to the bound of the constrained output y^{SP}, can be calculated for every time interval JT according to the following equation:

$$\xi^{SP}_{NMM} = f\left(u_1, \cdots, u_{JT}, \xi_1, \cdots, \xi_{NMM-1}, y^{SP}\right) \quad \text{with} \quad NMM = JT \times N\Phi \tag{5.21}$$

However, for NT time intervals, the probability of complying with the constraint for all time intervals can be computed by multivariate integration of a probability density function over all uncertain parameters as follows:

$$\Pr = \int_{-\infty}^{\infty} \cdots \int_{-\infty}^{\infty} \int_{-\infty}^{\xi^{SP}_{N\Phi}} \int_{-\infty}^{\infty} \cdots \int_{-\infty}^{\infty} \int_{-\infty}^{\xi^{SP}_{NMM}} \rho\left(\xi_1, \cdots, \xi_{NMM}\right) d\xi_{NMM} \cdots d\xi_1 \quad \text{with} \quad NMM = NT \times N\Phi \tag{5.22}$$

Each integration bound of the uncertain parameter ξ^{SP} corresponds to the bound of the constrained output y^{SP} within the corresponding interval. All the other uncertain parameters will be integrated over their entire space. For the case of two dynamic random variables (NΦ=2) the calculation will be simplified to

$$\begin{aligned} \Pr &= \int_{-\infty}^{\infty} \int_{-\infty}^{\xi^{SP}_2} \int_{-\infty}^{\infty} \int_{-\infty}^{\xi^{SP}_4} \cdots \int_{-\infty}^{\infty} \int_{-\infty}^{\xi^{SP}_{NMM-2}} \int_{-\infty}^{\infty} \int_{-\infty}^{\xi^{SP}_{NMM}} \rho\left(\xi_1, \cdots, \xi_{NMM}\right) d\xi_{NMM} \cdots d\xi_1 \\ &= \int_{-\infty}^{\infty} \int_{-\infty}^{\xi^{SP}_2} A_1\left(\xi_1, \xi_2, \xi^{SP}_3, \xi^{SP}_4, \cdots, \xi^{SP}_{NMM}\right) d\xi_2 d\xi_1 \end{aligned} \tag{5.23}$$

With

$$A_1 = \int_{-\infty}^{\infty}\int_{-\infty}^{\xi_4^{SP}} A_2\left(\xi_1,\xi_2,\xi_3,\xi_4,\xi_5^{SP},\xi_6^{SP}\cdots,\xi_{NMM}^{SP}\right)d\xi_4 d\xi_3$$

$$\vdots \qquad\qquad \vdots$$

$$A_{JT} = \int_{-\infty}^{\infty}\int_{-\infty}^{\xi_j^{SP}} A_{JT+1}\left(\xi_1,\cdots,\xi_{j-1},\xi_j,\xi_{j+1}^{SP},\cdots,\xi_{NMM}^{SP}\right)d\xi_j d\xi_{j-1} \quad \text{where } j=(JT+1)\times N\Phi$$

$$\vdots \qquad\qquad \vdots$$

$$A_{NT-1} = \int_{-\infty}^{\infty}\int_{-\infty}^{\xi_{NMM}^{SP}} A_{NT}\left(\xi_1,\cdots,\xi_{NMM}\right)d\xi_{NMM} d\xi_{NMM-1}$$

$$A_{NT} = \rho\left(\xi_1,\cdots,\xi_{NMM}\right)$$

Since only few discretization points are required for the integration over a relatively large integration space with an acceptable accuracy, the orthogonal collocation method on finite elements has been proved to be very efficient. Based on this, a calculation scheme has been derived where the first uncertain parameter ξ_1 is discretized in the first interval. For each resulting collocation point (NK), a value for the second uncertain parameter ξ_2^{sp} can be obtained which exactly corresponds to the bound of the constrained output y^{SP} within this interval and, thus, forming the bound for the second integration layer. Over the new derived integration space, the second uncertain parameter can be discretized. Thus, in case of two dynamic random variables, NK^2 collocation points result for the first interval. This procedure will then be repeated until the next-to-last integration layer. The approach can be represented by the following computation tree structure,

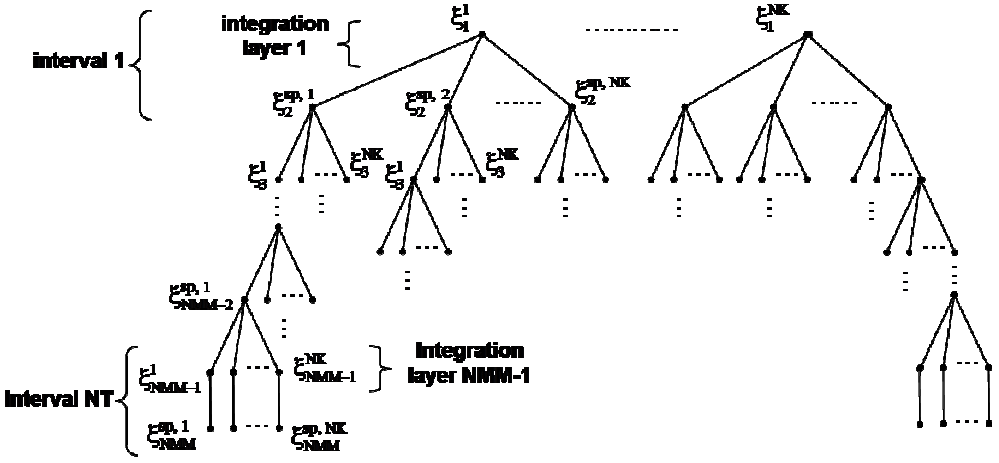

Figure 5.19: Computation tree structure for time-dependent uncertainties

Since the values below the integration bound are only used for calculations in the following integrals, only one value which corresponds to the bound of the constrained output is required for the last uncertain parameter of the last time interval. Thus, the probability of complying with the restrictions of the last interval under given values of the other uncertain variables and all control variables will be obtained. This value can also be seen as a part of the probability density function of the next-to-last integration layer. The integration along this layer leads to

the probability calculation concerning this layer. This procedure will be carried out up to the most superior integration layer and, thus, we finally obtain the originally wanted probability for fulfilling the constraints of the entire time horizon. Furthermore, to solve the NLP-problem with a standard NLP solver such as SQP, gradients of the objective function and the constraints with regard to the control parameters **u**(t) are additionally required. These gradients can be computed as follows:

$$\frac{\mathrm{d}\,\mathrm{Pr}}{\mathrm{d}\mathbf{u}} = \frac{\mathrm{d}}{\mathrm{d}\mathbf{u}} \int_{-\infty}^{\infty} \int_{-\infty}^{\xi_2^{SP}} \mathrm{A}_1\left(\xi_1, \xi_2, \xi_3^{SP}, \xi_4^{SP}, \cdots, \xi_{NMM}^{SP}\right) \mathrm{d}\xi_2 \mathrm{d}\xi_1$$

$$= \int_{-\infty}^{\infty} \left[\int_{-\infty}^{\xi_2^{SP}} \frac{\partial \mathrm{A}_1}{\partial \mathbf{u}} \mathrm{d}\xi_2 + \frac{\partial \xi_2^{SP}}{\partial \mathbf{u}} \cdot \mathrm{A}_1\left(\xi_1, \xi_2^{SP}, \xi_3^{SP}, \cdots, \xi_{NMM}^{SP}\right) \right] \mathrm{d}\xi_1 \tag{5.24}$$

Where

$$\frac{\mathrm{dA}_1}{\mathrm{d}\mathbf{u}} = \int_{-\infty}^{\infty} \left[\int_{-\infty}^{\xi_4^{SP}} \frac{\partial \mathrm{A}_2}{\partial \mathbf{u}} \mathrm{d}\xi_4 + \frac{\partial \xi_4^{SP}}{\partial \mathbf{u}} \cdot \mathrm{A}_1\left(\xi_1, \xi_2, \xi_3, \xi_3^{SP}, \cdots, \xi_{NMM}^{SP}\right) \right] \mathrm{d}\xi_3$$

$$\vdots \qquad\qquad\qquad \vdots$$

$$\frac{\mathrm{dA}_{NT-1}}{\mathrm{d}\mathbf{u}} = \int_{-\infty}^{\infty} \left[\int_{-\infty}^{\xi_{NMM}^{SP}} \frac{\partial \rho}{\partial \mathbf{u}} \mathrm{d}\xi_{NMM} + \frac{\partial \xi_{NMM}^{SP}}{\partial \mathbf{u}} \cdot \rho\left(\xi_1, \xi_2, \cdots, \xi_{NMM-1}, \xi_{NMM}^{SP}\right) \right] \mathrm{d}\xi_{NMM-1}$$

5.3.1 Illustrative example: a semi-batch reactor under time-dependent uncertainty

In order to assess the applicability of the developed approach to allowing for dynamic random variables, in this section a simple semi-batch reactor example is considered where a sequential reaction system ($\mathrm{A} \rightarrow \mathrm{B} \rightarrow \mathrm{C}$) takes places (Fig. 5.20). Both reactions are assumed to be first order. Basically, the aim is to achieve a certain concentration of the desired product B and minimize the batch time by means of manipulating the feed flow rate $F_e(t)$. For the sake of illustration, the cooling system is neglected and thus the reactor temperature is also a time-varying operational degree of freedom. By this means, an energy balance can be omitted and the actual model is simply composed of the component balances, and the equations for the reaction rates. The model parameter and data are summarized in Appendix A4.

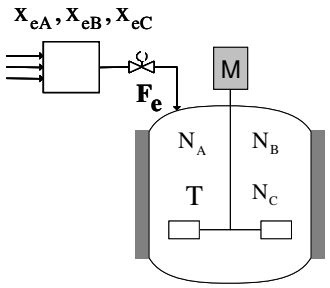

Figure 5.20: Scheme of the semi-batch reactor.

The chance-constrained optimization problem can be posed as:

$$
\begin{aligned}
&\min_{T,\ F_e,\Delta t} \quad t_f \\
\text{s.t.} \quad &\text{model equations and} \\
&\int_{t=0}^{t_f} F_e(t)dt = 162\text{mol} \\
&N_C(t_f) \le N_C^{max} \\
&\Pr\left\{N_B(t_f) \ge N_B^{min}\right\} \ge 98\% \qquad (5.25) \\
&T^{min} \le T(t) \le T^{max} \\
&F_e^{min} \le F_e(t) \le F_e^{max} \\
&\xi(t) = \left\{x_{eA}(t), x_{eB}(t)\right\}
\end{aligned}
$$

The total feed amount is restricted to 162mol. In addition to the deterministic constraints, the defined single chance constraint corresponds to the end-point restriction on the concentration of B and is to be satisfied with a probability level of 98%. In this case study, the time-varying uncertainties are assumed to be the feed flow concentration $x_{ei}(t)$.

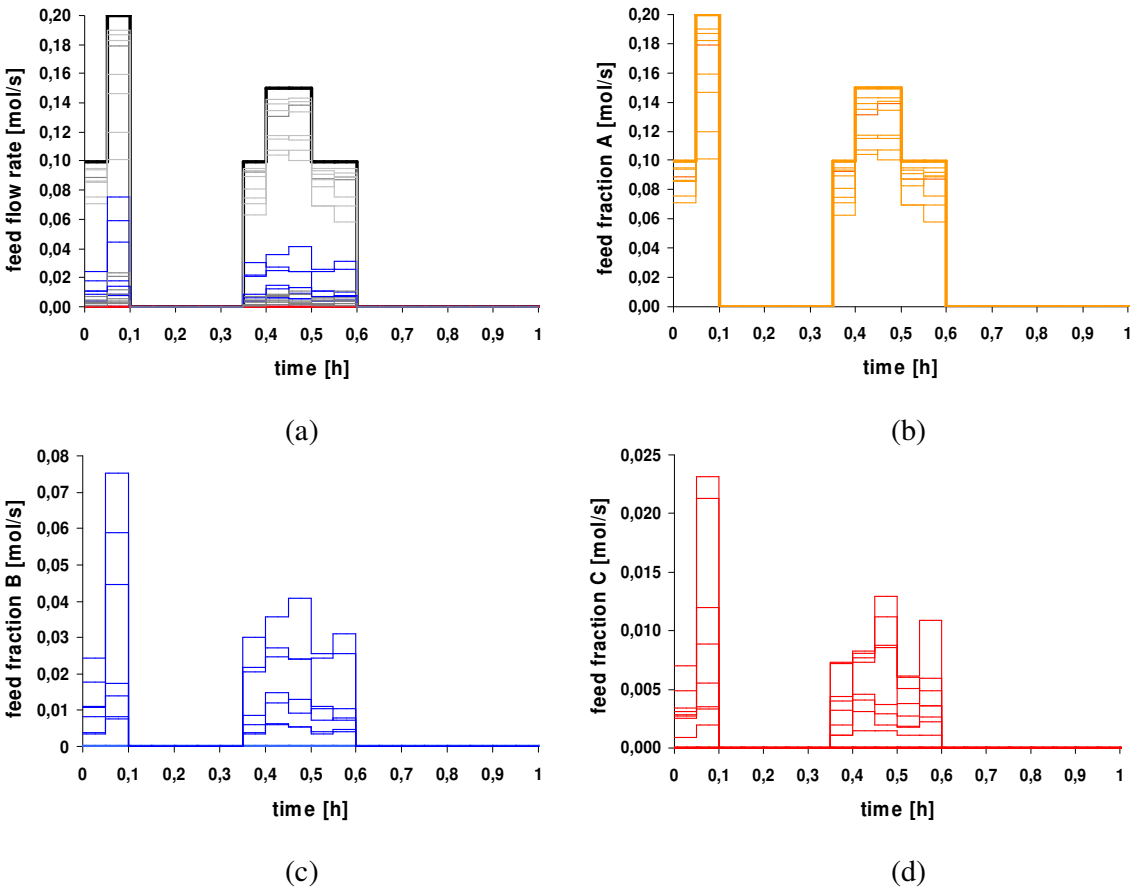

Figure 5.21: Feed flow and molar flow disturbance profiles.

Since in the nominal optimization is assumed that the feed flow only consist of A, the bold lines in Figure 5.21a-b represent the deterministic problem solution of (5.25) with regards to the feed flow rate and the corresponding molar flow of A. Furthermore, the thin lines in all

illustrations in Figure 5.21 characterize the time-dependent behaviour of the molar flow of all components in (a) and for each of them in (b)-(d), respectively.

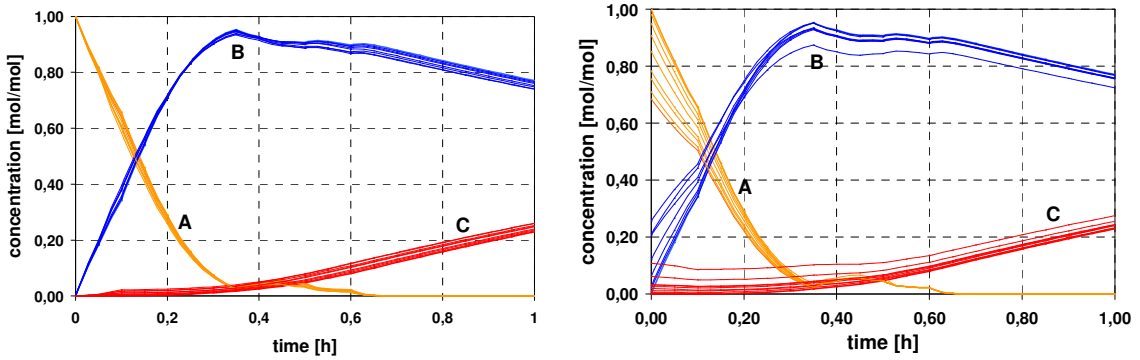

Figure 5.22: Concentration profiles in the reactor for (a) nominal and (b) uncertain initial composition.

Based on the outcomes in Figure 5.22, the influence of the uncertainties on the composition during the batch operation is pointed up. In Figure 5.22b, in particular, the concentration changes due to the uncertain initial operating conditions underscore the fact that a classical open-loop implementation of off-line calculated nominal outputs may not lead to the optimal performance. Furthermore, constraint complying can not be assured unless a conservative strategy is implemented such as an extended reaction time, lower feed rate or temperature in order to force the reaction to fully consume the reactant.

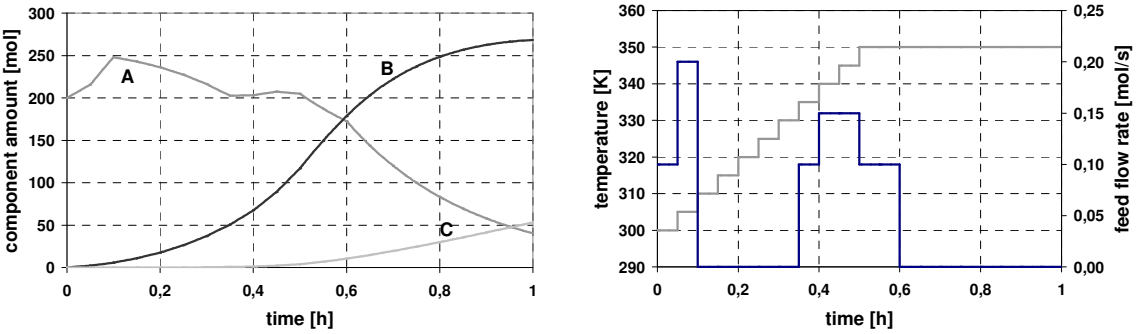

Figure 5.23: Robust optimal profiles: reactors component amount (*left*); temperature and feed flow rate policies (*right*).

The resulting robust optimal trajectories of the operational degree of freedom and the state variables are illustrated in Figure 5.23. A piecewise constant profile of the reactor temperature is determined. It can be seen that the desired product B is initially converted relatively slow. Towards the end of the batch process both restrictions for B and C, respectively, are however fulfilled. Moreover, the feed flow rate is high in the beginning in order to assure a fast ignition of the reaction. During this period A is accumulated in the reactor. Afterwards the feed flow rate is decreased drastically due to the static potential in the reactor. In order to achieve the desired conversion of B, the remaining feed is again supplied to the reactor. The developed strategies are robust and may be particularly effective for meeting path and terminal constraints under time-varying uncertainties.

5.4 Summary

In this chapter, a new approach to chance constrained programming of large-scale nonlinear *dynamic systems* has been presented. In dynamic processes, in particular, there are parameters which are usually uncertain, but may have a large impact on the targets like the objective value and the constrained outputs. The stochastic property of the uncertainties is explicitly included in the problem formulation. The method is based on the employment of a monotonic relation between output constraints and at least one uncertain variable, so that the probabilities and their gradients can be achieved by numerical integration of the probability density function of the multivariate uncertain variables by collocation in finite elements. The new approach involves new efficient algorithms for realizing the required reverse projection for dynamic systems and hence the probability and gradient computation with an optimal number of collocation points. Another novelty of this approach lies in the efficient computation of single and joint constraints and their gradients.

Moreover, the chance-constrained optimization approach has been extended to deal with such stochastic optimization problems where *no monotonic relation* between constrained output and any uncertain input variable can be guaranteed. Especially for those cases which involve chemical chain reactions or other complex reaction systems which strongly depend on the decision variables whether there is monotony or not. A two-stage reactor system has been investigated to demonstrate the potential of the new approach. Here, the novel chance constrained optimization approach has been used to address the problem of optimal process design under uncertainty and process variability, in which optimal operational considerations and robustness analysis are simultaneously considered. The formulation of individual pre-defined probability limits of complying with the restrictions incorporates the issue of feasibility and the contemplation of trade-off between *profitability* and *reliability*.

Since optimal operation and control problems involve the determination of time-varying profiles through dynamic optimization, such problems turn out to be even more complex in practical situations where the handling of time dependent uncertainties becomes a significant issue. Moreover, some parameters may exhibit a drift with respect to time, which could be due to several causes. In time these changes may gradually relieve resulting in a drift in the nominal values or measurements. Therefore, novel algorithms have been integrated to consider time-dependent uncertainties. The influence of these uncertain variables on the output constraints will propagate through the nonlinear dynamic process from time interval to time interval. Thus, the solution of the problem has the feature of prediction and robustness.

In order to show the scope of the proposed approach, in the next Chapter, the stochastic dynamic optimization of a large-scale dynamic system under uncertainty is considered to show the analytical steps of the approach, and to demonstrate the efficiency of the proposed optimization framework.

Chapter 6

Robust Dynamic Optimization of a Large-Scale Process System

Due to the growing competition, dynamic optimization of batch processes has attracted more attention in recent years since it is a natural choice for reducing production costs, improving product quality, and meeting safety requirements and environmental regulations (Bonvin et al., 2001). However, batch processes are inherently transient and their operation demands the determination of time-varying trajectories rather than a set of time-invariant operating conditions. In the production of low-volume, high-value specialty chemicals, batch distillation is one of the most common operations. Although it has long been recognized that continuous distillation is much more energy efficient and less labor intensive than batch distillation, batch distillation has continued to be an important technology due to the greater operational flexibility that offers. This operational flexibility of batch distillation columns makes them particularly suitable for smaller, multi-product or multi-purpose operations. In particular, when chemical reactions and physical separations have some overlapping operating conditions the combination of these tasks in a single process unit can offer significant benefits. These benefits could involve avoidance of reaction equilibrium restrictions, higher conversion, selectivity and yield, removal of side reactions and recycling streams, circumvention of non-reactive azeotropes, and finally, reduction of investment costs and energy demands through heat integration (Reuter, 1994). Although there is an intensive literature on batch distillation, relatively little has been published on reactive batch distillation.

The most outstanding feature of batch distillation is its flexibility. It allows for operating with completely different feed stocks and product specifications. However, this flexibility along with the nature of unsteady state of the process poses challenges in design and operation. In the chemical industry, conservative operation policies of batch processes are mostly determined by heuristic rules. Conservatism is necessary here to guarantee feasibility despite process disturbances. Although the capital investment required for a batch column is less than a continuous column, the unsteady state nature of batch distillation results in higher operating costs. Furthermore, in industrial practice, optimal control problems in batch distillation involve finding an open loop solution for the policies profiles. The trajectories are then followed by a controller to optimize the selected performance index. These trajectories are then optimal when the mathematical model accurately represents the physical phenomena. However, compensation without considering the uncertainty properties is, in fact, the *wait-and-see* strategy and has several drawbacks. First, it is always *a posteriori*. Second, the

system propagates the disturbances to connecting systems. Third, a feedback can not ensure constraints on open-loop variables. In many cases it is impossible to on-line measure some variables which describe product properties (e.g. composition, viscosity, density). These variables have to be open-loop under the uncertainties but they should be confined to a specified region corresponding to the product specifications.

As shown in the previous chapters, dealing with dynamic and uncertainty is a key problem for optimal design and operation. The techniques developed in the present thesis for the chance-constrained optimization of dynamic systems have been illustrated for examples of limited complexity. In order to demonstrate the efficiency of the developed approaches, the chance-constrained optimization framework is applied to an industrial scale process. For this purpose, the reactive batch distillation process is treated here. The comparison of the stochastic results with the deterministic results is presented to indicate the robustness of the stochastic optimization. The achievements are an important step towards the implementation of robust optimal operating policies on real uncertain processes.

6.1 Problem definition: An industrial reactive batch distillation process

The detailed modelling of batch distillation processes formulates a large-scale nonlinear differential and algebraic equation (DAE) system. Thus, in most of the previous studies concerning batch distillation optimization, simplified models have often been employed as a compromise between the model accuracy and the solution possibility of the optimization problem (Farhat et al. 1990, Reuter et al., 1989, Ahmad et al. 1998, Diwekar 1995, Low and Sorensen 2002). Thus far no reports on experimental studies of batch distillation processes optimization of an industrial scale have been found in the open literature. In this chapter, an industrial semi batch distillation process with a transesterification taking place in the reboiler is considered. Since a conventional batch process run was carried out on the industrial site, the model was validated with measured experiment data. Thus, a detailed dynamic model is used to describe the batch process more accurately.

6.1.1. Process description

An industrial reactive semi batch distillation process composed of a total condenser, a column with 30 bubble-cap trays, a reboiler, and two accumulators (main-cut and off-cut) is considered. A slightly endothermic transesterification of two esters and two alcohols takes place in the reboiler, which can be described as follows:

Educt ester (A) + Educt alcohol (B) ↔ Product ester (C) + Product alcohol (D)
Methyl Myristat + Isopropanol ↔ Isopropyl Myristat + Methanol

At the beginning of the batch operation 6.9 m^3 of pure educt ester, 2.6 m^3 of a mixture consisting of educt alcohol and product alcohol of the off-cut from the last batch, 0.4 m^3 of pure educt alcohol, and 80 kg of the homogeneous catalyst are charged to the reboiler. This leads to the initial molar fraction composition of 0.2944, 0.1329, 0.3532, and 0.2195 for the components A to D, respectively. The reboiler is then stirred and heated with the pressurized steam. During the start-up period the batch column is usually operated with total reflux. An inert gas is introduced to keep the column at a constant operating pressure. During the batch, a limited amount of educt alcohol will be fed to the reboiler in order to intensify the reaction. Moreover, the product alcohol, which is the lightest component, is distillated from the reboiler. By this means, the reaction will be shifted toward the product side. The use of an

excess of educt alcohol and the simultaneous removal of the product alcohol through distillation are very effective in displacing the reaction equilibrium towards the product side and hence to a high reaction rate. During the main cut period the product alcohol is collected in the first distillate accumulator according to a given purity specification, while in the off-cut period the reboiler reaction temperature will be increased such that the still remained educt ester can react to an acceptable extent in an attempt to avoid an additional special separation step. At the end of the batch process, a mixture consisting of the product ester and the educt alcohol will be obtained in the reboiler and separated then by a recovery column. The accumulated off-cut will be recharged to the reboiler of the next batch. In the real plant, the temperatures, flow rates, and pressures of the different positions (Fig. 6.1) can be measured on-line, while the composition measurements are provided via an off-line chromatographic analysis. Some control loops are implemented to ensure a stable process operation. The samples composition from the condenser and the reboiler are taken hourly and analyzed to obtain the composition profiles.

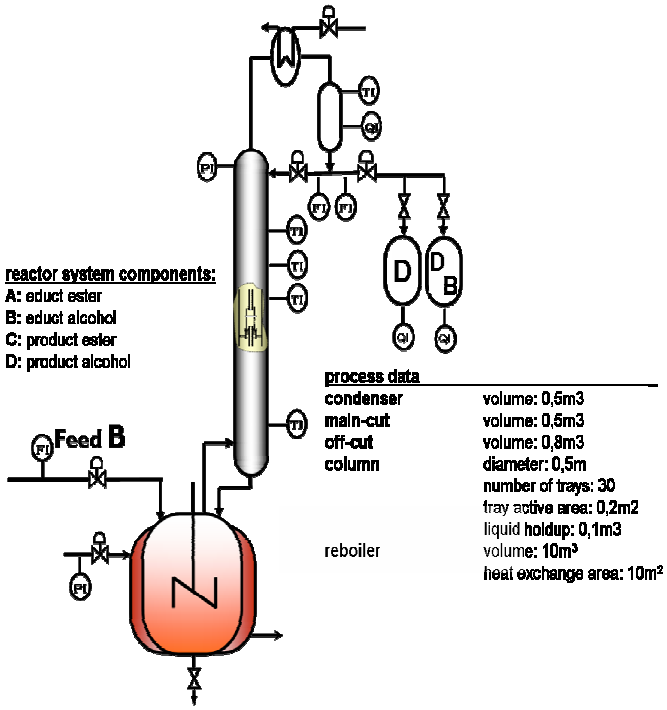

Figure 6.1: Flowsheet of the reactive semi batch distillation process

6.1.2. Process modelling and simulation

A detailed tray-by-tray model is used to describe the batch column. Included are component balance, energy balance and vapor-liquid equilibrium of each tray in the unit model. The holdup, the pressure drop of each tray, and non-equimolar flow in the column are taken into consideration. The vapor-liquid equilibrium is described with nonideal liquid phase computed by the NRTL model. The reaction kinetic is incorporated to the model to depict the chemical reaction in the reboiler. The component compositions of the liquid and the vapor phases, the liquid and vapor flow rates, and the temperature are the variables of each tray, i.e. the total number of the variables are: (number of components x 2 + 3) times the number of trays. Thus, a large complex dynamic system composed of nonlinear differential algebraic equations (DAEs) is formulated. A detailed description of the model is given in Appendix A5. The model parameters required are the constants of the Antoine component vapor pressure

equation, of the component heat capacity correlation, and of the NRTL model which are taken from Reid et al. (1987) and Gmehling et al. (1977), respectively. The kinetic parameters of the endothermic transesterification are taken over by the experimental study of Reuter (1994).

To efficiently simulate the reactive semi batch operation, collocation on finite elements is also used to discretize the dynamic model equations in each time interval. The dependent variables are approximated with Lagrange polynomials with shifted roots of Legendre polynomials (Finlayson, 1980). To keep the variables continuity between intervals, the last collocation point is defined as the starting point of the next interval. The Newton-Raphson algorithm is then applied to solve the algebraic equations derived from the discretization. By this means, the operation of the process is simulated from interval to interval. To take advantage of the dominant block tridiagonal structure of the Jacobian matrix, a Gauss elimination approach for sparse matrices is employed. As defined in the previous chapter, the developed simulation program can directly be incorporated into the optimization framework following the sequential strategy (Li et al., 1998).

However, prior to the simulation, the pressure, holdup, and tray efficiency parameters of the model have to be computed. The pressure of each tray can be calculated through interpolation between the top and bottom operating pressures. The holdup of each tray is usually determined from the tray volume. Furthermore, since the value of the Murphree tray efficiency is typically in the range between 0.7 and 1.0 its determination is conventionally carried out through trial-and-error by comparing the simulated results with those of the measured experiment data. To overcome this drawback, in the next section, an approach to improve the reliability of the initial state is introduced.

6.1.3. Physical initialization

In batch distillation operation there are uncertainties which affect the trajectory computed for the operation policies. Some of the static uncertainties are even translated into dynamic uncertainties due to the time-dependent nature of the process and some of them are not. In several systems encountered in pharmaceutical, specialty chemical and biochemical industries, the thermodynamic models are not exact or there is not enough data to predict the behaviour caused by non-idealities (Rico-Ramirez et al., 2003; Ulas et al., 2004). These thermodynamic uncertainties represent static uncertainties, which in most cases can be characterized by probability distributions functions. However, since batch distillation is of unsteady state nature, static uncertainties are translated into time-dependent uncertainties which affect the optimal operating conditions. For instance, variability observed in initial variables, such as the amounts of feed, and the feed initial composition, are static uncertainties. Since these are initial values in batch operation the uncertainties in these variables are not translated into dynamic uncertainties. It implies though that the profile determined for the optimal policies need to be moved to a new starting point and re-evaluated for the accurate, optimum performance.

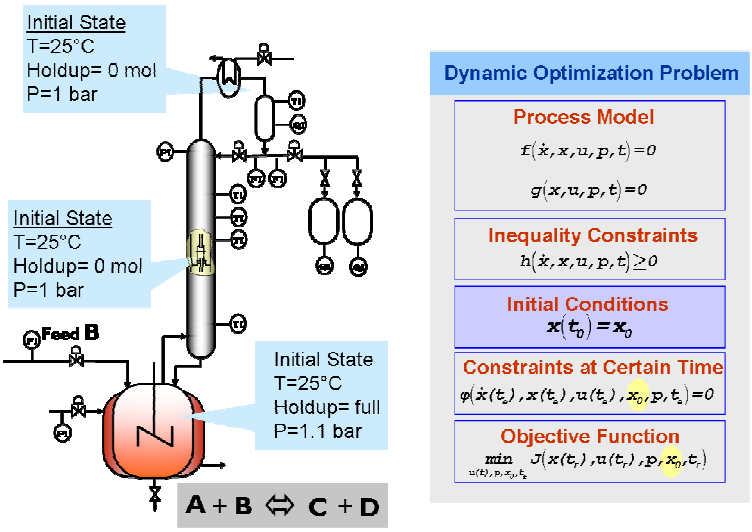

Figure 6.2: Initial conditions for the formulation of an optimization problem with time-dependent restrictions

Moreover, a further inherent characteristic of batch distillation is that a batch (reactive) column will frequently be started up from the cold and empty state. Furthermore, as stated before, the amount, the composition as well as the nature of the components in the initial charge may be variable from batch to batch. Therefore, modelling and simulation of the batch distillation start-up operation from a given initial state plays an important role in the optimal design and operation of such process, particularly with regard to reactive batch distillation. Owing to the dynamic nature, initialization of such a system is a challenging problem. However, the initial state, in previous studies on optimization and control of batch distillation, is assumed to be a pseudo-warm state (Diwekar et al., 1991b; Mujtaba et al., 1998; Sorensen et al., 1994). Due to the unsteady state operation point for batch distillation, the most common solution for this problem is trial-and-error. In most available simulation software of batch distillation, a pseudo-warm state is also applied (Jimenez et al., 2000). In this thesis, a hybrid model for simulation of start-up operation for batch distillation with overlapping chemical reactions is proposed. Thus, the proposed model includes both equation and variable discontinuity. A detailed tray-by-tray model for the reactive batch distillation has been developed. The total equation system consists of mass balance, energy balance, vapour-liquid equilibrium relations and tray hydraulics. During the start-up phase each tray will be described from a non-equilibrium phase, in which only mass and energy transfer are taking place, to an equilibrium phase in which the vapour-liquid equilibrium is held (Wang et al., 2003). The switching point between these two phases is decided by the relationship of bubble point temperature at the operating pressure. The equilibrium state is attained tray by tray from bottom to top of the column, whereas the liquid hold-up of each tray is mainly filled due to the reflux flow. Figure 6.3 shows the state transition of the trays in the batch column during start-up. At certain time point, a tray may be at the state of empty (EM), liquid accumulation (LA) or vapour-liquid equilibrium (VLE).

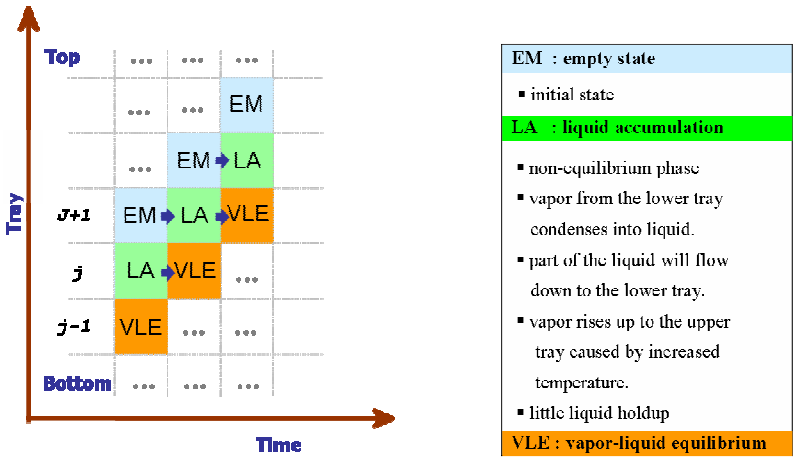

Figure 6.3: Tray state transition during the start-up.

6.1.3.1 Start-up procedure

Turning on the heater in the reboiler commences the startup operation. When the temperature of the reboiler charge reaches its bubble point, the first vapor rises to the lowest tray from the bottom. Due to the condensation of the rising vapor on the tray, its state changes then from EM (empty) to the state of LA (liquid accumulation). Simultaneously, the condensed liquid in this tray is heated by the rising vapor. When the temperature reaches the bubble point, the tray state will be switched from LA to the equilibrium state VLE. Subsequently, the rising vapor from this tray reaches then the tray above and will be condensed there. As shown in Figure 6.3 (left) the transition sequence of the batch column trays during the startup upwards is EM→LA→VLE. When the vapor attains to the condenser, the reflux drum level will gradually increase. Provided that a certain liquid level in the reflux drum is achieved, the reflux valve will be opened. After that the holdup in the trays will significantly be incremented tray by tray from top of the column to the bottom due to the reflux flow. The startup phase is usually completed when the lowest tray of the batch column arrives at its maximum holdup which also means that all trays have achieved their VLE state, respectively.

6.1.3.2 Simulation of reactive batch distillation starting from a cold and empty state

Based on the observation and analysis of the described start-up procedure, the model describing the startup operation should specify two different switching properties on a batch column tray. The first switching is from the non-equilibrium phase to the equilibrium phase. The non-equilibrium phase is defined by the EM and LA states during which there is no thermal separation on the tray. Due to the temperature increase the vapor leaves then the tray which implies that the tray state is now switched from the non-equilibrium phase to the VLE phase. In order to determine the switching event, the bubble point pressure is used as the first switching parameter. However, the tray is initially filled with air or inert gas until the bubble point pressure on the tray reaches the operating pressure of the column. By this means, the vapor leaving the tray will force up the air or inert gas to the trays above. The rising vapor leads to a pressure drop and thus the pressure on the tray will be increased (Fig. 6.4). The second switching parameter is due to the use of two different weir heights according to the structure and geometry of the trays. A lower weir used before the reflux valve is opened and the higher weir after this (Fig. 6.5). In order to describe the different separation effect with respect to these two different liquid holdups, a semi-theoretical tray efficiency formula is used

(Wang et al., 2003). Therefore, the model proposed is a hybrid one including both equation and variable discontinuity. In the numerical implementation the number of equations and state variables are not the same in different operating phases. It should be noted that the empty state EM does not need to be modeled. Besides, in the LA phase mass, component and energy balances as well as the Francis-weir formula are used to detail the condensation process. To describe the VLE state all MESH equations and hydraulic relations are required (see Appendix A6).

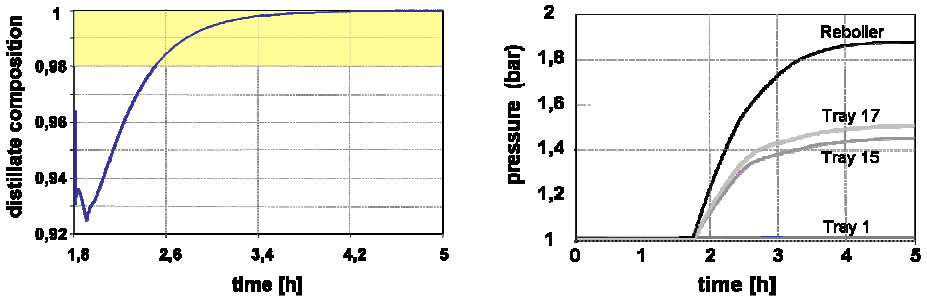

Figure 6.4: Simulated profiles of the distillate composition and the trays pressure.

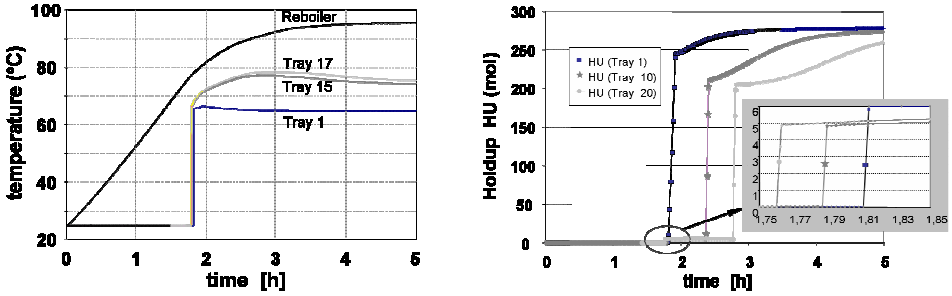

Figure 6.5: Simulated start-up profiles of the batch column temperature and the holdup transition.

The presented profiles in the Figures 6.4 and 6.5 show the simulation of the startup period beginning from a cold and empty state (ambient conditions). It should be reminded that the reactor volume is 10 m^3. In Figure 6.5 (left) the reboiler temperature increases steadily during the start-up along with the distillation of the light components. The holdup transition with its different weir heights is shown in Figure 6.5 (right) where, in particular, the holdups on the trays increase due to the reflux flow. The enlargement of the figure shows the holdup during the column heating through the rising vapor. Furthermore, due to the conservative operation – total reflux- during the startup, which is the common operation on industrial site, the purity of the product alcohol (Fig. 6.4 left) is definitely much higher than its specification (0.98 mol/mol). This is primarily due to the inappropriate reflux ratio profile at the operation beginning. Besides, since the product alcohol can not be removed rapidly from the reboiler, the reaction will be lowered.

Based on the simulation results of the start-up, alternative operations can be derived. So for instance, since the product alcohol purity attained at the very beginning of the start-up procedure is higher as required (Fig. 6.4 left) it is not necessary to wait until the last batch column tray is filled by the liquid flow stream due to the reflux. By this means, distillate product can be withdrawn just after the reflux drum has reached a certain level such that a suitable corresponding reflux ratio can be established by taking care of the maximum vapour

load. The decision of the time point, when to remove the distillate product, can be determined through simulation of the start-up phase with the method of the physical initialization introduced in this section.

6.1.3.3 Optimal operation of reactive batch distillation including the start-up phase

In this section, the optimal operation problem of an industrial reactive semi-batch distillation column including the startup period is solved. The aim is the minimization of the total batch time subject to the model equation system (see appendix A6). The total equation system consists of mass balance, energy balance vapor-liquid equilibrium relations and tray hydraulics. The tray hydraulics is related to the geometry of the trays and essential for computing the pressure drop and holdup of each tray. The reaction kinetic is added to the model to depict the slightly endothermic trans-esterification in the reboiler. Following the process description in 6.1.1, during the batch a limited amount of educt alcohol will be fed to the reboiler in order to increase the reaction rate in the desired direction.

To simulate and optimize the process efficiently, the orthogonal collocation on finite elements is used to discretize the dynamic model equations in each time interval. Since the dynamic system exhibits both continuous and discrete aspects, a difficulty in solving the model equations is to deal with state variables which will be switched from non-equilibrium to an equilibrium phase. In addition, discontinuity also arises while the liquid holdup of each tray is filled from the top of the column to the bottom. To overcome those problems, a multiple time-scale strategy is proposed to guarantee a smooth transition between the different transition states during the start-up period (Fig. 6.6).

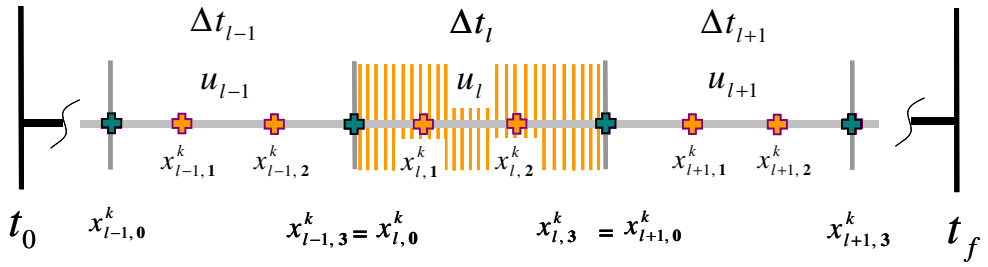

Figure 6.6: Multiple time-scale strategy.

In this strategy, the large time intervals are to be long enough for the practical realization as well as for the reduction of the computation time in the sensitivity calculation for the optimization. In order to keep the continuity of the variables, the last collocation point is used as the starting point of the next interval. Furthermore, small time intervals are adjusted in the simulation and their length is kept more flexible to guarantee the convergence in the Newton iteration. In case of non-convergence, a step length adjustment will be activated to reduce the step length until convergence is achieved. Moreover, the last collocation point of a small time interval must be one of the collocation points of the large time interval. Simulation studies have shown that one advantage of the collocation method is that the solutions of state variables at the same time point are almost independent of the step length. Therefore, the state variables at those large intervals can be used to compute the sensitivities. By this means, the gradient calculation has to be done only at the end of one large time interval. As a result, both the number of decision variables and the computation time for the sensitivity calculation can be significantly reduced.

The independent variables i.e. the only decision variables of the problem to be optimized using the NLP solver SQP, following the sequential strategy, are the feed flow rate into the reactor, and the reflux ratio. In addition, the lengths of the different time intervals are also considered as independent variables in order to conveniently handle the fraction switching time between the fractions and the total batch time. In order to compare the optimal results with those of the experimental run, the total amount of product alcohol recovered in the main cut fraction is restricted to a lower bound predetermined by experimental data. Furthermore, there are two constraints: one concerning to the average distillate composition at the end of the main cut period and the second one is related to the bottom purity at the end of the batch process, respectively.

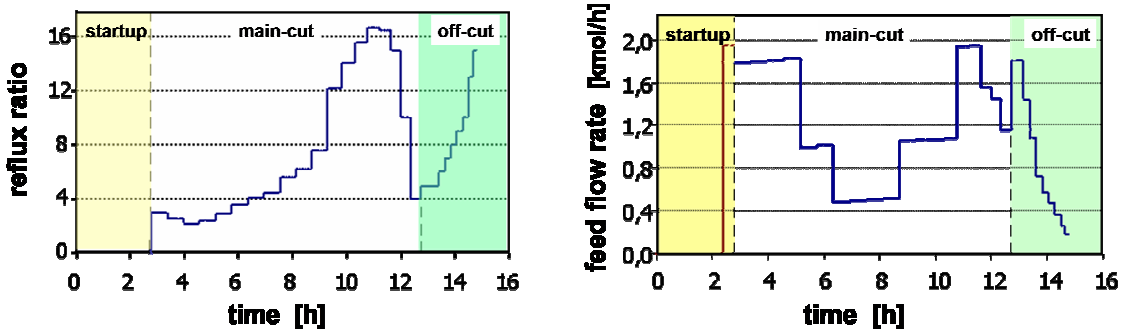

Figure 6.7: Optimal profiles of the reflux ratio and the feed flow rate.

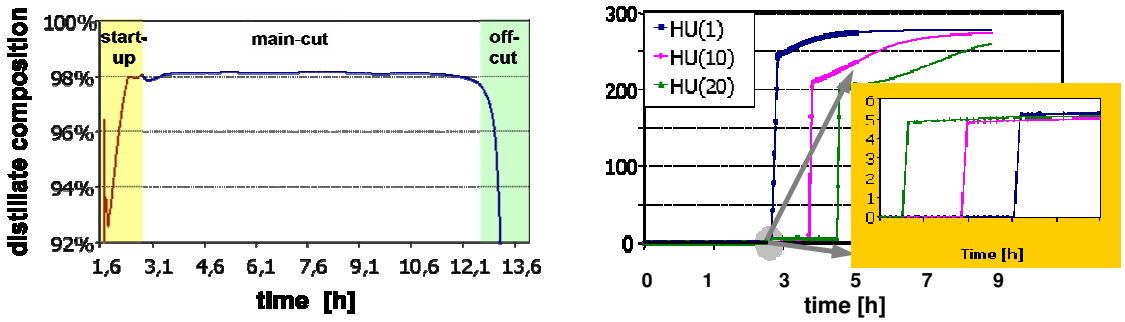

Figure 6.8: Optimal distillate composition and holdup transition profiles.

The optimal policies for the feed flow rate and the reflux ratio indicate both the thermal separation and chemical reaction effects (Fig. 6.7). The more product alcohol in the entire column, the less reflux ratio we need to satisfy the purity restrictions. A slow increase of the reflux ratio in the first 6 hours is allowed, since a large amount of product alcohol results from the drastic increase of the feed flow of the educt alcohol. However, when the feed flow has reached its maximum value, the reflux ratio needs to increase drastically in order to ensure the distillate purity constraint. The decrease of the reflux ratio after 11.5 h can be explained by the time delay between the feed supply of educt alcohol and the resulting effect of the formation of product alcohol caused by the chemical reaction. However, the average distillate composition at the end of the main fraction is to be fulfilled and not its instantaneous value. Moreover, to meet the purity requirement of the educt ester at the end of the batch process, an amount of feed is needed to react at the end of the charge. Figure 6.8 left shows the instantaneous value of the concentration at the top of the column, but the inequality constraint defined in the optimization problem refers to the cumulative value at the end of the main-cut period. Figure 6.8 right shows the holdup transition during the whole startup procedure. The

optimization outcomes show significant improvements in operation efficiency in comparison to conventional startup strategies. In particular, due to the reflux ratio strategy, which begins just after the reflux drum is filled up, the total batch time can be reduced. Furthermore, depending on the column geometry, liquid tray hold-up, vapor load and the reflux drum volume, in some cases the actual optimal reflux ratio strategy will be executed while the batch column trays are filled. For some systems, for the sake of simplicity, it might be more convenient to determine at first a feasible, reliable initial state from which a mathematical optimization can be carried out. However, to decide when and how much reflux ratio is appropriate, the simulation i.e. the model-based optimization including the start-up phase from a cold and empty batch column is required. The shown results clearly indicate the effectiveness and efficiency of the approach.

6.2 Deterministic Off-line Optimization

As stated before batch processes are inherently dynamic and thus the complete profiles of the decision variables are needed in order to define their optimal operating policies. In most studies, deterministic model-based optimization approaches have been performed for batch distillation processes using a nominal model (Low et al., 2002; Li et al., 1998; Arellano-Garcia et al. 2002, 2003). However, uncertainty in the model parameters or in the operating environment might have detrimental effects on the optimized process. Thus, since the operation policy developed is highly sensitive to the parameters and boundary conditions, product specifications may often be violated when implementing it in the real plant.

6.2.1 Optimization problem formulation

To evidence the performance of the developed approach (Chap. 5), the deterministic optimization of the large-scale nonlinear dynamic process described in section 6.1.1 is carried out at first. For this purpose, the model employed is the same as the one described in section 6.1.2 and Appendix A5. This model has been validated with experimental data (Li et al., 1998). Furthermore, based on the modeling approach for the startup of reactive batch distillation processes starting from a cold and empty state, a feasible reliable initial state is generated from which the deterministic model-based optimization is performed. Nonetheless, in view of the expected computational load required for the stochastic optimization, which strongly depends on the number of uncertain variables considered as well as on the total number of intervals with regard to the gradient computation, the process is scale-down without loss of generality. Accordingly, the reactor dimension, the column diameter and the initial amount of the charge are reduced. By this means and based on the orthogonal collocation method (three points), the resulting tailored system has now 233x3x30=20.970 state variables and 90 control (independent) variables which include the reflux ratio R_v, the feed flow rate into the reactor F as well as the time length of the different intervals.

In this thesis, the posed dynamic optimization problems are solved using the sequential approach where the variables space is divided into state **x** and control space **u**. Therefore, only the control or independent variables are optimized by the NLP solver (e.g. SQP). The large-scale DAE system is discretized with the orthogonal collocation on finite elements, thus, the differential and algebraic (dependent) variables are solved throughout the integration of the DAEs with the Newton method, and the required sensitivities are computed based on the interval gradient information (Li et al., 1998). The whole batch time is discretized into 30 time intervals. The control variables are set as piecewise constant.

The aim of the optimization of the reactive semi-batch distillation process is the minimization of the total batch time. Hence, the objective function of the nonlinear dynamic optimization problem can be formulated as follows:

$$\min t_f \left(F(t), R_v(t), t_u, t_f\right) \tag{6.1}$$

Since the time-length of the different intervals are also regarded as independent variables, t_u and t_f refer to the switching time point from the main-cut to the off-cut period and the total batch time, respectively. Besides, the optimization problem is subject to equality constraints which include the model equations and an additional constraint which corresponds to the limited amount of educt alcohol M_1 to be fed to the reactor or reboiler:

$$\int_{t_0}^{t_f} F(t)dt = M_1 \tag{6.2}$$

It is also subject to inequality constraints including product purity specifications. So, the average composition of the product alcohol x_D accumulated during the main-cut period is at t_u:

$$x_D(t_u) \geq 0,98 \ \text{mol/mol} \tag{6.3}$$

According to the process operation requirements, the remaining educt alcohol in the reactor or reboiler should have been converted by the end of the batch process t_f as far as possible. Thus, an upper bound for the concentration of the educt alcohol is considered,

$$x_A(t_f) \leq 0.002 \ \text{mol/mol} \tag{6.4}$$

As a result, two time-dependent end-point purity restrictions are considered. In addition, the total amount of the product alcohol, D, collected in the main-cut period is restricted to a lower bound in order to assure a reasonable comparison with other optimal operational strategies

$$D(t_u) \geq D_{min} \tag{6.5}$$

Physical restrictions are also included in the optimization problem. These are among others an upper and lower bound for the reflux ratio R_v and the feed supply F:

$$R^L_{v,min} \leq R_v(t) \leq R^U_{v,max} \tag{6.6}$$

$$F^L_{min} \leq F(t) \leq F^U_{max} \tag{6.7}$$

6.2.2 Deterministic optimization results

The computed trajectories of the control variables for the optimal operation are illustrated in Figure 6.9. The optimal results in Figure 6.9, analogous to Figure 6.7, indicate again both the thermal separation and chemical reaction effects. The more product alcohol in the entire column, the less reflux ratio is required to comply with the product specifications. The policy of the feed flow rate shown in Figure 6.9 illustrates an optimal distribution of the educt alcohol during the batch in order to forward the reaction to the product side. However, since the supply of educt alcohol increases, the reflux ratio is augmented considerably in order to

guarantee the fulfillment of the distillate purity restriction. Furthermore, due to the time displacement between the feed flow rate of educt alcohol and the resulting effect of formation of product alcohol caused by the progress of the chemical reaction, the reflux ratio is reduced before the main-cut period is completed. Moreover, in consequence of the educt alcohol excess during the off-cut period, which guarantees the desired conversion in the reboiler, the reflux ratio is held down to favor the reaction rate. By this means, the end-point restriction concerning the remaining educt ester (6.4) can be fulfilled.

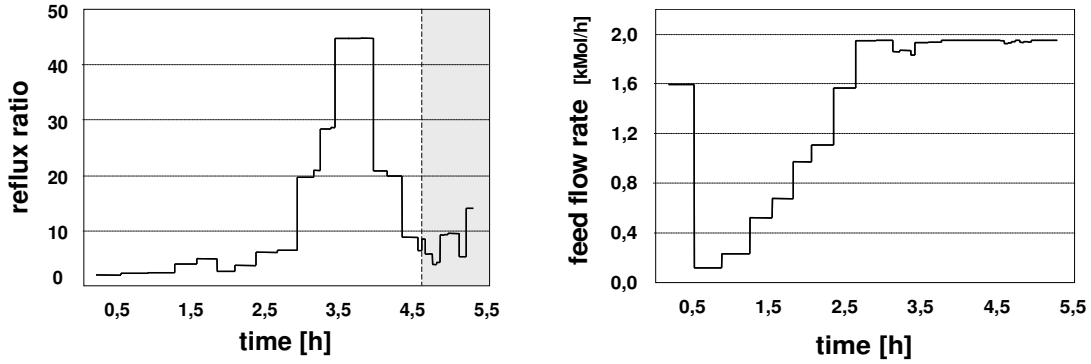

Figure 6.9: Optimal reflux ratio and feed flow rate profiles via deterministic optimization.

6.2.3 Impacts of the uncertain inputs to the constrained outputs

The purpose of this section is to illustrate the effect of uncertainty for the process treated above. Generally speaking, the design of chemical processes required a good deal of data, most of which are obtained from specific experiments or are estimated from correlations. The resulting design contains uncertainties, but their magnitudes may be unknown. In industrial practice, overdesign factors has commonly be applied to overcome this problem.

In this section, uncertainties are considered in order to simulate the impact of the uncertain inputs to the constrained outputs. In reactive batch distillation, the chemical reaction kinetic parameters are usually considered as uncertain parameters, since they are often determined through a limited number of experimental data. Furthermore, the amount and composition of the initial charge are also uncertain, since they are mostly product outputs of a previous batch. In this case study, the *Arrhenius* equation (Eq. 6.8) is used to describe the way the rate constant k varies with the absolute temperature T.

$$k = k_0 \cdot e^{-E/RT} \tag{6.8}$$

where E (*activation energy*) represents the energy difference between the reactants and an activated species. R is the gas constant. The term k_0 stands for the frequency factor. This is related to the frequency of molecular collisions in the collision theory and to the entropy term in the transition state theory. Taking the natural logarithm of both sides of the *Arrhenius* equation (6.8), it can be redefined as follows:

$$\ln k = -\frac{E}{RT} + \ln k_0 \tag{6.9}$$

Using a linear regression the slope and ordinate intercept of (6.9) can be determined. Figure 6.10 (a)-(d) shows the reaction rate based on different *Arrhenius* parameters. In the deterministic optimization the nominal values of E and k_0 are used. However, while remarkably accurate in a wide range of circumstances, the *Arrhenius* equation is not exact. Thus, the values of E and k_0 can be expressed as a probability density function (Fig. 6.10-a). Usually they are given in an area of validity (Fig. 6.10 b-d). By this means, the kinetic parameters are uncertain and thus they have a great impact on the output variables which are then also uncertain. This is particularly the case when both parameters are stochastic (Fig. 6.10-d).

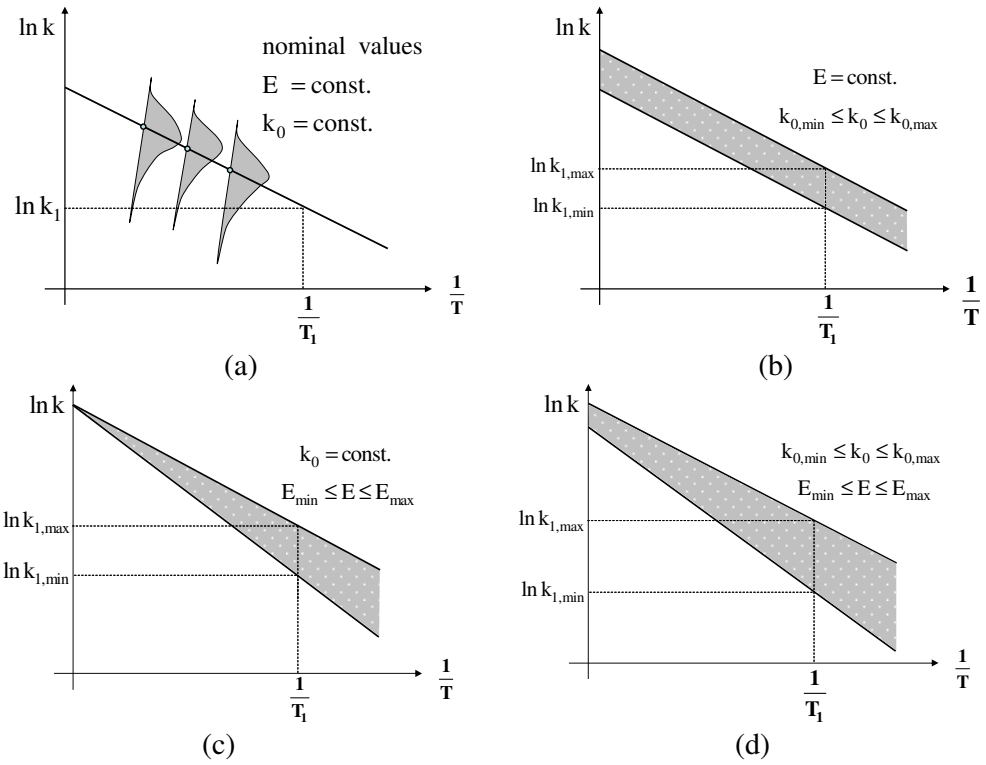

Figure 6.10: Reaction rate with different *Arrhenius* parameters.

In order to compare the performance results of the deterministic optimization with those of the stochastic optimization, the effect of the uncertainties is emphasized. Thus, the optimal operation of the reactive batch distillation based on the nominal values of the parameters is taken into account at first. Here, we assume that the two kinetic parameters, the frequency factor of the forward and reverse reaction, respectively, and the tray efficiency are uncertain. Besides, they have a correlated multivariate normal distribution according to Table 6.1. The terms of the correlation matrix are values that result from parameter estimation. It should be noted that the assumption that the *Arrhenius* constants are correlated and that all are normally distributed is not necessarily a practical assumption.

	expected values	standard deviation	correlation matrix
k_{01}	43093,9	5%	$\begin{bmatrix} 1 & 0,5 & 0,2 \\ 0,5 & 1 & 0,2 \\ 0,2 & 0,2 & 1 \end{bmatrix}$
k_{02}	15671,0	5%	
η	0,70	3%	

Table 6.1: Random parameters.

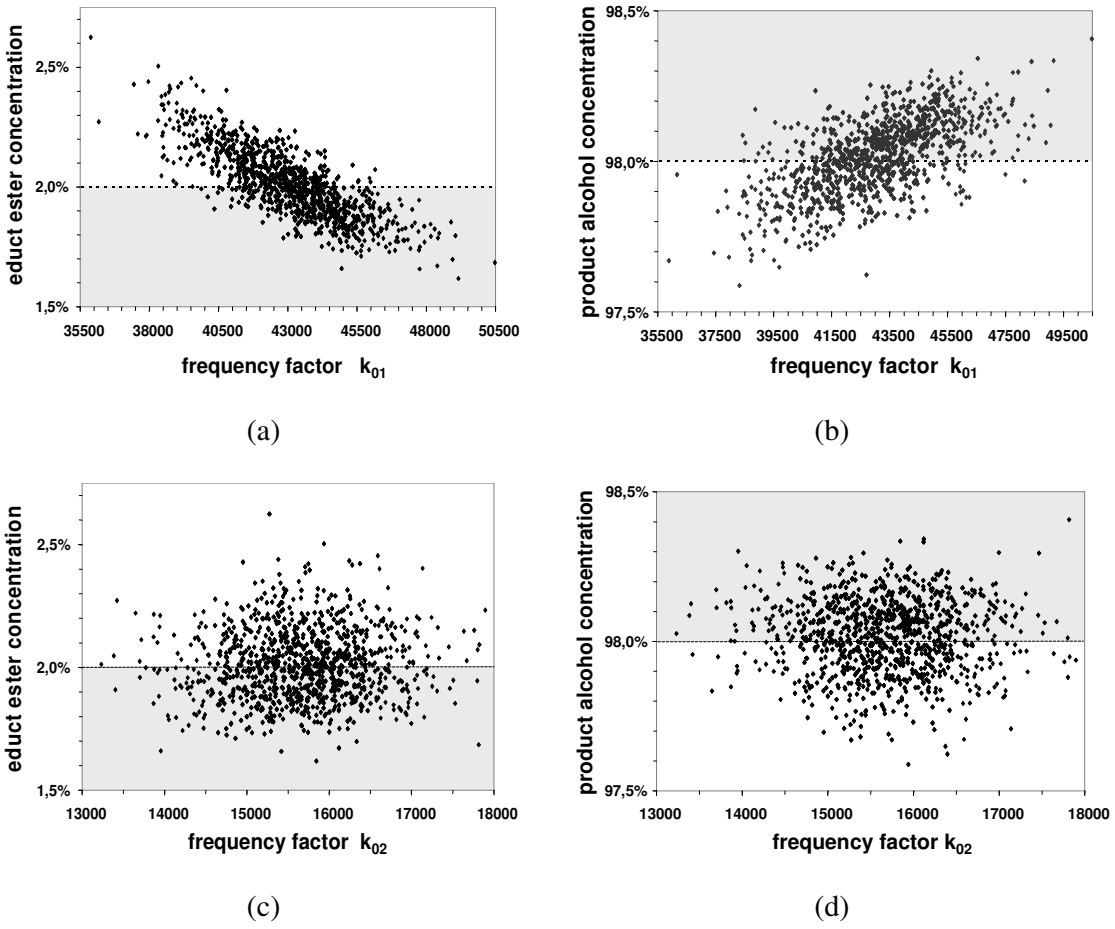

Figure 6.11: Impact of the uncertain frequency factors k_{01} and k_{02} on the constrained purity restrictions using the optimal policies determined through deterministic optimization.

From Figure 6.11 a-b, it can be noticed that though the frequency factor k_{01} has a negative correlation with the educt ester concentration, has it a positive correlation with the product alcohol concentration. This is based on the fact that the larger k_{01}, the higher the reaction rate and, thus, the products become purer. However, due to the lower value of k_{02} compared to k_{01}, the sampling correlation between k_{02} and the product concentrations (Fig. 6.11 c-d) is not clearly defined. Furthermore, the scatterplots in Figure 6.11 a-d show the constraints defining the feasible region (grey labeled) together with the simulation points calculated by propagating the parametric uncertainty through the model via Monte Carlo simulation with 1000 points. Sampling the random parameters based on the information of Table 6.1, it can be seen that the implementation of the deterministic optimization results will lead to about 50% of constraint violations. However, uncertainty and variability are inherent characteristics of any process system. Besides, for a quantitative understanding and control of transient processes, it is essential to relate the observed dynamical behavior to mathematical models. As stated in the previous chapters, these models usually depend on a number of parameters whose values are unknown or only known roughly. Furthermore, often only a part of the system's dynamics can be measured. Thus, the explicit consideration of the stochastic information of the uncertain input should be included in the optimization problem. By this means, an appropriate decision regarding the optimal policies will be taken in order to compensate between the objective function and the risk of constraint violation.

6.3 Stochastic Dynamic Optimization

Decision making inherently involves consideration of uncertain outcomes. Thus, we are confronted with decisions a priori for the future operation. The decisions should however be taken before the realization of the random inputs. These uncertain variables arise due to the unpredictable and instantaneous variability of different process condition, and can be constant or time-dependent in the future horizon. Moreover, the use of feedback control in order to compensate uncertainty can not ensure constraints on open-loop variables. Consequently, the consideration of uncertainties/disturbances and their stochastic properties in optimization approaches are necessary for robust process operation, and control. The stochastic distribution of the uncertain variables may feature different forms. The developed approach assumes though the availability of the uncertainty quantification and the knowledge of a process model. However, while a model which describes the process considered may be available, in many cases, the quantification of uncertainties represents a bottleneck in applying this approach. On the other hand, there has been an increasing attention on statistical analysis in the process industry. Furthermore, measurement instruments are increasingly installed to collect data from industrial processes. The mean and variance values can be determined based on historical data analysis. However, with the proposed optimization framework in Chapter 5 stochastic optimization with even an approximated distribution is more reliable than a deterministic optimization. In this thesis, uncertainties are assumed to have a correlated multivariate normal distribution, but the presented approach does not depend on the distribution form.

6.3.1 Chance constrained optimization problem formulation

In this section, the developed approach in Chapter 5 is applied also to the process described in 6.1.1. The uncertainty properties are included in the problem formulation. Thus, the model incorporates the probabilistic nature of the uncertain inputs. The resulting chance constrained optimization problem is formulated as follows,

$$
\begin{aligned}
&\min\ t_f\left(F(t), R_v(t), t_u, t_f\right)\\
&\text{s.t.}\quad \int_{t_0}^{t_f} F(t)dt = M_1\\
&\quad D(t_u) \geq D_{min}\\
&\quad \Pr\left\{x_D(t_u) \geq 0{,}98\ \text{mol/mol}\right\} \geq \alpha_1\\
&\quad \Pr\left\{x_A(t_f) \leq 0.02\ \text{mol/mol}\right\} \geq \alpha_2\\
&\quad R^L_{v,min} \leq R_v(t) \leq R^U_{v,max}\\
&\quad F^L_{min} \leq F(t) \leq F^U_{max}
\end{aligned}
\qquad (6.10)
$$

Uncertain variables are the frequency factors k_{01}, k_{02}, the activation energy E_1 and E_2, the tray efficiency η as well as the initial composition of the charge in the reboiler. To restrict the risk of constraint violation under the uncertainties, the product specifications in (6.3) and (6.4) are now expressed as ***single*** chance constraints at first. These impose lower bounds on the probability that the specified purity restrictions are fulfilled. Thus, α_1 and α_2 are the user-defined probability levels to hold the two specifications. Following the solution approach in this thesis, the stochastic programming problem will then be relaxed to an equivalent deterministic NLP problem. As indicated in the previous chapters, the main challenge lies in the computation of the probabilities of holding the constraints as well as their gradients.

6.3.2 Inverse mapping of the feasible region

Due to the nonlinear propagation, it is difficult to gain the stochastic distribution of output variables. Thus, nonlinear chance constrained programming remained as an unresolved problem. As stated before, in this thesis, the computation of the output probability distribution is avoided. Instead, an equivalent representation of the probability is derived by mapping the chance constrained region of the outputs back to a bounded region of the uncertain inputs. However, before the developed optimization framework can be applied, it needs to be proved whether there exists a strict monotonic relationship between constrained output and uncertain input or not. For this purpose, the impacts of the uncertain parameters on the constrained output variables are analyzed. Using the trajectories of the controls determined by the deterministic optimization, the constrained outputs are computed with values around the expected value of the uncertain parameters through simulation.

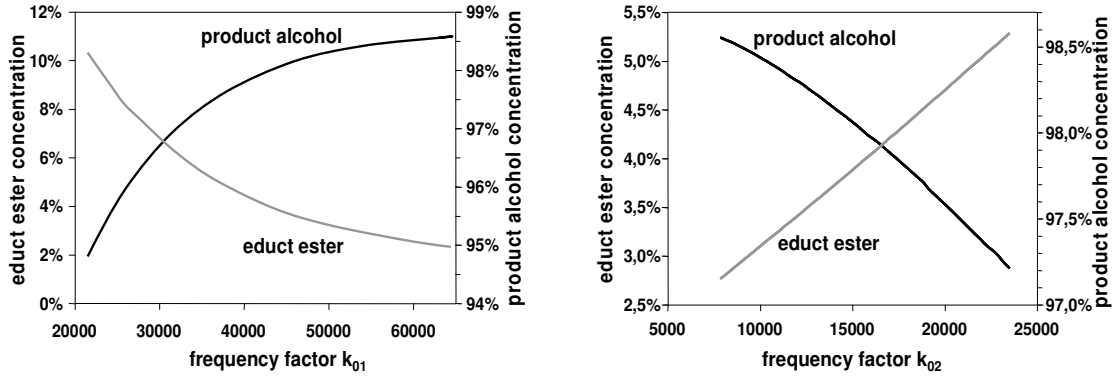

Figure 6.12: Impact of the frequency factors on the purity restrictions.

The simulation results show in Figure 6.12 that the two frequency factors have a strong impact on the output constraints in all regions. They have a monotonic relationship to both product restrictions. As shown in Figure 6.13, the tray efficiency exhibits also a strongly monotonic relation to the constrained output variables in the probabilistic constraints at any rate. The tray efficiency causes a strongly negative effect on the purity constraints in lower regions while causing a slightly positive effect in upper regions. By this means, there is a positive correlation $\eta \uparrow \Rightarrow x_D \uparrow$, which corresponds to the distillate purity restriction, and, on the other hand, a negative correlation related to the educt ester constraint $\eta \uparrow \Rightarrow x_A \downarrow$.

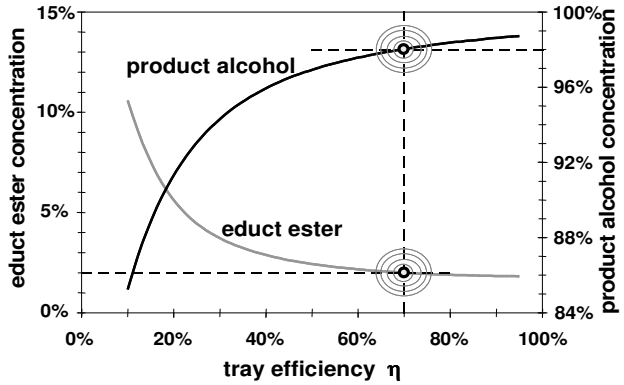

Figure 6.12: Relation between tray efficiency and the constraint output variables.

In this case study and due to numerical reasons concerning the convergence reliability, the tray efficiency η is chosen as the uncertain variable ξ_S, which has, in fact, a strict monotone relation to both output constraints, thus, the principals of the developed approach in 5.1.1 can be applied to solve the stochastic nonlinear dynamic optimization problem. Due to the positive monotony, the boundary of the constrained variable in the output region corresponds to the limit value ξ_S^L for ξ_S in the input region. Thus, we can then transform the originally chance constraints:

$$\Pr\left\{x_D(t_u) \geq x_D^{SP}\right\} \quad \text{to} \quad 1-\Pr\left\{\eta \leq \eta^L\right\} \text{ and} \tag{6.11}$$

$$\Pr\left\{x_A(t_f) \leq x_A^{SP}\right\} \quad \text{to} \quad \Pr\left\{\eta \geq \eta^L\right\} \tag{6.12}$$

However, this boundary depends also on the realization of the other uncertain variables $(\xi_S, \cdots, \xi_{S-1})$. They are computed on each collocation point of these variables. The computation of the time-dependent uncertain variable boundaries is carried out through inverse mapping of the feasible output region according to:

$$\eta^L(t) = F^{-1}\left(k_{01}, k_{02}, E_1, E_2, n_0, x_D(t_u), R_v(t), F(t), \Delta t\right) \tag{6.13}$$

$$\eta^L(t) = F^{-1}\left(k_{01}, k_{02}, E_1, E_2, n_0, x_A(t_f), R_v(t), F(t), \Delta t\right) \tag{6.14}$$

where n_0 and Δt denote the initial composition of the charge and the different lengths of the time intervals, respectively. Accordingly, the corresponding bound of the random variable in the numerical integration can be determined based on these relations (6.13) and (6.14). However, due to the model complexity of the reactive batch distillation, there is no explicit expression for these expressions. Thus, in order to solve the nonlinear dynamic optimization problem with time-dependent constraints, uncertain parameters occurring throughout the entire operation, and different values of **u** in different time intervals, the dynamic solver introduced in chapter 5 is required (see Fig. 5.4). One main task is the iterative determination of the tray efficiency which exactly generates the output variables values x_D^{SP} and x_A^{SP} by given trajectories of the independent variables. This occurs however with different combinations of the other uncertain parameters. By this means, a raster results from the five-point-collocation which is extended over the space of the uncertain variables (Fig. 6.13).

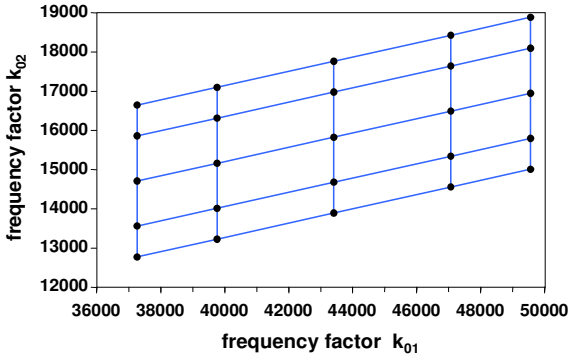

Figure 6.13: Collocation points of the frequency factors.

In Figure 6.13, the grid points correspond to the integration bounds for the probability computation. Thus, the *dynamic solver* is called 25 times for each probability. The computation of η^L follows the reverse projection (inverse mapping) approaches presented in 5.1.1. In order to emphasize the advantages of both approaches for the specific case of the reactive batch distillation system, several studies were accomplished. For this purpose, the number of required simulation calls can be seen as a degree of efficiency. Thus, Figure 6.14 shows a representative example for the probability computation of complying with both product constraints and their corresponding simulation calls.

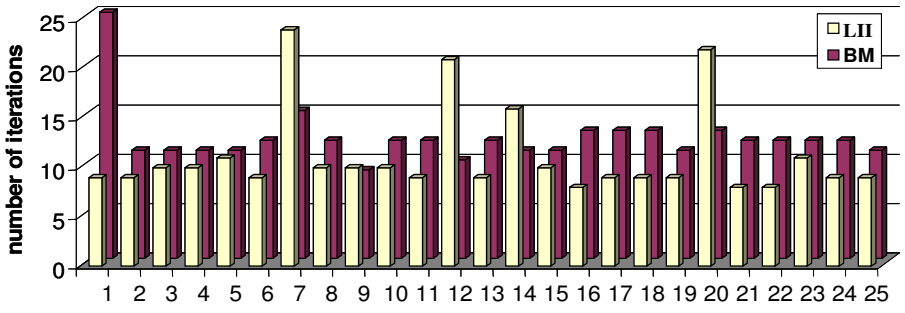

(a)

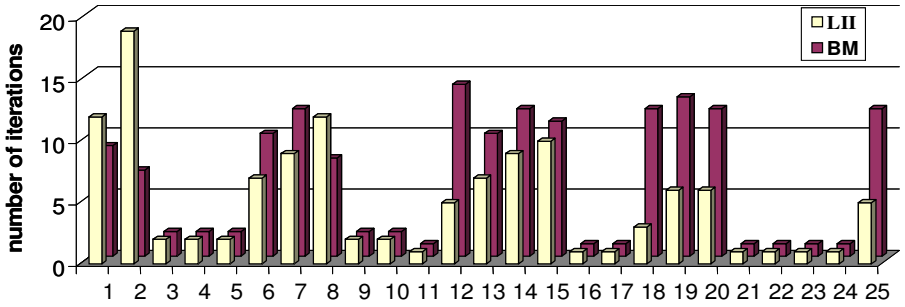

(b)

Figure 6.14: Number of required simulation calls for both approaches, *linear inverse interpolation* **LII,** and *bisectional method* **BM**.

In Figure 6.14 a-b, it can be seen that the number of simulation calls is apparently lower for LII than using BM. However, this does not apply to all collocation points. The cases, where just one or two simulations calls are required, can be explained by the fact that the sought reverse projection bound η^L lies outside of the search range $[-3\sigma, +3\sigma]$ and thus no further computation is needed. Accordingly, the BM requires for the example above a total of 466 simulation calls while the LII approach implies presently 406 calls for the computation of both single probabilities. At an average, the iterative determination of η^L with LII is approx. 10% faster. Therefore, it is selected for further computation related to the system treated in this chapter (Arellano-Garcia et al., 2003b).

6.3.3 Computation of the probability gradients

Another main task of the *dynamic solver* is finally the sensitivity computation. As shown in section 5.1.1.2, the method for the computation of the gradients with respect to the decisions variables **u** is based on the formulation of the total differential of the model equations **g**:

$$\mathrm{d}\mathbf{g} = \left[\frac{\partial \mathbf{g}}{\partial \boldsymbol{x}}\frac{\partial \boldsymbol{x}}{\partial \mathbf{u}}\right]\mathrm{d}\mathbf{u} + \left[\frac{\partial \mathbf{g}}{\partial \xi_{\mathrm{s}}^{\mathrm{L}}}\frac{\partial \xi_{\mathrm{s}}^{\mathrm{L}}}{\partial \mathbf{u}}\right]\mathrm{d}\mathbf{u} + \left[\frac{\partial \mathbf{g}}{\partial \mathbf{u}}\right]\mathrm{d}\mathbf{u} = \mathbf{0} \tag{6.15}$$

As exemplified in the previous chapter, Equation (6.15) can generally be reformulated as follows:

$$\left[\frac{\partial \mathbf{g}}{\partial \boldsymbol{x}} \quad \frac{\partial \mathbf{g}}{\partial \xi_{\mathrm{s}}^{\mathrm{L}}}\right]\begin{bmatrix}\dfrac{\partial \boldsymbol{x}}{\partial \mathbf{u}} \\ \dfrac{\partial \xi_{\mathrm{s}}^{\mathrm{L}}}{\partial \mathbf{u}}\end{bmatrix} = -\left[\frac{\partial \mathbf{g}}{\partial \mathbf{u}}\right] \tag{6.16}$$

The application of the approach to the reactive semi-batch distillation leads though to a large-scale system of equations generated after discretization of the models equations with the orthogonal collocation method. The derived equation system can be formulated as follows:

$$\underbrace{\begin{bmatrix}\mathbf{J}_1 & & & & & \mathbf{C}_1 & & \\ \mathbf{A}_2 & \mathbf{J}_2 & & & & \mathbf{C}_2 & & \\ & \ddots & \ddots & & & \vdots & & \\ & & \mathbf{A}_i & \mathbf{J}_i & & \mathbf{C}_i & & \\ & & & \ddots & \ddots & \vdots & & \\ & & & & \mathbf{A}_{m-1} & \mathbf{J}_{m-1} & \mathbf{C}_{m-1} & \\ & & & & & \mathbf{A}_m & \mathbf{J}_m & \end{bmatrix}}_{\mathfrak{I}} \underbrace{\begin{bmatrix}\boldsymbol{x}_{\mathrm{u},11} & \cdots & \cdots & \boldsymbol{x}_{\mathrm{u},1m} \\ \vdots & \ddots & & \vdots \\ \vdots & & \ddots & \vdots \\ \boldsymbol{x}_{\mathrm{u},m1} & \cdots & \cdots & \boldsymbol{x}_{\mathrm{u},11}\end{bmatrix}}_{\Omega} = -\underbrace{\begin{bmatrix}\mathbf{F}_1 & & & & \\ & \mathbf{F}_2 & & & \\ & & \ddots & & \\ & & & \mathbf{F}_{m-1} & \\ & & & & \mathbf{F}_m\end{bmatrix}}_{\Gamma} \tag{6.17}$$

Where $\mathbf{J}_i$ denotes the Jacobian matrix at the time interval i, and m is the total number of time intervals which result from the discretization,

$$\mathbf{J}_i = \left.\frac{\partial \mathbf{g}}{\partial \boldsymbol{x}}\right|_i \tag{6.18}$$

$\mathbf{C}_i$ represents the gradients of the model equations with respect to the bound value,

$$\mathbf{C}_i = \left.\frac{\partial \mathbf{g}}{\partial \xi_{\mathrm{s}}^{\mathrm{L}}}\right|_i \tag{6.19}$$

In contrast, $\mathbf{A}_i$ describes the derivative of the model equations with respect to the variables $\boldsymbol{x}$ which correspond to the previous interval (i-1),

$$\mathbf{A}_i = \left.\frac{\partial \mathbf{g}}{\partial \boldsymbol{x}}\right|_{i-1} \tag{6.20}$$

$\mathbf{F}_i$ denote the derivative with respect to the decision variables $\mathbf{u}$,

$$\mathbf{F}_i = \left.\frac{\partial \mathbf{g}}{\partial \mathbf{u}}\right|_i \tag{6.21}$$

Thus, all these variables can be derived from the model equations. In Equation (6.17) the rows of the first matrix on the left hand side represent the model equations in their respective intervals, while die columns denote the variables $\boldsymbol{x}$ which also include the constrained outputs y_i. However, since the constrained outputs y_i are defined by their specifications y_i^{SP}, its corresponding column will be replaced by the uncertain inputs ξ_s^L. Moreover, since the formulated nonlinear dynamic optimization problem under single chance constraints in (6.10) encloses output constraints for fixed end time points, namely, at the end of the main-cut period and at the end of the batch process, the gradients $\mathbf{C}_i$ are also located in the last column of the matrix $\mathfrak{I}$. By this means, all model equations of the intervals (i = 1,…., m-1) do not depend on the other variables of the last time interval m since the last column in $\mathfrak{I}$ stands for the uncertain input variable ξ_s^L. Thus, $\mathbf{J}_m$ represents the modified Jacobian matrix where the constrained outputs are replaced by ξ_s^L. In fact, the actual unknowns at the present system of equations (6.17) are the derivatives of $\boldsymbol{x}$ at the interval i with respect to the decision variables $\mathbf{u}$ at the interval j ($\partial \boldsymbol{x}/\partial \mathbf{u}$). They are represented in $\boldsymbol{\Omega}$ (6.17) by $\boldsymbol{x}_{\mathbf{u},ij}$. However, primarily the values $\boldsymbol{x}_{\mathbf{u}}$ of the last row of $\boldsymbol{\Omega}$ are of interest since they include the desired gradients $\partial \xi_s^L / \partial \mathbf{u}$. Furthermore, in $\mathfrak{I}$ are the matrices $\mathbf{A}_i$, which stand for the derivative of the model equations of the current interval with respect to the variables of the previous interval, only at the column of the last collocation point taken, since these operate as initial values for the current interval.

However, since the individual matrices in (6.17) are very large, the solution of the whole equation system poses some difficulties. So for instance, the entries of $\mathfrak{I}$, namely, $\mathbf{J}_i$, $\mathbf{A}_i$, and $\mathbf{C}_i$ are even matrices, each of them has the dimension 699×699 while the dimension of $\mathbf{F}_i$ and $\boldsymbol{x}_{u,ij}$ is 699×b, respectively. Here, b stands for the number of control variables which depends on the number of intervals m. The unknowns of the equation system are computed using the Gauss elimination approach. By this means, the matrix $\mathfrak{I}$ in (6.17) is transformed to an upper triangular matrix which features a main diagonal composed of unit matrices, while the matrix $\boldsymbol{\Gamma}$ is converted to a lower triangular matrix. The allocation of the matrix $\boldsymbol{\Omega}$, however, remains unchanged.

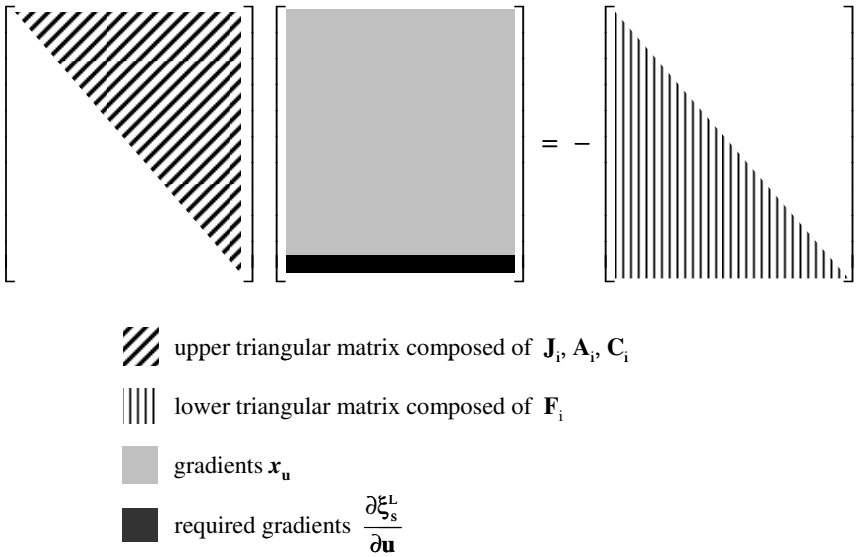

Figure 6.15: Structure of the equation system after the Gauss elimination (Arellano-Garcia et al., 2003c).

By means of the structure illustrated in Figure 6.15, the required gradients of the reverse projected bound value ξ_s^L with respect to the control variables **u** can easily be computed. Furthermore, around 60% of the initially computing time could be saved by exploiting the structure of the sparse matrices $\mathbf{A}_i$ and $\mathbf{C}_i$.

The computational strategy for solving the nonlinear chance constrained optimization problem is illustrated in Figure 5.4. The gradient vector is simultaneously computed to the probability computation of each single chance constraint by numerical integration in the limited area of the uncertain inputs. For this purpose, the optimal number of collocation points and intervals is firstly determined based on a trade-off between computational time and accuracy. In this case study, in particular, the five-point collocation is more efficient than the three-point-collocation at any rate, so for instance, with two intervals the error of probability computation is always less than 1%.

6.3.4 Stochastic optimization results

In this section, the results of the stochastic optimization problem formulated in (6.10) including single chance constraints are presented. Figure 6.16 shows the resulting optimal operation policy for the reactive semi-batch distillation process. Compared to the results of the deterministic approach, the reflux ratio is slightly higher, which is necessary in order to reduce the risk of violating the purity constraints. This inevitably means that the total batch time has to be a little longer (5.6h) than that of the deterministic approach (5.28h).

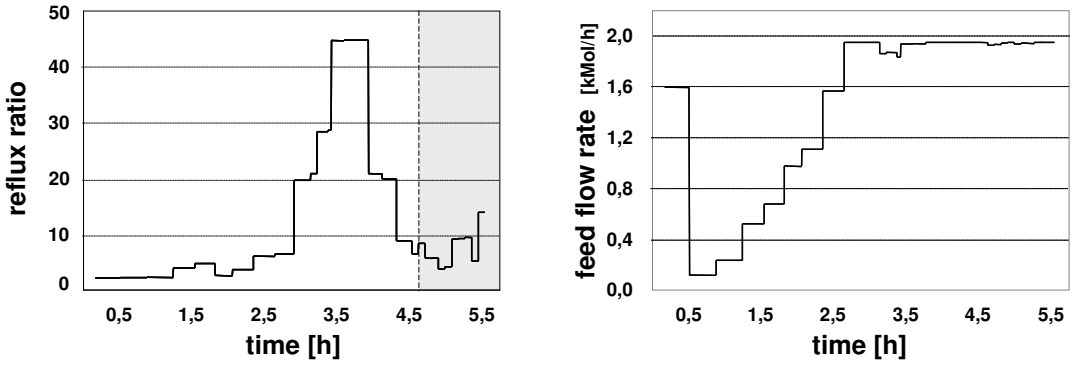

Figure 6.16: Optimal reflux ratio and feed flow rate profiles via stochastic optimization.

The deterioration of the objective value is obviously the price for a higher robustness. However, it can easily be seen in Figure 6.17 that the desired robustness is achieved. Using again Monte Carlo simulation, the distribution of the constrained output variables are illustrated according to the operation policy obtained by the stochastic approach. Setting the probability level for both chance constraints to the value of 96%, by the robust optimization policy, the risk of violation is reduced to less than 4%.

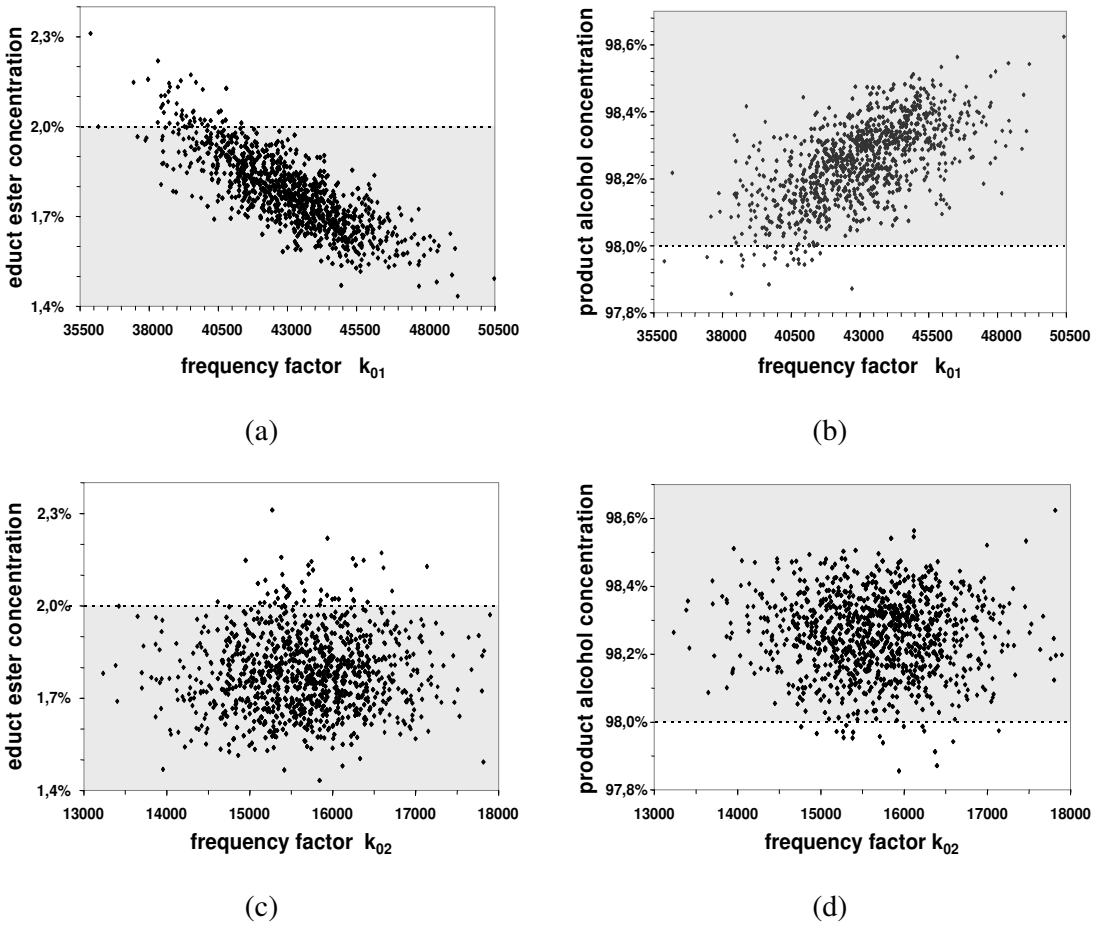

Figure 6.17: Impact of the uncertain frequency factors k_{01} and k_{02} on the constrained purity restrictions using the optimal policies determined through stochastic optimization.

The numerical results presented in Figure 6.17 a-d point up the efficiency of the developed approach. Since the uncertainty attributes are considered, the problem solution is a decision a priori. The predefined probabilities to comply with the constraints are held under the influence of several uncertainties, thus, the decision is robust. Furthermore, it provides a comprehensive relationship between the performance criteria and the probability level of fulfilling the constraints. This issue can be used as a measurement for evaluating and selecting operation policies. By this means, conservative or aggressive decisions can be prevented.

6.3.5 Feasibility analysis with chance constraints

In this section, we focus on the analysis of the impact of chance constraint probability limits on the optimal process operation policies in terms of robustness and feasibility, in particular with regard to the optimized value of the objective function. These probability limits (α=confidence level) can be seen as a criterion for robustness of the optimized strategies. Obviously a high confidence level to ensure the constraints will be preferred. However, due to the properties of the uncertain input and the restrictions of the controls and outputs, it is often impossible to find an operation policy with a 100% guarantee for complying with the constraints. Thus, as already introduced in chapter 4 as well, a maximum confidence level max-α needs to be found first.

The knowledge of max-α is essential, so for instance, if a value greater than max-α is chosen, the feasible region will be empty. Moreover, below max-α the optimized value of the objective function deteriorates with an increasing probability limit due to the decrease of the feasible region. Hence, those regions where an increase of the probability limit α causes only a little deterioration of the optimized objective function are of special interest. Consequently, the relationship between the probability levels and the corresponding values of the objective function can be used for a suitable trade-off decision between profitability and robustness. Tuning the value of α is also an issue of the relation between feasibility and profitability. The solution of a defined problem, however, is only able to arrive at a maximum value max-α which is dependent on the properties of the uncertain inputs and the restriction of the controls.

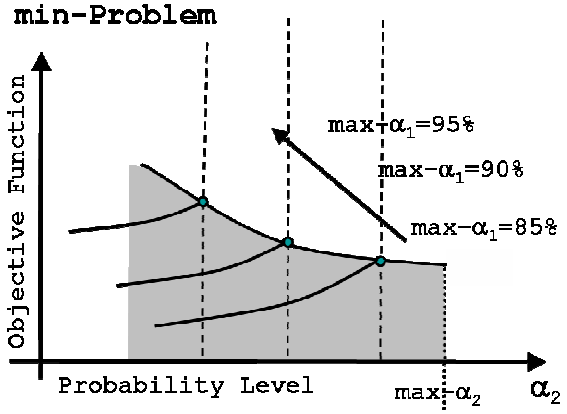

Figure 6.18: Feasible region according to the probability levels and the objective function

In Figure 6.18, we consider the case of a minimization problem subject to two single probabilistic constraints representing α_1 and α_2 the probability levels, respectively. If we assigned to α_2 a certain probability level, we can then compute, as stated in Equation 6.22, the corresponding maximum achievable probability level for α_1 and vice versa. For this purpose, we replace the original objective function and solve then the optimization problem,

$$
\begin{aligned}
&\max \ \alpha_1 \\
&\text{s.t.} \ \ \mathbf{g}(\dot{\boldsymbol{x}}, \boldsymbol{x}, \mathbf{y}, \mathbf{u}, \boldsymbol{\xi}) = 0, \quad \boldsymbol{x}(t_0) = \boldsymbol{x}_0 \\
&\qquad \Pr\{\, y_1(\mathbf{u}, \boldsymbol{\xi}, t) \le y_2^{SP} \} \ge \alpha_1 \\
&\qquad \Pr\{\, y_2(\mathbf{u}, \boldsymbol{\xi}, t) \le y_2^{SP} \} \ge \alpha_2 \\
&\qquad \boldsymbol{x}_{min} \le \boldsymbol{x} \le \boldsymbol{x}_{max} \\
&\qquad \mathbf{u}_{min} \le \mathbf{u} \le \mathbf{u}_{max}, \qquad t_0 \le t \le t_f
\end{aligned}
\tag{6.22}
$$

The aslope solid lines within the gray area represent the isolines for max-α_1. Since they have a monotonic relation, the value of objective function will be degraded if α_1 is increased. Now, we repeat the computation for a lower value of α_2. We get here again the maximum achievable probability level which is, in fact, greater than the one calculated before. If we continue doing the computation for further values of α_2 we obtain different pairings of α_2 and the corresponding maximum value for α_1. By connecting all the resulting points to each other, a feasibility boundary arises under which every combination of α_1 and α_2 leads to a feasible solution. Moreover, from the maximal achievable probability level for α_2 results a defined feasible area. If pairing values outside of this area are chosen, the feasible region will be

empty and the SQP algorithm can not find a feasible solution. Moreover, one can analyze for the reactive batch distillation the profile of the function value changing again the probability level and decide a suitable trade-off between profitability and reliability. For this purpose, the chance constrained optimization problem (6.10) is solved several times with different paring values of α_1 and α_2.

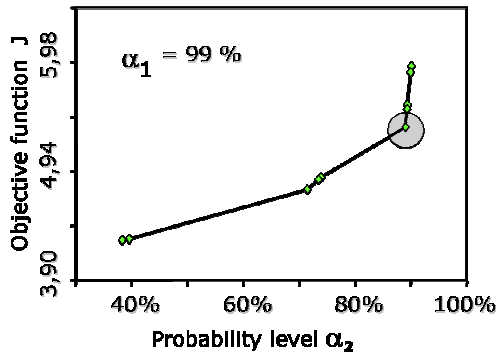

Figure 6.19: Trade-off between probability level and objective function

Since the results are to be used for finding trade-off decisions between robustness and the benefit of the objective value, the optimized values are computed for different probability levels. In Figure 6.19, α_1, the probability level of the distillate product purity is fixed at 99%. It represents the case that almost no risk can be afforded towards a violation of the distillate product purity. We then change the confidence level for holding the bottom purity restriction α_2. It is worthwhile to note the significant increase of the objective value from the confidence level of 92% on. From this point on, it is obvious that not much reliability can be gained by increasing the batch time. The opposite occurs in regions of lower probabilities. For a trade-off decision the point, at which the low increase ends and the significant increase begins, can be chosen (Arellano-Garcia et al., 2004a).

6.3.6 Joint chance constrained optimization

The stochastic optimization problem formulate in (6.10) has more than one restriction, thus, distinction has to be made between single and joint probabilistic constraints. A joint chance constraint requires the reliability in the output feasible region as a whole, while single chance constraints demand the reliability in the individual output feasible region. In addition, the joint probabilistic constraint leads to more robustness of all policies during the entire process. To consider a joint chance constraint, the two single chance constraints in (6.10) will be replaced by a joint chance constraint with the following formulation:

$$\Pr\left\{\begin{matrix} x_D(t_u) \geq 0{,}98 \ \text{mol/mol} \\ x_A(t_f) \leq 0.002 \ \text{mol/mol} \end{matrix}\right\} \geq \alpha \tag{6.23}$$

Due to the monotonic relations $\eta \uparrow \Rightarrow x_D \uparrow$ and $\eta \uparrow \Rightarrow x_A \downarrow$, both purity restrictions induce an upper bound of the tray efficiency, η, in the integral for computing the probability of violation (or a lower bound for the probability of being feasible). Follwing the principles in section 5.1.2, we have also the convenient case that there is only an upper bound, but no lower bound. This means that in each step, the reverse function is computed for each purity restriction according to Equation (5.10) and (5.11) so that we have for each one a corresoponding upper bound for η:

$$\xi_S^{L,1} = F^{-1}(\xi_1, \cdots, \xi_{S-1}, y_1^{SP}, \mathbf{u}, t) = \eta_1^L \tag{6.24}$$

$$\xi_S^{L,2} = F^{-1}(\xi_1, \cdots, \xi_{S-1}, y_2^{SP}, \mathbf{u}, t) = \eta_2^L \tag{6.25}$$

Then the higher one will be taken as the upper bound for the integration:

$$\xi_S^L = \max\left\{\eta_1^L, \eta_2^L\right\} \tag{6.26}$$

It is worthwhile to note that different values of η_1^L and η_2^L are generated through reverse projection at different values of the other uncertain parameters. Taking the last point from the curve in Figure 6.19 (i.e. $\alpha_1 = 99\%$ and $\alpha_2 = 93\%$), some corresponding curves of η_1^L and η_2^L are illustrated in Figure 6.20. It can be seen that the higher value according Equation (6.26) alternates between η_1^L and η_2^L in different situations.

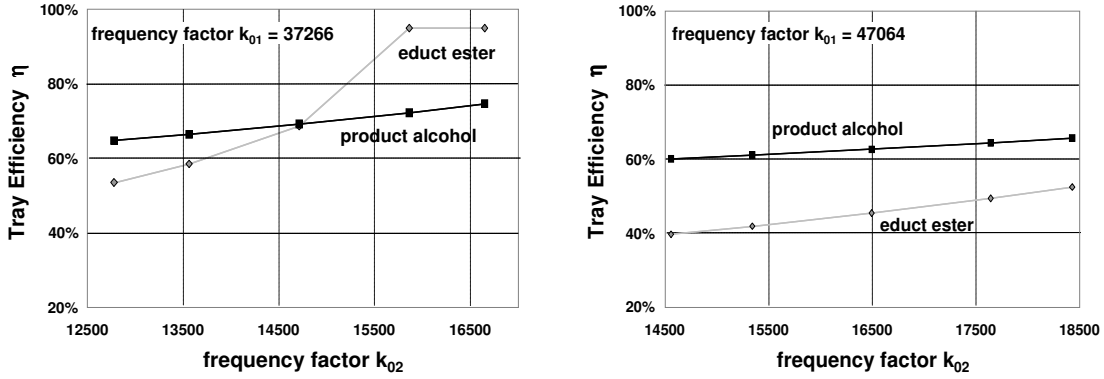

Figure 6.20: Tray efficiency over frequency factors

Due to this alternating behaviour, it can be concluded that the joint probability resulting from a determined operation policy is always significantly lower than both single constraints. This fact can be confirmed in Figure 6.21, showing the results of both constrained outputs by the optimal operation policy and 1000 samples of the uncertain paramerters through Monte Carlo simulation. Moreover, it can be seen that the optimal policy will result in a higher reliability for holding the product alcohol purity than that of the educt ester purity.

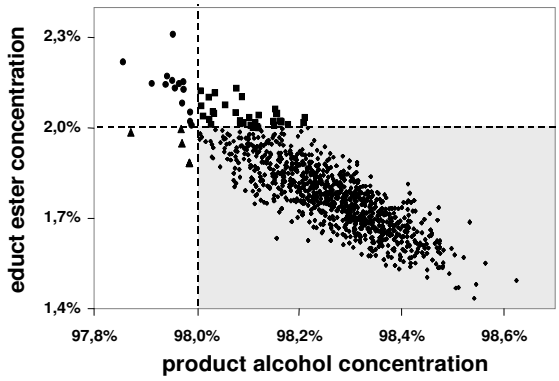

Figure 6.21: Constrained output after stochastic optimization.

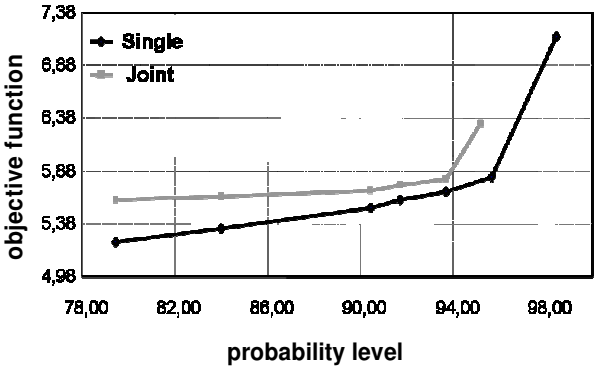

Figure 6.22: Comparison between single and joint constraints.

With those results, regions which are attractive for trade-off decisions between robustness and the objective value can easily be identified and thus are a suitable basis for decision making. In Figure 6.22 the comparison between single and joint probabilistic for the stochastic optimization of the reactive batch distillation is shown. It can be seen that the joint chance constraint is more severe than the single chance constraints with the same value ($\alpha_{1,2} = 96\%$) for the probability levels. Thus, if the constraints are related to safety consideration of a process operation, a joint chance constraint may be preferred. By this means, optimal operational considerations and robustness analyses can simultaneously be considered.

6.4 Summary

In this chapter, the application of the new approach to chance constrained programming of large-scale nonlinear dynamic systems has been presented. The stochastic property of the uncertainties is included in the problem formulation. Following the idea introduced in chapter 5, a monotonic relation between output constraints and at least one uncertain variable is used so that the probabilities and their gradients can be achieved by numerical integration of the probability density function of the multivariate uncertain variables by collocation in finite elements. The new approach involves new efficient algorithms for realizing the required reverse projection for dynamic systems and hence the probability and gradient computation with an optimal number of collocation points. Another novelty of this approach lies in the efficient computation of single and joint constraints and their gradients. In general, the approach is relevant to all cases when uncertainty can be described by any kind of joint correlated multivariate distribution function.

The scope of the optimization framework is evidenced by application to a reactive semi-batch distillation process under several uncertainties. The aim was the minimization of the total batch time subject to product purity restrictions at certain time points. A comparison of the stochastic results with the deterministic results has been made with respect to the objective values and the reliability of satisfying the purity constraints. The formulation of individual pre-defined probability limits of complying with the restrictions incorporates the issue of feasibility. Thus, a feasibility analysis for the stochastic optimization problem was offered. The results obtained by the implementation with a higher probability level showed that the consideration of uncertainties with chance constraints leads to a trade-off between the objective value and robustness. Furthermore, a comparison between the effect of single and joint constraint has been presented. These results can be used for a trade-off decision between robustness and profitability to select optimal and robust operation policies.

Chapter 7

Chance Constrained On-line Optimization

Model-based process control has become significant during the last few decades. However, for a quantitative understanding and control of time varying phenomena in process systems, it is essential to relate the observed dynamical behavior to mathematical models. Due to the generally limited quality and quantity of input-output data used to fit the model, the model will not be an exact representation of the true process. Thus, the practical implementation of model-based techniques often leads to a significant discrepancy between reality and simulation. These models usually depend on a number of parameters whose values are unknown or only known roughly. Furthermore, often only a part of the system's dynamics can be measured. Therefore, a plant model unavoidably involves uncertainties. They are either endemic due to the external disturbances or introduced into the model to account for imprecisely known dynamics. These uncertainties or disturbances are often multivariate and correlated stochastic sequences. Moreover, the use of feedback control in order to compensate uncertainties can not ensure compliance of constraints on open-loop variables. Thus, a close-loop control requires on-line measured values of controlled variables. Many variables in the engineering practice can not, though, be measured on-line. These variables often represent the product quality and, thus, their control is desired. To overcome this problem, measurable variables are chosen as controlled variables in order to control the product quality indirectly. This concept is schematically illustrated in Figure 7.1. Here, the measurable output variable $\mathbf{y}$ will be controlled at their set-points $\mathbf{y}^{SP}$ by using the control variables $\mathbf{u}$. On the other hand, control of $\mathbf{y}^{C}$ is preferred, but, due to the lack of on-line measurement it has to be open-loop. In these cases, $\mathbf{y}^{C}$ needs to be constrained unlike $\mathbf{y}$.

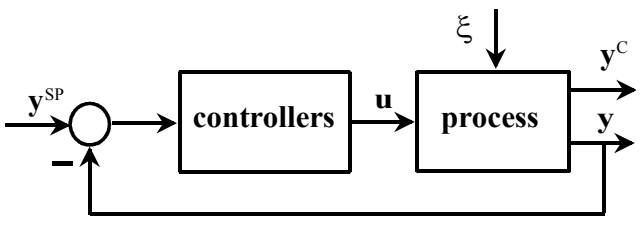

Figure 7.1: The open-closed framework.

To guarantee yet the product quality, the common procedure in industrial practice is to select an extremely conservative set-point value. This implicates that the product quality will be unnecessarily much higher than specified and, thus, the operation costs will be much higher than necessary. Consequently, an optimal set of set-points for the controllers is needed which are neither conservative nor aggressive. In addition, constrained variables for safety or environmental considerations are often monitored but not close-loop controlled. Thus, it is required to evaluate the probability of violating these constraints at the decided operation point. For this purpose, in this chapter, chance constrained optimization is proposed, i.e. the objective function (e.g. costs) is improved and the constraints with regard to $\mathbf{y}^C$ are then to be satisfied with a predefined confidence level. Thus, unlike the problem definition above, where controls are decision variables, in the closed framework the set-points of the measurable outputs are defined as decision variables. The controls will react based on the realization of the uncertain inputs and, thus, they are uncertain variables. Consequently, the consideration of uncertainties/disturbances and their stochastic properties in optimization approaches are necessary for robust process control.

In order to emphasize this issue, in this chapter, two methods based on a nonlinear model predictive control NMPC scheme are proposed to solve close-loop stochastic dynamic optimization problems assuring both robustness and feasibility with respect to state output constraints within an online framework. The main concept lies in the consideration of unknown and unexpected disturbances in advance. The first one is a new **deterministic approach** based on the *wait-and-see* strategy. The key idea is here to anticipate, in particular, violation of output hard-constraints, which are strongly affected by instantaneous disturbances, by backing off of their bounds along the moving horizon with a decreasing degree of severity leading then to the generation of a trajectory consisting of the modified constraint bounds. This trajectory is however dependent on the amount of measurement error and parameter variation including uncertainty. The second method is based on the **stochastic approach** proposed in this thesis to solve nonlinear chance-constrained dynamic optimization problems under uncertainties. The key aspect is the explicit consideration of the stochastic properties of both exogenous and endogenous uncertainties in the problem formulation (*here-and-now* strategy). The approach considers a nonlinear relation between the uncertain input and the constrained state output variables. Accordingly, the stated inequality constraints are to be complied with a predefined probability level. Thus, the solution of the problem has the feature of prediction, robustness and being closed-loop.

Furthermore, towards an **integration of dynamic real-time optimization and control** of transient processes, a two-stage strategy is considered which is characterized through an upper stage corresponding to a dynamic optimization problem and a lower stage related to a tracking control problem. The performance of the developed methodologies is assessed via an application to a semi-batch reactor under safety constraints, where a strongly exothermic series reaction conducted in a non-isothermal batch reactor is considered to explain the analytical steps of the developed approaches, and to demonstrate the applicability of the proposed online framework.

7.1 Problem statement

In contrast to continuous processes which have been subject to several rigorous optimization studies, batch and semi-batch reactors are often still operated using recipes which are based on heuristics and experience. Due to its ability to include constraints directly in the computation of the control moves, nonlinear model predictive control offers advantages for the optimal operation of transient chemical plants (Morari and Lee, 1999). However,

numerous robust predictive controllers suffer from excessively conservative control because they rely upon open-loop predictions of future system uncertainty (Kothare et al., 1996). Open-loop predictions overestimate the uncertainty in future outputs (Lee and Yu , 1997, Ma et al., 1999, Nagy and Braatz, 2004). Furthermore, since the true process optimum occasionally lies on a boundary of the feasible region defined by one or more active constraints, the process is forced into an infeasible region due to the uncertainty in the parameters, external disturbances, and measurement errors (Chisci et al., 2001). Thus, the risk of infeasibility at every sampling instant represents another critical issue in MPC. Hence, the formulation of soft constraints has become common to handle state output constraints, in which penalty terms concerning the constraints are included in the objective function. This prevents infeasibility problems by allowing violations of the constraints (Mayne, 2000). On the other hand, approaches based upon relaxation are, in fact, inapplicable for processes with safety restrictions which are not supposed to be violated at any time point. Recently, deterministic approaches to handling robustness in MPC (Mhaskar et al., 2005) and to ensuring state constraint satisfaction via modification of the constraints for steady state processes (Dubljevic et al., 2005) have been proposed. Besides, although NMPC can inherently exhibit a certain degree of robustness (De Nicolao et al., 2000), for safety-critical transient processes, however, an explicit consideration of uncertainty and disturbances is needed.

7.1.1 Process description and model

A strongly exothermic series reaction conducted in a non-isothermal fed-batch reactor is considered (Figure 7.2). The reaction kinetics are second-order for the first reaction producing B from A, and an undesirable consecutive first-order reaction converting B to C. The reaction scheme is given as follows,

$$2A \xrightarrow{K_1} B \xrightarrow{K_2} C \tag{7.1}$$

The intermediate product B is deeemed to be the desired product. In order to prevent the risk of runaways, batch reactors are usually equiped with two cooling systems, a jacket around and a coil inside the reactor. In this case study, only the dynamic of the jacket cooling system is explicitly considered while the temperature of the cooling system inside is used as an operational degree of freedom. In addition, for safety reasons, the potentially hazardous process is operated in a fed-batch manner. However, in industrial practice, the simple feeding strategy with a constant dosing rate over the entire batch time is commonly used.

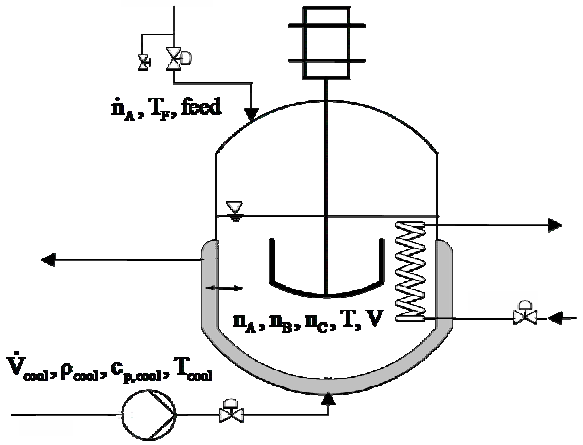

Figure 7.2: Scheme of the semi-batch reactor and its cooling system.

The restricted industrial acceptance of model-based optimization techniques is caused by the availability of detailed dynamic models. Their lack of reliability together with the presence of uncertainty has motivated the investigation of process improvement via chance-constrained online optimization. In this case study, a detailed first-principle model of the exothermic fed-batch process is given by a set of DAEs based on mass balance,

$$\frac{dn_A}{dt} = -\nu_A k_{01} e^{-\frac{E_1}{RT}} \frac{n_A^2}{V} + feed \tag{7.2}$$

$$\frac{dn_B}{dt} = -k_{02} e^{-\frac{E_2}{RT}} n_B + k_{01} e^{-\frac{E_1}{RT}} \frac{n_A^2}{V} \tag{7.3}$$

$$\frac{dn_C}{dt} = k_{02} e^{-\frac{E_2}{RT}} n_B \tag{7.4}$$

reactor energy balance,

$$\frac{d}{dt}\left\{T \cdot n_S \cdot \sum_i^{comp} (c_{p_i} x_i)\right\} = \dot{Q}_{reac} + \dot{Q}_{feed} + \dot{Q}_{cool}^{HT} \tag{7.5}$$

cooling jacket energy balance,

$$\frac{d\overline{T}_{cool}}{dt} = \frac{\dot{V}_{cool} \cdot \rho_{cool} \cdot c_{p,cool} \cdot \left(T_{cool,in} - \overline{T}_{cool}\right) - \dot{Q}_{cool}^{HT}}{V_{cool} \cdot \rho_{cool} \cdot c_{p,cool}} \tag{7.6}$$

and the constitutive algebraic equations

$$\begin{aligned} \dot{Q}_{reac} = -\sum_i^{comp}\left(h_i \frac{dn_i}{dt}\right) = &\left(h_{0A} + c_{pA}\left(T - T_0\right)\right)\frac{dn_A}{dt} + \left(h_{0B} + c_{pB}\left(T - T_0\right)\right)\frac{dn_B}{dt} \\ &+ \left(h_{0C} + c_{pC}\left(T - T_0\right)\right)\frac{dn_C}{dt} \end{aligned} \tag{7.7}$$

$$\dot{Q}_{feed} = \left(h_{0A} + c_{pA}\left(T_F - T_0\right)\right) \cdot feed \tag{7.8}$$

$$\dot{Q}_{cool}^{HT} = -k_{HT} \cdot A \cdot \left(T - \overline{T}_{cool}\right) = -k_{HT}\left(\frac{\pi d^2}{4} + 4\frac{V}{d}\right)\left(T - \overline{T}_{cool}\right) \tag{7.9}$$

$$n_S = n_A + n_B + n_C \tag{7.10}$$

$$V = \frac{n_A \tilde{M}_A + n_B \tilde{M}_B + n_C \tilde{M}_C}{n_A \overline{\tilde{\rho}}_A + n_B \overline{\tilde{\rho}}_B + n_C \overline{\tilde{\rho}}_C} n_S \tag{7.11}$$

$$n_S \sum_i^{comp}\left(c_{p_i} x_i\right) = c_{p_A} n_A + c_{p_B} n_B + c_{p_C} n_C \tag{7.12}$$

In these equations V denotes the varying volume, n_i the molar amount of component i, T, T_F, $\overline{T}_{cool}$, T_{cool}, the reactor, dosing, jacket and cooling medium temperatures, respectively. h_{0i} are the specific standard enthalpies, k_{HT} the heat transfer coefficient, d the scaled reactor diameter, A the heat exchange surface, $\tilde{M}_i$ molecular weights, ρ_i densities and c_{pi} are heat capacities. Additional data and parameters corresponding to the batch reactor model are given in appendix A7. The resulting model comprises 5 differential and 2 algebraic state variables, as well as 3 time-varying operational degrees of freedom which are the feed flow rate into the reactor, the cooling flow rate, and the length of the different time intervals.

7.1.2 Physical and safety restrictions

The consideration of physical, in particular, safety aspects is essential. They often determine the recipe design procedure and limit the achievable performance. Thus, their contemplation is required in order to operate the process closer to the existing constraints. The developed model considers both the reactor and the cooling jacket energy balance. Thus, the dynamic performance between the cooling medium flow rate as manipulated variable and the controlled reactor temperature is also included in the model equations. Thereby, it can be guaranteed that later the computed temperature trajectory can be implemented by the controller. Furthermore, whilst the reaction proceeds, the reactor's volume diminishes so that the computation of the corresponding cooling capacity is adapted according to the remaining cooling jacket area. Besides, since the heat removal is limited, the temperature is controlled by the feed rate of the reactant A (semi-batch operation mode), and the flow rate of the cooling liquid $\dot{V}_{cool}$. At the start, the reactor partly contains the total available amount of A. The remainder is then fed and its feed flow rate is optimized to maximize the yield. However, the accumulation of A at the start of the batch time must be prevented, otherwise, as the batch proceeds; exhaustion of the cooling system capacity can not be avoided.

Maximal reactor temperature

In order to guarantee operability within a specified operating regime it should be assured that the occurring heat development can be discharged through the cooling system at any time. Thus, there exists a maximal allowable reactor temperature starting from which the maximum cooling performance is not longer enough so as to run the process within the specified product requirements. By this means, there is an upper bound according to the critical reactor temperature which should not be exceeded at any time point during the whole batch process. Consequently, the following condition results:

$$\dot{Q}_{reac}\left(T_{max}\right) \leq \left|\dot{Q}_{cool}^{HT,\,max}\left(T_{max}\right)\right| \tag{7.13}$$

This means that in each time point it must be possible to lower both reactor temperature and cooling jacket temperature with the maximum available cooling flow rate in order to fulfill condition (7.13). This leads to:

$$\frac{dT}{dt} \leq 0 \quad \text{and} \quad \frac{d\overline{T}_{cool}}{dt} \leq 0 \tag{7.14}$$

In that case, the relations given in (7.14) are inserted in the equations (7.5) and (7.6), respectively. Derived from this the following equations result:

$$\overline{T}_{cool}^{min} = \overline{T}_{cool} \leq \frac{-\dot{Q}_{reac}}{k_{HT}\left(\frac{\pi d^2}{4} + 4\frac{V}{d}\right)} + T \tag{7.15}$$

$$\dot{V}_{cool}^{min} \geq \frac{\dot{Q}_{reac}}{\rho_{cool} \cdot c_{p,cool} \cdot \left(\overline{T}_{cool} - T_{cool,in}\right)} \tag{7.16}$$

Equation (7.15) indicates the minimal required cooling jacket temperature in order to comply with condition (7.14) while equation (7.16) denotes the minimal needed cooling pump capacity in order to remove the reaction heat. This issue is illustrated in Figure 7.3.

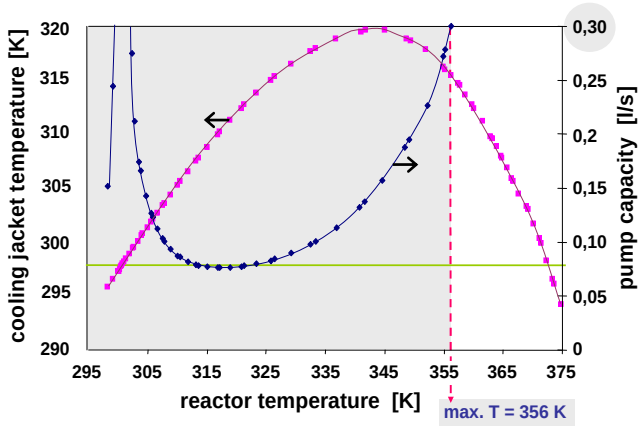

Figure 7.3: Simulated minimal cooling jacket temperature and cooling pump capacity.

From Figure 7.3, it can be seen that after the reactor exceeds the temperature of 300K, a sufficient large gradient exists for heat removal over the cooling jacket. Besides, the required minimum temperature of the cooling medium in the cooling jacket is higher than the cooling inlet temperature. Moreover, for lower reactor temperatures the necessary pump capacity is rather low, it escalates though for higher reactor temperatures and reaches at 356K its maximal value of 0,3 l/s, which is predefined by the pump design. Thus, the maximal permitted operating temperature for the reactor can be specified explicit.

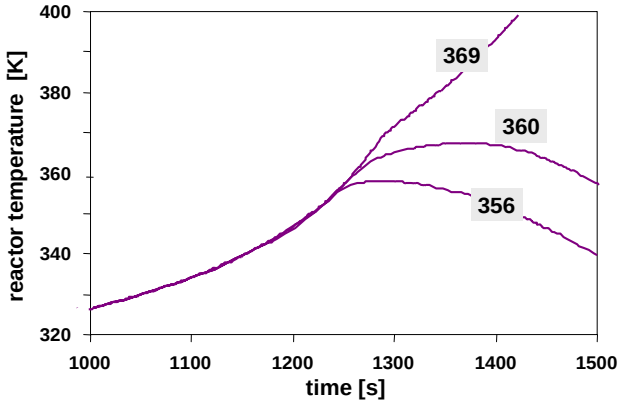

Figure 7.4: Reactor temperature during the heating process.

Figure 7.4 corresponds to the case study when the reactor is charged with the entire amount of A and the cooling system is switched off. As soon as the reactor temperature arrives at a certain temperature, the cooling pump will be put into operation at full capacity. In the first case (T=356K) represented in Figure 7.4, it can be seen that the reactor temperature can be lowered with a slight delay. It achieves the maximum value of 358K. On the other hand, if the pump starts up when the reactor temperature is at 360K, then, a further temperature rise can not be stopped and the reactor is not controllable any longer. A runaway can not be avoided by switching on the pump at 369K.

Safety restriction to avoid runaways

The operation of the fed-batch reactor requires not only operability within specified operating regimes but also in non-specified. Since the reaction is strongly exothermic specific awareness is necessary in order to ensure that the determined operation remains safe. In this study, the particular scenario of a sudden cooling failure is taken into account. However, since the time instant of a possible failure is not known a priori, a safety constraint is incorporated which has to be complied with during the whole path. This implies verification through dynamic simulation at every time point. Thus, based on the thermal explosion theory used for the analysis and design of reaction processes under safety considerations, the adiabatic temperature rise ΔT_{ad} is considered to deal with the dynamic of the cooling system failure (Abel et al., 2000). However, since the maximum achievable temperature after failure is primarily of interest at any time point, once a runaway has started, it can be assumed that the feed is stopped immediately and that the reaction will carry on under adiabatic conditions. Consequently, the heat produced by the reaction will cause a temperature rise whose extent depends on the momentary concentrations, reactor temperature, cooling jacket temperature, the heat capacity of the reactor content as well as on the reactor heat. This can be calculated by a stationary energy balance around the reactor assuming adiabatic conditions. Thus, with the reactor temperature T in progress, the adiabatic end temperature T_{ad} can then be described as follows,

$$T_{ad} = T(t) + \Delta T_{ad} \tag{7.17}$$

It results then,

$$T_{ad} = \frac{\left(h_{0A} + c_{PA}\left(T - T_0\right)\right)n_A + \left(h_{0B} + c_{PB}\left(T - T_0\right)\right)n_B + \left(h_{0C} + c_{PC}\left(T - T_0\right)\right)n_C}{\left[c_{PC}\left(n_C + \frac{n_A}{2} + n_B\right) + C_{P,cool} \cdot \rho_{cool} \cdot V_{cool}\right]} + \frac{C_{P,cool} \cdot \rho_{cool} \cdot V_{cool} \cdot T_{cool} + \left[n_C + \frac{n_A}{2} + n_B\right]\left(c_{PC} T_0 - h_{0C}\right)}{\left[c_{PC}\left(n_C + \frac{n_A}{2} + n_B\right) + C_{P,cool} \cdot \rho_{cool} \cdot V_{cool}\right]} \tag{7.18}$$

Hence, the Equation (7.18) represents a further algebraic relation which can also be used to restrict the variable T_{ad} by a temperature limit converting the dynamic treatment of the cooling system failure to a path constraint. In order to emphasize this issue, the development of the reactor temperature, the cooling jacket temperature as well as the reaction performance is illustrated in Figure 7.5 considering the current entire feed amount in the reactor (500mol of A) and a switched-off cooling. Due to the stationary balance, the instantaneous increase of the temperature is not covered, the heat produced, however, is transferred relatively fast to the

cooling jacket reaching temperature compensation. Furthermore, the maximum possible temperature without heat dissipation to the environment is 683K. Because of the heat transfer to the cooling jacket, the adiabatic end temperature of the reactor content plus cooling jacket is 564K. On the other hand, if the initial feed amount of A is reduced, for instance to 240mol, then the end temperature will be decreased to 497K. Thereby, it becomes clear that supplying A during the batch is the most appropriate operation mode in order to comply with the safety regulation because of its sensitivity to the adiabatic end temperature. By this means, the initial amount of A represents also an additional degree of freedom.

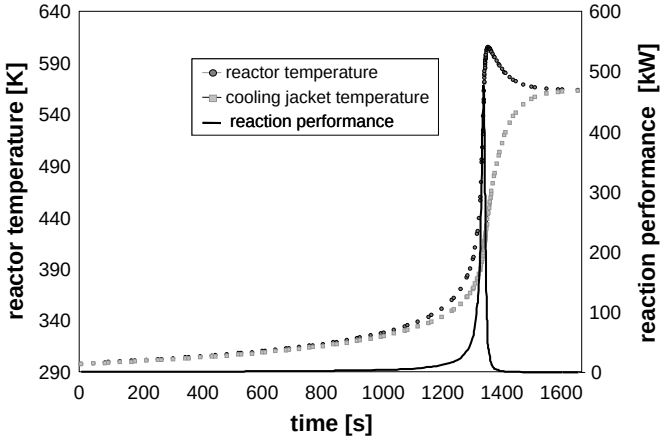

Figure 7.5: Batch heating-up procedure with switched-off cooling.

Thus, the Equation (7.18) represents rather a regulation for the reactor operation. If this regulation/constraint is complied, it can then be guaranteed that in case of cooling failure, the reactor will not exceed a certain stationary final temperature at any time point. Figure 7.6 shows the simulation results for T_{ad}=500K and a cooling failure after 2364s with subsequent switch-off of the cooling pump.

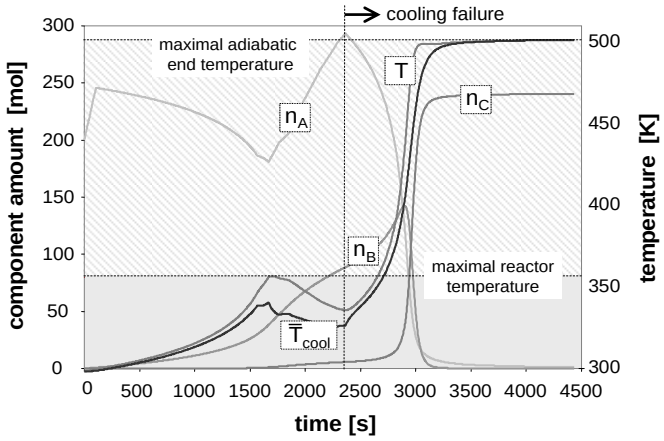

Figure 7.6: Simulation of cooling failure.

By this means, the limitations of the cooling system (pump capacity) can explicitly be taken into account for the optimization. In addition, both maximum temperature constraints have to be enforced during the complete batch time. The selected cooling medium is *Aral Farolin U* which can be applied for a temperature range from -10 to 320 °C. Therefore, it does not represent a source of danger in non-specified operating regimes.

7.1.3 Problem formulation

The optimal operational strategy for the semi-batch reactor is now to be calculated such that the physical and safety restrictions derived in the previous section are also considered. Moreover, the open-loop optimal control problem needs to be solved first and represents a prerequisite for the consecutive optimization with moving horizons involved in NMPC. The objective function is basically chosen depending on the nature of the problem. Thus, there are, in general, two practical optimization problems related to batch operation: maximization of product concentration in a fixed batch time or minimization of batch operation time in order to determine an optimal reactor temperature profile. The first problem formulation is applied to a situation where the increase of the desired product amount is required while batch operation time is fixed. This is due to the limitation of complete production line in a sequential processing. However, in some circumstances, we need to reduce the duration of batch run to allow the operation of more runs per day. This requirement leads to the minimum time optimization problem. In this problem definition, both issues are combined, thus, the objective is to maximize the production of B at the end of the batch (CB_f) while reducing the total batch time t_f,

$$\min_{\dot{V}_{cool},\,feed,\,\Delta t,\,n_{A,0}} \left(-CB_f + \lambda \cdot t_f\right) \quad \text{with} \quad \lambda = 1/70 \tag{7.19}$$

subject to the equality constraints i.e. process model equations (7.2)-(7.12) as well as path and end point constraints. The numbers in brackets [.] to the left denotes the current number of constraints. First, a limited available amount of A, which is to be converted by the final time, is fixed to,

$$[1] \qquad n_{A,total}(t_f) = n_{A,0} + \int_{t_0=0}^{t_f} n_A(t)\,dt = 500\,\text{mol} \tag{7.20}$$

At the final batch time the reactor temperature must not exceed a limit in order to include also the shut-down procedure,

$$[2] \qquad T(t_f) \le 303\ \text{K} \tag{7.21}$$

The safety restrictions are defined as path constraints. The adiabatic end temperature is used amongst others to determine the temperature after failure, as indicator for the educt accumulation, as operation mode regulation, and as process monitoring aid. Handling this constraint ensures that even in the extreme case of a total cooling failure no runaway will occur.

$$[3\text{-}42] \qquad T(t) \le 356\ \text{K} \tag{7.22}$$

$$[43\text{-}82] \qquad T_{ad}(t) \le 500\ \text{K} \tag{7.23}$$

In addition, in order to prevent too large fluctuations of the control variables, the feed and cooling flow rate changes from interval to interval are restricted to an upper bound. This has a positive effect on the convergence particularly with regard to the initial values for the optimization run. However, these limitations can also be modified during the optimization run. For instance, close to the end of the batch process only the absolute amount of heat

discharged is of interest for the maximization of product B. Thus, the allowed changes of the cooling flow rate between the neighboring intervals are smaller.

[83-122] $$\left\| \dot{V}_{cool}(t+1) - \dot{V}_{cool}(t) \right\| \leq 0,05 \tag{7.24}$$

[123-162] $$\left\| feed(t+1) - feed(t) \right\| \leq 0,2 \tag{7.25}$$

The optimization problem definition includes also the vector of states with known initial conditions $\boldsymbol{x}_0$. The decision variables are the feed flow rate into the reactor (0-3 mol/s), the cooling flow rate (0-0,3 l/s), the length of the different 40 time intervals (60-180s) as well as the initial amount of A, $n_{A,0}$, in the reactor. This results in 121 decision variables for the entire optimization horizon.

7.1.4 Optimal nominal solution

In this section, the open-loop optimal results are presented. In the nominal optimization the uncertainty is basically discharged. Figure 7.7 shows the resulting nominal trajectories of the feed and cooling flow rate. During the first few intervals the feed flow rate is determined at a higher value such that the constraints (7.22) and (7.23) are not violated. After a certain feed amount has been added the feed flow rate is drastically reduced. By this means, a fast ignition of the reaction and a quick conversion can also be ensured.

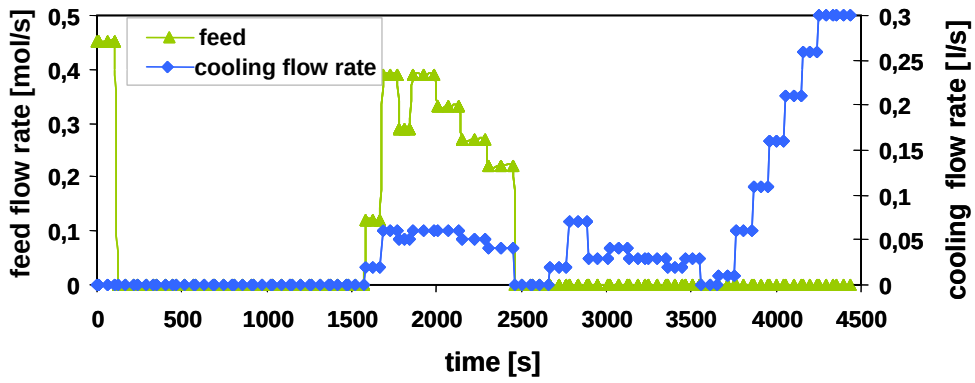

Figure 7.7: Optimal nominal trajectories of the feed and cooling flow rates.

As soon as the reactor temperature is about to reach its limit value the cooling and, in particular, the feed flow rate is again increased. At this time the conversion is sufficiently fast to prevent the accumulation of A. After 2500s, when the total feed amount has been supplied, the reactor temperature increases rapidly again and arrives at its maximum allowable value where it evolves along its upper limit during a long time period (Fig. 7.8). Subsequently, in order to comply with the shut-down end-point constraint (7.21), the cooling rate is increased progressively.

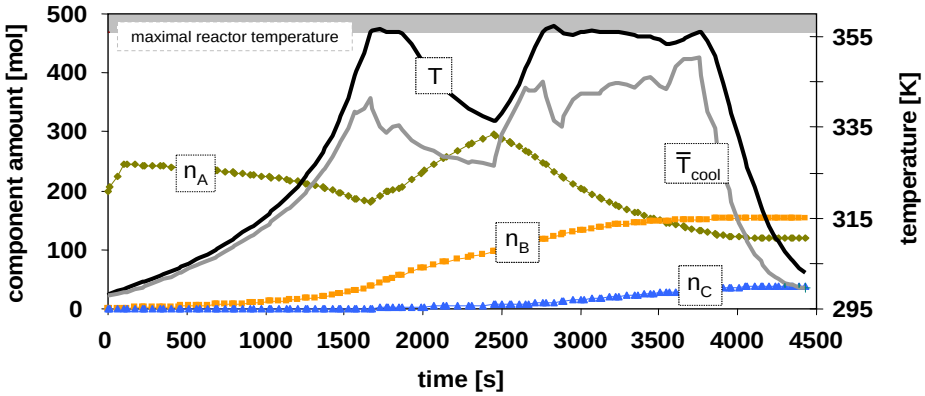

Figure 7.8: Optimal profiles of the components amount, the reactor and the cooling jacket temperature at nominal optimum.

The time-dependent amount of the different components, the reactor as well as the cooling jacket temperatures are depicted in Figure 7.8. From Figures 7.8 and 7.9, it can be seen that the safety restrictions and the feed flow rate determine the reactor temperature evolution. Furthermore, the adiabatic end temperature is decisive during the first half of the process run while in the second part the process is operated almost with maximum reactor temperature until the shut-down period starts. The change of the different time interval lengths can also be noticed. The sum of all 40 time intervals represents the total time. The duration of each individual interval has however a detrimental effect on the applied operational strategy.

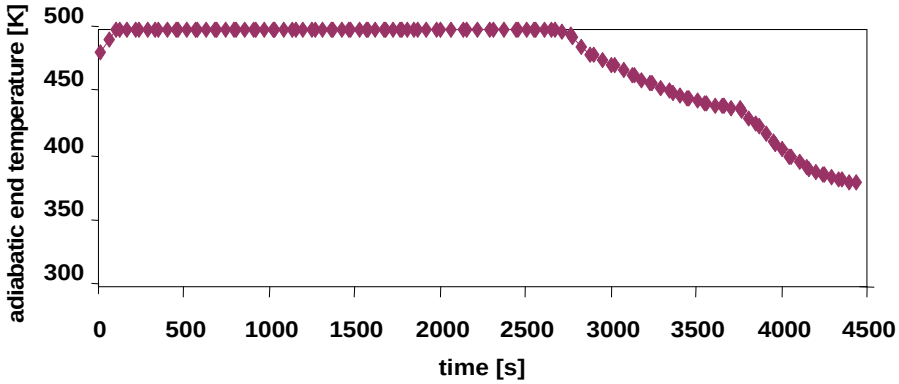

Figure 7.9: Trajectory of the adiabatic end temperature at nominal optimum.

The evolution of the adiabatic end temperature for the nominal operation is depicted in Figure 7.9. It can be seen that the adiabatic end temperature reaches its upper limit right from the start and remains at this value during the heating process with switched-off cooling (up to 1500s) and maintains this value through a large part of the batch time. By this means, the reactor temperature and, in particular, the adiabatic end temperature is an active constraint over a large time period. This poses a potential threat. Although operation at this nominal optimum is desired, it typically cannot be achieved with simultaneous satisfaction of all constraints due to the influence of uncertainties and/or external disturbances. However, the safety constraints should not be violated at any time point. Thus, in this chapter, two methods based on a nonlinear model predictive control scheme are proposed to implement such an optimal strategy despite disturbances solving close-loop dynamic optimization problems assuring robustness with respect to state output constraints within an online framework.

7.1.5 NMPC simulation results

Batch processing offers greater flexibility in the production of specialty and pharmaceutical chemicals. Thus, the trend in the chemical industry towards high value products has increased interest in the optimal model-based control of batch processes (Bonvin, 2001). Due to its ability to directly include constraints in the computation of the control moves, nonlinear model predictive control NMPC presents advantages for the optimal operation of transient chemical plants. Moreover, it provides a systematic methodology to handle constraints on manipulated and controlled variables not being limited to a certain model structure (Allgöwer et al., 1999).

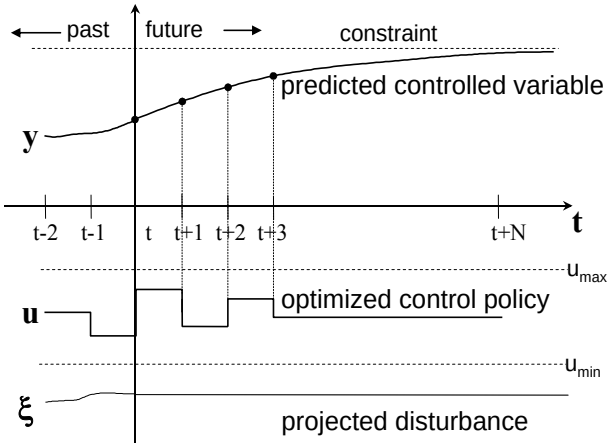

Figure 7.10: Principles of model predictive control

The principle of MPC is shown in Figure 7.10. The model predictive controller uses a process model to predict the future, and then computes the future control trajectory that optimizes a performance objective based on the sum squares of the differences between model predicted outputs and a desired output variable trajectory over a prediction horizon solving an open-loop optimization problem. The value for the control move at the current sampling instance is implemented, i.e. the manipulated variables of the first time interval are applied. At the next sampling instance, new measurements are collected and the control calculation is repeated. By this means, the time window is shifted into the future where the whole procedure is repeated (Figure 7.15). These steps update the control move calculations to consider the latest measurement information. However, most of the research efforts have mainly been directed towards the regulation problem for stationary problems. Recently, a growing number of works have studied the application of MPC to batch and semi-batch processes. However, most of the processes are nonlinear and while linear models are good approximations if the process is kept close to an operating point, this is not the case when the process changes operating point or is subject to high perturbations (Camacho, 1999).

7.1.5.1 Open-loop strategy implementation

Based on the open-loop optimal control trajectories of the critical state variables (see 7.1.4), in this section, a deterministic NMPC scheme is implemented for the exothermic fed-batch process. In order to implement the open-loop strategy, the 40 intervals from the open-loop optimization are divided into small intervals with the same length but not smaller than 6 seconds. The time length values for the intervals with regard to the decision variables are taken over from the off-line optimization results. In contrast, the values of the temperature for

the beginning of each new interval are linear interpolated with the previous values of the off-line trajectory.

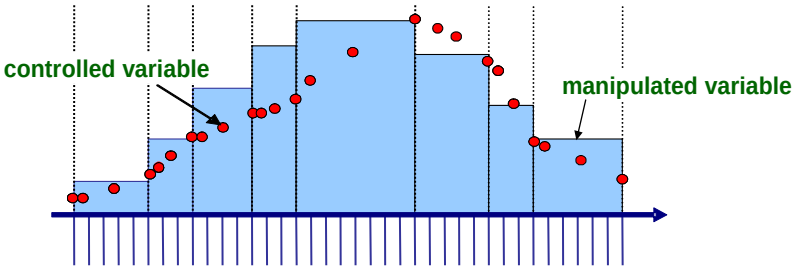

Figure 7.11: Modification of the time interval length based on the multiple-time-scaling approach.

The adjustment of the interval lengths is accomplished by a developed *multiple-time-scaling* strategy which is based on the orthogonal collocation method in finite elements. The strategy is applied for both discretization and implementation of the optimal policies according to the controller's discrete time intervals (6-12s). Thereby, it results around 600-700 intervals. In Figure 7.11, the approach is illustrated schematically.

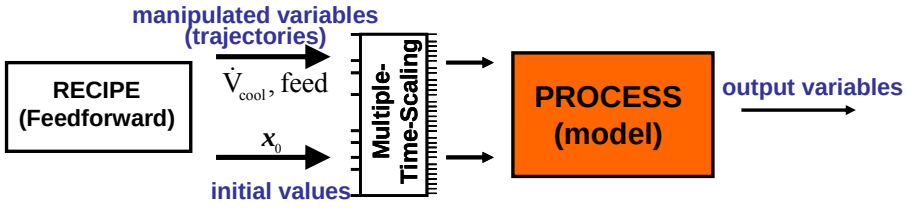

Figure 7.12: Implementation of the open-loop strategy.

In Figure 7.12, the open-loop strategy implementation according to the feedforward strategy is presented, i.e. the reactor is operated with the optimal trajectories of the feed and cooling flow rate determined by the off-line deterministic optimization. However, during the course of a typical batch, process variables swing over wide ranges and process dynamics go through significant changes due to nonlinearity. Furthermore, batch processes are characterized by significant uncertainties, a certain number of noisy measurements, and the fact that the controlled properties are usually not measured on-line. Thus, in order to show the sensitivity to disturbances the model described in section 7.1.1 is extended to include also the catalyst activity a. Thereby, a further factor of influence on the system is realized. For this purpose, a simple approach is used to describe a homogeneous distributed catalyst in the system considered. The catalyst is assumed to influence the main reaction A→B, primarily. So far it was assumed that the total amount of A is available for the reaction, this is however not the case if the reaction is catalyzed. In fact, using a catalyst supposes a decrease of the catalyst activity and, thus, a limited conversion of the available educt A. This is mainly attributed to the fact that the reaction takes place on the catalyst surface and this is not fully available in the course of the reaction any longer. In a simplified form, the catalyst activity can be described as a relationship between the current reaction rate and the reaction rate with the fresh catalyst (t=0). However, if the deactivation mechanism is more complex, the catalyst kinetics can then not be described independent from the reaction kinetics (non-separable kinetics). In this case study, the catalyst activity is considered directly as a factor of the reaction term in the component balances. The reaction term of the reaction A-B results in,

$$r'_{A-B} = - \; a(t) \cdot k(T) \cdot c_A \qquad (7.26)$$

The kinetics of the catalyst activity is described as follows,

$$\frac{da_{A-B}}{dt} = -K_{decay} \cdot (a_{A-B})^2 \cdot \frac{n_A}{V} \tag{7.27}$$

where K_{decay} and $a_{A\text{-}B}$ denote the catalyst decay rate and the catalyst diminution (second order), respectively (Fogler, 1999). Furthermore, the inlet temperature of the cooling medium into the cooling jacket has been assumed so far to be a constant parameter during the off-line optimization. However, due to weather or heat input through the cooling pump depending on its momentary performance, the inlet temperature is rather subject to fluctuations. The impact of these changes on the feedforward strategy is depicted in Figure 7.13.

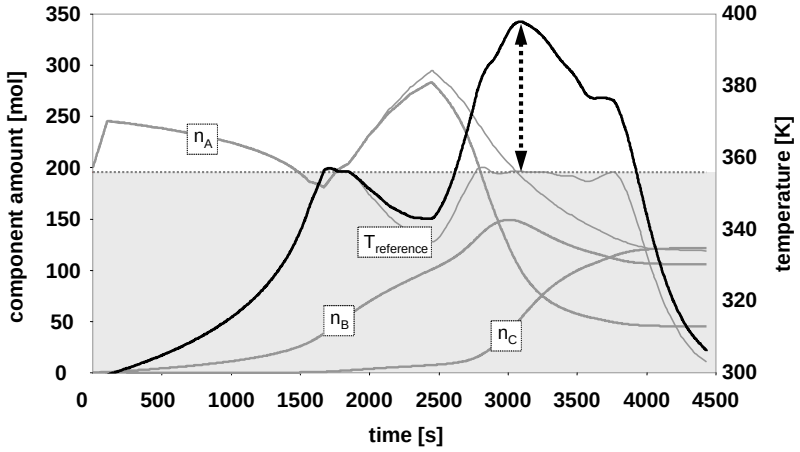

Figure 7.13: Simulation results of the open-loop strategy implementation with $\Delta T_{cool,\,in}$=2K.

The simulation results of the batch operation for an increment of only 2K with regard to the cooling inlet temperature from originally 298K to 300K are illustrated in Figure 7.13. Here, it becomes obvious that the operating conditions deviate significantly from the nominal optimal conditions determined in the open-loop optimization. In particular, the reference trajectories of the educt A in the reactor and the reactor temperature at each time point differ from the simulated trajectories. This has evidently an effect on the yield. However, although operation at the nominal optimum is desired, it typically cannot be achieved with simultaneous satisfaction of all constraints, because of the influence of external disturbances (Loeblein and Perkins, 1999). Thus, an NMPC based approach is proposed to implement such an optimal strategy despite disturbances.

7.1.5.2 Close-loop Optimization

In this section, a nonlinear model predictive controller is implemented which assures the compliance with the operating conditions tracking the path of the reference trajectory. The feed flow rate control is not included in the close-loop. Based on simulation studies, the reactor temperature possesses a higher sensitivity with respect to model uncertainty and disturbances. Its impact on the reaction rate is crucial for the course and conversion of the reaction. By this means, the moving horizon tracking controller will then increase the system robustness against external disturbances at some extent.

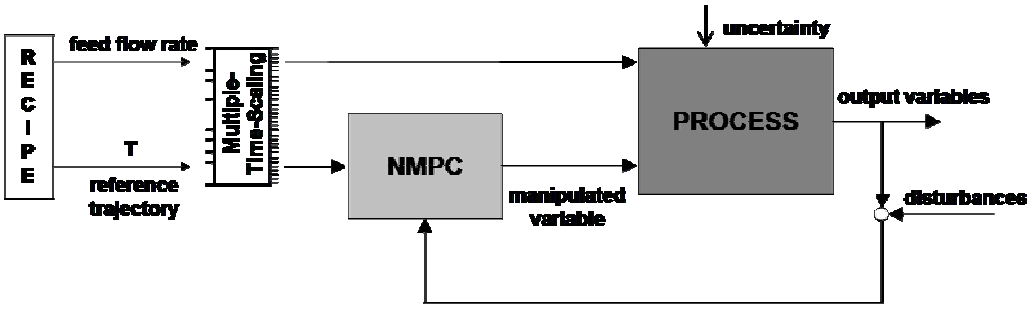

Figure 7.14: NMPC scheme for the tracking control problem.

The process/plant model, which also includes now some disturbances such as catalyst decay and fluctuations of the inlet cooling temperature, is discretized using the orthogonal collocation method with three points. In contrast, these disturbances are assumed to be constant parameters within the NMPC process model, which is discretized with the implicit Euler method. Due to the short horizon and the small intervals, both large deviation and error reproduction are not expected. Thus, with constant step length, the computation time can be reduced. This is particularly important with regard to the simulation and the gradient computation for the optimization. It should be noted that the time required for the solution of the optimization problem is restricted through the interval length within the moving horizon.

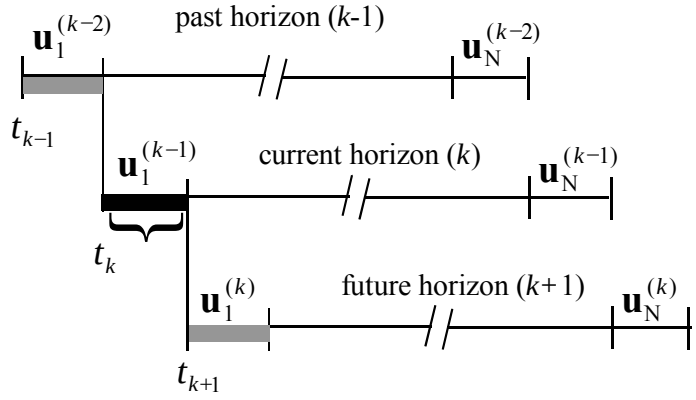

Figure 7.15: Close-loop optimization with the moving horizon.

As shown in Figure 7.14, in oder to implement the developed recipe the length of the diverse time intervals are first adjusted through the *multiple-time-scaling* approach. The NMPC controller receives then the discret set-point trajectory determined via open-loop optimization. However, the performance of the model based control approach relies on the proper estimation of current and future states. Thus, at the end of each corresponding time interval and in time-discrete distance the controller is updated with the current process state. This occurs through measurements at the beginning of each interval. For this purpose, the values of the components amounts, the reactor and cooling jacket temperatures are required in order to fully describe the process state. Since the measurements (here the current values from the process simulation) can commonly not be measured accurately, in this case study, these values are corrupted with white noise e.g. component amount 8%, temperature 2%. Subsequently, they are smoothed with a first order filter. By this means, fast disturbances can efficiently be rejected by the controller.

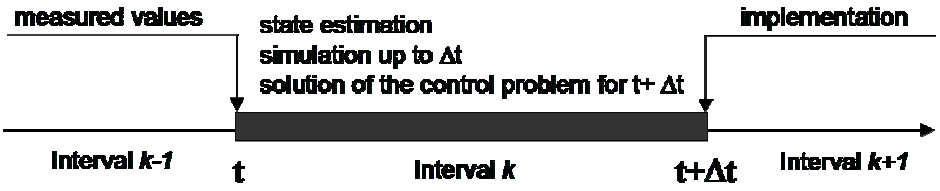

Figure 7.16: Tasks during the current interval.

In case the available time within the interval is not sufficient to solve the NMPC problem, a trigger is activated that holds the current control signal for the next interval. Furthermore, as stated before, proper state estimation is crucial for the success of the NMPC application. Extended Kalman filter (EKF) has been widely used in process control applications, however its performance strongly depends on the accuracy of the model (Nagy and Braatz, 2003, 2004). To avoid highly biased model predictions, some of the model parameters are estimated together with the states. In this case study, the state information is however assumed to be available. For further details concerning the state estimation, we refer to the paper of Haseltine and Rawlings (2005).

7.1.5.3 Tracking problem without safety restrictions

For the online optimization of the semi-batch process, the momentary criteria on the restricted controller horizon with regard to the entire batch operation are insufficient. Therefore, the original objective (7.19) must be substituted by an appropriate alternative that can be evaluated on the local nonlinear MPC prediction horizon,

$$\min_{\dot{V}_{cool}} \quad \mathcal{J}\left(N_1, N_2, N_U\right) = \sum_{j=N_1}^{N_2} \delta(j) \cdot \left[\hat{y}(t+j \mid t) - w(t+j)\right]^2 + \sum_{j=1}^{N_U} \lambda(j) \cdot \left[\Delta u(t+j-1)\right]^2 \tag{7.28}$$

Accordingly, the cooling flow rate becomes now a manipulated variable while the resulting time-variant reactor temperature is taken as reference trajectory. In equation 7.28, the first term of the function stands for the task of keeping as close as possible to the calculated open loop optimal trajectory of the critical variables $\hat{y}$ (e.g. the reactor temperature, which can easily be measured online), whereas the second term corresponds to control activity under the consideration of the systems restriction. Moreover, the control and prediction horizons are chosen equal, to avoid large deviations of the predicted quantities from their setpoints due to the transient character of the process. N_1 and N_2 denote the number of past, and future time intervals, respectively. N_U stands for the number of controls. Both the prediction T_p and control horizon T_C comprise 8 intervals. The corresponding parameters of the objective function are given in Table 7.1.

T_P	prediction horizon	8 intervals
T_C	control horizon	8 intervals
λ	MV variation weighting factor	3000
δ	offset weighting factor	$\alpha^{(Tp-j)}$ with α=0,7

Table 7.1: Objective function parameters.

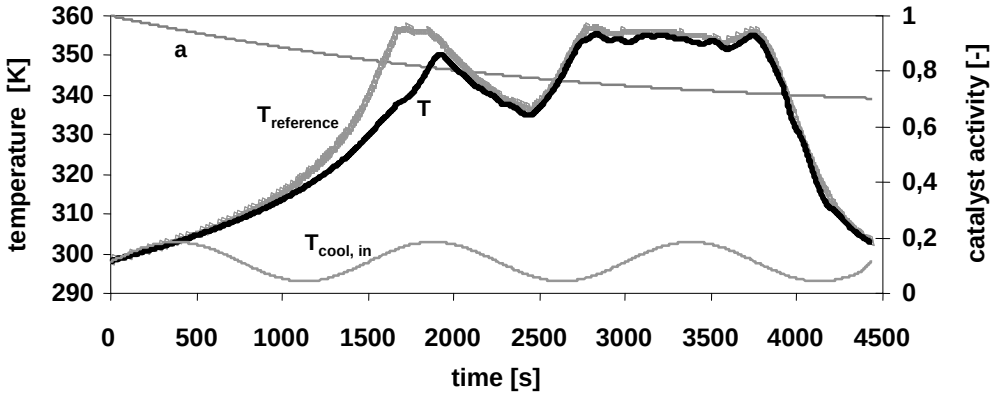

Figure 7.17: NMPC-based control of the exothermic fed-batch reactor under several disturbances without safety restrictions.

The parameters of the objective function in Table 7.1 are determined in such a way that the best possible control quality can be achieved compensating for disturbances and model uncertainties. Thus, in order to examine the robustness of the developed strategies, diverse disturbance scenarios are integrated simultaneously. The inlet temperature fluctuations are simulated with a sinus oscillation of +/-5K around its nominal value of 298 K and a period duration of 1500 seconds. In order to include the impact of the catalyst activity decay, an initial catalyst activity is considered with a(t = 0) = 100% and a specific decay rate of K_{decay}=0,000006. Thus, a gradual poisoning of the catalyst is simulated with a final reduced activity of 70% at the process end. Moreover, white noise with a maximum deviation of 8% for the component amounts and 2% for the temperature are assumed. The time constant of the filter is 15 seconds.

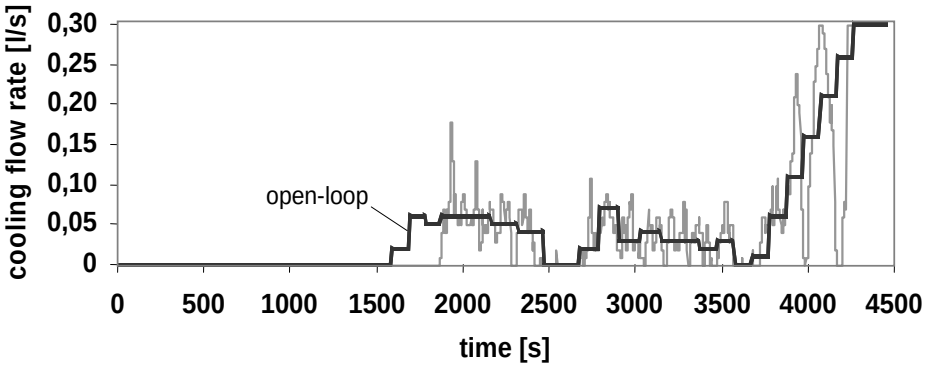

Figure 7.18: Trajectories of the cooling flow rate with regard to open and close-loop optimization.

Despite several disturbances the NMPC simulation results show almost perfect tracking regarding the reference temperature, in particular, after 2000 seconds. The deviations at the beginning are due to the lower catalyst activity in combination with a smaller heat development as assumed in the open-lop optimization. Thus, the difference between the reference trajectory and the actual reactor temperature is not based on the control activity. On the contrary, the controller responds rather appropriately extending the heating period until the reference trajectory is reached.

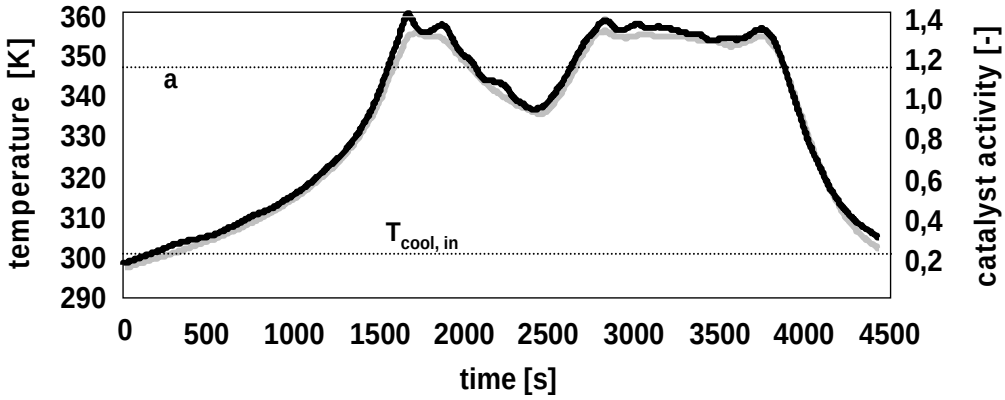

Figure 7.19: NMPC-based control with time-invariant values for the catalyst activity and the inlet cooling temperature.

However, without considering safety restrictions the implemented controller features some deficiencies. Figure 7.19 and 7.20 show the results for another scenario using the same parameters from Table 7.1. In this case study, the inlet cooling temperature (=301K) and the catalyst activity a=105% are assumed to be time-invariant representing the case of model mismatch. As a consequence, the reactor temperature is generally higher than in Figure 7.17. This is because of the controller model errors. The controller assumes a lower heat development and a higher cooling capacity than they actually arise with the implementation.

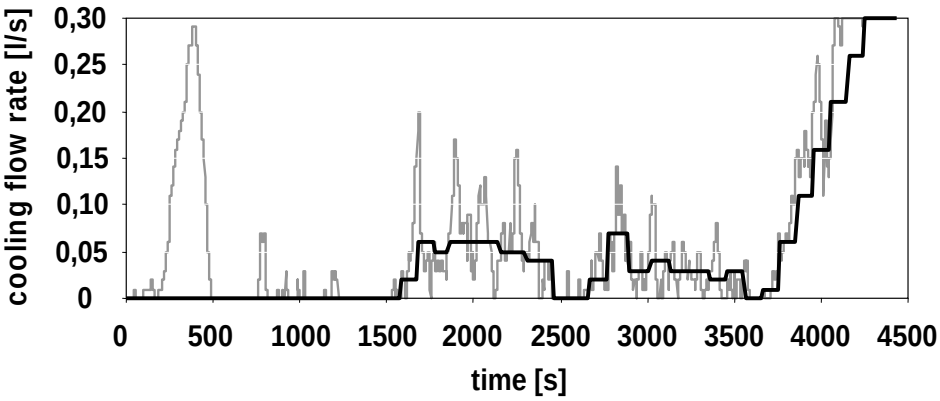

Figure 7.20: Trajectories of the cooling flow rate with respect to open and close-loop optimization for the second scenario.

At the beginning of the heating process, the cooling pump is activated although the inlet cooling temperature still runs above the reactor temperature (Fig. 7.20). In general, during the entire batch process the reactor temperature often lies above the reference trajectory and, as a result, it also exceeds the maximum allowed reactor temperature. This means that the reactor is operated in not allowed region where safety restrictions are not fulfilled. Consequently, the controller quality essentially depends on the model accuracy. In other simulated scenarios even a runaway can not be avoided. However, in a typical batch, process variables swing over wide ranges and process dynamics go through significant changes. Moreover, batch processes are characterized by significant uncertainties, a number of noisy measurements, and the fact that the controlled properties are typically not measured on-line. Therefore, the potential advantages of a model based control system are likely to lead to significant tracking errors. Thus, in order to guarantee that the determined optimal operation remains safe, safety restrictions are needed to be incorporated explicitly here.

7.2 A NMPC-Based On-line Optimization Approach

In this section, the safety restrictions described in section 7.1.2 are now explicitly considered in the NMPC-based control of the exothermic batch process including the equations (7.22) and (7.23). On the one hand, the adiabatic end temperature constraint which guarantees that the temperature evolution even in a case of cooling system failure does not exceed a critical safety limit. On the other hand, an upper limit corresponding to the reactor temperature which assures operability within specified operating regimes according to the maximum available pump performance. Both constraints are to be enforced during the complete batch time and are formulated as *hard-constraints* in the optimization problem. For this purpose, a nonlinear MPC scheme is proposed to solve close-loop dynamic optimization problems ensuring both robustness and feasibility with respect to output constraints. The main concept lies in the consideration of unknown and unexpected disturbances in advance. The novel *deterministic* approach is based on the *wait-and-see* strategy. The key idea is here to anticipate violation of output hard-constraints (safety restrictions), which are strongly affected by instantaneous disturbances.

In the nominal optimization of the exothermic fed-batch reactor, safety restrictions have been considered. They are formulated both as path and end time-point constraints. The open-loop resulting trajectories of the reactor temperature and the adiabatic end temperature are depicted in Figure 7.8 and 7.9. It can be observed that during a large part of the batch time both states variables evolve along the upper limit. The adiabatic end temperature, in particular, is an active constraint over a large time period. Even though operation at this optimum is preferred, it usually cannot be accomplished with simultaneous fulfillment of all constraints, due to the effect of external disturbances. Thus, in this section, an NMPC based approach is proposed to implement such an optimal strategy remaining safe despite disturbances.

The consideration of these output constraints for the control problem in the limited horizon does not naturally imply that a feasible operation can be guaranteed at each time point. Poorly defined constraints within the moving horizon can lead to a deadlock situation. That means that the system is maneuvered into a situation where the problem is infeasible and can not be solved with the given optimization variables and their limitations (Helbig et al, 1998). In connection with batch reactors a deadlock situation arises when a high educt accumulation takes place in the reactor leading to a heat development which exceeds the system cooling capacity. By this means, the reactor can not be controlled any longer and runs away.

In order to prevent such situations, a predictive optimization is necessary. This is however limited through the horizon length and, thus, is not necessarily enough in order to hold the process within a feasible operating region. Previous studies on this issue show that certain restrictions can be formulated so as to prevent a deadlock-situation. One possibility will be to work with special path constraints which consider worst case scenarios. Another alternative assuring feasibility can also be the restriction of the allowable deviation from the set-point trajectory. In this work, the main aim is to meet the safety constraints under all circumstances. Therefore, deviations from the originally determined trajectories to the possible disadvantage of the economic objectives are accepted.

7.2.1 Dynamic adaptive back-off strategy

Since the true process optimum occasionally lies on a boundary of the feasible region defined by one or more active constraints, the process is forced into an infeasible region due to the uncertainty in the parameters, external disturbances, and measurement errors. Thus, the risk of

infeasibility at every sampling instant represents another critical issue in model predictive control. Hence, the formulation of soft constraints has become common to handle state and output constraints, in which penalty terms on the constraints are included in the objective function. This prevents infeasibility problems by allowing violations of the constraints. On the other hand, approaches based upon relaxation are, in fact, inapplicable for processes with safety restrictions which are not supposed to be violated at any time point. Recently, deterministic approaches to handling robustness in MPC (Mhaskar et al., 2005) and to ensuring state constraint satisfaction via modification of the constraints for steady state processes have been proposed (Dubljevic et al., 2005). Besides, although NMPC can inherently exhibit a certain degree of robustness, for safety-critical transient processes, however, an explicit consideration of uncertainty and disturbances is needed.

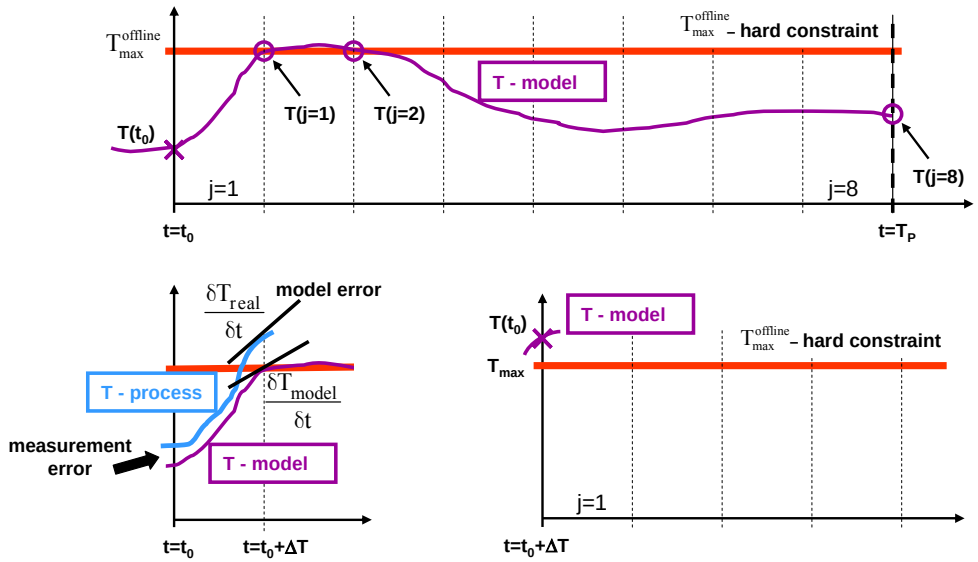

Figure 7.21: Course of the reactor temperature within the horizon.

This issue can be explained with an assumed trajectory of the reactor temperature (T-model) in Figure 7.21. This temperature is calculated with the controller model and it depends on the initial value $T(t_0)$ and on the cooling flow rate strategy within the horizon ($0 \le t \le T_P$). The cooling flow rate is determined through solution of the optimization problem such that the discrete values of the reactor temperature are feasible at the end of each interval, i.e. the maximum allowable reactor temperature T_{max} is not exceeded. In Figure 7.21, the values T(j=1) and T(j=2) lies on the bound of the feasible area, which means that the constraint is active. Besides, in Figure 7.21 at the bottom on the left, the implementation is represented. The reactor temperature at the end of the first interval differs from the predicted temperature due to the measurement and model errors and the hard-constraint is violated. For the sake of demonstration, a poor direction of action has been chosen. This does not mean that a constraint violation is always unavoidable.

The third diagram on the right in Figure 7.21 represents the issue which corresponds to the initial value for the optimization problem in the next interval. This value is determined through measurement and does not necessarily correspond to the actual process state. In this case, a feasible problem solution means that the decision variable (cooling flow rate) is selected in such a way that the reactor temperature will lie inside of the feasible region at the end of each interval. But, it is also possible that even the maximum system cooling capacity is not able to realize this demand. By this means, the optimization problem can not be solved. Thus, practical implementation of NMPC becomes difficult for any reasonably nontrivial

nonlinear system (Mayne D. Q., 2000). However, as illustrated in Figure 7.21, critical issues are robustness and the feasibility of the optimization problem, i.e. the presence of an input profile that satisfies the constraints.

In order to guarantee robustness and feasibility with respect to output constraints despite of uncertainties and unexpected disturbances, an adaptive dynamic back-off strategy is introduced into the optimization problem to guarantee that the restrictions are not violated at any time point, in particular, in case of sudden cooling failure. For this purpose, it is necessary to consider the impact of the uncertainties between the time points for re-optimization and the resulting control re-setting by setting, in advance, the constraint bounds much more severe than the physical ones within the moving horizon.

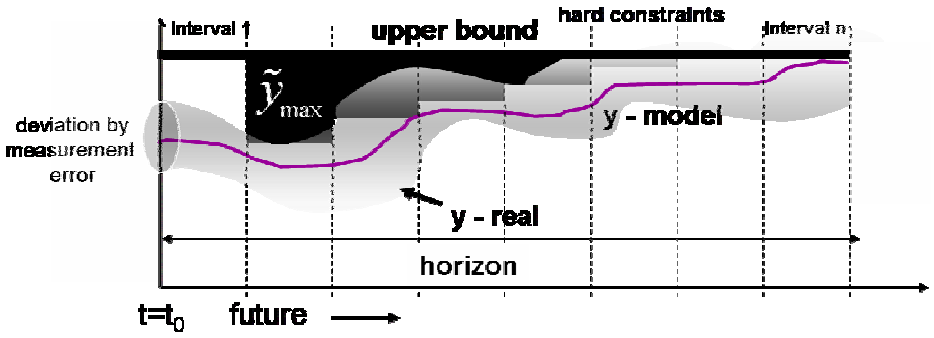

Figure 7.22: Back-off strategy within the moving horizon.

Thus, as shown in Figure 7.22 and 7.23, the key idea of the approach is based on backing-off of these bounds with a decreasing degree of severity leading then to the generation of a trajectory which consists of the modified constraint bounds along the moving horizon (8 intervals). For the near future time points within the horizon, these limits (bounds) are more severe than the real physical constraints and will gradually be eased (e.g. logarithmic) for further time points. The trajectory of these bounds is dependent on the amount of measurement error and parameter variation including uncertainty.

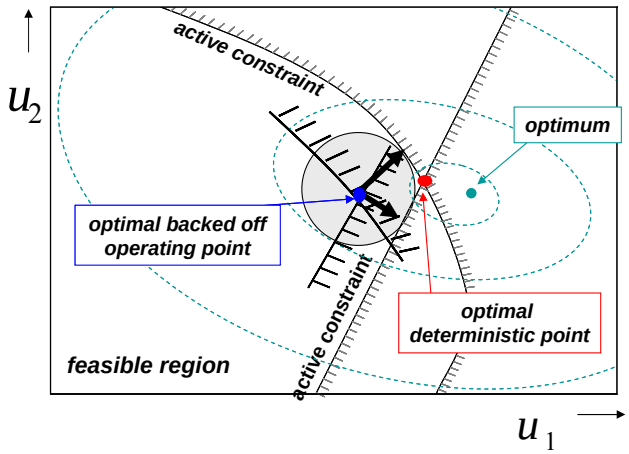

Figure 7.23: Back-off from active constraints.

As previously illustrated in Figure 7.8 and 7.9, the true process optimum lies on the boundary of the feasible region defined by the active constraints. Due to the uncertainty in the parameters and the measurement errors, the process optimum and the set-point trajectory would be infeasible. By introducing a back-off from the active constraints in the optimization,

the region of the set-point trajectory is moved inside the feasible region of the process to ensure, on the one hand, feasible operation, and to operate the process, on the other hand, still as closely to the true optimum as possible (Fig. 7.23). By this means, the black-marked area in Figure 7.22 illustrates the corrected bounds $\tilde{y}_{max}$ of the hard constraints. Here, it should however be noted that due to the severe bound at the computation of the previous horizon, the initial value at t_0 is rather far away from the constraint limit in the feasible area. Thus, in the first interval of the current moving horizon, the bound is set at the original physical limit to avoid infeasibility. The back-off adjustment starts from the second interval, i.e. from the time point on, where the next re-optimization begins. Since there will be more time points for re-optimization and thus for compensating disturbances, for the further remaining intervals within the moving horizon $\tilde{y}_{max}$ approaches to the original constrained bound. The size of $\tilde{y}_{max}$ strongly depends on parametric uncertainty, disturbances, and the deviation by measurement errors. Thus, the safety constraints for the adiabatic end temperature and the reactor temperature within the moving horizon are now reformulated as follows,

$$T(j) \leq 356\ \text{K} - \tilde{T}_{max} \cdot \alpha^{(j-2)} \tag{7.29}$$

$$T_{ad}(j) \leq 500\ \text{K} - \tilde{T}_{ad,\,max} \cdot \alpha^{(j-2)} \tag{7.30}$$

with $j = 2,....,8$, $\alpha = 0,5$, $\tilde{T}_{max} = 4\text{K}$ and $\tilde{T}_{ad,\,max} = 3\text{K}$. For the formulation of the NMPC-based online optimization, the parameters of the objective function (7.28) are also taken from Table 7.1. The hard-constraints and their back-offs, which are now to be included in the optimization problem, are formulated in the Equations (7.29) and (7.30), respectively. The manipulated variable is again the cooling flow rate. In order to compare the performances of the open-loop nominal solution and the nominal NMPC with the proposed dynamic adaptive back-off strategy, different disturbances have been considered. The developed close-loop optimization framework is depicted in Figure 7.24. The concept incorporates also a feasibility analysis with regard to the handling of safety constraints. For this purpose, the safety constraints are set at the beginning of each time step. By this means, the value of $\tilde{y}_{max}$ can be verified through simulation.

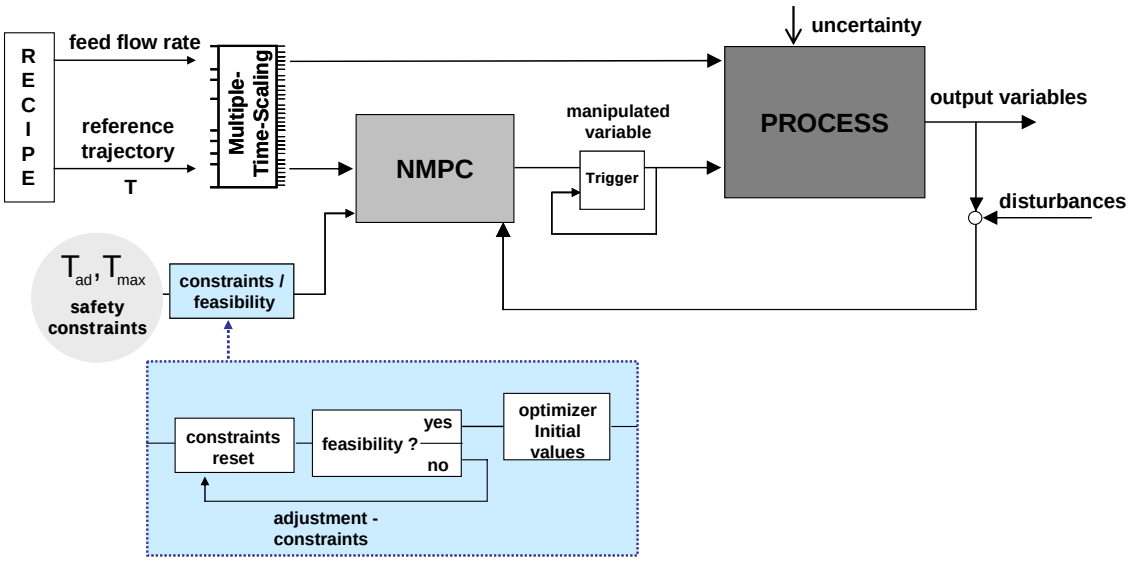

Figure 7.24: Close-loop optimization framework including hard output constraints.

In case the optimization algorithm does not find a solution, a trigger is activated that holds the current control signal for the next interval. Another important issue represents the initial values for the optimization. Here the values of the open-loop optimization are used as reference. Furthermore, by means of simulation, the constraint tightening (back-off) within the horizon can be estimated. This depends however on the size and effect of the arising uncertainties. The back-off is also to be selected as small as possible in order not to lose optimization potential. In case the required process knowledge is even not available then the back-off is determined in a conservative manner.

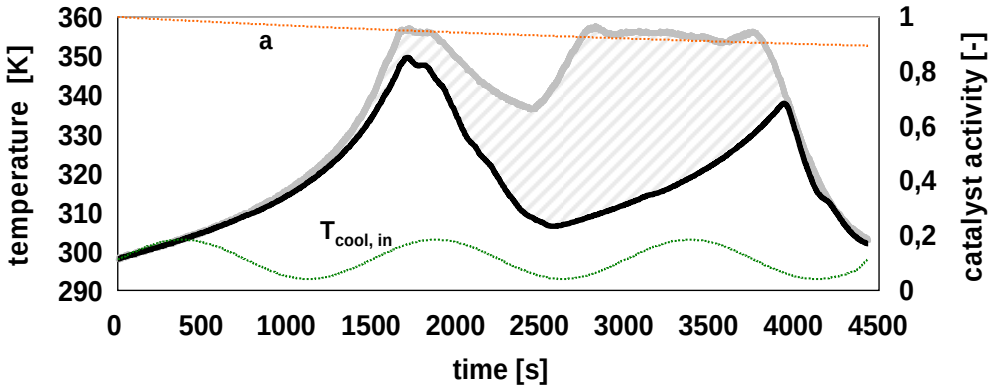

Figure 7.25: NMPC-based control of the exothermic fed-batch reactor considering safety restrictions under several disturbances.

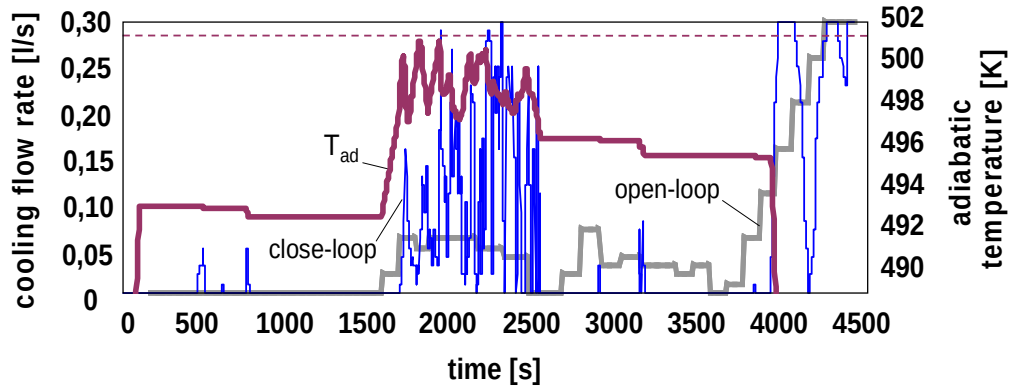

Figure 7.26: Optimal trajectory of the adiabatic temperature and the cooling flow rate with regard to open and close-loop optimization.

In order to show the relevance of the developed close-loop optimization framework, the robustness of the developed strategies considering the safety restrictions is illustrated in Figure 7.25 and 7.26. The optimal policies guarantee the constraints compliance both for nominal operation as well as for cases of large disturbances e.g. sudden cooling failure at any time-point. To emphasize this fact, diverse strong disturbance have been realized simultaneously. The inlet cooling temperature fluctuations are simulated with a sinus oscillation of +/-5K around its nominal value of 298 K and a period duration of 1500 seconds. Moreover, an initial catalyst activity is considered with a(t = 0) = 100% and a specific decay rate of K_{decay}=0,0000015, thus, the final reduced activity is 86% at the process end. Moreover, all measurements are corrupted with white noise with a maximum deviation of 2% for the temperature and 8% for the component amounts.

As depicted in Figure 7.25, the reactor temperature evidently differs from the reference temperature (hatched area). This is principally due to the lower reaction performance. The reactor temperature lags the reference temperature during the heating process. Moreover, since the controller does not have a direct influence on the feed supply, in case of imminent danger of exceeding the adiabatic end temperature, the controller can only lower the reactor temperature. Thus, as shown in Figure 7.26, T_{ad} reacts very sensitive during the time period when the feed flow is mainly supplied (1500-2500s). Furthermore, since the heat removal and the trajectory of the feed flow rate are determined in such a way that for a largest part of the operating time the process is run close to the feasible bounds, a higher activity of the controller can be observed in Figure 7.26. Thus, as the manipulated variable changes several peaks arise which basically appears within those ranges where the constraints are *active*. These peaks are mostly caused by measurement noise. This is also the resulting effect of increasing the educt amount in the reactor and thus raising the potential in the reactor. Although in the reference trajectory a temperature diminishment is provided, it is however not sufficient since a large amount of the educt has been accumulated due to the slower reaction as originally assumed. However, the constraint with regard to the adiabatic end temperature will then be violated if the reactor temperature is not lowered. The now lowered reactor temperature implies though a diminished reaction performance such that this effect will again be strengthened.

The explicit inclusion of the safety restrictions has assets and drawbacks. The main advantage is obviously the guarantee of compliance with the safety regulations at each time point during the operation. In general, the consideration of output-constraints leads to an increased activity of the manipulated variable. This is due to the relatively small horizon of the controller and the relatively large influence of the uncertainties. However, the temperature control is effectively implemented and the process is now robust regarding the compensation for *fast* disturbances and, thus, guaranteeing operability within specified operating regimes. The highest priority is though given to the fulfillment of the safety restrictions. This means that in case of threatening risk of exceeding the adiabatic end temperature the operating conditions can keenly deviate from the reference conditions. This arises primarily due to the time-variant changes of the catalyst activity. In other words, the effects of slow disturbances or drifting parameters can not be compensated satisfactorily. However, feasibility and robustness in particular with respect to output constraints have been achieved by the presented dynamic backing-off strategy. On the other hand, in order to compensate for such disturbances, in the following section the implementation of a next higher level in Figure 7.24 is proposed (see Fig. 7.27). This is definitely necessary since the selected operating conditions by the controller do not imply an optimal global solution for the operation. This is amongst others due to the rather limited horizon, the tracking of a given reference trajectory as well as the restricted actions which primarily concerns the cooling flow rate.

7.2.2 A two-level strategy for optimization based control

The size of the dynamic operating region around the optimum (see Figure 7.23) is affected by fast disturbances. These are, however, efficiently rejected by the proposed regulatory NMPC-based approach. On the other hand, there are, in fact, slowly time-varying non-zero mean disturbances or drifting model parameters which change the plant optimum with time (Loeblein and Perkins, 1999). Thus, a re-optimization, i.e., *dynamic real-time optimization* (D-RTO) may be indispensable for an optimal operation. When on-line measurement gives access to the system state, on-line re-optimization promises considerably improvement. Moreover, additional constraints can be formulated. In this case study, the state information is assumed to be available and parameters are estimated from available measurements.

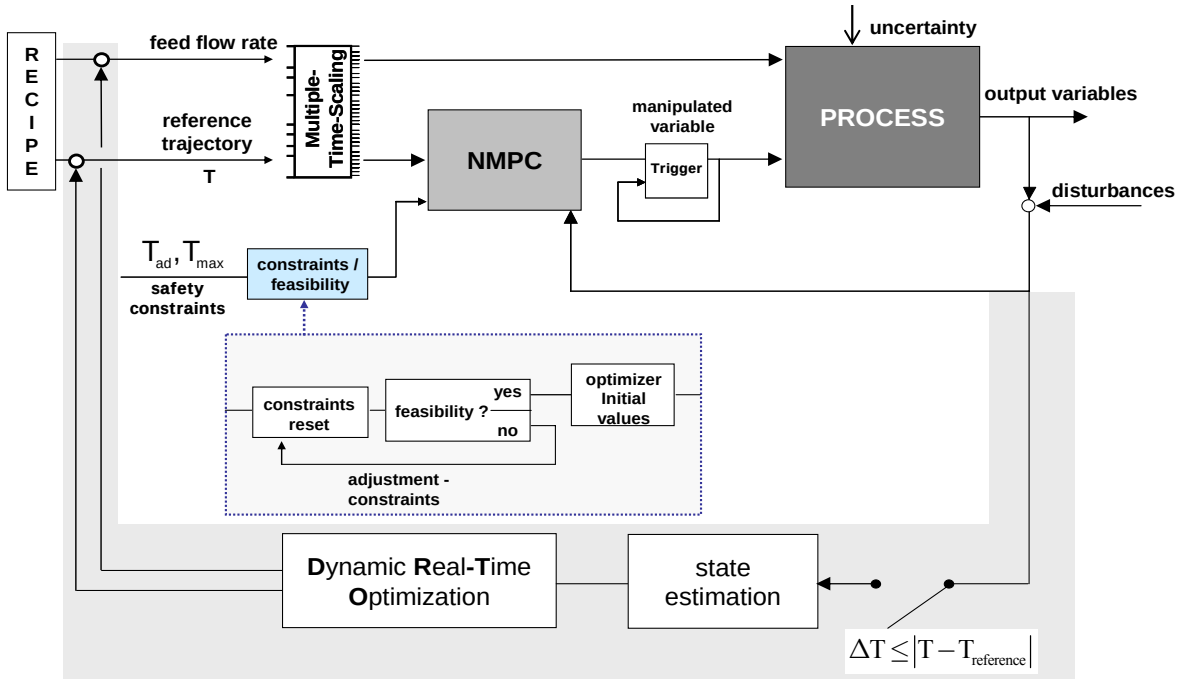

Figure 7.27: Online Framework: Integration of NMPC and dynamic re-optimization.

In order to compensate slow disturbances, the on-line dynamic re-optimization problem is automatically activated three times along the batch process time according to a trigger defined as the maximum allowable bounded difference, ΔT, between the actual reactor temperature and the temperature reference trajectory (see Fig. 7.28a). New recipes resulting from this are then updated as input to the on-line framework. Due to the different trigger time-points the current D-RTO problem progressively possesses a reduced number of variables within a shrinking horizon (Nagy and Braatz, 2003). However, as a result of this and a catalyst contamination, the final total batch time increases. But, despite the large model mismatch and the absence of kinetic knowledge nearly perfect control is accomplished. Thus, the resulting NMPC scheme embedded in the on-line re-optimization framework is viable for the optimization of the semi-batch reactor recipe while simultaneously guaranteeing the constraints compliance, both for nominal operation as well as for cases of large disturbances e.g. cooling failure situation at any time-point. The proposed scheme yields almost the same profit as the one of the off-line optimization operational profiles (see Table 7.2).

	CB_f [mol]	CC_f [mol]	t_f [s]
Nominal open-loop optimization	152,5	37,8	4434
NMPC / unconstrained	141,0	28,8	4434
NMPC / safety restrictions / dynamic back-off strategy	127,9	12,8	4434
NMPC / safety restrictions / dynamic back-off / D-RTO	148,8	36,8	4892

Table 7.2: Nominal optimal and NMPC simulation results under the consideration of several uncertainties and disturbances.

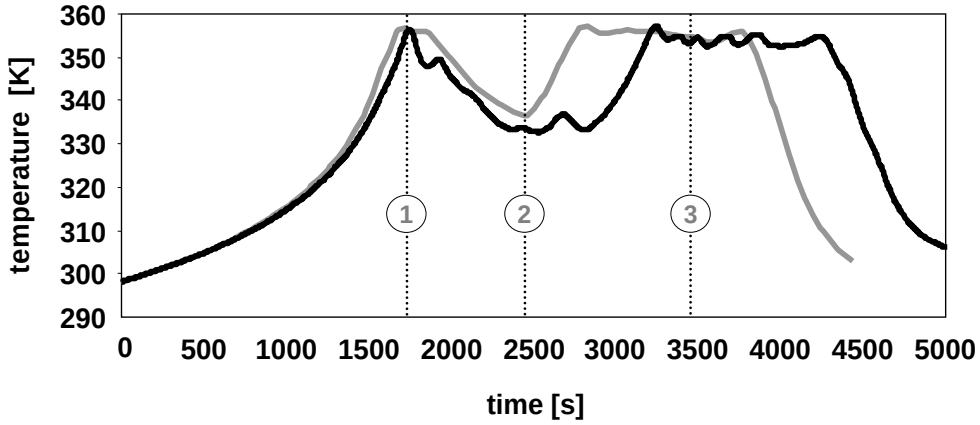

(a)

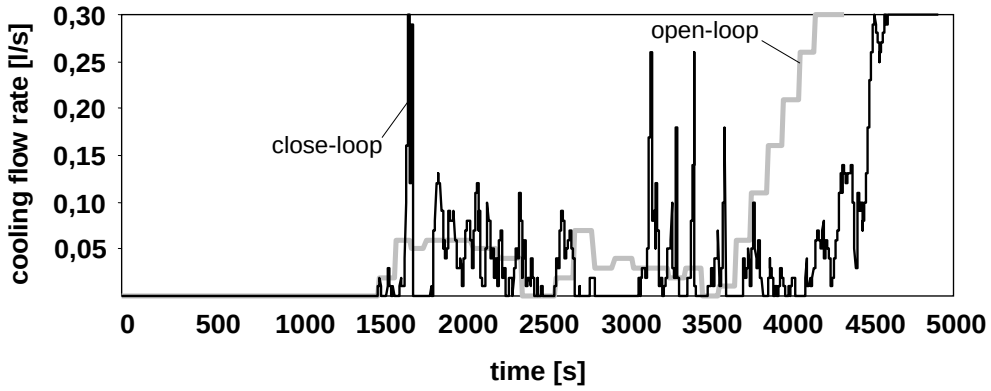

(b)

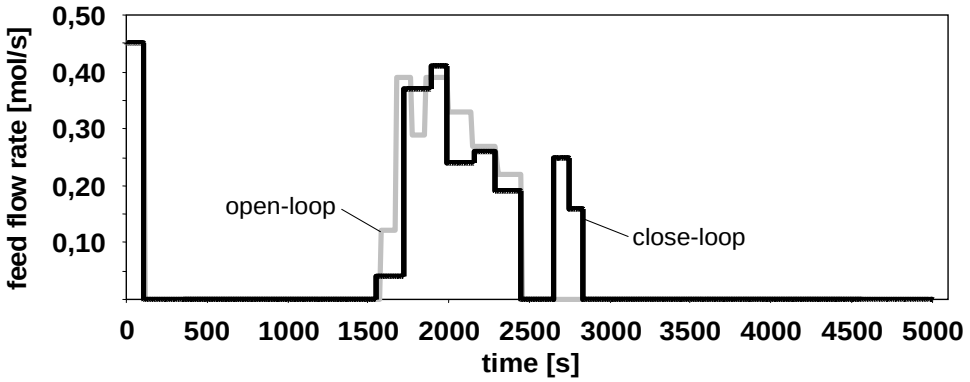

(c)

Figure 7.28: Implementation results of the online re-optimization: (a) reference and optimal reactor temperature; (b) open and close-loop optimal cooling flow rate; (c) open and close-loop optimal feed flow rate.

The online framework illustrated in Figure 7.27 basically provides a basis for feedback from the process to both the NMPC tracking controller and to the trajectory design level. This also means that the developed two-level strategy for the transient process relies in principle on the assumption that the existing disturbances can be divided into *fast* and *slowly time-varying* non-zero mean disturbances or drifting parameters. The update of new trajectories is however performed on a larger time-scale than the sampling time of the controller. The real output

variables and the current estimated catalyst activity are handed over to the re-optimization step as constant values for the triggered optimization run at the corresponding time-point. Besides, the information about the remaining or already employed educt A is imperative. This issue changes the total amount of A, $n_{A,total}$, to be still supplied and, therefore, the equality constraint (Eq. 7.20) needs to be readjusted. However, both online optimization and controller use the imperfect model as also assumed in the open-loop optimization. In the Figures 7.28a-c the implementation results of the online optimization in comparison with the nominal open-loop optimization are shown. The resulting new reference trajectories are updated three times during the batch run at 1700, 2450 and 3450 seconds. The different considered strong disturbances are again the oscillations of the inlet cooling temperature, a catalyst contamination with K_{decay}=0,0000021, as well as perturbed measurements with white noise. The objective function of the D-RTO is the same as in Equation (7.19). From Figure 7.28a-c, it is evident that a substantial improvement of the product yield can be obtained by re-optimizing the operating conditions. However, the required total time of operation has increased. An alternative to counter this problem might be to suitably adapt or restate the objective function of the D-RTO based on the new arising process conditions.

7.3 Robust Chance-Constrained NMPC under Uncertainty

Model predictive control has extensively been used in process control engineering. One reason for its popularity is the ability to directly include constraints in the computation of the control moves. However, since the prediction of future process outputs within an NMPC moving horizon is based on a process model involving the effects of manipulated inputs and disturbances on process outputs, the compliance with constraints on process outputs is more challenging than these on process inputs. Moreover, as the model involves uncertainty, process output predictions are also uncertain. This results in output constraints violation by the close-loop system, even though predicted outputs over the moving horizon might have been properly constrained. Consequently, a method of incorporating uncertainty explicitly into the output constraints of the online optimization is needed.

Moreover, as discussed in the previous section, the true process optimum occasionally lies on a boundary of the feasible region defined by one or more active constraints and, thus, representing a risk of infeasibility at every sampling instant. In addition, the dynamic operating region around the backed-off optimum is certainly not a rigid shape determined by the corresponding back-offs from the safety constraints but corresponds rather to a distribution with points which are closer to the nominal optimum (see Fig. 7.29) and thus leading to a better performance.

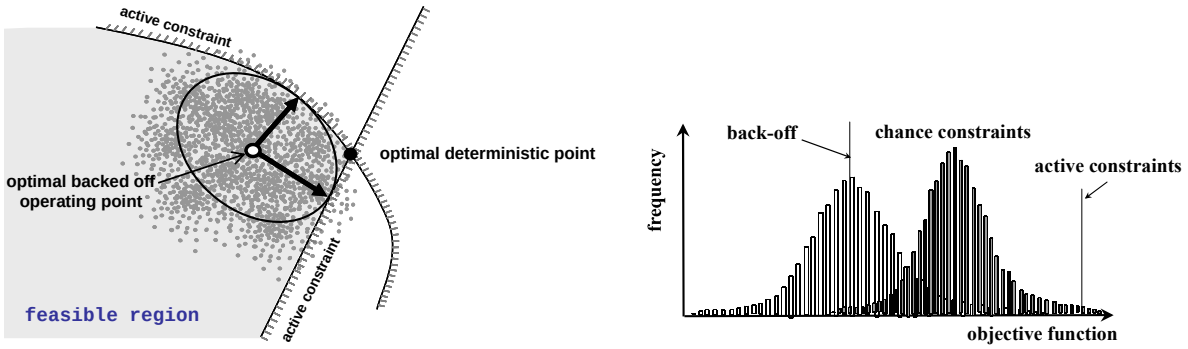

Figure 7.29: Distribution of the operating points.

Thus, in this section, a new robust nonlinear MPC scheme is proposed by means of using the chance constrained approaches developed in this Thesis. Here, in particular, close-loop stochastic dynamic optimization problems are solved assuring both robustness and feasibility with respect to output constraints. The main concept lies in the consideration of unknown and unexpected disturbances in advance. The approach considers a nonlinear relation between the uncertain input and the constrained output variables. The new controller solves a chance-constrained nonlinear dynamic optimization problem at each execution in order to determine the set of control moves that will optimize the expected performance of the system while complying with the constraints. The controller deals with model uncertainty and disturbances, which are assumed to be correlated multivariate stochastic variables, by replacing the deterministic inequality constraints in the NMPC formulation with chance constraints which are to be complied with a predefined probability level. The formulation and tuning of individual predefined probability limits of complying with the restrictions incorporates the issue of feasibility, and the contemplation of trade-off between the objective function (profitability) and robustness. Thus, the solution of the problem has the feature of prediction, robustness and being closed-loop.

7.3.1 Chance constrained linear MPC

For linear MPC with *single* chance constraints, the chance constraints can easily be transformed to linear deterministic inequalities where the uncertain variables in the prediction horizon are described as random variables with a probability distribution function, and the output constraints are formulated as chance constraints. It leads however to a QP problem and thus the solution can be derived analytically (Schwarm and Nikolaou, 1999). In cases of problems with a *joint* chance constraint, an explicit solution cannot be obtained, since the calculation of a joint probability of multivariate uncertain variables is needed. Here, the resulting linear chance constrained MPC problem is then transformed in a convex nonlinear optimization problem so that it can be solved with a standard NLP method. It should be noted that even if the uncertain inputs are uncorrelated, the outputs are correlated through the linear propagation. *Linear* MPC under probabilistic (chance) constraints have been proposed in (Li et al., 2000b, Wendt, 2005). In these studies, the distribution of disturbances are considered in the design of chance constrained MPC controllers, so that the resulting control performance is more robust than that from the conventional MPC design methods. However, unlike the linear case, for nonlinear (dynamic) processes the controls have also an impact on the covariance of the outputs.

7.3.2 Chance constrained nonlinear MPC

In this Section, the chance constrained programming framework developed is used to propose a robust nonlinear model predictive control strategy. As emphasized in the previous chapters, the main challenge lies here also in the mapping back of the output probability distribution as well as in the computation of the probabilities and their gradients. For this purpose, the approaches developed in this Thesis (see Chapter 5) are implemented. Based on the formulations for the tracking controller discussed in Section 7.2.1, the general chance constrained NMPC problem, which is solved at each sampling time k, can be formulated as follows:

$$\min_{V_{cool}} \quad \mathcal{J}(N_1, N_2, N_U) = \sum_{k=N_1}^{N_2} \delta(j) \cdot \left[\hat{\mathbf{y}}(t+k \mid t) - \mathbf{w}(t+k)\right]^2 + \sum_{k=1}^{N_U} \lambda(j) \cdot \left[\Delta \mathbf{u}(t+k-1)\right]^2$$

s.t.

$$\begin{aligned}
&\mathbf{x}(k+i+1 \mid k) = \mathbf{g}_1(\mathbf{x}(k+i \mid k), \mathbf{u}(k+i \mid k), \boldsymbol{\xi}(k+i)) \\
&\mathbf{y}(k+i \mid k) = \mathbf{g}_2(\mathbf{x}(k+i \mid k), \mathbf{u}(k+i \mid k), \boldsymbol{\xi}(k+i)) \\
&\mathbf{Pr}\{\mathbf{y}_{min} \le \mathbf{y}(k+i \mid k) \le \mathbf{y}_{max}\} \ge \boldsymbol{\alpha}, i = 1, \ldots, n \\
&\mathbf{u}_{min} \le \mathbf{u}(k+i \mid k) \le \mathbf{u}_{max}, i = 0, \ldots, m-1. \\
&\Delta \mathbf{u}_{min} \le \Delta \mathbf{u}(k+i \mid k) = \mathbf{u}(k+i \mid k) - \mathbf{u}(k+i-1 \mid k) \le \Delta \mathbf{u}_{max}
\end{aligned} \tag{7.31}$$

Where $\mathbf{g}_1$ are the first-principle model equations describing the dynamic changes of the state variables **x,** while $\mathbf{g}_2$ describe the state of the constrained variables **y** depending on the control variables **u** and the uncertain parameters ξ. The main novelty of the chance constrained NMPC relies basically on the explicit inclusion of the uncertainties in the problem formulation. The principles of the control strategy are schematically depicted in Figure 7.30. Based on the current output variable y(t) and the input u(t-1) the future N controls will then be computed such that the predicted outputs are restricted within the specified bandwidth with a given probability. Once the control is implemented including the realization of the disturbances, the new state at the time-point t+1 is accessible. The computation is then repeated in the next horizon.

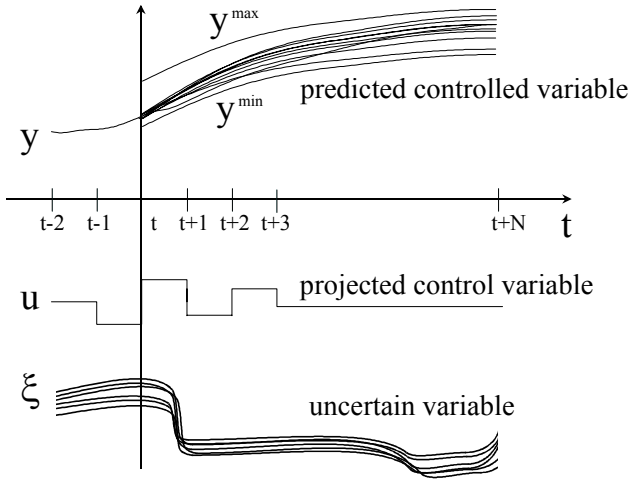

Figure 7.30: Principles of chance constrained model predictive control.

The efficiency of the chance-constrained controller is proved through application to the same scenario of the fed-batch reactor under safety constraints discussed throughout this Chapter. The resulting NMPC scheme is also embedded in the on-line optimization framework (Fig. 7.27). For the sake of simplicity, the objective function only includes the quadratic terms of the controls, since the outputs are confined in the chance constraints. Thus, the performance of the objective function from (7.31) is now redefined as follows,

$$\min_{V_{cool}} \quad \mathcal{J}(N_U) = \sum_{k=1}^{N_U} \left[\Delta \mathbf{u}(t+k-1)\right]^2 \tag{7.32}$$

subject to the entire first principle model described in Section 7.1.1. Besides, in order to compare the performance of the chance constrained NMPC with the dynamic adaptive back-off strategy; the constraint regarding the process shout down is neglected in the nominal open-loop optimization. Furthermore, while the hard-constraint with regard to the adiabatic end temperature (7.30) is still taken over, the safety restriction (7.29) corresponding to the maximum allowable reactor temperature is now formulated as a chance constraint within the moving horizon,

$$\Pr\{T(k+i\,|\,k) \le T_{max} = 356K\} \ge \alpha\,. \tag{7.33}$$

The decision variable is here the cooling flow rate too. Moreover, the relationship between the probability level and the corresponding value of the objective function can also be used here for a suitable trade-off decision between profitability and robustness. As previous discussed, tuning the value of α is also an issue of the relation between feasibility and profitability. The general solution of the defined NMPC problem (Eq. 7.31), however, is only able to arrive at a maximum value α^{max} which is dependent on the properties of the uncertain inputs and the restriction of the controls. The value of α^{max} can be computed through a previous probability maximization step. For this purpose, the original objective function (7.32) is replaced and the following optimization problem will then be solved:

$$\begin{aligned}
&\max \ \alpha \\
&\text{s.t.} \ \ \mathbf{g}(\dot{\mathbf{x}},\mathbf{x},\mathbf{y},\mathbf{u},\boldsymbol{\xi}) = 0,\ \mathbf{x}(t_0) = \mathbf{x}_0 \\
&\qquad \mathbf{h}_D(\dot{\mathbf{x}},\mathbf{x},\mathbf{y},\mathbf{u},\boldsymbol{\xi}) \le 0 \\
&\qquad \Pr\{\ T \le T_{max}\} \ge \alpha \\
&\qquad \mathbf{u}_{min} \le \mathbf{u} \le \mathbf{u}_{max},\ t_0 \le t \le t_f
\end{aligned} \tag{7.34}$$

where **g** represents the model equations, which form the equality constraints (see Section 7.1.1) and $\mathbf{h}_D$ are the deterministic inequality constraints. The maximization of α is equivalent to the computation of the highest probability value of complying with the constraint, which can be maximized as an ordinary objective function by setting the optimal values of the decision variables **u**. Solving the problem in Equation 7.34, a value of α^{max}=96,7% is achieved. In order to identify the potential of the proposed approach, the main disturbance assumed is the catalyst activity with a variance of 15%.

However, the use of this strategy for transient process with the consideration of uncertainties in advance has for those NMPC-Problems a great impact where the reference trajectory is very close to a defined upper bound of the constraint output at some time-periods. Thus, a comparison between the chance-constrained approach and the deterministic dynamic adaptive back-off strategy is meaningful in order to find further improvement of operation policies due to the stochastic approach.

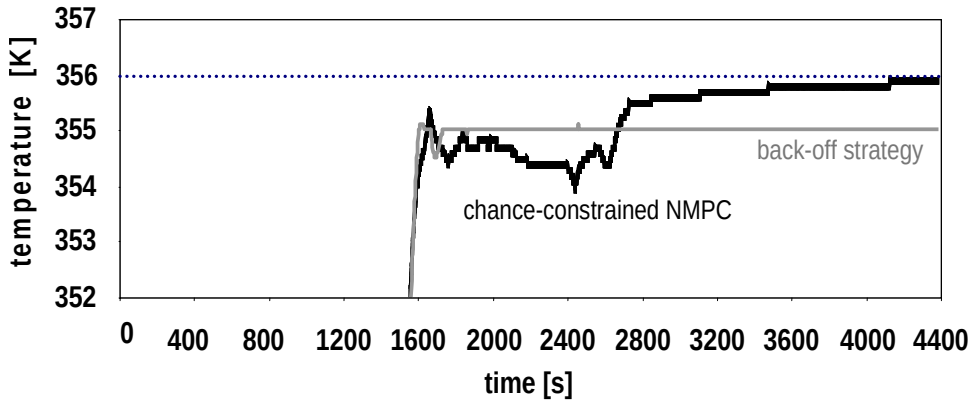

Figure 7.31: Reactor temperature trajectory of both strategies.

The resulting trajectories of the reactor temperature concerning both strategies are illustrated in Figure 7.31. It can be seen that the reactor temperature trajectory based on the back-off strategy reaches early a stationary value caused by fixed bounds of the temperature formulated in the corresponding optimization problem. The temperature curve of the chance-constrained approach shows several changes with lower values of temperatures compared to the back-off strategy just after the heating period, and higher values after the total feed amount has been supplied (see Fig. 7.32). This is caused by the fact that with the consideration of uncertainties in advance, the sensitivity changes of uncertain parameters towards the reactor temperature are also taken into consideration by means of the stochastic approach.

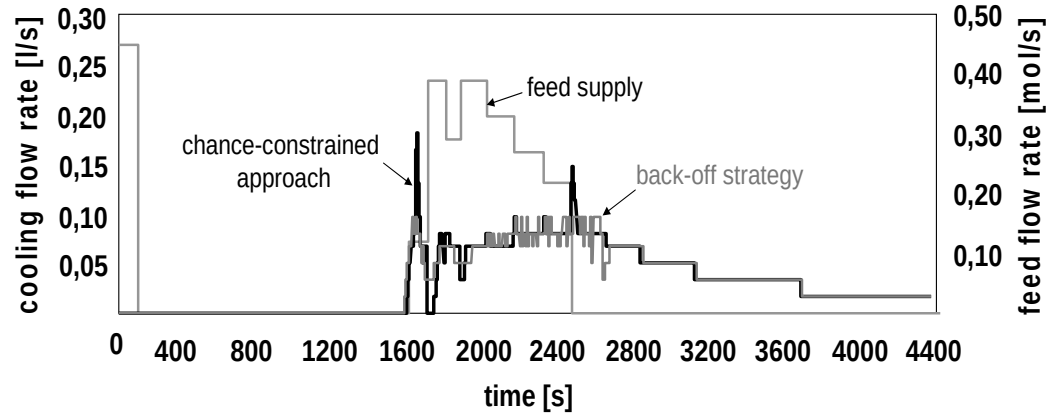

Figure 7.32: Optimal cooling flow rate for both strategies and the given feed supply.

Due to the higher sensitivities, the stochastic approach implements a more conservative strategy after 1600s and, thus, the operation may achieve more robustness than the back-off strategy. Towards the end of the process, the decrease of sensitivities is used for a closer approach to the maximum allowable reactor temperature and thus leading to a better objective value. Moreover, different confidence levels can be assigned to different time periods within the moving horizon by using single chance constraints. By this means, a decreasing factor, i.e., a lower confidence level for the future periods within the horizon can be introduced. As a result, the process operation will be as close as possible to the constrained boundaries. Thus, the chance-constrained strategy leads to an improvement of both robustness and the objective value.

7.4 Summary

Model-based process control of transient processes has become significant during the last few decades. However, transient processes are inherent dynamic and characterized by the fact that some of the controlled properties are commonly not measured on-line. Moreover, since nonlinear models are derived from input-output data, which inevitably contain significant bias and variance, the uncertainties and disturbances are required to be quantified and considered explicitly in the controller design and analysis. As demonstrated for the semi-batch reactor under safety restrictions, the potential advantages of a model-based control system are otherwise likely to lead to significant tracking errors.

In this chapter, two methods based on a nonlinear model predictive control NMPC scheme are introduced to solve close-loop dynamic optimization problems within an online framework. The key idea lies in the consideration of unknown and unexpected disturbances in advance i.e. anticipating, in particular, violation of output hard-constraints, which are strongly affected by instantaneous disturbances. The first approach is realized by means of an adaptive backing off of their bounds along the moving horizon with a decreasing degree of severity leading then to the generation of a trajectory consisting of the modified constraint bounds. This trajectory is however dependent on the amount of measurement error and parameter variation including uncertainty. In addition, towards an integration of dynamic real-time optimization and control of transient processes, a two-stage strategy is considered which is characterized through a higher level corresponding to a dynamic optimization problem and a lower level related to a tracking control problem.

In the chance-constrained control approach the known properties of some major disturbances can be integrated in the NMPC formulation. These are described with stochastic distributions, which can be achieved based on historical data. Moreover, since the influence of the uncertain variables on the output constraints propagate through the nonlinear process from time interval to time interval. The solution of the chance-constrained NMPC problem has the feature of prediction, robustness and being closed-loop. Due to the property of the moving horizon the developed control strategy is extended to on-line optimization under uncertainty. Thus, derived from the proposed approach, in this Chapter, a novel concept based on a nonlinear MPC scheme has been introduced to solve close-loop stochastic dynamic optimization problems assuring efficiently both robustness and feasibility with respect to input and, in particular, output constraints. The formulation of individual pre-defined probability limits of complying with the restrictions incorporates the issue of feasibility and the contemplation of trade-off between profitability and reliability. In order to demonstrate the performance of the developed concepts and the efficiency of the proposed online framework, both presented NMPC schemes are applied for the on-line optimization of a semi-batch non-isothermal reactor under safety (hard-) constraints and the influence of several disturbances.

Chapter 8

Conclusions and Future Research Directions

In the industrial practice, an overestimation of uncertainties, which is a widespread practice in the chemical industry, leads to conservative decisions resulting in an unnecessary deterioration of the economic performance. The main reason for these intuitive decisions in planning chemical process operations is due to the lack of systematic reliability analysis. In other cases, an aggressive strategy may be preferred due to profit expectations. This is very likely to lead to process constraint violations. Accordingly, a systematic way is required to evaluate the trade-off between profitability and reliability. To allow solving the optimization problems with inherent uncertainty, a promising chance-constrained programming approach has been developed and presented in this thesis. Its main feature is that the resulting decisions ensure the probability of complying with constraints, i.e., a sufficient confidence level of being feasible. Thus, using chance constrained programming, the relationship between the profitability and reliability can be quantified. In other words, the solution of the problem provides comprehensive information about the economical performance as a function of the desired confidence level of satisfying process constraints.

Therefore, in this thesis the aspects of uncertainty in process engineering problems have been addressed. The main challenge has been the solution of large-scale, complex optimization problems under uncertainties focusing on the development of a general chance-constrained programming framework to deal with different optimization problems as depicted in Figure 1.3. The resulting optimization problems are then relaxed into equivalent nonlinear optimization problems such that they can be solved by a nonlinear programming solver. The

major challenge when solving chance-constrained optimization problems lies in the computation of the probability and its derivatives of satisfying inequality constraints. Suitable algorithms and numerical approaches to addressing nonlinear, steady-state as well as dynamic optimization problems under uncertainty have been developed and applied to various optimization tasks with uncertainties, such as optimal design and operation as well as optimal control of processes under uncertainty.

This work presents a novel contribution to the research of optimization under uncertainty and provides theoretical developments and practical applications of chance-constrained programming. One of the main contributions is also that the solution of such problems based on the developed approaches can offer both optimal and reliable decisions such that the analysis of the outcomes allows for identifying the critical constraint which cuts off the largest part of the feasible region. This information is important for decision makers in order to relax the constraint, if necessary, so as to arrive at a meaningful decision. It has been clearly demonstrated that probabilistic programming is a promising technique in solving optimization problems under uncertainty in process system engineering.

8.1 Summary of contributions

Summarizing the major contributions of this thesis are:

Nonlinearity between constrained output and uncertain input

The approach considers a nonlinear relation between the uncertain input and the constrained output variables. In fact, the approach is relevant to all cases when uncertainty can be described by any kind of joint correlated multivariate distribution function. The essential achievement is the efficient computation of the probabilities of holding the constraints, as well as their gradients.

Mapping back or reverse projection of output probability distribution

In systems where the relation between uncertain and constrained variables is *nonlinear*, the type of the probability distribution function of the uncertain input is not the same as the one of the constrained output. Thus, due to the nonlinear propagation, it is difficult to obtain the stochastic distribution of output variables. For this reason, nonlinear chance-constrained programming remained an unresolved problem. In this thesis, new approaches are introduced to infer the output probability distribution. The basic idea is to avoid directly computing the output probability distribution. Instead, an equivalent representation of the probability is derived by mapping the probabilistic constrained output region back to a bounded region of the uncertain inputs. Thus, within the developed framework the probability computation of the output constraints is transformed to a multivariate integration in the limited area of uncertain inputs. Hence, the output probabilities and, simultaneously, their gradients can be calculated through multivariate integration of the density function of the uncertain inputs. For this purpose, efficient algorithms are introduced based on the orthogonal collocation on finite elements with an optimal number of collocation points. However, since multiple time intervals are considered, the reverse projection of the feasible output region is not trivial. Therefore, the approach also involves efficient algorithms for the computation of the required (mapping) reverse projection so as to deal with large-scale nonlinear dynamic processes.

Strict monotonic and non-monotonic relationship

Depending on the relation between the uncertain input and the output variables, the developed method relies upon the case of a strict monotonic relationship between the constrained output variables and at least one of the uncertain input variables. However, the chance-constrained programming framework has also been extended to address stochastic optimization problems where *no monotonic* relationship between constrained output and any uncertain input variable can be assured. Especially for those process systems where the decision variables are strongly critical to the question of whether there is monotony or not such that chance-constrained nonlinear dynamic optimization can now also be realized efficiently even for those cases where the monotony can not be guaranteed.

Consideration of single and joint constraints

In this work, we also focus on the analysis of the impact of chance constraint probability limits on the optimal policies in terms of robustness and feasibility, particularly with regard to the optimized value of the objective function. These probability limits can be seen as measurements of the robustness of the optimized strategies. Obviously a high confidence level to ensure the constraints will be preferred. However, due to the nature of the uncertain inputs and the restriction of the controls and outputs, it is often impossible to find an operation policy with a 100% guarantee for complying with the constraints. Thus a maximum confidence level needs to be found first. As part of this work, therefore, a systematic analysis, appropriate to the system complexity, has been developed to compute this value. The novelty lies in the efficient computation of single and joint constraints and their gradients.

Time-dependent uncertainties

Uncertain variables can be constant or time-dependent in the future horizon. They are, however, undetermined before their realization. Moreover, usually only a subset of variables can be measured. However, in this work novel efficient algorithms have been integrated to consider time-dependent uncertainties.

Integration of D-RTO and control level

Furthermore, for the integration of dynamic real-time optimization and control of transient processes, a two-stage strategy is considered which is characterized by an upper stage corresponding to a dynamic optimization problem and a lower stage related to a tracking control problem. For this purpose, two methods based on a nonlinear model predictive control (NMPC) scheme are proposed to solve close-loop stochastic dynamic optimization problems assuring both robustness and feasibility with respect to state output constraints within an online framework.

Dynamic adaptive back-off strategy

Feasibility and robustness with respect to input and output constraints have been achieved by the proposed backing-off strategy. The resulting NMPC scheme embedded in the on-line re-optimization framework is viable for the optimization of transient processes while simultaneously guaranteeing the constraints compliance - both for nominal operation as well as for cases of large disturbances e.g. failure situation.

Robust Nonlinear MPC under Chance Constraints

Since the prediction of future process outputs within an NMPC moving horizon is based on a process model involving the effects of manipulated inputs and disturbances on process outputs, the compliance with constraints on process outputs is more challenging than these on

process inputs. Furthermore, as the model involves uncertainty, process output predictions are also uncertain. This leads to output constraints violation by the close-loop system, even though predicted outputs over the moving horizon might have been properly constrained. Thus, a robust predictive control strategy is introduced for the online optimization of transient processes, in particular, under hard constraints leading to a chance-constrained nonlinear MPC scheme where the output constraints are to be held with a predefined probability with respect to the entire horizon. Due to the moving horizon approach, the control strategy can be extended to on-line optimization under uncertainty.

Finally, a number of example problems are discussed including the application of the optimization framework to a large-scale industrial process. Thus, the developed chance-constrained optimization framework demonstrates to be promising to address optimization problems under uncertainties. The different solution strategies have mainly been applied to transient processes. The solution provides a robust operation strategy in the future time horizon. Moreover, the relationship between the probability levels and the corresponding values of the objective function can be used for a suitable trade-off decision between profitability and robustness. Tuning the value of the different confidence levels is also an issue of the relation between feasibility and profitability.

8.2 Recommendations for future work

Derived from the ideas suggested in this thesis and along the lines of the presented development, several points were raised that call for further investigations and can lead to interesting extensions of this work.

Usually the distribution of an uncertain variable can be estimated through statistical regression from past data logs or through interpolation or extrapolation. There has been an explosive growth of computer-based process monitoring systems, which makes it relatively easy to acquire process data for utilization in distribution analysis. Uncertain variables may be correlated or uncorrelated and their stochastic distribution may also have different forms. The developed solution approaches are not dependent on the distribution of the random variables, whenever the probability distribution function of the random variables is known or can be approximated, the chance-constrained programming framework can be applied. However, the application of the approach to processes under uncertainties with other distributions may be a challenging future work. In this context, the development of appropriate algorithms to approximate a multivariate probability distribution function based on available data represents an interesting task to be tackled.

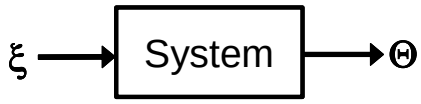

Figure 8.1: Defining (time-dependent) parameters as output variables.

Another interesting topic concerns the application of the developed approaches to reducing the confidence interval of estimated parameters (Θ). Here the random input ξ can be represented by means of uncertain operating conditions, measurement uncertainty amongst others (Fig. 8.1).

Beyond doubt, the most attractive work direction represents the extension of chance constrained programming in order to also consider integer variables for nonlinear dynamic systems, thus, leading to mixed-integer dynamic optimization problems under uncertainty. This, in fact, represents the most motivating challenge for the immediate future work.

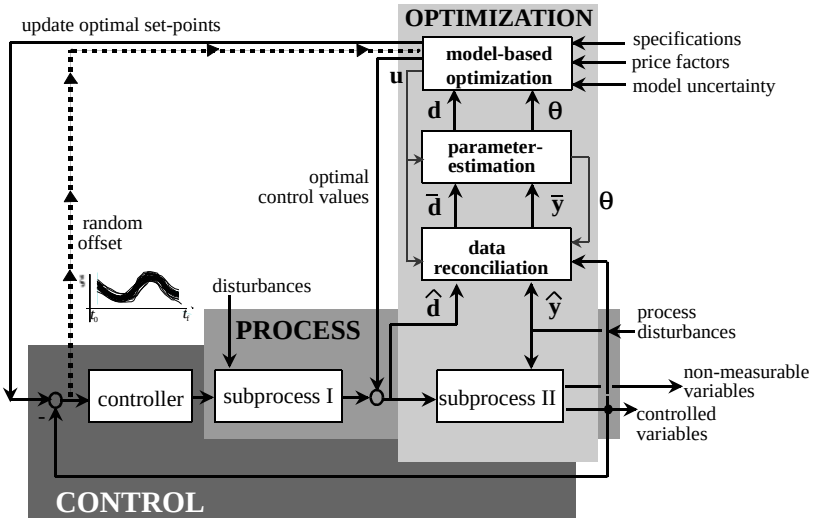

Figure 8.2: Close coordination and integration between process, control and optimization.

The case studies discussed in the previous chapters are mainly concerned with single unit operations. However, chemical processes are mostly composed of a large number of units which are interconnected with each other through flows of materials and energy including recycle streams. Thus, based on the promising results obtained in this thesis, the development of a unified framework for a *robust* tight integration and coordination of the different optimization and control tasks accounting for the uncertain operating conditions, uncertain model parameters and disturbances at different time scales, as illustrated in Figure 8.2, poses an interesting challenge for integrated chemical processes development. Together with the increasingly intensifying computer performance, the developed algorithms in this thesis, which some of them are still time-consuming for real-time control of large-scale systems, will lead to a broader applicability of optimization problems with probabilistic performance functions and constraints. Thus, chance constrained programming will further evolve into a promising technique in solving optimization problems under uncertainty in several applications and disciplines.

Appendix

Appendix A1: Theorem for the Maximal joint Probability of a Multivariate Normal Distribution (Li, P., Wendt, M., Arellano-Garcia, H., Wozny G., 2002).

Theorem: For a multivariate normal distribution the maximal value of the joint probability is achieved, if

$$\mu_{y(i)} = \frac{y_{\min} + y_{\max}}{2} \qquad i = 1, \cdots, N \tag{A1.1}$$

Proof: Let the probability density function of the output vector be

$$\varphi_N(\mathbf{y}) = \frac{1}{\left|\mathbf{R}_y\right|^{1/2} (2\pi)^{N/2}} e^{-\frac{1}{2}(\mathbf{y}-\boldsymbol{\mu}_y)^T \mathbf{R}_y^{-1}(\mathbf{y}-\boldsymbol{\mu}_y)} = \gamma e^{f(\mathbf{y})} \tag{A1.2}$$

where γ and $f(\mathbf{y})$ are the corresponding constant and function, respectively. The joint probability is then

$$P(\boldsymbol{\mu}_y) = \int_{y\min}^{y\max} \cdots \int_{y\min}^{y\max} \cdots \int_{y\min}^{y\max} \varphi_N(\mathbf{y}) dy(1) \cdots dy(i) \cdots dy(N) \tag{A1.3}$$

at the maximum point, there will be

$$\frac{\partial P(\boldsymbol{\mu}_y)}{\partial \mu_y(i)} = 0 \qquad i = 1, \cdots, N \tag{A1.4}$$

Since

$$\frac{\partial \varphi_N(\mathbf{y})}{\partial \mu_y(i)} = \gamma e^{f(\mathbf{y})} \frac{\partial f(\mathbf{y})}{\partial \mu_y(i)} \tag{A1.5}$$

From (A1.2)

$$\frac{\partial f(\mathbf{y})}{\partial \mu_y(i)} = -\frac{\partial f(\mathbf{y})}{\partial y(i)} \tag{A1.6}$$

From (A1.3) and (A1.4), it results

$$\int_{y\min}^{y\max}\cdots\int_{y\min}^{y\max}\left[\int_{y\min}^{y\max}\gamma e^{f(\mathbf{y})}df(\mathbf{y})\right]_i dy(1)\cdots dy(i-1)dy(i+1)\cdots dy(N)=0 \tag{A1.7}$$

That is

$$\begin{aligned}&\int_{y\min}^{y\max}\cdots\int_{y\min}^{y\max}\int_{y\min}^{y\max}\cdots\int_{y\min}^{y\max}\varphi_{N-1}[y(1),\cdots,y(i-1),y(i+1),\cdots,y(N)]_{y(i)=y\min}dy(1)\cdots dy(i-1)dy(i+1)\cdots dy(N)\\ =&\int_{y\min}^{y\max}\cdots\int_{y\min}^{y\max}\int_{y\min}^{y\max}\cdots\int_{y\min}^{y\max}\varphi_{N-1}[y(1),\cdots,y(i-1),y(i+1)\cdots,y(N)]_{y(i)=y\max}dy(1)\cdots dy(i-1)dy(i+1)\cdots dy(N)\end{aligned} \tag{A1.8}$$

It means

$$\Phi_{N-1}[y(1),\cdots,y(i-1),y(i+1),\cdots y(N)]_{y(i)=y\min}=\Phi_{N-1}[y(1),\cdots,y(i-1),y(i+1),\cdots y(N)]_{y(i)=y\max} \tag{A1.9}$$

Since Φ_{N-1} is the probability function of N-1 joint events of normally distributed variables, it is continuous and symmetric. Since $y_{\min} \neq y_{\max}$, then the mean of $y(i)$ must be at the center of $[y_{\min},\ y_{\max}]$.

Appendix A2: Collocation on finite elements for numerical integration (Finlayson, 1980)

The integration required has the form

$$\Omega=\int_{v_0}^{v_f}\omega(v)dv \tag{A2.1}$$

namely

$$\frac{d\Omega}{dv}=\omega(v),\quad \Omega(v_0)=0 \tag{A2.2}$$

The domain $[v_0, v_f]$ of the variable v will be discretized into subintervals ($[v_l, v_{l+1}], l=1,\cdots,L$). In each interval the integration function will be approximated by Lagrange-functions

$$\Omega(v)=\sum_{j=0}^{NC}\Gamma_j(v)\Omega_j \tag{A2.3}$$

where *NC* is the number of collocation points and Γ is the Lagrange-function

$$\Gamma_j(v) = \prod_{\substack{i=0 \\ i \neq j}}^{NC} \frac{v - v^{(i)}}{v^{(j)} - v^{(i)}} \tag{A2.4}$$

Ω_j and $v^{(j)}$ are the values of the integration and the random variable on the corresponding collocation points which are usually the zeros of the shifted Legendre-function, respectively. Thus the derivatives of Ω on the collocation points can be calculated

$$\left.\frac{d\Omega}{dv}\right|_{v_i} = \sum_{j=0}^{NC} \left.\frac{d\Gamma_j}{dv}\right|_{v_i} \Omega_j \quad i = 1, \cdots, NC \tag{A2.5}$$

From (A2.2) and (A2.5), the value of the integration on the collocation points can be calculated. For the continuity, we use the integrated value on the last collocation point of the current interval as the initial value of the next interval.

Appendix A3: Model equations and parameters of the dynamic reactor network system in section 5.2.2

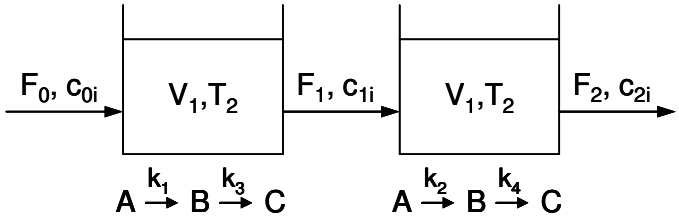

Figure A.3.1: Reactor network system.

Component balances for reactor 1:

$$V_1 \cdot \frac{\partial c_{1A}}{\partial t} - F_0 \cdot c_{0A} + F_1 \cdot c_{1A} + k_1 \cdot V_1 \cdot c_{1A} = 0 \tag{A3.1}$$

$$V_1 \cdot \frac{\partial c_{1B}}{\partial t} + F_1 \cdot c_{1B} - k_1 \cdot V_1 \cdot c_{1A} + k_3 \cdot V_1 \cdot c_{1B} = 0 \tag{A3.2}$$

$$V_1 \cdot \frac{\partial c_{1C}}{\partial t} + F_1 \cdot c_{1C} - k_3 \cdot V_1 \cdot c_{1B} = 0 \tag{A3.3}$$

Component balances for reactor 2:

$$V_2 \cdot \frac{\partial c_{2A}}{\partial t} - F_1 \cdot c_{1A} + F_2 \cdot c_{2A} + k_2 \cdot V_2 \cdot c_{2A} = 0 \tag{A3.4}$$

$$V_2 \cdot \frac{\partial c_{2B}}{\partial t} - F_1 \cdot c_{1B} + F_2 \cdot c_{2B} - k_2 \cdot V_2 \cdot c_{2A} + k_4 \cdot V_2 \cdot c_{2B} = 0 \tag{A3.5}$$

$$V_2 \cdot \frac{\partial c_{2C}}{\partial t} - F_1 \cdot c_{1C} + F_2 \cdot c_{2C} - k_4 \cdot V_2 \cdot c_{2B} = 0 \tag{A3.6}$$

Product amounts

$$\frac{\partial SD_1}{\partial t} - F_2 \cdot c_{2A} = 0 \tag{A3.7}$$

$$\frac{\partial SD_2}{\partial t} - F_2 \cdot c_{2B} = 0 \tag{A3.8}$$

$$\frac{\partial SD_3}{\partial t} - F_2 = 0 \tag{A3.9}$$

with,

$$k_1 = k_{01} \cdot e^{-\frac{E_{A1}}{RT_1}}; \quad k_2 = k_{01} \cdot e^{-\frac{E_{A1}}{RT_2}}; \quad k_3 = k_{02} \cdot e^{-\frac{E_{A2}}{RT_1}}; \quad k_4 = k_{02} \cdot e^{-\frac{E_{A2}}{RT_2}}$$

$$c_{0A} = 1; \quad c_{0B} = 0; \quad c_{0C} = 0$$

Auxiliary equations

$$CB = \frac{\int_0^{t_f} F_2\, c_{2B}\, dt}{\int_0^{t_f} F_2\, dt} \tag{A3.10}$$

$$PB = \int_0^{t_f} \left(F_2\, c_{2B} - F_0\, c_{0B} \right) dt \tag{A3.11}$$

$$UT_i = \int_0^{t_f} QP_i\, dt + \sum_{II=2}^{MM} \left| T_i(II) - T_i(II-1) \right| \cdot \rho \cdot c_P \cdot V_i \tag{A3.12}$$

where MM is the total number of intervals II and i=1,2. The independent (decisions) variables are the length of the different time intervals TD(II), the feed flow rate F_0(II), the reactor temperatures T_1(II) and T_2(II), and the reactor volumes V_1(II) and V_2(II), II represents the current interval. The dependent variables are the concentrations: c_{1A}, c_{1B}, c_{1C}, c_{2A}, c_{2B}, c_{2C}, the product amounts SD_1, SD_2, SD_3, and the heat flux QP_1, QP_2 for both reactors, which are necessary in order to keep constant the reactor temperature in the respective interval II. In this case study, the activation energies, the frequency factors, and the reaction enthalpies are assumed to be uncertain.

uncertain parameters ξ		**expected value μ**		**Standard deviation σ**
activation energy	E_{A1}	36.400,00	J / Mol	10%
activation energy	E_{A2}	34.600,00	J / Mol	1%
frequency factor	k_{01}	840.000,00	1 / min	10%
frequency factor	k_{02}	76.000,00	1 / min	10%
reaction enthalpy	ΔH_1	21,20	kJ / Mol	5%
reaction enthalpy	ΔH_2	63,60	kJ / Mol	5%
density	$\rho = \rho_A = \rho_B = \rho_C$	1.180,00	kg / m³	5%
heat capacity	c_p	3,20	kJ / kg K	5%

Table A3.1: Stochastic properties of the uncertain inputs.

Correlation matrix:

$$\begin{array}{c} \\ E_{A1} \\ E_{A2} \\ k_{01} \\ k_{02} \\ \Delta H_1 \\ \Delta H_2 \\ \rho \\ c_p \end{array} \begin{array}{c} \begin{array}{cccccccc} E_{A1} & E_{A2} & k_{01} & k_{02} & \Delta H_1 & \Delta H_2 & \rho & c_p \end{array} \\ \begin{bmatrix} 1,0 & 0,5 & 0,3 & 0,2 & 0,1 & 0,0 & 0,0 & 0,0 \\ 0,5 & 1,0 & 0,5 & 0,3 & 0,2 & 0,1 & 0,0 & 0,0 \\ 0,3 & 0,5 & 1,0 & 0,5 & 0,3 & 0,2 & 0,1 & 0,0 \\ 0,2 & 0,3 & 0,5 & 1,0 & 0,5 & 0,3 & 0,2 & 0,1 \\ 0,1 & 0,2 & 0,3 & 0,5 & 1,0 & 0,3 & 0,1 & 0,0 \\ 0,0 & 0,1 & 0,2 & 0,3 & 0,3 & 1,0 & 0,2 & 0,0 \\ 0,0 & 0,0 & 0,1 & 0,2 & 0,1 & 0,2 & 1,0 & 0,1 \\ 0,0 & 0,0 & 0,0 & 0,1 & 0,0 & 0,0 & 0,1 & 1,0 \end{bmatrix} \end{array} \tag{A3.13}$$

Furthermore, since the utility costs UT_i are proportional to the absolute value of the current temperature deviation. The relation of the utility costs to the reactor temperature deviation is approximated by an exponential function (Eq. A3.14), which is smooth also around the point of the current temperature and thus easy to differentiate,

$$\left|T_i(II) - T_i(II-1)\right| = \left|T_i(II) - T_i(II-1)\right| + \frac{1}{k}\exp\left(-k\left|T_i(II) - T_i(II-1)\right|\right) \tag{A3.14}$$

also

$$\left|QP_i\right| = \left|QP_i\right| + \frac{1}{k}\exp\left(-k\left|QP_i\right|\right) \tag{A3.15}$$

with k=20.

Appendix A4: Model equations and parameters of the semi-batch reactor in section 5.3.1

Component balances

$$\frac{dx_A}{dt} = -k_{01}\ e^{-\frac{E_{A1}}{RT}} x_A \tag{A4.1}$$

$$\frac{dx_B}{dt} = -k_{02} e^{-\frac{E_{A2}}{RT}} x_B + k_{01}\ e^{-\frac{E_{A1}}{RT}} x_A \tag{A4.2}$$

$$\frac{dx_C}{dt} = k_{02}\ e^{-\frac{E_{A2}}{RT}} x_B \tag{A4.3}$$

parameter	value	parameter	value
k_{01}	20000 1/s	E_{A2}	53000 J/mol
k_{02}	10000 1/s	R	8.314 J/mol/K
E_{A1}	48890 J/mol	$N_A(t=0)$	200 mol

Table A4.1: Model parameter.

Appendix A5: Model of the reactive semibatch distillation

The model considered in the deterministic and stochastic optimization in the sections 6.2 and 6.3 is based on the following assumptions:

1) constant holdup in the condenser and on the trays
2) constant tray pressure
3) total condenser without subcooling
4) ideal vapor phase on each tray
5) negligible vapor holdup
6) ideal heat exchange in the condenser and reboiler.

The trays are numbered from the condenser (j=1) to the reboiler (j=NST). The variables on each tray are the component compositions of both liquid and vapor phases, the liquid and vapor flow rates, as well as the temperature. With the above assumptions, the following DAE system is formulated

Total condenser: $j = 1$

Component balance

$$HU_1 \frac{dx_{i,1}}{dt} = V_2 y_{i,2} - (L_1 + D) x_{i,1} \tag{A5.1}$$

Summation equation:

$$\sum_{i=1}^{NK} x_{i,1} = 1 \tag{A5.2}$$

The energy balance is replaced wit the following relationship

$$\sum_{i=1}^{NK} K_{i,1} x_{i,1} = 1 \tag{A5.3}$$

Total mass balance

$$L_1 = \frac{\left[1 + R_V(T_j)\right] V_2}{R_V(T_j)} \tag{A5.4}$$

Internal trays: $j = 2, NST - 1$

Component balance

$$HU_j \frac{dx_{i,j}}{dt} = L_{j-1} x_{i,j-1} + V_{j+1} y_{i,j+1} - L_j x_{i,j} - V_j y_{i,j} + r_{i,j} \tag{A5.5}$$

Vapor-liquid equilibrium

$$y_{i,j} = \eta_j K_{i,j} x_{i,j} + (1-\eta_j) y_{i,j+1} \tag{A5.6}$$

Summation equations

$$\sum_{i=1}^{NK} x_{i,j} = 1 \qquad \sum_{i=1}^{NK} y_{i,j} = 1 \tag{A5.7}$$

Energy balance

$$HU_j \frac{dH_j^L}{dt} = L_{j-1} H_{j-1}^L + V_{j+1} H_{j+1}^V - L_j H_j^L - V_j H_j^V \tag{A5.8}$$

Reboiler: $j = NST$

Component balance

$$HU_j \frac{dx_{i,j}}{dt} = L_{j-1} x_{i,j-1} + V_{j+1} y_{i,j+1} - L_j x_{i,j} - V_j y_{i,j} + r_{i,j} \tag{A5.9}$$

Vapor-liquid equilibrium

$$y_{i,j} = \eta_j K_{i,j} x_{i,j} + (1-\eta_j) y_{i,j+1} \tag{A5.10}$$

Summation equations

$$\sum_{i=1}^{NK} x_{i,NST} = 1 \qquad \sum_{i=1}^{NK} y_{i,NST} = 1 \tag{A5.11}$$

Based on the assumption of ideal heat exchange, the energy balance of the reboiler can be replaced as follows

$$V_{NST} - L_{NST-1} = D \tag{A5.12}$$

Total mass balance

$$\frac{dHU_{NST}}{dt} = L_{NST-1} - V_{NST} + F_{NST} \tag{A5.13}$$

and the volume of the reaction

$$V_{R,NST} = HU_{NST} \left(\sum_{i=1}^{NK} \frac{x_{i,NST} M_i}{\rho_i (T_{NST})} \right) \tag{A5.14}$$

Phase equilibrium:

$$K_{i,j} = \frac{p_{i,j}^0}{p_j}\gamma_{i,j}(T_j, x_{i,j}) \qquad \text{(A5.15)}$$

Antoine equation

$$\ln p_{i,j}^0 = A_i + \frac{B_i}{C_i + T_j} \qquad \text{(A5.16)}$$

The activity coefficient $\gamma_{i,j}$ is calculated by the NRTL model.

Enthalpy

$$H_j^V = \sum_{i=1}^{NK} y_{i,j} h_{i,j}^V \qquad H_j^L = \sum_{i=1}^{NK} x_{i,j} h_{i,j}^L \qquad \text{(A5.17)}$$

where the vapor and liquid molar enthalpy of a component can be computed respectively with

$$h_{i,j} = \Delta H_{298i} + \int_{298}^{T} c_{p_{i,j}} dT \qquad \text{(A5.18)}$$

and

$$c_{p_{i,j}} = a_{i,0} + a_{i,1} T_j + a_{i,2} T_j^2 + a_{i,3} T_j^3 \qquad \text{(A5.19)}$$

Reaction rate

$$r_{i,NST} = k_H C_{A,NST} C_{B,NST} - k_R C_{C,NST} C_{D,NST} \qquad \text{(A5.20)}$$

with the Arrhenius equation:

$$k = k_0 \exp\left(-\frac{E}{RT_{NST}}\right) \qquad \text{(A5.21)}$$

There are $(2NK + 3)$ variables and the same number of equations per tray.

Appendix A6: A hybrid model for the start-up of the reactive batch column starting from the cold and empty state

In section 6.1.3, a hybrid model for the simulation of the start-up operation of batch distillation with overlapping chemical reactions is proposed. The proposed model includes both equation and variable discontinuity (Wang et al., 2003). A detailed tray-by-tray model has been developed. The total equation system consists of mass balance, energy balance,

vapor-liquid equilibrium relations and tray hydraulics. Below are given some auxiliary equations

Liquid flow rate:

$$L_j = \alpha \; l_{weir} \left(\frac{h_j^{liq} - \beta \;\; h_j^{tray}}{\beta} \right)^{1.5} \Big/ vol_j^{liq} \tag{A6.1}$$

with

$$h_j^{liq} = HU_j vol_j^{liq} / A_{tray} \tag{A6.2}$$

Gas velocity:

$$w_j \;=\; V_j \frac{\sum_{i=1}^{NK} y_{i,j} \dfrac{M_i}{\rho_{i,j}^{V}(T_j)}}{A_f} \tag{A6.3}$$

Vapor flow:

$$V_j \quad vol_j^{vap} / A_{act} = \sqrt{\frac{\Delta p_j^{dry}}{\lambda} \Big/ \rho_j^{vap}} \tag{A6.4}$$

Wet pressure drop:

$$\Delta P_{wet}(j) = \bar{\rho}_j^{L} \quad g \quad \left(h_j^{\omega} + h_j^{0\omega} \right)$$
(A6.5)

where the average liquid density is calculated by

$$\bar{\rho}_j^{L} \;=\; \frac{\sum_{i=1}^{NK} x_{i,j} M_i}{\sum_{i=1}^{NK} x_{i,j} \dfrac{M_i}{\rho_{i,j}^{L}(T_j)}} \tag{A6.6}$$

Dry pressure drop:

$$\Delta P_{dry}(j) \;=\; \zeta_W \frac{\bar{\rho}_j^{V}}{2} w_j^2 \tag{A6.7}$$

here the average vapor density is

$$\bar{\rho}_j^V = \frac{\sum_{i=1}^{NK} y_{i,j} M_i}{\sum_{i=1}^{NK} y_{i,j} \frac{M_i}{\rho_{i,j}^V(T_j)}} \tag{A6.8}$$

Tray efficiency

$$\eta_j = \frac{1}{1+\mu \frac{\sum_{i=1}^{NK} k_{i,j} MW_i}{h_j^L \rho^L T_j}} \tag{A6.9}$$

μ has been taken over from Perry et. al., (1997).

Appendix A7: Process data and parameter of the exothermic batch reactor

parameter	value	parameter	value
ν_A	2	d	3 dm
T_0	273 K	ρ_{cool}	900 g/dm^3
R	8,31441 J/mol/K	$c_{p,cool}$	3,1 J/g/K
c_{pA}	92,3 J/mol/K	T_{cool}	298 K
c_{pB}	154,2 J/mol/K	k_{HT}	10 W/dm^2/K
c_{pC}	173,9 J/mol/K	V_{jacket}	6,98 dm^3
$\tilde{M}_A$	25 g/mol	Feed	mol/s
$\tilde{M}_B$	50 g/mol	$\dot{V}_{cool}$	dm^3/s
$\tilde{M}_C$	50 g/mol	h_{0A}	48500 J/mol
ρ_A	550 g/dm^3	h_{0B}	36500 J/mol
ρ_B	800 g/dm^3	h_{0C}	30000 J/mol
ρ_C	900 g/dm^3	E_1	48890 J/mol
k_{01}	500 1/s	E_2	53000 J/mol
k_{02}	10000 1/s		

Table A7.1: Model parameter.

Bibliography

Abel, O., Helbig, A., Marquardt, W., Zwick, H., Daszkowski, T. (2000). Productivity optimization of an industrial semi-batch polymerization reactor under safety constraints. *J. Proc. Cont.* **10**, 351-362.

Abel, O., Marquardt, W. (2000). Scenario-integrated modeling and optimization of dynamic systems. *AIChE J.* **46**(4), 803-823.

Acevedo, J., Pistikopoulos, E. N. (1998). Stochastic optimization based algorithms for process synthesis under uncertainty. *Comput. Chem. Eng.,* **22**(4/5), 647-671.

Adjiman, C. S., Androulakis, I. P., Floudas, C. A. (1998). A global optimization method, αBB, for general twice--differentiable NLPs -- II. Implementation and computational results, *Comput. Chem. Eng.,* **22**(9), 1159-1178.

Ahmad, B. S.; Zhang, Y.; Barton, P. I. (1998). Product sequences in azeotropic batch distillation, *AIChE J.,* **44**, 1051-1071.

Ahmed, S., Sahinidis N. V. (1998). Robust process planning under uncertainty, *Ind. Eng. Chem. Res.* **37**, 1883-1892.

Allgöwer, F., Badgwell T. A., Qin J. S., Rawlings J. B., Wright S. J. (1999). Nonlinear predictive control and moving horizon estimation – An introductory overview, *Advances in Control – High lights of ECC'99*, 391-449, Springer, Berlin.

Arellano-Garcia, H., Henrion, H., R., Li P., Möller, A., Römisch, W., Wendt, M., Wozny, G. (1998). A Model for the On-line Optimization of Integrated Distillation Columns under Stochastic Constraints, DFG-Schwerpunktprogramm "Echtzeit-Optimierung grosser Systeme", Preprint 98-32.

Arellano-Garcia, H., Martini, W., Wendt, M., Li P., Wozny, G. (2002). Improving the Efficiency of Batch Distillation by a New Operation Mode, in: J. Grievink and J. v. Schijndel, Proc. ESCAPE12, Elsevier, 619-624.

Arellano-Garcia, H.; Martini, W.; Wendt, M.; Li, P.; Wozny, G. (2003a). Dynamic Optimization of a Reactive Semibatch Distillation Process under Uncertainty ESCAPE-13, June 1-4, 2003, Lappeenranta, Finland, Proceedings pp. 551-556.

Arellano-Garcia, H., Martini W., Wendt M., Wozny, G. (2003b). Chance constrained batch distillation process optimization under uncertainty, *International Symposium on Foundations of Computer-Aided Process Operations*, Coral Springs, Florida, Jan. 12-15, 2003, Proceedings pp. 609-612.

Arellano-Garcia, H., Martini W., Wendt M., Li P., Wozny G. (2003c). Nichtlineare stochastische Optimierung unter Unsicherheiten, *Chem.-Ing.-Tech.*, 72, 814-822.

Arellano-Garcia, H.; Martini, W.; Wendt, M.; Li, P.; Wozny, G. (2004a). Evaluation Strategies of Optimized Batch Processes under Uncertainties by Chance Constrained Programming. *8th International Symposium on Process Systems Engineering (PSE8)*, January 5.-10. 2004, Kunming, Proceedings pp. 148-153.

Arellano-Garcia, H.; Martini, W.; Wendt, M.; Wozny, G. (2004b). Robust Operational Process Design under Uncertainty. *International Symposium on Foundation of Computer-Aided Process Design (FOCAPD)*, July 11-16, 2004, Princeton, Proceedings pp. 505-508.

Balasubramanian, J., Grossmann, I: E. (2003). Scheduling optimization under uncertainty- an alternative approach. *Computers and Chemical Engineering*, **27**, 469-490.

Bansal, V., Perkins, J. D., Pistikopoulos, E. N. (2000). Flexibility analysis and design of linear systems by parametric programming, *AIChE J.*, **46**, 335-354.

Bansal, V., Perkins, J. D., Pistikopoulos, E. N. (2002). Flexibility analysis and design using a parametric programming framework, *AIChE J.*, **48**, 2851-2868.

Bates, D. M., Watts, D. G. (1988), Nonlinear Regression Analysis and its Applications, Wiley.

Benders, J. F. (1962). Partitioning procedures for solving mixed-variables programming problems. *Numer. Math*., **4**, 238.

Bernardo, F. P., Pistikopoulos, E. N., Saraiva, P. M. (1999). Integration and computational issues in stochastic design and planning optimization problems, *Ind. Eng. Chem. Res.,* **38**, 3056-3068.

Biegler, L. T., Cervantes, A. M., Wächter, A. (2002). Advances in simultaneous strategies for dynamic process optimization, *Chem. Eng. Sci.*, **57**, 575-593.

Birge, J. R., Louveaux, F. (1997), Introduction to Stochastic Programming, Springer, New York.

Bonny, L., Domenech, S., Floquet, P., Pibouleau L. (1994), Strategies for slop cut recycling in multicomponent batch distillation. *Chem. Eng. Process.*, **33**: 15-23.

Bonvin, D., Srinivasan, B., Ruppen, D. (2001). Dynamic optimization in the batch chemical industry. In: Chemical Process Control - 6. Tucson, AZ.

Calafiore, G., Dabbene, F. (2002). A probabilistic framework for problems with real structured uncertainty in systems and control, *Automatica*, **38**, 1265-1276.

Camacho, E. F., Bordons C. (1999). Model Predictive Control, Springer, Berlin.

Cervantes, A., Biegler, L. T. (1998). Large-scale DAE optimization using a simultaneous NLP formulation, *AIChE J.*, **44**, 1038-1050.

Chisci, L., Rossiter, J. A., Zappa, G. (2001). System with persistent disturbances: Predictive control with restricted constraints, *Automatica*, **37** (7).

Clay, R. L., Grossmann, I. E. (1997). A Disaggregation Algorithm for the Optimization of Stochastic Planning Models", *Comp. Chem. Eng*., **21**, 751.

Damert, K., Dittmar, R., Hartmann, K. (1977). Sensitivity analysis and optimization of complex chemical process systems by the conjugate process method. *International Chemical Engineering*, **17**(4), 624.

Dantzig, G. B. Linear programming under uncertainty. *Manage. Sci*. 1955, **1**, 197.

Dantzing, G. B., Wolfe, P. (1960). The decomposition principle for linear programs. *Oper. Res.* **8**, 101.

Darlington J., Pantelides C.C., Rustem B., Tanyi, B.A. (1999). An algorithm for constrained nonlinear optimization under uncertainty. *Automatica,* **35**, 217.

De Nicolao, G., Magni, L., Scattolini, R. (2000). Stability and Robustness of Non-linear Receding Horizon Control, In F. Allgöwer (Ed.) Nonlinear Model Predictive Control, 3-22.

Dimitriadis, V. D., Pistikopoulos, E. N. (1995). Flexibility analysis of dynamic-systems, *Industrial & Engineering Chemistry Research*, **34**, 4451 – 4462.

Dittmar, R., Hartmann, K. (1976). Calculation of optimal design margins for compensation of parameter uncertainty. *Chemical Engineering Science*, **31**, 563-568.

Diwekar, U. M., Rubin, E. S. (1991a). Stochastic modeling of chemical processes, *Comput. Chem. Eng.,* **15**(2), 105-114.

Diwekar, U. M., Madhavan, K. P. (1991b). Multicomponent batch distillation column design, *Ind. Eng. Chem. Res.,* **30**, 713-721.

Diwekar, U. M., Rubin, E. S. (1994). Parameter design methodology for chemical processes using a simulator, *Ind. Eng. Chem. Res.,* **33**, 292-298.

Diwekar, U. M. (1995). Unified approach to solving optimal design-control problems in batch distillation, *AIChE J.,* **38**(10), 1551-1563.

Diwekar, U. M., Kalagnanam, J. R. (1997). Efficient sampling technique for optimization under uncertainty, *AIChE Journal,* **43**(2), 440-447.

Diwekar, U. (2003). Introduction to Applied Optimization, *Kluwer Academic Publishers*, ISBN 1-4020-7456-5.

Dua, V., Pistikopoulos, E. N. (2002). A Multiparametric Approach for Mixed Integer Quadratic Engineering Problems. *Comput. Chem. Eng*., **26**, 715.

Dubljevic, S., Mhaskar, P., El-Farra, N. H., Christofides, P. D. (2005). Predictive Control of Transport-Reaction Processes, *Comp. & Chem. Eng*., **29**, 2335-2345.

Egly, H., Ruby, V., Seid, B. (1979). Optimum design and operation of batch rectification accompanied by chemical reaction, *Comput. Chem. Eng.,* **3**, 169-174.

Engel, V., Stichlmair J., Geipel W. (1997). IChemE Symposium No. 142, 939.

Farhat, S., Czernicki, M., Pibouleau, L., Domenech, S. (1990). Optimization of multiple fraction batch distillation by nonlinear programming, *AIChE J.,* **36**, 1349-1360.

Feehery, W. F., Barton, P. I. (1998). Dynamic optimization with state variable path constraints. *Computers Chem. Engng.* **22** (9), 1241-1256.

Finlayson, B. A. (1980). Nonlinear Analysis in Chemical Engineering. McGraw-Hill, New York.

Fishman, G. (1999). Monte Carlo: Concepts, Algorithms, and Applications, Springer, New York.

Floudas, C. A., Gümüs, Z. H., Ierapetritou, M. G. (2001). Global optimization in design under uncertainty: feasibility test and flexibility index problems, *Ind. Eng. Chem. Res.*, **40**, 4267-4282.

Fogler, Scott H. (1999). Elements of Chemical Reaction Engineering, Prentice Hall Int. London.

Gallant, A.R. (1987). Nonlinear Statistical Models, NY: Wiley.

Gill, P. E., W. Murray, and M. A. Saunders, (1997). SNOPT: An SQP Algorithm for Large-scale Constrained Optimization, Report NA 97-2, Department of Mathematics, University of California, San Diego.

Gmehling, J.; Onken, U.; Arlt, W. Vapor-Liquid Data Collection; DECHEMA: Frankfurt, 1977.

Grossmann, I. E., R. W. H. Sargent (1978), Optimum design of chemical plants with uncertain parameters, *AIChE J.*, **24**, 1021-1029.

Grossmann, I. E., Halemane, K. P., Swaney, R. E. (1983). Optimization Strategies for Flexible Chemical Processes," *Compur. Chem. Eng.,* **7**, 439 .

Grossmann, I. E., Morari, M. (1984). Operability, resilience and flexibility – process design objectives for a changing world, Proc. Int. Conf. On Foundations of Computer-Aided Process Design, *CACHE Publications*, 931-1010.

Grossmann, I. E., Floudas, C. A. (1987). Active constraint strategy for flexibility analysis in chemical processes, *Comp. Chem. Eng.*, **11**, 675-693.

Gupta, A. and C. D. Maranas (2000). A Two-Stage Modeling and Solution Framework for Multidite Midterm Planning under Demand Uncertainty, *Ind. Eng. Chem. Res.* **39**, 3799.

Halemane K. P., Grossmann I. E. (1983). Optimal Process Design under Uncertainty, *AIChE Journal*, **29**, 425.

Haseltine, E. L., Rawlings, J. B. (2005). Critical evaluation of extended Kalman filtering and moving horizon estimation. Ind. Eng. Chem. Res., **44**(8), 2451-2460.

Helbig, A., Abel, O., Marquardt, W. (1998). Model Predictive Control for the On-line Optimization of semi-batch reactors, In American Control Conference, 1695–1699, Philadelphia, PA.

Henrion R., Römisch W. (1999a), Metric regularity and quantitative stability in stochastic programs with probabilistic constraints, *Mathematical Programming*, **84**, 55-88.

Henrion, R. (1999b), Qualitative stability of convex programs with probabilistic constraints, V.H. Nguyen, J.-J. Strodiot and P. Tossings (eds.): *Optimization* (*Lect. Notes in Economics and Mathematical Systems,* **481**).

Henrion, R., Li P., Möller A., Steinbach M., Wendt M., Wozny G. (2001). Stochastic Optimization for Chemical Processes Under Uncertainty, *Online Optimization of Large Scale Systems*, Grötschel et al. eds., Springer-Verlag, 455-476.

Honkomp, S. J., Mockus, L., Reklaitis, G. V. (1999). A framework for schedule evaluation with processing uncertainty, *Comput. Chem. Eng.,* **23**, 595-609.

Ierapetritou, M. G., Acevedo, J., Pistikopoulos, E. N. (1996a). An optimization approach for process engineering problems under uncertainity, *Comput. Chem. Eng.,* **20**(6/7), 703-709.

Ierapetritou, M. G., Pistikopoulos, E. N., Floudas, C. A. (1996b). Operational planning under uncertainty, *Comp. Chem. Eng.*, **20**, 1499-1516.

IMSL (1987), MATH/Library, User's Manual, Houston, Texas.

Jimenez, L., Basualdo, M., Toselli, L., Rosa, L. (2000). Dynamic modeling of batch distillation: comparison between commercial software, In Proceedings Escape-10, 1153-1158.

Jobson, J. (1991), *Applied Multivariate Data Analysis*, Springer, Berlin.

Johnston, L. P. M., Kramer, M. A. (1998). Estimating state probability distributions from noisy and corrupted Data, *AIChE J.*, **44**, 591-602.

Kall, P., and S. W. Wallace, Stochastic programming. New York: Wiley, (1994).

Kim K. J., Diwekar, U. M. (2002). Efficient combinatorial optimization under uncertainty. 1. Algorithmic development, *Ind. Eng. Chem. Res.*, **41**, 1276-1284.

Kothare, M. V., Balakrishnan, V., Morari, M. (1996). Robust constrained model predictive control using linear matrix inequalities, *Automatica*, **32**, 1361-1379.

Lee, J. H., Yu, Z. H. (1997). Worst-case formulations of model predictive control for systems with bounded parameters. *Automatica*, **33**, 765-781.

Leineweber, D. B., Bock, H. G. , Schroder, J. P. (1997). Fast Direct Methods for Real- Time Optimization of Chemical Processes, Proc. of 15th IMACS World Congress on Scientific Computation, A. Sydow, ed., *Modeling and Applied Mathematics*, **6**, 451.

Li, P., Arellano-Garcia, H., Wozny, G., Reuter, E. (1998). Optimization of a semibatch distillation process with model validation on the industrial site, *Ind. Eng. Chem. Res.*, **37**, 1341-1350.

Li, P., Wendt, M., Wozny, G. (2000a), Probabilistically Constrained Generalized Predictive Control, *ADCHEM 2000, 14-16.6.2000, Pisa, Italien.*

Li, P., Wendt, M. (2000b), Robust Model Predictive Control under Chance Constraints, Process System Engineering PSE´2000, July 16-21, Keyston, Colorado, USA.

Li, P., Wendt, M., Arellano-Garcia, H., Wozny, G. (2002). Optimal Operation of Distillation Processes under Uncertain Inflows Accumulated in a Feed Tank, *AIChE Journal*, **48**, 1198.

Li, P.; Wendt, M.; Wozny, G. (2003). Optimale Produktionsplanung für verfahrenstechnische Prozesse unter unsicheren Marktbedingungen. *Chemie-Ingenieur-Technik*, **75**, 832-842.

Li, P.; Wendt, M.; Arellano-Garcia H., Wozny, G. (2004). Process Optimization and Control under Chance Constraints.*International Symposium on Advanced Control of Chemical Processes* (ADCHEM), January 10.-14., 2004, Hong Kong, Proceedings pp 962-967.

Liu M. L., Sahinidis N. V. (1998). Robust process planning under Uncertainty. *Ind. Eng. Chem. Res.*, **37**, 1883.

Loeve, M., Probability Theory (1963), Van Nostrand-Reinhold, Princeton, New Jersey

Loeblein, C., Perkins, J. D. (1999). Analysis and structural design of integrated on-line optimization and regulatory control systems, *AIChE Journal*, **45**, 1030-1040.

Logsdon, J. S.; Biegler, L. T. (1992). Decomposition strategies for large-scale dynamic optimisation problems. *Chem. Eng. Sci*., **47**, 851.

Low K. H., Sorensen, E. (2002). Optimal Operation of Extractive Distillation in Different Batch Configurations, *AIChE Journal*, **48**(5), 1034-1050.

Ma, D. L., Chung, S. H., Braatz R. D. (1999), Worst-case performance analysis of optimal batch control trajectories, *AIChE J*., **45**, 1469-1476.

Maranas, C.D. (1997). Optimal Molecular Design Under Property Prediction Uncertainty, *AIChE Journal*, **43**(5), 1250-1264.

Maybeck, P.S. (1995). Stochastic models, estimation, and control. Arlington: Navtech.

Mayne, D. Q., Rawlings, J. B., Rao, C. V., Scokaert P. O. M. (2000). Constrained model predictive control: Stability and optimality, *Automatica*, **36**, 789-814.

Mhaskar, P., El-Farra, N. H., Christofides, P. D. (2005). Robust hybrid predictive control of nonlinear systems, *Automatica*, **41** (2), 209-217.

Morari, M., Lee J. H. (1999). Model predictive control: past, present and future. *Comp. Chem. Eng.*, **23**, 667-682.

Mueller, D. E. (1956). A method for solving algebraic equations using an automatic computer. *Mathematical tables and other aids to computation*, **10**, 208-215.

Mujtaba, I. M., Macchietto, S. (1998). Holdup issues in batch distillation-binary mixtures, *Chem. Eng. Sci.,* **53**(14), 2519-2530.

Nagy, Z. K., Braatz, R. D. (2003). Robust nonlinear model predictive control of batch processes, *AIChE Journal*, **49**(7), 1776–1786.

Nagy, Z., Braatz, R. D. (2004). Open-loop and close-loop robust optimal control of batch processes using distributional and worst-case analysis, *Journal of Process Control*, **14**, 411-422.

Nocedal, J., S. J. Wright (1999), Numerical Optimization, Springer, New York.

Ostrovsky, G. M., Volin, Y. M., Barit, E. I., Senyavin, M. M. (1994). Flexibility analysis and optimization of chemical plants with uncertain parameters, *Comp. Chem. Eng.*, **18**, 755-767.

Ostrovsky, G. M., Volin, Y. M., Golovashkin, D. V. (1998). Optimization problem of complex system under uncertainty, *Comput. Chem. Eng.,* **22**(7/8), 1007-1015.

Ostrovsky, G. M., Achenie, L. E. K., Wang, Y. P., Volin Y. M. (2000). A new algorithm for computing process flexibility, *Ind. Eng. Chem. Res.*, **39**, 2368-2377.

Painton, L. A., Diwekar, U. (1995). Stochastic annealing under uncertainty, *European Journal of Operations Research*, **83**, 489.

Pearson, R. K. (2001). Exploring Process Data, *J. Process Control*, **11**, 179.

Petkov, S. B., Maranas, C. D. (1998). Design of Single Product Campaign Batch Plants under Demand Uncertainty, *AIChE Journal*, **44**, 896.

Phenix, B.D., Dinaro, J.L., Tatang, M.A., Tester, J.A., Howard J.B., McRae, G.J. (1997). Incorporation of Parametric Uncertainty into Complex Kinetic Mechanisms: Application to Hydrogen Oxidation in Supercritcal Water, *Combustion and Flame*.

Perry, R. H., Green, D. W., Maloney, J. O. (1997). Perry's chemical engineers' handbook, 7th ed., McGraw-Hill, New York.

Pistikopoulos, E. N., Mazzuchi T. A. (1990). A novel flexibility analysis approach for processes with stochastic parameters, *Comp. Chem. Eng*., **14**, 991-1000.

Pistikopoulos, E. N., Ierapetritou, M. G. (1995a). Novel approach for optimal process design under uncertainty, *Comp. Chem. Eng*., **19**, 1089-1110.

Pistikopoulos, E. N., (1995b). Uncertainty in Process Design and Operations, *Comput. Chem. Eng.,***19,** S553.

Prékopa, A. (1995). Stochastic Programming. Kluwer, Dordrecht, 1995.

Reid, R. C.; Prausnitz, J. M.; Poling, B. E. (1987). The Properties of Gases and Liquids; McGraw-Hill, New York.

Reuter, E., Wozny G., Jeromin L. (1989), Modeling of multicomponent batch distillation processes with chemical reaction and their control systems, *Comput. Chem. Eng.* **13**, 499-510.

Reuter, E. (1994). Simulation und Optimierung einer chemischen Reaktion mit überlagerter Rektifikation, VDI Fortschritt-Berichte, Reihe 3: Verfahrenstechnik, Nr. 394.

Rico-Ramirez, V., Diwekar, U., Morel, B. (2003). Real option theory from finance to batch distillation. Compuetrs and Chemical Engineering, 27, 1867.

Rooney, W. C., Biegler, L. T. (1999). Incorporating joint confidence regions into design under uncertainty, *Comput. Chem. Eng.,* **23**, 1563-1575.

Rooney, W. C., Biegler L. T. (2001). Design for Model Parameter Uncertainty Using Nonlinear Confidence Regions, *AIChE Journal*, **47**, 1794-1804.

Sahinidis, N. V. (2004). Optimization under uncertainty: State-of-the-art and opportunities, *Computers & Chemical Engineering*, **28**(6-7), 971-983.

Saltelli, A., Chan, K., Scott, E.M. (2000). Sensitivity Analysis. John Wiley and Sons, Chichester.

Samsatli, J.N., Papageorgiou, L. G., Shah, N. (1998). Robustness Metrics for Dynamic Optimization Models under Parameter Uncertainty, *AIChE J.*, **44**, 1993-2006.

Schwarm, A. T., Nikolaou, M. (1999). Chance-constrained Model Predictive Control, *AIChE Journal,* **45**, 1743.

Seber G. A. F., Wild, C. (1989). Nonlinear regression. Wiley, New York.

Sørensen, E., Skogestad, S. (1994). Control strategies for reactive batch distillation, *J. Process Control,* **4**, 205-217.

Steinbach, M., (1995). Fast Recursive SQP Methods for Large-scale Optimal Control Problems, PhD Dissertation, Universitaet Heidelberg,.

Straub, D. A., Grossmann, I. E. (1993). Design optimization of stochastic flexibility, *Comp. Chem. Eng*., **17**, 339-354.

Swaney, R. E., Grossmann, I. E. (1985a). An index for operational flexibility in chemical process design. Part I: formulation and theory, *AIChE J.*, **31**, 621-630.

Swaney, R. E., Grossmann I. E. (1985b). An index for operational flexibility in chemical process design. Part II: computational algorithms, *AIChE J.*, **31**, 631-641.

Subrahmanyam, S., Pekny, J. F., Reklaitis, G. V. (1994). Design of Batch Chemical Plants under Market Uncertainty, *Ind. Eng. Chem. Res.*, **33**, 2688.

Szántai, T. Habib, A. (1998). On the k-out-of-r-from-n: F system with unequal element probabilities. In: Gianessi, F. et al. (eds.), New Trends in Mathematical Programming. Kluwer, 289-303.

Szántai, T. (1988), A computer code for solution of probabilistic-constrained stochastic programming problems, In: Numerical Techniques for Stochastic Optimization (Y. Ermolive & R. J.-B. Wets, eds.), New York: Springer Verlag, 229-235.

Takamatsu, T., Hashimoto, I., Shioya, S. (1973). Design margins for parameter uncertainty. *J. of Chem. Engrg. Of Japan*, **6**(5), 553.

Tayal M.C., and Diwekar U.M. (2001). Novel Sampling Approach to Optimal Molecular Design under Uncertainty, *AIChE Journal*, **47**, 609-628.

Terwish, P., Ravemark, D., Schenker, B., Rippin, D. W. T. (1998). Semi-Batch optimization under uncertainity: Theory and experiments, *Comput. Che. Eng.,* **22**(1-2), 201-213.

Tørvi, H., Hertzberg, T. (1997). Estimation of uncertainty in dynamic simulation results, *Comput. Chem. Eng., Suppl. (21): 181-185*.

Ulas S., Diwekar, U. (2004). Thermodynamic uncertainties in batch processing and optimal control. *Computers & Chemical Engineering*, **28**(11), 2245-2258.

Uryasev, S. (Ed.), Probabilistic Constrained Optimization: Methodology and Applications, Dordrecht: Kluwer Academic Publishers, 2000.

Varvarezos, D.K., Grossmann, I. E., Biegler, L. T. (1992). An Outer Approximation Method for Multiperiod Design Optimization, *Ind. Eng. Chem. Res.,* **31**,1466-1477.

Vassiliadis V. S., Pantelides, C. C., Sargent, R. W. H. (1994a). Solution of a class of multistage dynamic optimization problems, 1. Problems without path constraints. *Ind. Eng. Chem. Res*., **33**, 2111.

Vassiliadis, V. S.; Pantelides, C. C.; Sargent, R. W. H. (1994b). Solution of a class of multistage dynamic optimization problems, 2. Problems with path constraints. *Ind. Eng. Chem. Res*., **33**, 2123.

Vassiliadis, C. G.; Pistikopoulos, E. N. (2001). Maintenance scheduling and process optimization under uncertainty , *Computers & Chemical Engineering*, **25**, 217 – 236.

Vasquez, V. R., Whiting, W. B. (1999). Effect of systematic and random errors in thermodynamic models on chemical process design and simulation: A Monte Carlo approach, *Ind. Eng. Chem. Res.,* **38**, 3036-3045.

Vasquez, V. R., W. B. Whiting (2000). Uncertainty and sensitivity analysis of thermodynamic models using equal probability sampling. *Comput. Chem. Eng*, **23**, 1825-1841.

Wang, L., Li, P., Wozny, G., Wang, S. (2003). A startup model for simulation of batch distillation starting from a cold state, *C&CE*, **27**(10), 1485-1497.

Wendt, M.; Li, P.; Wozny, G. (2000). Batch Distillation Optimization with a Multiple Time-Scale Sequential Approach for Strong Nonlinear Processes, ESCAPE-10, 7-10.5.2000, Florence.

Wendt, M., Li, P., Wozny G. (2002). Nonlinear Chance Constrained Process Optimization under Uncertainty. *Ind. Eng. Chem. Res.*, **41**, 3621-3629.

Wendt, M. (2005). Untersuchung zur stochastischen Online Optimierung kontinuierlicher Destillationsprozesse unter Unsicherheiten, PhD Thesis, Berlin University of Technology, Germany.

Wets, R. J. B. (1994), Challenges in Stochastic Programming, *IIASA Working Paper*, WP-94-032, Laxenburg.

Wets, R. J. B. (1996). Challenges in Stochastic Programming, *Math. Pi-og.,* **75**, 115.

Whiting, W., Vasquez, V., Meerschaert, M. (1999). Techniques for Assessing the Effects of Uncertainties in Thermodynamic Models and Data. *Fluid Phase Equilibria*, **158**, 627-641.

Xin Y, Whiting W. (2000). Case studies of computer-aided design sensitivity to thermodynamic data and models, *Ind. Eng. Chem. Res.,* **39**, 2998-3006.